Enhancement of Hygrothermal Properties of Bio-based Thermal Insulation Materials via Sol-gel Technology

Hussain, Atif

Award date:
2018

Awarding institution:
University of Bath

Enhancement of Hygrothermal Properties of Bio-based Thermal Insulation Materials via Sol-gel Technology

Atif Hussain

A thesis submitted for the degree of Doctor of Philosophy

University of Bath
Department of Architecture and Civil Engineering

September 2018

Abstract

This study involves the modification of a bio-based aggregate, hemp shiv, using functionalised silica-based coatings. This is the first time sol-gel technology is used in the treatment of hemp shiv to develop sustainable thermal insulation building materials with enhanced hygrothermal properties. Bio-based materials such as hemp shiv have a tendency to absorb large amounts of water due to their hydrophilic nature and highly porous structure. In contrast, the high porosity of hemp shiv provides excellent moisture buffering and thermal insulating properties. In this work, the hydrophilicity of the hemp shiv was reduced without compromising its moisture buffering ability.

A detailed investigation into the physical and chemical properties, surface roughness, porosity and microstructure of hemp shiv is presented. Application of coatings on hemp shiv was found to alter the properties of hemp shiv. The focus of this work was to particularly enhance the water-resistance of hemp shiv without significantly altering the morphology and microstructure of hemp shiv.

The coatings were formulated by the cohydrolysis and polycondensation of tetraethoxyorthosilicate (TEOS). The effect of methytriethoxysilane (MTES) and hexadecyltrimethoxysilane (HDTMS) as functionalising agents in the coating was evaluated. The impact of precursors and their concentration in the coating formulation showed varying results on the hydrophobicity and roughness of hemp shiv. Furthermore, the porosity of hemp shiv was affected by the number of coating layers thereby blocking the pores responsible for the moisture buffering behaviour of hemp shiv. The selected coating formulation was found to increase the hydrophobicity of hemp shiv providing water contact angles up to 118° and reducing the water absorption rates by 250% without showing a significant reduction in the moisture absorption capacity.

Novel thermal insulation building composites were developed using the coated hemp shiv in both a silica and a starch-based matrix. The composites were characterised for their hygrothermal, physical and mechanical properties where it was found that the sol-gel coating reduced water absorption capacity without affecting the moisture buffering ability of the composites. The newly designed light weight high performance composites have potential as sustainable thermal insulators and can establish innovative concepts for global application.

Acknowledgements

First and foremost, I would like to express my sincere gratitude to my lead supervisor Dr Mike Lawrence who has trained me to become a successful researcher. Without his expertise and dedication, I would not have been able to work on the ISOBIO project and perform this pioneering piece of work. I am extremely thankful to my co-supervisor Dr Juliana Calabria-Holley who has been always willing to share her knowledge and help me keep a positive attitude throughout my PhD.

I would like to acknowledge the European Union Horizon 2020 - ISOBIO project for funding this PhD. I would also like to thank Dr Martin P. Ansell, Dr Yunhong Jiang, Dr Helen Cornwell, Prof Pete Walker and Dr Andy Shea for providing insightful comments and helpful suggestions during the ISOBIO team meetings.

The work in this thesis was carried out in the Department of Architecture and Civil Engineering at University of Bath, UK between October 2015 and September 2018 and I would like to thank all the laboratory staff for their assistance. I would also like to thank all my friends at University of Bath for those amusing and entertaining yet highly knowledgeable conversations at the Research Hub.

A part of the experimental work was carried out in the Department of Wood Science and Forestry at Laval University, Quebec, Canada under the Canadian Queen Elizabeth II Scholarship Programme involving an exchange for 6 months (May 2016-October 2016). Special thanks to Professor Pierre Blanchet for giving me this opportunity to work with him and I am grateful to Dr Diane Schorr for her support and advice.

With great pleasure, a massive thanks to my special friend “Wish” for her continuous support and understanding without whom this PhD journey wouldn’t be enjoyable. With her virtual presence, I never felt alone while working during those endless late nights, ignoring the Earth’s distance and time difference! Lastly, I would like to thank my family for their love and blessings in the successful completion of my PhD.

Contents

List of Figures

List of Tables

List of abbreviations

BET – Brunauer–Emmett–Teller
BS – British Standard
CFC – Chloro-fluoro carbons
CM – Confocal microscopy
CT – Computed tomography
CVD – Chemical vapour deposition
DMF – Dimethyl formamide
DSC – Differential scanning calorimetry
DTG – First derivative of weight loss thermogram
DVS – Dynamic vapour sorption
EDX – Energy dispersive X-ray
EMC – Equilibrium moisture content
EU – European Union
FIB – Focused ion beam
FTIR – Fourier transform infrared
GCMS – Gas chromatography mass spectrometry
HDTMS - Hexadecyltrimethoxysilane
IEA – International Energy Agency
ISO – International Organization for Standardization
IUPAC – International Union of Pure and Applied Chemistry
MBV – Moisture buffer Value
MC – Moisture content
MIP – Mercury intrusion porosimetry
MTES - Methyltriethoxysilane
RH – Relative humidity
SEM – Scanning electron microscopy
TEM – Transmission electron microscopy
TEOS – Tetraethyl orthosilicate
TGA – Thermogravimetric analysis
TMOS – Tetramethyl orthosilicate
WA – Water absorption
WCA – Water contact angle
XPS – X-ray photoelectron spectroscopy

Chapter 1

Introduction

This Chapter gives an overview on current concerns in building sector related to energy efficiency, importance of thermal insulation materials, scope and objectives of this PhD, layout of this thesis and dissemination details of this research.

1.1 Background

The United Kingdom is one of the founding members of the International Energy Agency (IEA). A deep de-carbonisation of the UK's energy system is under process in which the country plans to cut down its greenhouse gas emissions. Buildings have been responsible for consumption of over 40% of the global energy which amounts to emit 8.1 Gt of carbon dioxide emissions (CO_2e) annually, equivalent to 33% of the greenhouse gas emissions worldwide. Without any corrective actions, the IEA predicts these figures to almost double by 2050 (Lawrence, 2015; United Nations, 2009).

According to the International Energy Agency (IEA), UK had an electricity consumption of 5.08 MWh/capita and CO_2 emission of 5.99 t CO_2/capita during the year 2015 (Agency for Natural Resources and Energy, 2017). The IEA UK energy data shows the total electricity supplied to the country was 342,668 GWh in 2015. Figure 1.1 shows the share of electricity production by fuel type in 2015 in which the combustible fuels contribute to majority of the UK's electricity demand. In terms of energy consumption in UK, the residential sector consumes one-third of the total energy produced. Electricity and natural gas contribute to 20% and 34% of UK's total final energy consumption respectively (International Energy Agency, 2015).

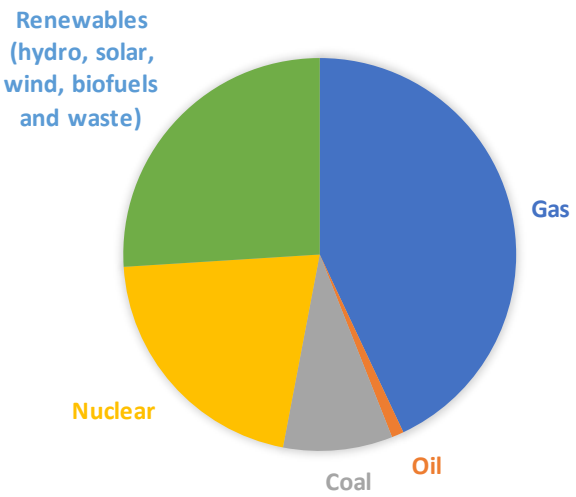

Figure 1.1. Electricity production by fuel type in UK in 2015 (International Energy Agency, 2017).

In the UK, the building sector contributes significantly higher CO_2e equivalent at over 50% of the total UK carbon emissions. Therefore, in order to reduce the net UK carbon emissions, the UK Climate Change Act of 2008 set a target reduction of net UK carbon emission of at least 80% by 2050 compared to the 1990 baseline. Other acts and legislation referring to the construction industry include the 2016 Zero Carbon Policy, the Code for Sustainable Homes and the Low Carbon Construction Action Plan which target reductions of embodied carbon in the fabric of buildings (International Energy Agency, 2012; Lawrence, 2015).

In the EU, buildings have been responsible for almost 40% of total energy consumption and 36% of carbon emissions (EU, 2010). Currently, almost 35% of the buildings in EU are over 50 years old and 75% of the buildings are energy inefficient (European Commission, 2018). Therefore, the EU has proposed the renovation of existing buildings which would potentially lead to a reduction in total energy consumption of 5-6% and lower CO_2 emissions of 5% (European Commission, 2018). The main EU policies that target the improved energy performance of buildings are the "2010 Energy Performance of Buildings Directive" and the "2012 Energy Efficiency Directive". The Energy Performance Directive is directed towards all new buildings being zero-energy buildings by 2020. The Energy Efficiency Directive promotes the use of energy more efficiently at all stages, from production to consumption and sets a 20% energy efficiency target by 2020 within EU countries.

One of the strategies developed for the reduction in carbon emissions is to improve thermal insulation for both new build and retro-fit so that the in-use or operational energy consumption can be lowered. The concept of building insulation has been widely known for decades due to its advantages in reducing energy consumption and maintaining a comfortable indoor environment. Thermal insulation serves to reduce energy consumption over the whole year by enhancing the efficiency of both heating and cooling systems. Saving energy results in reduced costs as well as having a positive impact on the environment by lowering carbon emissions. The Green Deal and PassivHaus programme are

initiatives leading to more energy efficient buildings through better thermal insulation and building design (International Energy Agency, 2012).

However, reducing the embodied energy within a building is also a significant factor which needs immediate attention. The embodied energy of a building can be described as the energy that is needed to extract, process, transport and construct the building and its materials and components. For the achievement of a highly energy optimised building design, both the operational energy and the embodied energy of the building need to be taken into account. The total energy that is used by a building during its lifetime is a combination of its operational energy and embodied energy as seen in Figure 1.2.

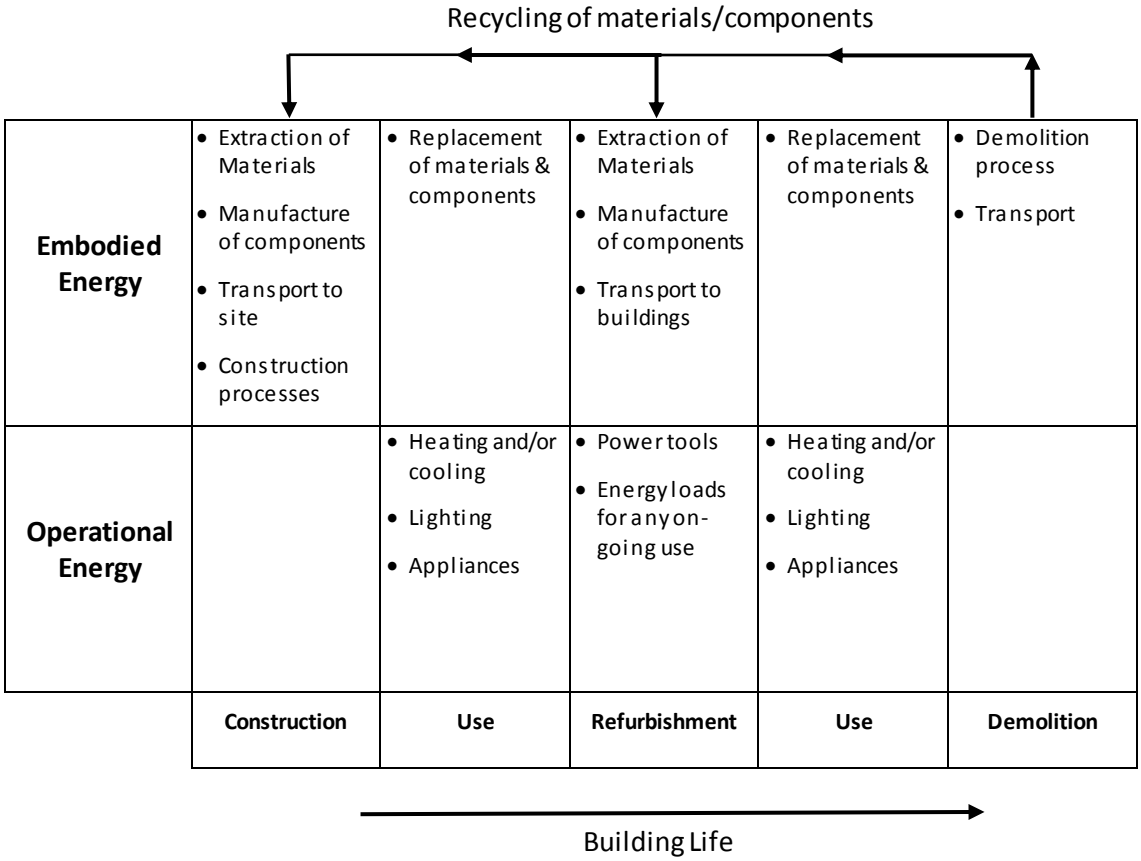

Figure1.2 Operational and embodied energy components of a building during its lifetime (Yohanis & Norton, 2002).

Operational energy currently accounts for the majority of the building energy consumption which includes cooling, heating, lighting and equipment usage. In 2008, operational energy accounted for 83% of the total energy usage when

compared to only 17% represented by the embodied energy of the building (Morrell, 2010). Currently the main emphasis is to target the reduction in the operational energy through heavy insulation, triple glazed windows, building orientation for best use of solar gain, ventilation, high efficiency equipment and so on. The net result of the Acts and Codes (2016 Zero Carbon Policy, the Code for Sustainable Homes and the Low Carbon Construction Action Plan) is that when these buildings become more energy efficient, embodied energy will play a more significant role towards the total percentage of the carbon emissions. Therefore, there is a need to emphasise not only the reduction of operational energy consumption but also the reduction of embodied energy of the building fabric (Lawrence, 2015).

1.2 Types of Thermal Insulation materials

The different types of thermal insulating materials available can be broadly classified into four categories as seen in Figure 1.3. Inorganic fibrous materials such as glass wool and stone wool account for 60% of the insulation products market in Europe and oil-based foamy materials such as polystyrene, polyisocyanurate and polyurethane account for a further 27% of the insulation market. All the remaining materials account for less than 13% of the European insulation market (Papadopoulos, 2005).

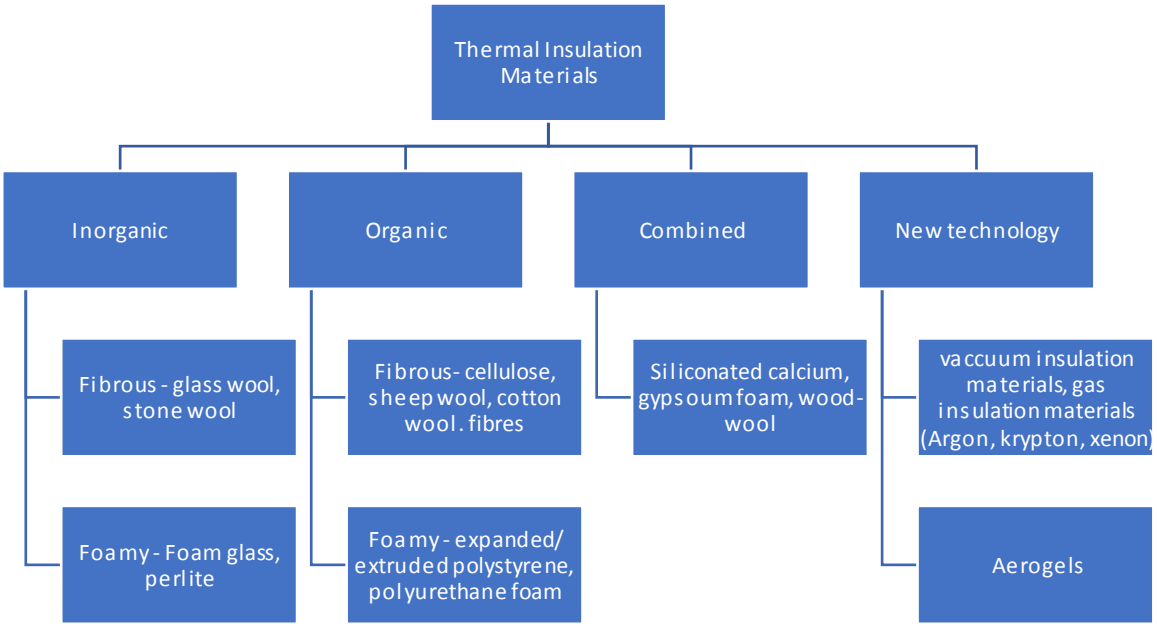

Figure 1.3. Types of thermal insulation materials (Papadopoulos, 2005).

Oil-based insulation products show very low thermal conductivity as can be seen in Table 1.1. However these polymeric products such as expanded and extruded polystyrene require blowing agents in their production process which, after the phase out of chloro-fluoro carbons (CFCs), are mainly CO_2 and pentane. Compared to using CFC blowing, CO_2 is not as efficient in producing low density foams due to its high level of diffusivity and low solubility in polymers. This results

in poorer thermal performance and an increase in atmospheric CO_2 due to release of excess CO_2 (Yang et al., 2009). On the other hand, pentane has been reported to increase smog and ground ozone levels (Danny Harvey, 2007). Mineral fibre materials often require adhesives and water repellent oils to be added during their manufacture in order to enhance their mechanical properties.

Table 1.1. Characteristics of some insulating materials (Sutton, Black, Walker, & BRE, 2011).

Material		Thermal conductivity (W/m.K)	Density (kg/m3)	Availability
Synthetic Materials	Mineral fibre	0.032−0.044	24	Boards, semi, rigid boards, rolls
	Glass fibre	0.038-0.041	16-48	Boards, semi, rigid boards, rolls
	Polyurethane foam	0.023-0.026	30	Boards
	Expanded polystyrene (EPS)	0.033-0.035	12-48	Boards
	Extruded polystyrene (XPS)	0.037-0.038	30-45	Boards
Natural Materials	Wood fibre	0.038-0.050	30–40	Boards, semi, rigid boards, rolls
	Hemp	0.038-0.040	80-110	Semi-rigid slabs, batts
	Straw Bale	0.06	110–120	Boards
	Paper (cellulose)	0.035-0.040	32	Loose batts, semi-rigid batts
	Cork	0.038- 0.070	200-250	Boards, granulated

Table 1.2 Ranking commercially available insulation materials (Papadopoulos, 2005).

Property	Inorganic		Organic	
	Fibrous	**Foamy**	**Fibrous**	**Foamy**
Thermal properties	o	o/-	o	o/+
Moisture resistance	o/+	+	o	o/+
Fire resistance	+	+	o	o
Decay resistance	+	+	o	+
Harmful emissions	o/-	o	o/+	-
Use of CFC, HCFC, CO_2	NA	-	NA	o
Handling safety	o	+	+	+
Toxicity during fire	NA	+	+	o/-
Embodied energy	+	o	o/+	o
Recycling	o	o		+
Waste disposal	+	+	+	o/-
Cost	+	-	o/-	o

(+): Good; (o): average; (−): poor; NA: not applicable

The commercially available organic and inorganic insulation materials have been ranked in Table 1.2 based on their performance and health & safety. The use of bio-based thermal insulation products in the building sector has stimulated considerable interest during the past few years, although synthetic thermal insulators currently dominate the industry (Hills, Norton, & Newman, 2009). The thermal conductivity of bio-based materials is relatively high compared to that of

oil-based foamy insulations or mineral fibre materials. This is mainly due to addition of binders to the bio-based materials that increase the overall thermal conductivity of the composite. Increasing the thickness of the bio-based insulation materials can improve its thermal resistance and make their performance comparable with synthetic materials. However, this would lead to disadvantages such as an increase in cost, need for more land space and an increase in the impact associated with retrofitting solutions. Nevertheless there are some advantages to using bio-based materials compared to synthetic materials such as low embodied energy, ability to sequester CO_2 and their hygroscopic nature. The physical, thermal and hygroscopic properties of bio-based materials will be discussed in detail in literature review in Chapter 2.

1.3 Scope of research

The use of bio-based materials (derived from plant sources) has become increasingly popular for the production of economical engineering materials in the construction industry (Faruk, Bledzki, Fink, & Sain, 2012). Bio-based materials have numerous advantages over conventional non-renewable building materials such as lower embodied energy, lower CO_2 emissions of buildings and the demand for operational energy can be significantly reduced through passive environmental control (Lawrence, 2015).

Several studies have examined the ability of bio-based materials used in construction to absorb and release moisture in response to changes in relative humidity in the surroundings which creates a breathable wall. These materials act as a hygric buffer and eventually reduce the energy demands for air conditioning (Tran Le, Maalouf, Mai, Wurtz, & Collet, 2010). The response to varying humidity conditions is linked to their pore structure and pore connectivity where the moisture condenses and evaporates on the surface of the material and within its pores.

Insulation material made from hemp (*Cannabis Sativa* L.) is gaining interest in the construction industry although currently they have a small share in the European thermal insulation market. Towards the end of the 20th century, a bio-based building material was rediscovered which used the woody core or shiv of hemp combined with lime based binders to produce hemp-lime composites. Many studies have been conducted over the recent years to optimise the hemp characteristics, curing conditions and binder content during the production of hemp based concrete. Hemp insulation materials show good hygrothermal properties by regulating humidity inside buildings and has a low environmental impact (Collet, Chamoin, Pretot, & Lanos, 2013).

Bio-based materials such as hemp shiv are generally very porous with low density due to the structure of the plant stem from which they are derived. The excellent insulation and hygroscopic properties of hemp shiv are related to its highly porous

structure and the presence of long tubes and channels. However, this high porosity is responsible for its large water absorption capacity. Moreover, the presence of cellulose, hemicellulose and lignin in bio-based materials contributes to the presence of hydrophilic hydroxyl groups in their structure.

This leads to certain challenges in the use of bio-based materials:

- Chemical composition: The hydrophilic nature of bio-based materials makes them incompatible with hydrophobic thermoset/thermoplastic polymers which leads to poor adhesion in the matrix interface resulting in lower mechanical strength of the polymeric bio-based composites (Gassan, Gutowski, & Bledzki, 2000; Kabir, Wang, Lau, Cardona, & Aravinthan, 2012).

- Manufacturing: During the manufacture of bio-based composites such as hemp-lime, water is added in significant excess amounts compared to what is actually needed for the hydration of hydraulic lime. This leads to long drying times ranging from several months to over a year which are not acceptable to be employed at an industrial scale (Arnaud & Gourlay, 2012). Moreover, the large water absorption capacity of bio-based materials can even cause problems in all production phases preventing binder adhesion and ultimately in the end product stage when undesirable water comes into contact with the composite or if the surroundings are humid (Kymainen, Hautala, Kuisma, & Pasila, 2001).

- Miscibility: Mixing bio-based material such as hemp shiv with binders is quite a challenge in that the shiv competes with the binder for the available water. Due to this reason, purely hydraulic binders like hydraulic lime or cement cannot hydrate completely, leading to a powdery inner core in the hemp-lime walls which is poorly bound. (Elfordy, Lucas, Tancret, Scudeller, & Goudet, 2008). In addition, the sugars present on the surface of the shiv interfere with the setting of

hydraulic binders, resulting in lower mechanical strength (Ahmad, Bing, Oderji, & Mohsan, 2018).

- Durability and resilience: Another major issue associated with the use of bio-based materials is that they are prone to natural decay, which generally is triggered by a combination of humidity and warmth. In presence of excess moisture, these materials are susceptible to decay and therefore it is not advisable to use them below damp proof courses or in areas which could get wet (Marceau et al., 2017).

- Environmental factors: Higher moisture contents can also occur in vapour permeable walls made with hygroscopic bio-based materials due to environmental factors such as: rainfall causing direct wetting, absorption of moisture from the ground rising in the walls, pressure differential leading to diffusion of water vapour across the wall and flooding (Lawrence, Heath, & Walker, 2009; Straube & Schumacher, 2003).

- Decay and degradation: Excess moisture levels can affect the long-term durability of the walls made with bio-based wall materials as it can promote microbial activity and fungal growth. The degradation of the material is accelerated under certain environmental conditions that are favourable for the micro-organisms such as nutrient availability, oxygen concentration temperature, moisture and duration of exposure (Hoang, Kinney, Corsi, & Szaniszlo, 2010; Nielsen, Holm, Uttrup, & Nielsen, 2004).

Further details on effect of pore structure and chemical composition of hemp shiv on hydrophilicity are given in Chapter 2. The sensitivity of bio-based materials to moisture uptake can be reduced by pre-treatment of the material. Several studies have been reported on the use of coupling agents and surface treatments on natural fibres to improve mechanical and thermal properties of the fibre reinforced

polymeric composites (M. Abdelmouleh, Boufi, Belgacem, & Dufresne, 2007; Mekki Abdelmouleh, Boufi, Salah, Belgacem, & Gandini, 2002; Bledzki, Mamun, Lucka-Gabor, & Gutowski, 2008; Kabir et al., 2012; Mwaikambo & Ansell, 2002). Chemical pre-treatment of natural plant fibres have been reported to produce better bonding with a polymer matrix interface due to an improvement in their hydrophobic characteristics (Belgacem & Gandini, 2005; Valadez-Gonzalez, Cervantes-Uc, Olayo, & Herrera-Franco, 1999).

There is a need to develop a novel treatment method for the hemp shiv in order to enhance its water resistance thereby improving the shiv-binder interfacial adhesion, reducing susceptibility to decay and decreasing drying times at manufacturing stage. This will allow for the production of a more resilient bio-based material which is resistant to water but which still allows water vapour to permeate thereby retaining the hygroscopic characteristics of the hemp shiv. This will be the focus of this PhD work.

The sol-gel technique is a highly versatile method to deposit silica based coatings possessing single or multi functionality (C. Brinker & Scherer, 1990). These thin mesoporous coatings have high structural homogeneity and their adhesion can be tailored to different substrates. Sol-gel based hydrophobic and water repellent coatings have been investigated on different plant based materials such as wood and cellulosic fibres detailed in Chapter 2. Sol-gel treatment is also known to significantly reduce the flammability of wood and the fire resistance properties can be further enhanced by phosphorus or boron based additives (Mai & Militz, 2004).

The work done during this PhD is supported by the ISOBIO project funded by the European Union Horizon 2020 programme under grant agreement no. 636835. The ISOBIO project relates to the ‘Materials for Building Envelopes’ work programme topic of the Horizon2020 call for Energy Efficient Buildings. The objective of the ISOBIO project is to bring new bio-based insulation panels and renders into the mainstream for the purpose of creating more energy efficient buildings. The project aims to develop a novel combination of existing low energy, low embodied carbon materials, producing durable composite construction

materials. One key technology that is targeted to be developed in the ISOBIO project is the pre-treatment of bio-based aggregates to render them more resistant to bio-degradation through hydrophobic treatment with sol-gels, whilst maintaining their valuable hygrothermal qualities.

1.4 Aims and objectives

This thesis aims to develop robust hydrophobic composites coupling bio-based materials and sol-gel technology. A hydrophobic sol-gel coating is proposed to provide water resistance and enhance hygrothermal properties of hemp derived materials. This is the first time that sol-gel technology is used to engineer the surface of hemp shiv.

The objectives of this thesis are listed below:

- Investigation of the porosity and pore structure of hemp shiv;
- Formulation and development of water repellent coatings using the sol-gel process;
- Investigation of different sol-gel precursors to optimise the hydrophobicity of the coating formulation;
- Investigation of any change in physical and chemical properties of hemp shiv after application of selected sol-gel coating formulations;
- Development of novel thermal insulation composites using sol-gel coated hemp shiv;
- Characterisation of these novel thermal insulation composites for their thermal, hygroscopic, physical and mechanical properties.

1.5 Thesis layout

The contents of this PhD thesis is divided into 9 chapters and illustrated in Figure 1.4.

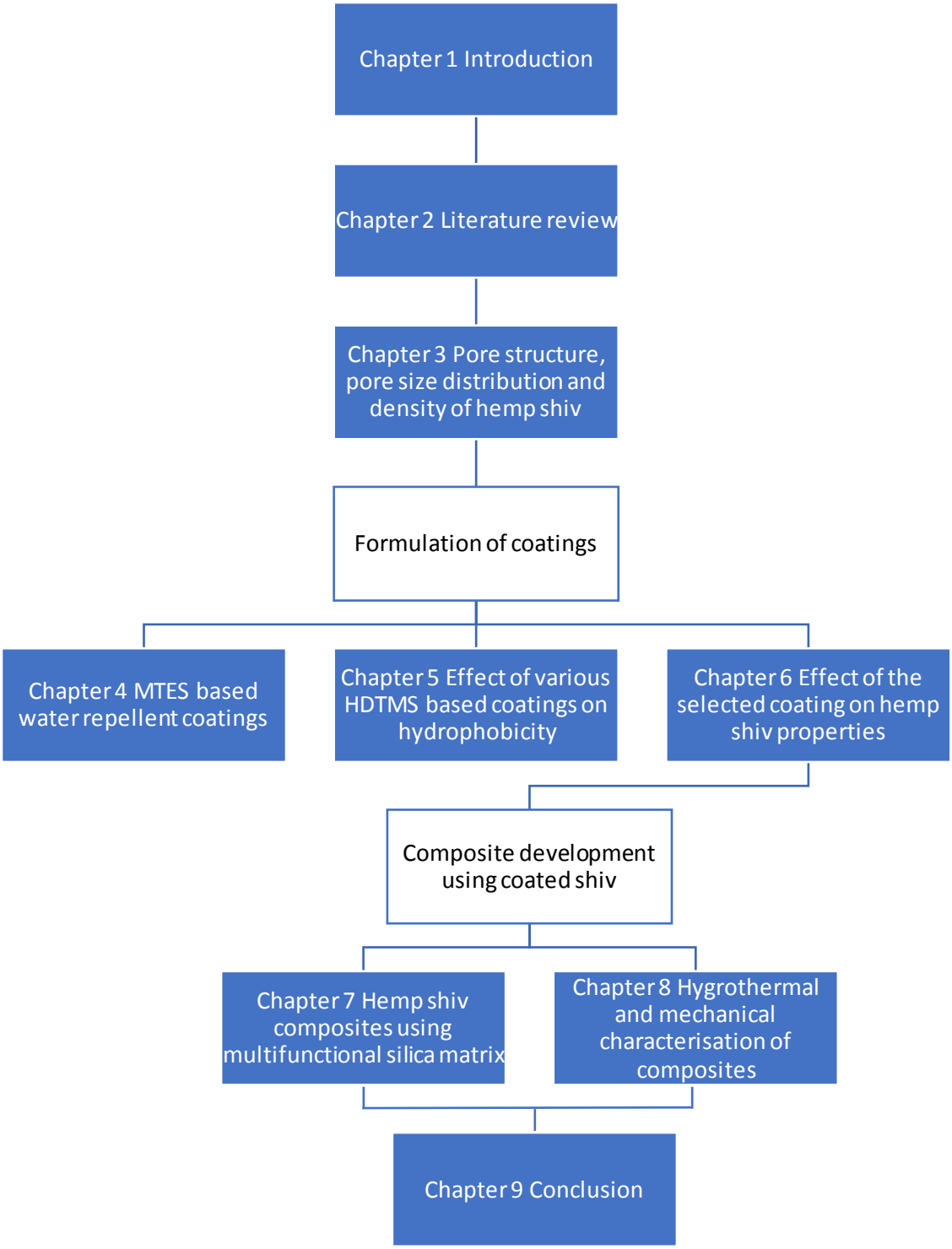

Figure 1.4. Layout of the PhD thesis.

Chapter 1 provides an overview on the impact of thermal insulation in building industry, use of current insulation materials in the industry, identification of research gaps and the objectives of this PhD thesis to overcome these issues.

Chapter 2 gives a detailed insight to what is already known in the field of bio-based thermal insulation and current hemp insulation materials, reviews existing approaches on treatment of plant-based materials and the current application of sol-gel technology on cellulose-based materials.

Chapter 3 studies the pore structure, pore size distribution and density of hemp shiv. The results from various experimental techniques have been analysed for determining the porosity of hemp shiv. **The content of this chapter is from a paper that has been published in the journal: Royal Society Open Science.**

Chapter 4 studies the development and application of a methyltrimethoxysilane (MTES) based coating on hemp shiv. The alteration of chemical and physical properties of the coated hemp shiv have been investigated in this chapter. **The content of this chapter is from a paper that has been published in Journal of Sol-Gel Science and Technology.**

Chapter 5 studies the formulation of new coatings using hexadecyltrimethoxysilane (HDTMS) and different catalysts to obtain a hydrophobic surface on hemp shiv. The impact of these coatings on the surface roughness and morphology of hemp shiv have been evaluated. **The content of this chapter is from a paper that has been published in the journal: Applied Surface Science.**

Chapter 6 studies the impact of the selected coating formulation on the moisture buffering performance of hemp shiv. The changes in chemical and physical properties of coated hemp shiv have been studied. **The content of this chapter is from a paper that has been submitted to the journal: Construction and Building Materials.**

Chapter 7 includes the development of composites from hemp shiv in a multifunctional silica matrix. The science behind the composite manufacturing process has been investigated and the durability of these composites have been evaluated. **The content of this chapter is from a paper that has been published in the journal: Composites Part B: Engineering.**

Chapter 8 discusses the development of composites using sol-gel coated hemp shiv and a starch based binder. The composites have been characterised for their thermal, hygroscopic and mechanical properties and their performance has been compared hemp shiv composites from Chapter 7. **The content of this chapter is from a paper that has been submitted to the journal: Construction and Building Materials.**

Chapter 9 restates the research importance of this thesis, highlighting the main work, draws the conclusions and suggests future work.

1.5 Dissemination

The research work from this PhD thesis has been disseminated in 10 journal articles, a book chapter and 6 conferences.

Publications in international and peer reviewed journals

- Hussain, A., Calabria-Holley, J., Schorr, D., Jiang, Y., Lawrence, M., & Blanchet, P. (2018). Hydrophobicity of hemp shiv treated with sol-gel coatings. *Applied Surface Science*, 434, 850–860. https://doi.org/10.1016/j.apsusc.2017.10.210

- Hussain, A., Calabria-Holley, J., Jiang, Y., & Lawrence, M. (2018). Modification of hemp shiv properties using water-repellent sol–gel coatings. *Journal of Sol-Gel Science and Technology*, 86(1), 187–197. https://doi.org/10.1007/s10971-018-4621-2

- Hussain, A., Calabria-Holley, J., Lawrence, M., Ansell, M. P., Jiang, Y., Schorr, D., & Blanchet, P. (2018). Development of novel building composites based on hemp and multi-functional silica matrix. *Composites Part B: Engineering*, *156*, 266–273. http://doi.org/10.1016/J.COMPOSITESB.2018.08.093

- Jiang, Y., Ansell, M.P., Lawrence, M., & Hussain, A. (2018). Cell wall microstructure, pore size distribution and absolute density of hemp shiv. *Royal Society Open Science*, 5, 171945. https://doi.org/10.1098/rsos.171945

- Jiang, Y., Bourebrab, M. A., Sid, N., Taylor, A., Collet, F., Pretot, S., Hussain, A., Ansell, M.P., Lawrence, M. (2018). Improvement of Water Resistance of Hemp Woody Substrates through Deposition of Functionalized Silica Hydrophobic Coating, While Retaining Excellent Moisture Buffering Properties. *ACS Sustainable Chemistry & Engineering*, *6*(8), 10151–10161. https://doi.org/10.1021/acssuschemeng.8b01475

- Viel, M., Collet, F., Lecieux, Y., François, M., Colson, V., Lanos, C., Hussain, A., & Lawrence, M. (2018). Resistance to mold development assessment of bio-based building materials, *Composites Part B: Engineering*, *158*, 406–418. https://doi.org/10.1016/j.compositesb.2018.09.063

Book chapter

- Ansell, M.P., Lawrence, M., Jiang, Y., Shea, A., Hussain, A., Calabria-Holley, J., Walker, P. (2018). 10 - Natural plant-based aggregates and bio-composite panels with low thermal conductivity and high hygrothermal efficiency for applications in construction. *In Nonconventional and Vernacular Construction Materials (2nd Ed.),* K. A. Harries & B. Sharma (Eds.). Woodhead Publishing. (Accepted)

Articles under review

- Hussain, A., Calabria-Holley, J., Lawrence, M., & Jiang, Y., Preparation of hydrophobic surface on hemp shiv while retaining its moisture buffering ability, *Construction and Building Materials*. (Under review)

- Hussain, A., Calabria-Holley, J., Lawrence, M., & Jiang, Y., Hygrothermal and Mechanical Characterisation of Novel Hemp Shiv Based Thermal Insulation Composites, *Construction and Building Materials*. (Under review)

- Jiang, Y., Ansell, M.P., Lawrence, M., & Hussain, A., Comparison studies of the moisture and heat sorption characteristics of fibre and shiv (hemp and flax) as building insulation materials, *Cellulose*. (Under review)

- Heidari, M.D., Hussain, A., Jiang, Y., Calabria-Holley, J., Blanchet, P., Lawrence, M., & Amor, B., Regionalized life cycle assessment of bio-based materials in construction, case study: hemp shiv treated with sol-gel coatings, *Building and Environment* (In preparation).

International Conferences

- Hussain, A., Schorr, D., Blanchet, P. Calabria-Holley, J., & Lawrence, M., (2017) "Hydrophobic Sol-Gel Coatings on Bio-Based Materials – Influence of Catalyst and Solvent Concentration" in 2nd International Conference on Bio-based Building Materials & 1st Conference on ECOlogical valorisation of GRAnular and FIbrous materials ECOGRAFI, in Clermont-Ferrand France, June 21-23.

- Hussain, A., Calabria-Holley, J., Jiang, Y., & Lawrence, M., (2017) "Induced binding effect of cellulose-based building materials via sol-gel technology" in 19th International Sol-gel Conference, in Leige – Belgium, September 3-8.

- Hussain, A., Calabria-Holley, J., Jiang, Y., & Lawrence, M., (2018) "Functionalised silica based surface coating for Enhancing the Hygroscopic Properties of Bio-based Building Insulation Materials" in SurfCoat Korea 2018 Conference, in Incheon – South Korea, March 28-30.

- Jiang, Y., Ansell, M.P., Jia, X., Hussain, A. & Lawrence, M., (2017) "Physical Characterisation of Hemp Shiv: Cell wall structure and Porosity" in 2nd International Conference on Bio-based Building Materials & 1st Conference on ECOlogical valorisation of GRAnular and FIbrous materials ECOGRAFI, in Clermont-Ferrand France, June 21-23.

- Viel, M., Collet, F., Lecieux, Y., François, M., Colson, V., Lanos, C., Hussain, A., & Lawrence, M., (2018) "Évaluation de la durabilité de matériaux de construction biosourcés" in RUGC 2018 36èmes Rencontres de l'AUGC, ENISE/LTDS, Saint Etienne, France, 19-22 June.

- Viel, M., Collet, F., Lecieux, Y., François, M., Colson, V., Lanos, C., Hussain, A., & Lawrence, M., (2018) "Développement d'une méthode d'évaluation de la durabilité: application à des composites biosourcés" in EcoMat2018, in Saint-Nazaire, France, 10-12 October.

Chapter 2

Literature review

This Chapter provides a detailed insight on hemp and reviews the physical, chemical and hygrothermal characteristics of hemp based materials. The application of existing hydrophobic treatments and sol-gel technology on plant based materials have been discussed.

2.1 Introduction

Bio-based materials come from by-products of various plants that are cultivated for their seeds such as wheat, sunflower and rape. It is beneficial to develop co-production of these materials with food and crop industry as cultivating these plants solely for use in the construction industry would be of lesser advantage from an economical as well as environmental perspective. Bio-based materials also come from parts of parts of fibrous plants such as hemp and flax. The fibres can be extracted and the woody core is chopped into smaller pieces called shiv. Such fibrous plants can be beneficial to the agricultural sector by being part of the crop rotation system.

Bio-based materials have the ability to capture CO_2 from the atmosphere during their lifetime. As they grow they use atmospheric CO_2 through photosynthesis producing O_2. When plant based materials are used to produce building materials, the sequestered CO_2 is locked up within the building. This concept results in the production of extremely low embodied energy materials. Embodied energy is the cost of energy involved in construction of a building or development of a material. Construction materials like concrete, fired bricks, cement etc. need a lot of energy during their manufacture and transportation which is mainly derived from burning fossil fuels. This leads to an increase in the CO_2 emissions in the atmosphere contributing to global warming.

The embodied energy of a building could be reduced by using recycled or renewable materials in the building fabric rather than synthetic materials. Bio-based materials are completely renewable as they harvested and regenerated within years. The main source of energy required for the growth of plant-based material through photosynthesis is solar energy. Therefore construction materials made from plant sources need lesser energy and if grown locally, they can even save on transportation costs and energy. A house constructed using hemp-lime for its 80m^2 external walls would sequester 10.8 tonnes of CO_2e in embodied energy (Lawrence, Shea, Walker, & De Wilde, 2013).

This chapter provides a review of literature on hemp shiv as a bio-based insulation thermal insulation material studying its physical properties and chemical composition. Since this is the first time that sol-gel coatings will be used on hemp shiv in this thesis, this chapter provides an overview on the use of sol-gel technology on other cellulose based materials as well as the existing treatment methods on bio-based materials to enhance their hydrophobicity.

2.2 Hemp

Insulation material made from hemp (*Cannabis Sativa* L.) is gaining interest in the construction industry although currently they have a small share in the European thermal insulation market. From the IAL Consultants data, Europe had a thermal insulation market of approximately 9.6 billion euro in 2012 (Lekavicius, Shipkovs, Ivanovs, & Rucins, 2015). In Europe, hemp straw is currently utilised in the form of fibres, shiv, and hemp dust. The major uses of hemp and their breakdown based on industry are listed in Table 2.1. From the research point of view, amongst bioaggregates, hemp shiv is the most studied in literature and is widely used in the construction and building industry.

Table 2.1 Utilisation of hemp in Europe (Carus, 2013).

HEMP INDUSTRIAL USES		
Fibre (31.7%)	**Shiv (54.1%)**	**Dust (14.2%)**
Biocomposites (4.5%) Paper and Pulp (17.3%) Insulation (8.2%) Textile (1.6%)	Bedding material (33.6%) Construction (8.3%)	Fuel - Pelletizing for incineration (2.8 %)

2.2.1 Origin and processing

Industrial hemp is produced in over 30 countries worldwide including France, UK, Canada, Australia, Germany, Netherlands and Austria. Although most of Europe have favourable climatic conditions for growing hemp, only a few countries grow considerable amounts of hemp. The countries the produce hemp in Europe are shown in Figure 2.1. The largest cultivator of hemp in Europe is France growing around 16,000 ha in 2017 (Association, 2018).

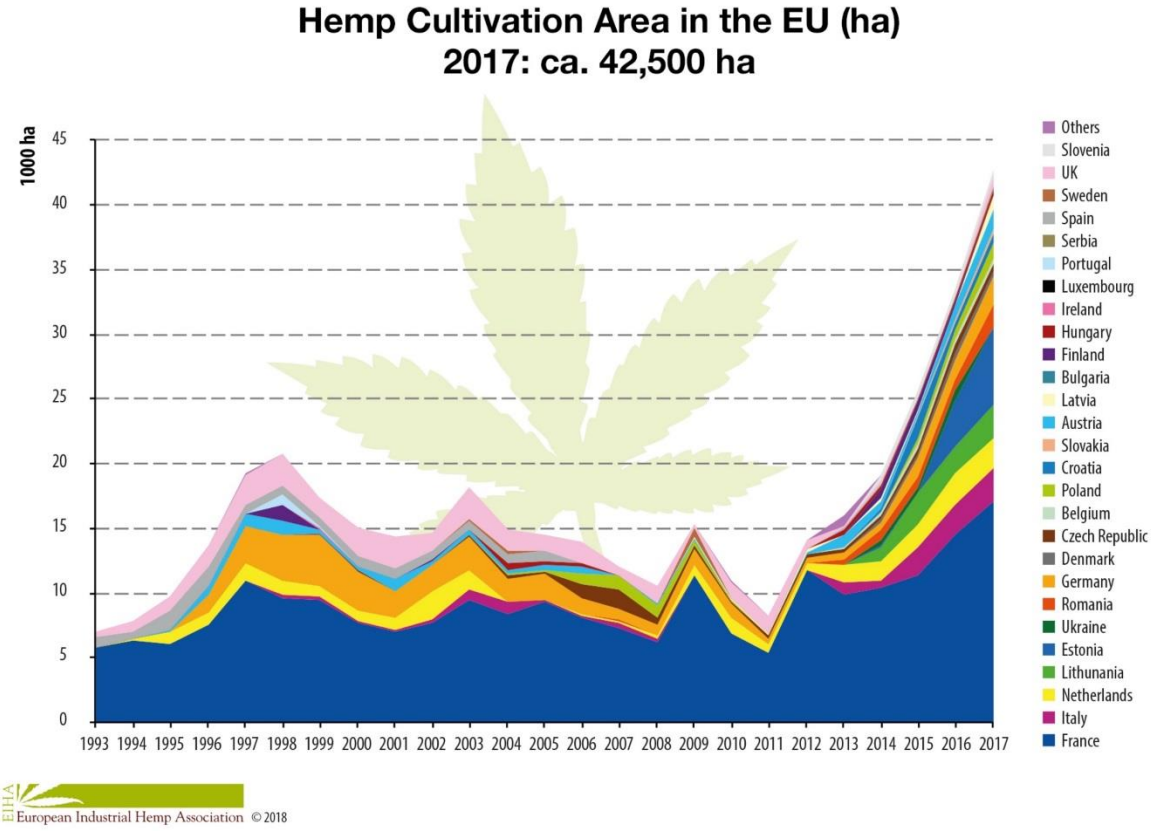

Figure 2.1 Hemp cultivation in Europe 1993-2017 (Association, 2018; Carus, 2017).

The vegetal nature of hemp is responsible for its intrinsic variability in the physical characteristics and chemical composition. The variability factors that influence the characteristics and quality of the plant raw material include:

- Selection of seed variety
- Sowing date
- Weather conditions

- Soil
- Topological conditions
- Plant maturity during harvesting
- Harvesting and processing procedure

Hemp is easy to grow without the need of herbicides and fertilizers. Following harvest, the hemp stem undergoes retting and mechanical defibration. The process conditions employed for the breakdown of the hemp stem into shiv can influence the aggregate size, residual fibre content, fibre length, composition and content of fibres and dust and presence of other organic and inorganic contaminants (Hirst, 2013).

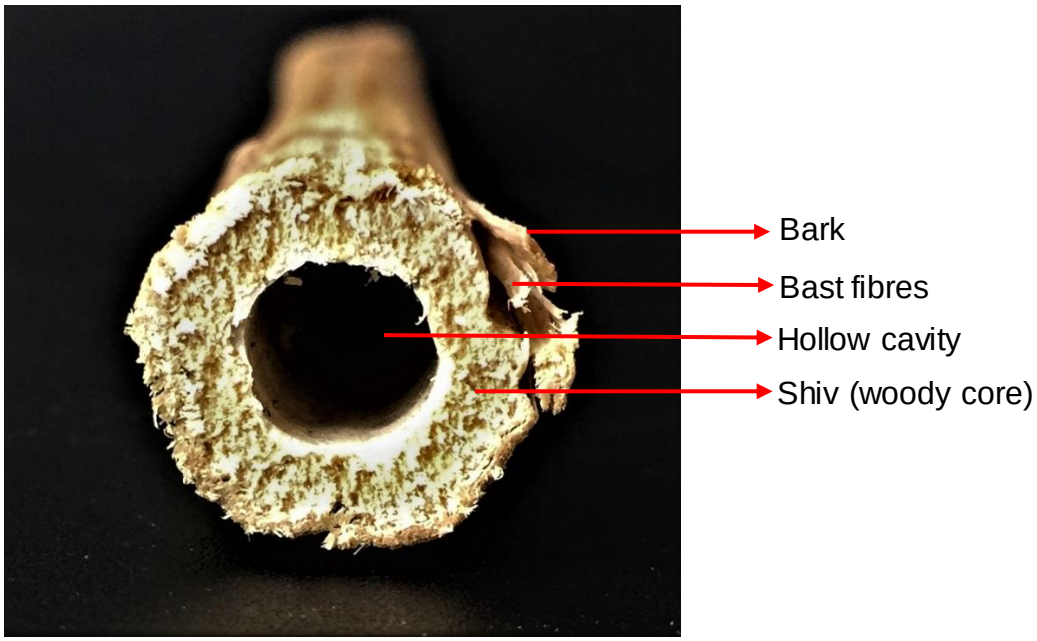

Figure 2.2 Photograph of a cross section of dried hemp stem.

The technical hemp has two major products of industrial importance: bast fibres used mainly in textile, paper and insulation industry, and shiv (also known as hurds) used in the building industry for manufacture of lightweight composites. The hemp stem contains approximately 20-40 wt% of bast fibres and 60-80 wt% of shiv (Thygesen, Daniel, Lilholt, & Thomsen, 2005). Figure 2.2 shows the cross section of a dried hemp stem. The bast fibres are known to have high quality whereas the shiv is the least valuable part of the hemp shiv being chemically similar to wood (Lekavicius et al., 2015).

2.2.2 Hemp based composites

Many studies have been conducted over the recent years to optimise the hemp characteristics, curing conditions and binder content during the production of hemp based concrete. Towards the end of the 20th century, a bio-based building material was rediscovered which used the woody core or shiv of hemp and lime based binders to produce hemp concrete.

Hemp shiv has very low conductivity compared to lime due to its porous structure. Due to the presence of hemp shiv, this material is lightweight, breathable and has insulating properties. Hemp concrete has be shown to have better thermal performance compared to conventional concrete (Benfratello et al., 2013). Hempcrete can be sprayed or cast and can be used for insulating floors, roofs or as plasters. Hemp based bricks are also produced in a similar manner to hemp based concrete. Other uses of hemp shiv in lightweight constructions are production of biodegradable boards for mobile homes and package material.

The hemp insulation products currently available in the market are listed in Table 2.2. It can be seen that most of the currently available hemp related industrial insulations are composed of hemp fibres and natural, recycled or synthetic binders with additional chemicals added for increasing fire resistance or to avoid mould growth. Based on the quantitative relationship between hemp shiv and fibre, increasing the production and supply of fibre to the industry results in higher production of shiv automatically. As seen from Table 2.1, there is a huge potential for increasing the utilisation of hemp shiv in the industry for production of sustainable construction materials.

Table 2.2 Hemp based thermal insulation products in industry (Lekavicius et al., 2015).

Thermal Insulator Brand	**Composition**	**Thermal Conductivity [W/m.K]**	**Density [kg/m^3]**	**Reference**
NatuHemp	Hemp fibre (95%), recycled adhesive binder (5%)	0.039	30	(Black Mountain Insulation)
Nature PRO	Hemp fibre	0.04	28	(NaturePRO)
Thermo-Hemp	Hemp fibre (82-85%), bi-component fibre (10-15%), $NaHCO_3$ (3-5%)	0.038	30-42	(Thermo-Hemp)
Thermafleece Natra Hemp	Hemp (60%), recycled polyester (30%), polyester resin (10%)	0.04	-	(Thermafleece)
Hemptechnol-ogy Breathe	Hemp (47.5%), flax (47.5%), polyester (5%)	0.039	-	(Hemptechnology)
Isonat végétal	Hemp fibres (42.5%), recycled cotton (42.5%) and polyester (15%)	0.039-0.041	35	(Végétal)
Fibranatur Isolant Ouate de Chanvre	Hemp fibres (85%), polyester binder	0.042	30	(Fibranatur)
Biofib' Hemp	Hemp fibres(90%), polyester binder	0.04	30-40	(Biofib')
Lenofon - Hemp Fibre Panel	Hemp fibre, small amount of bi-component fibres and soda	0.041	38	(Lenofon)
Technilaine	Hemp fibres (85%), synthetic binder (15%)	0.04-0.048	25-30	(Technichanvre)
STEICO Canaflex	Hemp fibres, ammonium phosphate, polyolefin fibres	0.043	40	(STEICO)

2.2.3 Structure of stem

Figure 2.3 Photograph of a dried stalk of hemp stem.

Figure 2.4 Cross section of hemp stems (Manitoba Agriculture Canada, 2018)

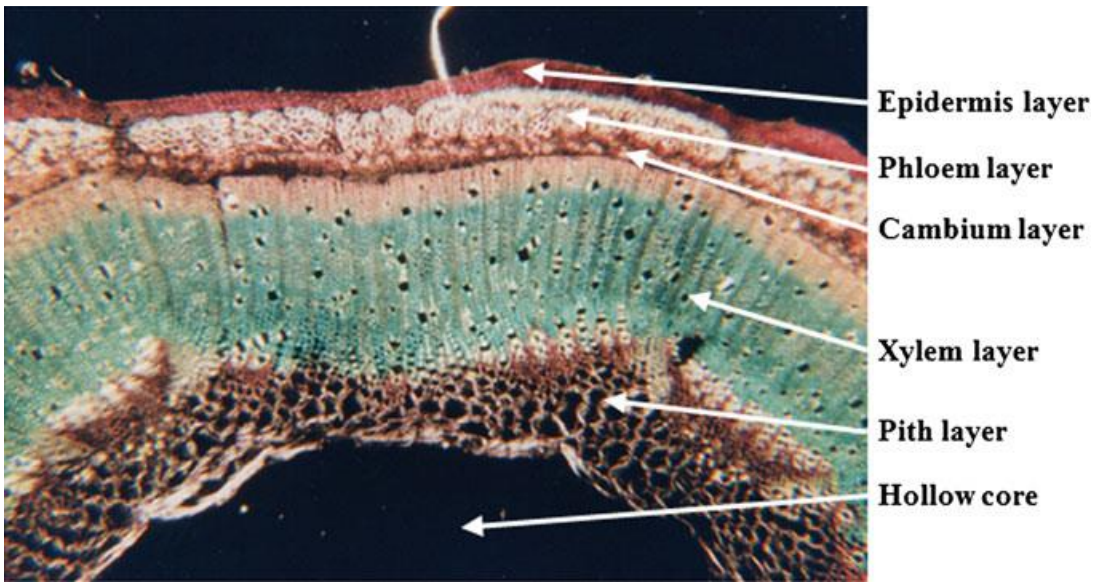

Figure 2.5 Micrograph showing hemp stem cross section at 90x magnification (Vignon & Dupeyre, 1995).

The dried stalk of hemp with unwrapped fibres and the woody core at the centre is shown in Figure 2.3. The cross section of hemp stem at harvest is shown in Figure 2.4.

The complex structure of the hemp stem cross section under an optical microscope after staining can be seen in Figure 2.5. The pink colour represents tissues rich in cellulose and green colour represents cells rich in lignin.

The different layers of the hemp stem are (Amziane & Collet, 2017; British Columbia, 1999):

- Hollow cavity or core at the centre of the stem
- Pith layer also known as the medulla layer. This layer contains parenchyma cells that are soft and spongy with intercellular spaces.
- A thick xylem layer that composes of woody tissues. Their main function is to support the plant and vessels through transportation of water and minerals. This layer of the hemp stem forms the shiv.

- Cambium layer which is the growth region producing secondary xylem on the inside and secondary phloem on the outside. This layer forms the area of separation between the bast fibres and shiv during the process of defibration.

- Phloem layer, composing mainly the bast fibres, and involved in the transportation of sugars and nutrients. The bast fibres are divided into two types: (i) primary bast fibres that are long fibres (5-55mm in length) and have low lignin content and; (ii) secondary bast fibres which are shorter (2mm in length) and contain high content of lignin.

- Epidermis is the outermost layer of the stem that protects the plant.

2.2.4 Chemical Composition

Hemp shiv are mainly composed of xylem tissues which are generally dead and empty. These longitudinal tubes are accountable for the porous structure of hemp shiv. The complex structure of xylem cell walls contain: (i) middle lamella connecting the neighbouring xylem cells and mainly composed of pectin; (ii) primary wall composed of cellulose and hemicellulose and; (iii) secondary cell wall composed of cellulose, hemicellulose and lignin (Dinwoodie, 1989).

Cellulose, hemicellulose and lignin are the three main structural components of a cell wall. Other organic and inorganic components like pectin, wax, ash, fats and water-soluble substances are also present in minor percentages.

The combination of cellulose and hemicellulose is also known as holocellulose and it forms the major component of bio-based aggregates. Holocellulose is rich in hydroxyl groups that are responsible for the absorption of water molecules through hydrogen bonding (Rowell, 2012).

The chemical composition of hemp shiv from previous studies is reported in Table 2.3. The chemical composition of the shiv can be influenced by various factors as listed in Section 2.2.1. Moreover, depending on the analytical method for assessing the biomass composition, some difference in results can be seen.

Table 2.3 Chemical composition of hemp shiv.

Study	Cellulose	Hemi-cellulose	Lignin	Pectin	Waxes	Ash
(Balčiunas, Vejelis, Vaitkus, & Kairyte, 2013)	36-41	31-37	19-21			
(Gandolfi, Ottolina, Riva, Fantoni, & Patel, 2013)	44	25	23	0.6	1.8	1.2
(Diquélou, Gourlay, Arnaud, & Kurek, 2015)	47.3	18.3	21.8			3.7
(Diquélou et al., 2015)	45.6	17.8	23.3			2.6
(Diquélou et al., 2015)	49.2	21	21.9			3.5
(Hustache & Arnaud, 2008)	48	12	28			2
(Sedan, Pagnoux, Smith, & Chotard, 2008)	48	12	28			
(Thomsen, Rasmussen, Bohn, Nielsen, & Thygesen, 2005)	48	21-25	17-19			
(de Groot, 1998)	37.7	26.8	22.1			
(Van der Werf, 1994)	34.5	17.8	20.8			
(Vignon & Dupeyre, 1995)	44	18	28	4	1	2
(Bedetti & Ciareli, 1976)	38	31	18			

2.3 Porosity, pore structure and density

Bio-based aggregates have a complex microstructure and high porosity which are responsible for their physical properties. Usually these aggregates have low density which results in low thermal conductivity values. However most bio-based aggregates are not used as structural or load bearing materials due to their low strength which is a result of their density. They are usually suitable as fillers in composites to lower the thermal conductivity of the reinforced composites. The porous structure of bio-based aggregates allows them to absorb and release moisture with varying humidity conditions making them excellent moisture buffering materials.

Porosity in a material represents the fraction of voids in that material. These voids can be: either interconnected leading to the exterior surface and can be called "open voids"; or they can be inaccessible and called as "closed voids". The total porosity (Φ) is defined as the ratio of void volume (V_V) to the bulk or total volume of the sample (V_T).

$$\emptyset = \frac{V_V}{V_T} \qquad \text{Eq (2.1)}$$

The porosity of a material can also be expressed in terms of bulk volume percentage. In hemp shiv, the pores arise during the growth of xylem cells in the living plant having the function to support the plant tissues through nutrient and water transportation from the roots. The high porosity, low density and complex pore structure is responsible for the properties of bio-based aggregates such as thermal conductivity, hygroscopicity and water absorption behaviour.

Anovitz and Cole (2015) summarised ten different methods to determine the porosity and pore size distribution on core or crushed rock materials. The various techniques that could be used to determine sample porosity are shown in Figure 2.6. It should be noted that these techniques have different measurement capabilities as they are based on different principles. Bio-based aggregates have

an enormous range in scale for their pore sizes and therefore a single technique cannot determine the total porosity of the aggregate. A combination of techniques and comparison of porosity results may give an insight into the complex pore structure of bio-based aggregates.

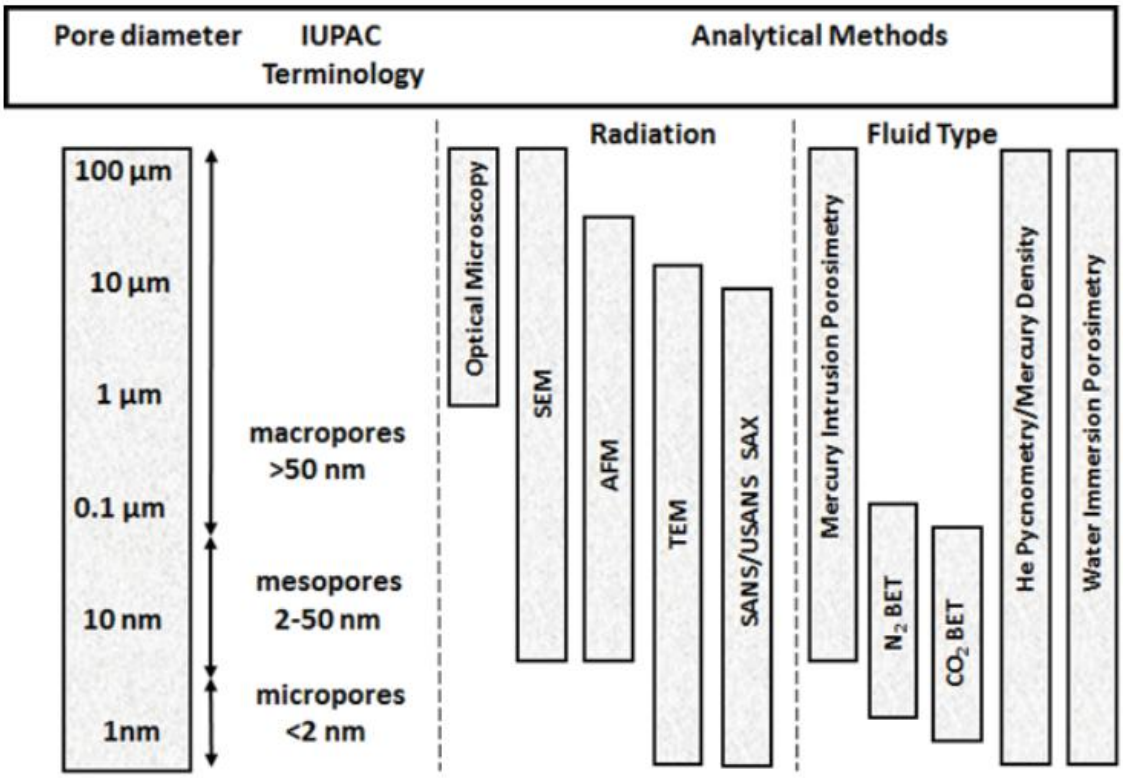

Figure 2.6 Determination of porosity using various methods and their scale range (Anovitz & Cole, 2015).

The porosity of hemp shiv has not been fully characterised so far as it is a complicated process. The presence of inaccessible pores can influence the results. Moreover, the quantification of porosity is a difficult in hemp shiv as the voids can range from a few nanometres to several micrometres. There is no single method that can determine the porosity of this vast scale range. Other factors that can affect the porosity measurements depending on the testing method could be sample deformation, hydrothermal variation and presence of bottle ink pores with narrow pore openings. Figure 2.7 shows the pore structure of a hemp shiv sample.

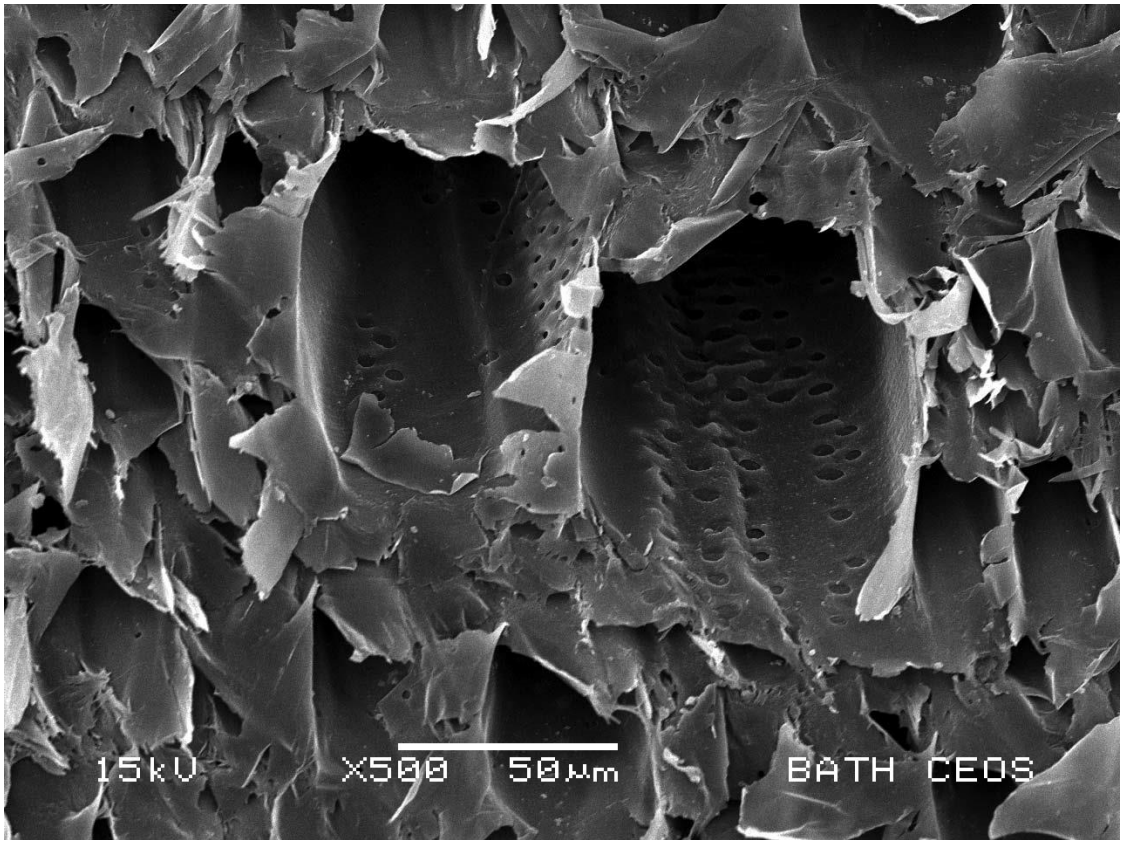

Figure 2.7 Cross section of hemp shiv showing its pore structure (Lawrence et al., 2013)

The microstructure has been investigated recently in several studies. Magniont *et al.* (2012) studied a cross section of hemp shiv that was embedded in resin and polished using scanning electron microscopy. It was observed that hemp shiv was mainly comprised of conducting vessels with diameter ranging between 10 and 20 µm. Furthermore, in the longitudinal section, few vessels with larger diameter were also observed.

Lawrence *et al.* (2013) reported that the microstructure of hemp shiv exhibited pores with diameter of 50 µm and these pores were connected to smaller pores having a diameter of 10 µm through 1 µm connecting pores. Dubois, Evrard and Lebeau (2014) studied a section of hemp shiv using X-ray microtomography. The total porosity of the aggregate was observed to be high and a typical tubular structure of mesoscopic pores was reported.

Another method that can characterise pores in the range of 1-100 nm is the BET analysis that involves nitrogen adsorption. The limitation of using this method is that they do not provide any insight on the pores larger macropores, which have been seen under the electron microscope in hemp shiv samples. Other studies reporting porosity of hemp shiv have used displacement liquids which could be polar or non-polar liquids. Nguyen, Picandet, Amziane & Baley (2009) used the pycnometer with toluene as the displacement fluid and found out that hemp shiv aggregates had an inter-porosity of 60% while fibrous hemp shiv possessed an inter-porosity of 76.6%. Manger (1963) mentioned that majority of the total porosity measurements can vary greatly with bulk volume/grain volume or bulk density/grain density approaches, and the absolute porosity measurements are made by absorption methods by using different liquids or gases.

Mercury intrusion porosimetry (MIP) is another measurement technique for the determination of porosity and pore size distribution. This technique can be used to obtain information on pores having a wide scale range - from a few nanometres to a hundred micrometres in diameter. The limitations of using this technique include the risk of sample crushing at high pressures that is required for analysis. Moreover, this method is unable to differentiate between inter-particle and intra-particle porosity, especially for powdered samples. Furthermore, this technique determines the diameter of the pore throat and does not take into account the actual pore size for ink bottle pores with narrow points of connection. As a result, this technique has the tendency to overestimate smaller pores at the expense of larger pores. Therefore, where ink bottle pores are present, the pore size distribution given by MIP analysis might tend to be shifted towards the smaller pores. However the total porosity given by MIP can be considered to be valid. At the maximum intrusion pressure either all pores would have been intruded with mercury or the pore walls would have been crushed and their equivalent volume intruded eventually (down to the effective limit of MIP of approximately 3.5 nm)(Jiang, Lawrence, Ansell, & Hussain, 2018).

The cell wall density of hemp shiv or any porous material is quite complicated as well. For determining the density of the bioaggregate, it is essential that all pores

need to be accessible for the displacing liquid or gas. This means that all voids in the cell wall should be filled with the displacing liquid or gas to get correct results.

Gas pycnometry is an accurate method for measuring the absolute density of cell walls, which is based on the Archimedes' principle of displacement of an inert gas, such as helium, nitrogen or argon. Although the method of gas pycnometry is relatively simple compared with other methods, there are few publications dealing with investigations of the cell wall density or porosity of bio-based aggregates using this procedure, owing to the complicated sample preparation. Hill et al. (2005) prepared samples of pine using a Soxhlet extraction for 8 h with a solvent system composed of toluene, methanol and acetone (4 : 1 : 1 by volume). Samples were then oven-dried for 12 h at 105 °C and cooled in a desiccator before placing into a helium pycnometer. The cell wall density of the untreated pine sample was 1.42 g cm^{-3}. Zauer, Pfriem, & Wagenführ (2013) studied the cell wall density of wood determined by gas pycnometry. The results clearly showed that misinterpretation of the results is possible due to unfavourable sample preparation in relation to the different wood anatomies.

2.4 Hygric characteristics

Several studies have discussed the ability of bio-based materials used in construction to absorb and release moisture in response to changes in relative humidity in the surroundings which creates a breathable wall. These materials act as a hygric buffer and eventually reduce the energy demands for air conditioning (Tran Le, Maalouf, Mai, Wurtz, & Collet, 2010). Creating a breathable wall and maintaining indoor relative humidity levels between 40 and 60% can have a positive impact on the wellbeing of residents, reducing bacterial growth, allergies and controlling respiratory problems (Maskell, Thomson, Walker, & Lemke, 2018).

The response to varying humidity conditions is linked to their pore structure and pore connectivity where the moisture condenses and evaporates on the surface of the material and within its pores. During this process, the thermal effects of latent heat are also taken into consideration as condensation/evaporation lead to release/absorption of heat respectively. This leads to an increased effective thermal mass, allowing the bio-based material to behave as a thermal buffer in addition to their hygric buffering characteristics (Hills, Norton, & Newman, 2009).

2.4.1 Sorption Isotherm

The equilibrium moisture content of a material with respect to the ambient relative humidity at a specified temperature can be given by the sorption isotherm. The moisture uptake takes place in three stages from dry state to humid state:

(i) Monolayer adsorption, where water molecules get adsorbed on internal walls of pores;

(ii) Polymolecular adsorption, where molecules of water adhere to the monolayer and;

(iii) Capillary condensation, where further water molecules fill the pore forming liquid bridges.

These phenomena can take place either individually or simultaneously depending on the pore structure of the substrate. A hysteresis can be observed between the adsorption and desorption curves. This hysteresis is usually related to the capillary condensation stage, suggesting the presence of ink bottle pores or inter-connected pores (Naono & Hakuman, 1993). Figure 2.8 shows a typical sorption isotherm for hemp lime sample using dynamic vapour sorption (DVS) instrument.

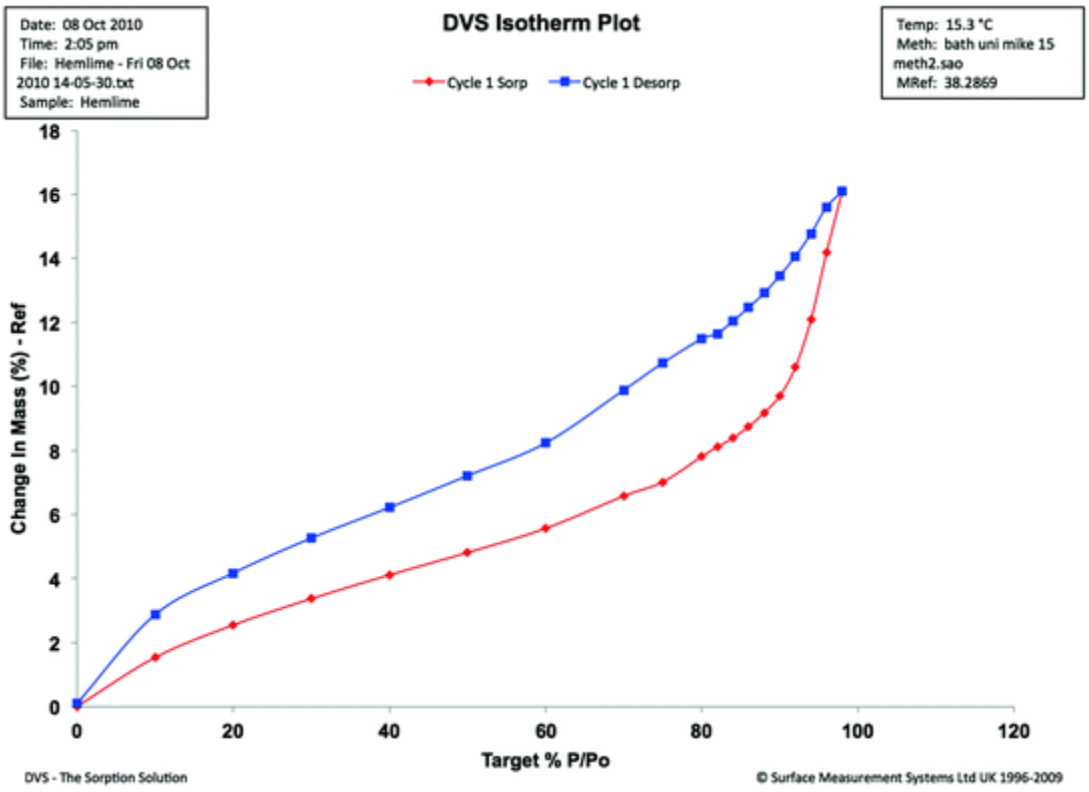

Figure 2.8 Adsorption-desorption isotherm of hemp lime sample (Lawrence & Jiang, 2017)

Bio-based aggregates are highly hygroscopic. Amziane & Arnaud (2013) reported that hemp concrete has a much higher water uptake (approx. 6-8 folds more) when compared to other building materials such as aerated autoclaved concrete and vertical perforated bricks. The porosity of hemp shiv can be affected by addition of binder such as lime thereby affecting its hygroscopic behaviour. It was seen that hemp shiv showed a higher sorption curve when compared to hemp lime, however hemp lime had a larger hysteresis when compared to hemp shiv (Latif, Lawrence, Shea, & Walker, 2015).

2.4.2 Moisture buffering capacity

The moisture buffering ability of a hygroscopic material can be measured by the moisture buffer value (MBV). Hygroscopic materials have the ability to adsorb and release moisture responding to changes in surrounding relative humidity in order to create an equilibrium. Moisture buffering capacity can regulate the fluctuations in humidity in internal spaces. Moreover, the moisture buffering performance of a material also depends on the vapour permeability, exposure area, surface treatments of the material and ventilation rate (Latif et al., 2015).

Several studies have reported the moisture buffering capacity of hemp concretes (Collet, Chamoin, Pretot, & Lanos, 2013; Latif et al., 2015; Tran Le et al., 2010) and they have followed the Nordtest protocol (Rode, 2005). This method measures the practical moisture buffer value of the specimens under dynamic conditions. The MBV value represents the amount of moisture adsorption and desorption, per unit open surface area, under daily cyclic variation of relative humidity according to following equation:

$$MBV = \frac{\Delta m}{A.(RH_{high} - RH_{low})} \qquad \text{Eq (2.2)}$$

where MBV: moisture buffer value (g/(m^2 %RH)), Δm is moisture uptake/release during the period (kg), A is open surface area (m^2), $RH_{high/low}$ is relative humidity level (%) respectively.

Figure 2.9 gives the ranges practical MBV value classes and Figure 2.10 compares the MBV values for usual building materials found in literature. Using the Nordtest protocol, it has been reported that the moisture buffer value of hemp concrete is generally higher than 2 g/(m^2 %RH) which makes it an excellent hygric regulator. On the other hand, the moisture buffering capacity of concrete is poor with less than 0.5 g/(m^2 %RH). For gypsum, the MBV value is nearly 1 g/(m^2 %RH) making it a moderate regulator, whereas for wood fibreboard it is 1.8 g/(m^2 %RH) making it a good hygric regulator.

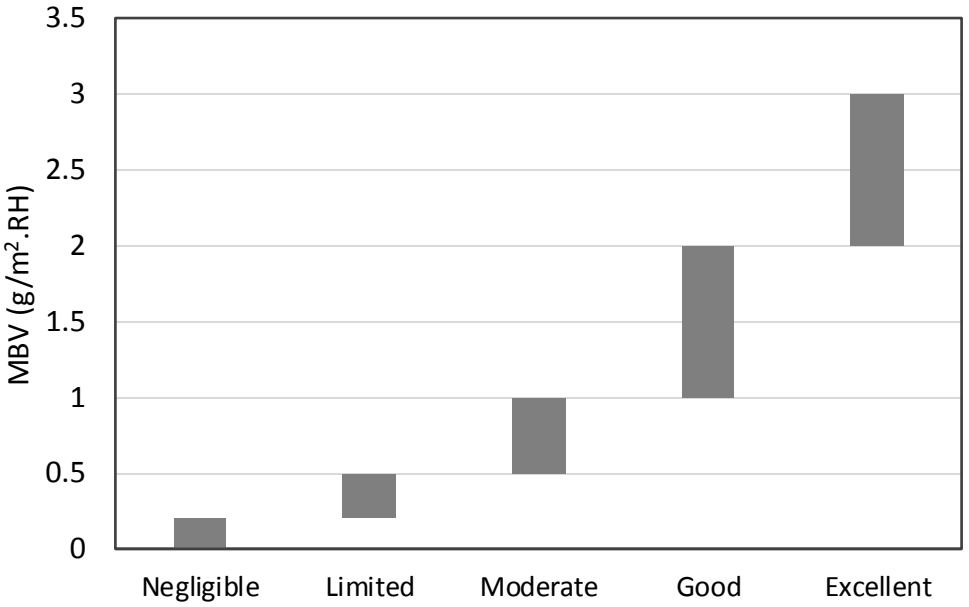

Figure 2.9 Practical moisture buffer value classes (Collet et al., 2013).

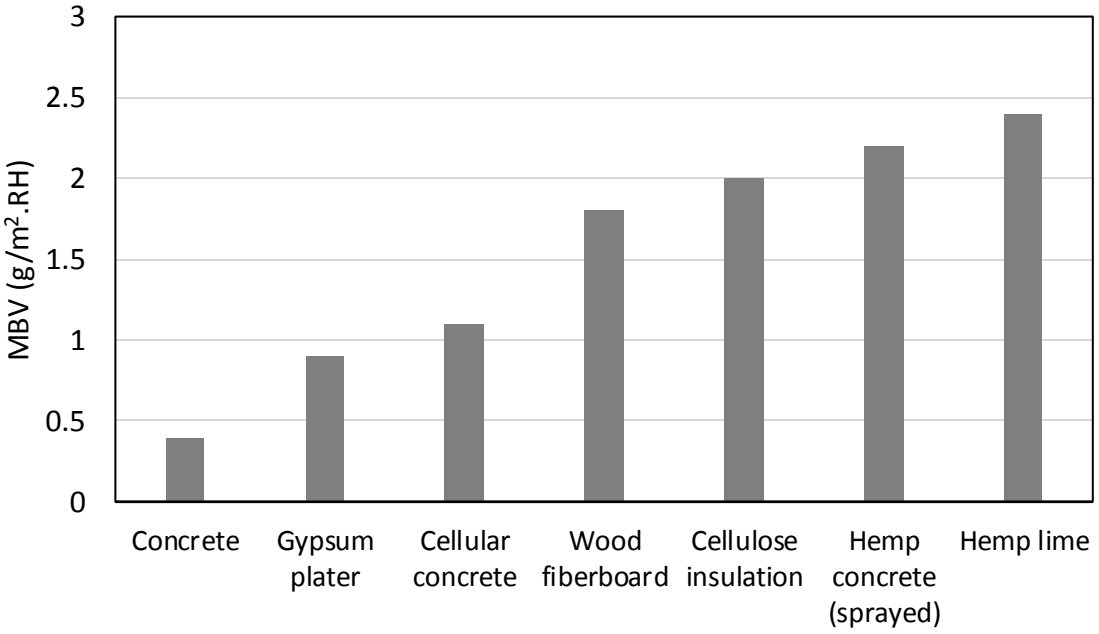

Figure 2.10 Moisture buffer value of general building materials (Collet & Pretot, 2012; Rode, 2005)

2.4.3 Vapour permeability

The ability of a porous material to transfer moisture due to a vapour pressure gradient can be expressed by the vapour permeability of the material. The transfer of moisture during this process can take place due to three factors: diffusion (self-collision of water molecules), effusion (collision of water molecules with the pore walls) and liquid transfer (associated with capillary condensation) (Collet et al., 2013). The water vapour permeability and the diffusion resistance factor of thermal insulation materials can be measured using the British Standard BS EN 12086 (2013) under isothermal conditions (23 °C) and at two sets of relative humidity: dry cup and wet cup.

Considering bio-based insulation material to be a part of a vapour permeable wall, significant benefits can be offered such as indoor air quality and robustness of fabric (Osanyintola & Simonson, 2006). When moisture is allowed to penetrate through the fabric of this wall, due to the vapour permeable and hygroscopic behaviour of the structure, the risk of moisture build-up is considerably reduced (Zhang, Yoshino, & Hasegawa, 2012). Under suitable environmental conditions, bio-based materials are durable and long-lasting.

Since bio-based aggregates have high porosity, they have been reported to have high water vapour permeability or low water vapour resistance factor. For solid concrete, the water vapour diffusion resistance factor is extremely high about 130, while for hemp concrete it ranges between 5-12 (Walker, Pavia, & Mitchell, 2014). The water vapour permeability for hemp concrete has been observed to increase with increase in relative humidity and therefore, it is a dependent on the external relative humidity (Collet et al., 2013). However, it was reported that the water vapour permeability of hemp concrete remained unaffected by the type of binder (Walker & Pavía, 2014).

2.5 Thermal conductivity

Thermal insulation is a material or combination of materials, that, when properly applied, retard the rate of heat flow by conduction, convection, and radiation. It retards heat flow into or out of a building due to its high thermal resistance. Thermal insulators resist flow of heat due to entrapment of air in the pores within the material. These pores prevent the movement of air and suppress convective heat transfer (Al-Homoud, 2005).

Thermal insulators, as part of building materials and some industrial hardware, have been used since quite some time as a means of saving energy. Thermal conductivity and wall thickness are the two main parameters that allows the selection of a proper insulating material. Thermal conductivity is the time rate of steady state heat flow (W) through a unit area of 1m thick homogeneous material in a direction perpendicular to isothermal planes, induced by a unit (1K) temperature difference across the sample. The SI unit of thermal conductivity, k-value, is W/m.K.

Thermal conductivity depends on the mean temperature within the material and its moisture content. It gives the heat conducting capacity of a material. Therefore comparing the thermal conductivity data of different insulators gives good knowledge to estimate the efficiency of the insulating material to resist heat.

Thermal conductivity of a material can be measured either by steady state methods such as heat flow meter and guarded hot plate or transient methods such as hot wire and hot disk. Transient methods like the hot disk allows simultaneous measurement of thermal conductivity, thermal diffusivity, heat capacity and temperature. Moreover, using a dynamic measurement method reduces the measurement time when compared to steady state measurement methods.

Figure 2.11 compares the thermal conductivity values of various bio-based materials and their respective densities (Agoua, Allognon-Houessou, Adjovi, & Togbedji, 2013; Aigbomian & Fan, 2013; Al Rim, Ledhem, Douzane, Dheilly, & Queneudec, 1999; Magniont et al., 2012; Taoukil et al., 2013; Walker & Pavía, 2014).

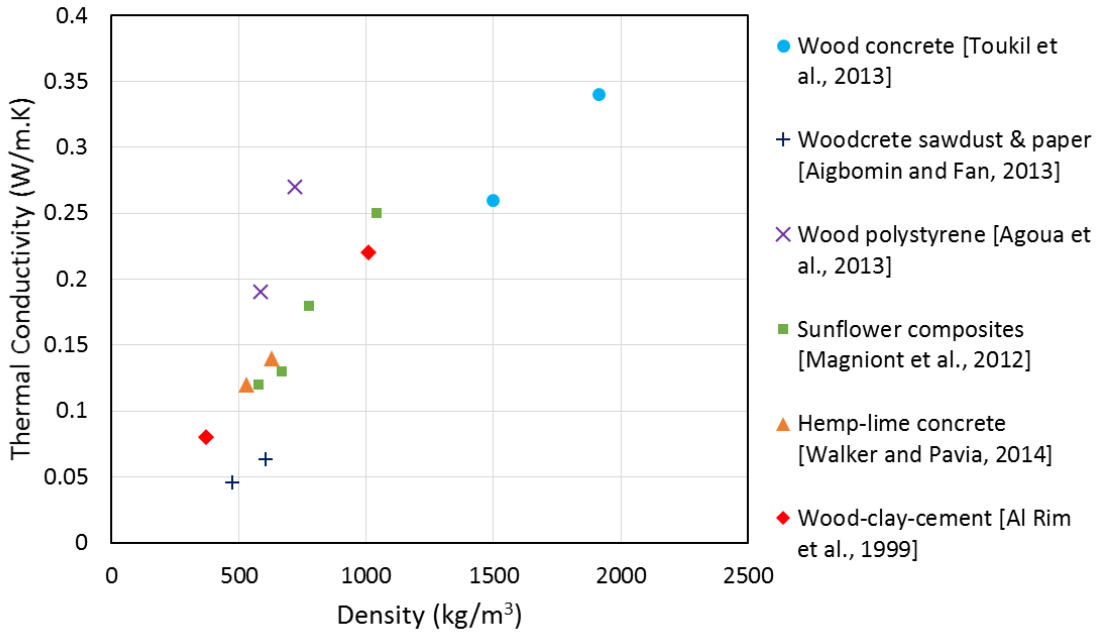

Figure 2.11 Thermal conductivity of bio-based composites vs density (Amziane & Collet, 2017)

In general, bio-based materials are light in weight and have low thermal conductivity making them good insulation materials. However, the thermal conductivity of the bio-based composite is also influenced by other factors such as aggregate, binder, aggregate to binder ratio and water content. The density can be affected by the formulation, binder content and production method thereby influencing the thermal conductivity as well (Collet & Pretot, 2014; Elfordy, Lucas, Tancret, Scudeller, & Goudet, 2008).

.

The thermal conductivity of bio-based composites is highly dependent on the type and proportion of binder used in the formulation. Stefanidou, Assael, Antoniadis, & Matziaroglou (2010) prepared 15 formulations using six binders such as lime, brick dust, white cement and pozzolans. The thermal conductivity for these formulations was found to be in the range of 0.16 – 0.39 W/m.K. White cement showed the highest conductivity and mixture of lime and pozzolan showed the lowest. Moreover, using similar mass proportions, traditional binder such as lime was found to be less conductive when compared to cement. Addition of pozzolanic materials reduced the thermal conductivity of mixtures when compared to pure lime. Furthermore, higher water to binder ratio in the formulation increased binder porosity and reduced the thermal conductivity of the binder.

In another study, it was observed that hemp concretes made with cement binder had lower thermal conductivity of 0.06 W/m.K than hemp concrete composed of lime binder having thermal conductivity of 0.08 W/m.K. It was found out that for the same hemp:binder:water ratio, hemp concretes made with cement binder had lower density than hemp concrete with the lime binder, even though the cement binder had a higher density than the lime binder. It was concluded that microstructural changes caused an increase in porosity and decrease in thermal conductivity due to a physico-chemical interaction between hemp shiv and the binder (Gourlay & Arnaud, 2010).

The characteristics of the bio-aggregate also influences the thermal conductivity of the composite. The species, origin and processing can affect the morphological characteristics of the bio-based aggregate. Stevulova et al. (2014) investigated composites made with hemp from different origins and found out for same ratios of hemp:binder, the thermal conductivities were different. It was observed that the hemp which had higher conductivity showed stronger structure and it was suggested that this species had smaller pores in its microstructure.

The binder to aggregate ratio can have an impact on the thermal conductivity of the final composite. Various studies have showed that as the aggregate content is increased, the thermal conductivity decreases for the composite (Al Rim et al.,

1999; Benfratello et al., 2013; Collet & Pretot, 2014). This is due to the decrease in density of the composite as usually the aggregate has lower density when compared to the binder. Higher aggregate content increases the overall porosity of the composite (Al Rim et al., 1999). However, it has also been reported the increase in aggregate content is not always linearly proportional to the decrease in thermal conductivity of the composites (Benfratello et al., 2013; Collet & Pretot, 2014).

2.6 Water absorption

Bio-based aggregates have a tendency to absorb huge amounts of water due to their highly porous structure. It has been reported that the hydrophilicity of bio-aggregates leads to competition with hydraulic binders that need water for hydration and cohesion (Arnaud & Gourlay, 2012; Nguyen et al., 2009). The short term water absorption behaviour of hemp shiv can be seen in Figure 2.12.

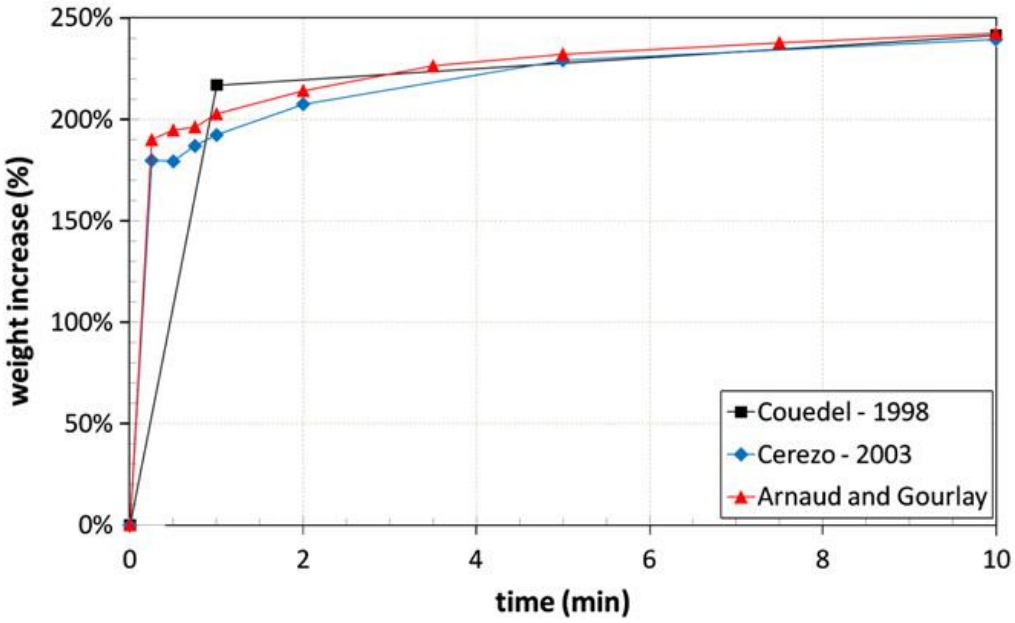

Figure 2.12 Water capillarity of a hemp shiv particle (Arnaud & Gourlay, 2012).

Arnaud & Gourlay (2012) reported that hemp shiv has a tendency to absorb water about 2-3 times its dry weight and the degree of saturation was found to be over 95% after 10 minutes of immersion. It has been reported that hemp shiv not only has higher water absorption rate but also absorb high amounts of water in the very first minutes compared to different plant materials (Kymainen, Hautala, Kuisma, & Pasila, 2001).

In another study published in the RILEM 2017 state of the art report (Amziane & Collet, 2017), pieces of shiv were immersed in water and the absorption curve was divided into three successive parts:

- Water adsorption on the hemp shiv surface
- Water absorption in the structure of the hemp shiv
- Diffusion of air trapped in the shiv structure.

The first part corresponding to the adsorption of water shows almost an instantaneous mass gain of hemp shiv. From Figure 2.12, the region corresponds to the rapid mass gain within the first minute of immersion. This initial water absorption for hemp shiv is almost 200% of its weight at dry state. It has been suggested that the biggest pores dominate the initial slope of the curve. These pores are connected to each other and are able to absorb large amounts of water (Kymainen et al., 2001).

The second part corresponds to the absorption of water within the internal structure of the plant walls. This diffusive behaviour can last from 14 to 24 hours. This stage is also influenced by the thickness of the hemp shiv particles and it can slowed down quickly if the shiv is thin moving to equilibrium faster when compared to a thicker piece of hemp shiv. Moreover, the tubes present inside the shiv structure may have different densities between individual shiv pieces leading to different properties (stiffness, length, orientation).

The third stage is extremely slow and corresponds to the release of air that has been trapped in the hemp shiv particle.

From the absorption curve, it can be highlighted the initial water absorption of significantly high in hemp shiv. This can be attributed to not only the chemical composition of hemp shiv containing large number of hydroxyls, but also to the rough surface of the material. Wettability of a material is a combination of chemical composition and the surface roughness of the material.

2.7 Hydrophobicity and Hydrophilicity

Wettability of a solid surface is a fundamental property of materials and it influences the applicability of the material. The surface energy and surface roughness determines the wetting nature of the material by a liquid.

Considering a drop of water or any liquid is placed on the surface of a smooth solid material, the liquid will spread to either greater or lesser extent, which is influenced by the surface energies of the liquid and the solid. This concept can be explained the interfacial tensions between the solid-liquid (γ_{SL}), solid-vapour (γ_{SV}) and liquid-vapour (γ_{LV}) interfaces. When a molecule of liquid is surrounded by the same liquid, it is held together by cohesion forces such as van der Waals which are exerted on the molecule from all directions. However, when the liquid molecule is at the boundary with air or vapour, it is in a higher state of energy as it has only forces exerted on it towards the liquid. The air-liquid forces are not as strong as the liquid-liquid forces, therefore the molecules at the boundary get attracted towards the centre of the liquid. This surface layer of molecules at the boundary forms a film and creates a surface tension between the liquid-air interface denoted by γ_{LV}. Similarly, the surface tension between solid-air interface is denoted by γ_{SV}. When the liquid is brought in contact with a solid, the interfacial tension between the solid-liquid is denoted by γ_{SL}.

The contact angle (θ) of a drop of liquid on a solid surface is determined by the interfacial tensions between solid-liquid (γ_{SL}), solid-vapour (γ_{SV}) and liquid-vapour (γ_{LV}) and is given by Young's equation:

$$\cos\theta = \frac{\gamma_{SV} - \gamma_{SL}}{\gamma_{LV}} \qquad \text{Eq (2.3)}$$

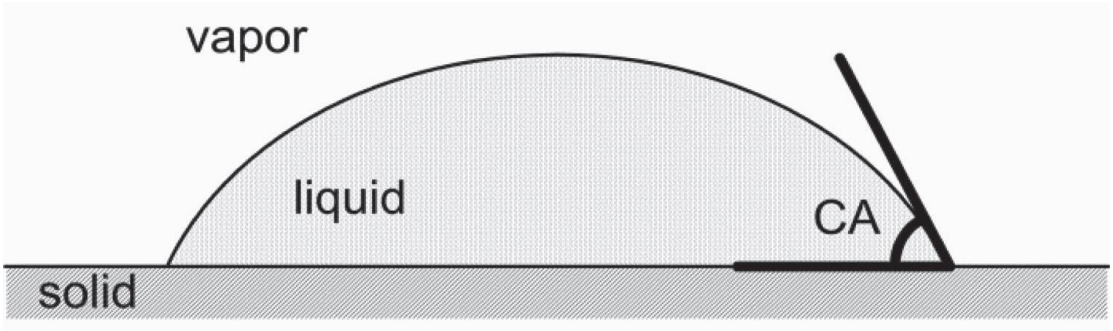

Figure 2.13 Contact angle determination of solid surface (Teisala, Tuominen, & Kuusipalo, 2014)

If water is used as the wetting liquid, then the contact angle between the liquid and solid is called water contact angle (WCA). When the drop of water comes into contact with a solid surface as seen in Figure 2.13, the following situations arise:

- For WCA <90°, water tends to spread on the solid surface and wets the surface. In this case, the surface is called hydrophilic.
- For WCA >90°, the surface repels the spreading of water. In this case, the surface is called hydrophobic.

Young's equation is only valid for surfaces that are entirely smooth and homogenous which is not the case in real life scenarios. Considering Young's equation, the highest contact angle can be achieved on a surface which has the lowest surface energy or the lowest γ_{SV}. It should be noted that the lowest surface energy so far recorded is for a surface obtained using closely aligned hexagonal-packed CF_3 groups with a value of 6.7 mJ/m^2. Using Eq (2.3), this would lead to a maximum WCA of 120° which does not justify the properties of naturally occurring superhydrophobic surfaces with WCA >150°. In reality, surfaces are rarely smooth and therefore roughness plays an important role in surface wetting.

2.8 Surface Roughness

A perfectly flat and smooth surface is hard to find in nature and therefore Young's approach needed to be modified using the surface roughness factor. Therefore, Wenzel modified Young's Equation and described the contact angle (θ') of a rough surface using the equation:

$$\cos\theta' = \frac{r(\gamma_{SV} - \gamma_{SL})}{\gamma_{LV}} = r\cos\theta \qquad \text{Eq (2.4)}$$

Where the parameter "r" is roughness factor and is defined as the ratio between the actual surface area to the geometrically projected area.

Since the roughness factor is always higher than 1, higher surface roughness results in increased hydrophilicity for hydrophilic materials. Similarly, for hydrophobic surfaces, higher surface roughness enhances the hydrophobicity of the material.

In the scenario where partial wetting takes place, that is, the surface has micro scale protrusions which cannot be filled by the liquid and instead filled by air, the wettability is then described by the Cassie-Baxter equation:

$$\cos\theta'' = r_f f\cos\theta + f - 1 \qquad \text{Eq (2.5)}$$

where r_f is the ratio between the actual wetted area divided by the projected wetted area, f is the fraction of projected area that has been wetted by liquid. Eq 2.5 is applicable in cases only when the liquid just touches the top of the substrate surface. If the liquid partially penetrates through the surface, then more complex equations are required. A schematic illustration of the wetting conditions are represented in Figure 2.14.

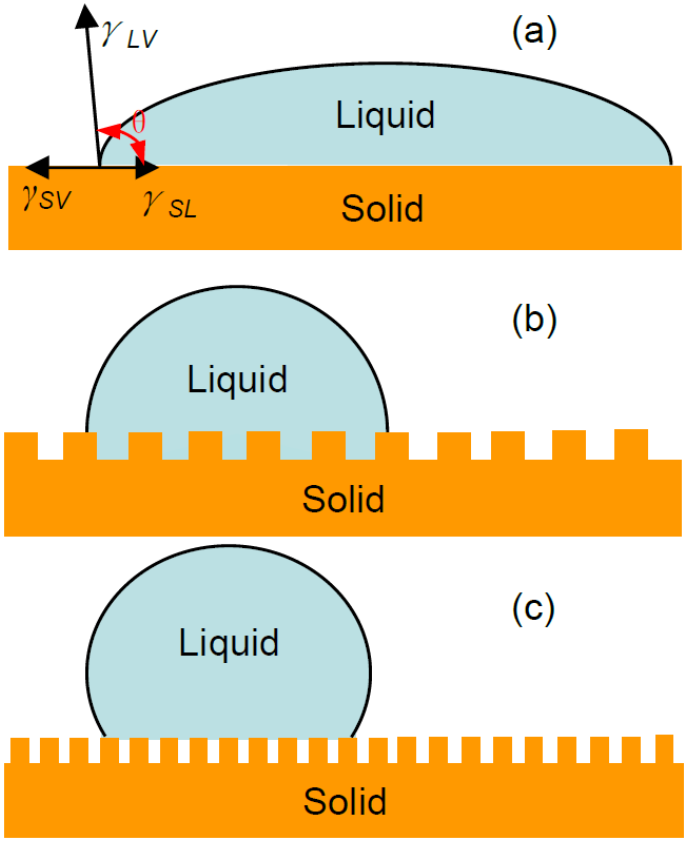

Figure 2.14 Schematic illustration of the wetting states; (a) Young's (b) Wenzel, and (c) Cassie regimes (Song & Rojas, 2013).

2.9 Common hydrophobic treatments for cellulose-based materials

To achieve maximum hydrophobicity from a cellulose-based surface, the treatment should chemically modify the surface resulting in low surface energy and the treatment must also create roughness at micrometer scale on the surface. Various treatment methods have been used in literature for obtaining hydrophobic surfaces on cellulose based materials. The most common approaches include deposition of spray or dip coatings, chemical vapour deposition (CVD), plasma processing techniques and in situ nanoparticle growth and their characteristics are presented in Table 2.4.

*Table 2.4. Common treatment methods for fabrication of hydrophobic surfaces on cellulose based materials in literature (Teisala et al., 2014).(*represents dry methods and **represents wet chemical methods; time scales for fast, moderate and slow are <1s, 1-2 min, 1 hour or more, respectively.*

Treatment	**Processing steps**	**Methodology nature**	**Coating thickness (nm)**	**Coating durability**
Dip-coating	3-5	Slow	>100	Good/ moderate
Spray coating	1*-3**	Fast*/ slow**	>100	Moderate/ weak
Polymerisation techniques	>5	Slow	±100	Good/ moderate
In situ nanoparticle growth	1* or >5**	Slow	±100	Moderate
CVD and plasma	1-2	Moderate/ slow	≤100	Moderate

Dip coating: The most common method for producing a hydrophobic coating on cellulose-based materials such as cotton or paper. The steps involved in the coating process include dipping the substrate in the coating liquid, drying and curing. The coating liquid usually consists of organic solvent, hydrophobic agents and can additionally contain micro- or nanoparticles for enhancing the roughness

and polymeric binders. Coatings produced by this process are generally durable due to the strong binding effect and good surface roughness.

Spray-coating: An easy route to develop hydrophobic coatings on cellulose based materials with potential for industrial scale up. Conventional spray coating techniques involve spraying of coating liquid over the material, and the coating formulation can be very similar to that of the dip-coating process. The coating process usually involves three steps; spraying, drying and curing. It may also involve an additional step for hydrophobization. Recent researches report novel single step spray coating process without the need of drying, curing or hydrophobization steps. Although this is a rapid treatment process, the coatings fabricated on the material may not be as durable as the dip-coating process.

Polymerisation: hydrophobic coatings can be fabricated using controlled chemical reactions. Limitations of using this technique include their speed of the coating process and the number of steps involved.

In situ nanoparticle growth: this technique can be used to develop structures on a nano/micro scale in a controlled manner on the surface of cellulose based materials. Although the fabrication of this coating is a single step process, it is not an efficient method as the nanoparticle growth is time consuming.

CVD and plasma processing: Techniques such as plasma etching or plasma enhanced CVD allow alteration of the chemical composition and the fine physical structure of cellulose based materials. The process involves two steps, the first one enhancing the roughness by etching and the second step depositing a thin layer of hydrophobic coating. Porous materials having rough surfaces can be treated using only CVD without requiring an additional roughening step. Drawbacks of using these techniques include the time consumption of the process and the high cost, particularly in the case for plasma etching.

2.10 Sol-gel technology

The sol-gel process refers to preparation of a sol consisting of small particles dispersed as a colloid that evolves into a continuous network structure called a gel. The formation of a sol takes place through well-known hydrolysis and condensation reactions of inorganic alkoxide precursors to form a colloidal suspension.

Metal alkoxides are most widely used precursors as they react readily with water. The most popular metal alkaoxides used in the sol-gel process are tetraexthoxysilane (TEOS) and tetramethoxysilane (TMOS), however, alkaoxides of titanates, aluminates, borates and zirconates are also used in the sol-gel process.

Sol-gel chemistry can be traced back to early 19th century, although it had become a topic of interest during the mid-1970 when extensive investigation was carried out on the chemical process. Since then, sol-gel technology has been used to produce molded gels, xerogels, fibers, films and molecular cages having widespread application in various fields.

To understand the sol-gel chemistry, the sol-gel reactions and the process have been studied in detail. A detailed insight to the sol-gel process has been provided by (C. Brinker & Scherer, 1990) which can be listed in the following steps:

1. Hydrolysis and condensation of alkoxide precursors
2. Gel-formation via polycondensation
3. Syneresis or aging
4. Gel drying
5. Calcination (if required)

The above steps influence the formation of the gel and controlling these steps determine the gel characteristics. We will focus on the sol-gel reaction mechanism and the factors influencing the reaction to get an insight to sol-gel chemistry of coatings.

Sol-gel reactions comprise of a series of hydrolysis and condensation reactions of an alkoxysilane (Figure 2.15). The sol-gel chemistry is strongly affected by the process parameters such as nature of the R-group, the alkoxide:water ratio and presence of catalysts. The type of catalyst is responsible for the relative rates of hydrolysis and condensation and this determines the structure of the gel.

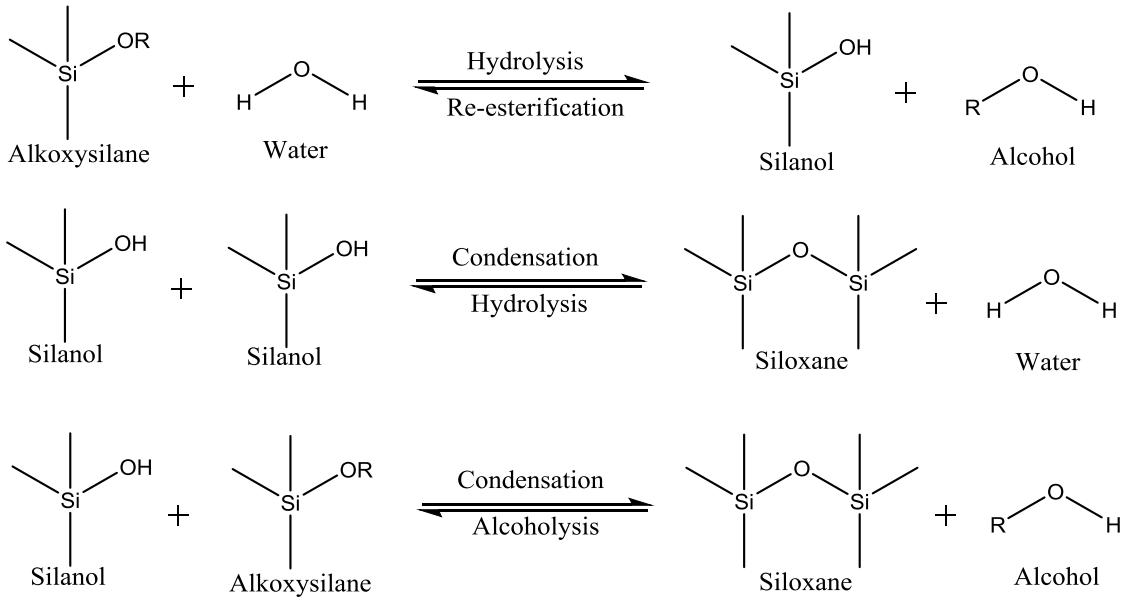

Figure 2.15. Sol-gel reaction scheme (C. Brinker & Scherer, 1990).

The hydrolysis reaction can be catalysed by an acid or base as the neutral reaction is extremely slow. During hydrolysis, one of the alkoxy groups is replaced with a pentacoordinate transition state during acid and base catalysis. Acid catalysed hydrolysis gives a positive charge whereas base catalysed hydrolysis gives a negative charge on the transition state molecule. This provides the transition state with an electron withdrawing (-OH) or electron donating (-OR) power. From literature it is evident that hydrolysis gets progressively slower in acidic conditions and faster in basic conditions (Silva & Airoldi, 1997).

Condensation stage results in formation of siloxane bonds. Similar to hydrolysis, condensation via acid and base catalysts results positive and negative charges on the transition state respectively. As seen in Figure 2.15, condensation takes place in two steps. Before the first step, if hydrolysis is complete then the

transition state has more sites for next condensation step. Since the degree of hydrolysis is faster in basic conditions, more sites are available for multiple condensation steps resulting in small highly branched agglomerates. In acidic conditions, condensation starts before completion of hydrolysis resulting in chain like structures (Danks, Hall, & Schnepp, 2016).

2.11 Hydrophobic sol-gel coatings on cellulose-based materials

The sol-gel technique is a highly versatile method to deposit silica based coatings possessing single or multi functionality (C. Brinker & Scherer, 1990). These thin mesoporous coatings have high structural homogeneity and their adhesion can be tailored to different substrates (Calabria A. et al., 2010). Sol-gel based hydrophobic and water repellent coatings have been investigated on different plant based materials such as wood (Donath, Militz, & Mai, 2004; Boris Mahltig, Swaboda, Roessler, & Böttcher, 2008; Wang, Liu, et al., 2011) and cellulosic fibres (Bae et al., 2009; B. Mahltig & Böttcher, 2003; Song & Rojas, 2013). It has proved to be an efficient treatment on cellulose based materials to provide hydrophobicity through the use of organic molecules during the sol-gel preparation. Recent researches conducted on hydrophobicity of cellulose based materials through sol-gel technology have been listed in Table 2.5. Sol-gel treatment significantly reduces the flammability of wood and the fire resistance properties can be further enhanced by phosphorus or boron based additives (Mai & Militz, 2004). Other researchers have demonstrated that using titania based nanosols on cotton fabrics result is providing excellent UV protection (Xue, Jia, Chen, & Wang, 2008).

Fluoro containing silanes have been used in various studies to control the surface roughness and chemical properties of the substrate resulting in very high contact angles. However, fluoroalkyl compounds have certain disadvantages. They are not eco-friendly as they are responsible for emission of fluorine compounds into the environment during and after the coating process. They are a potential threat to health if they come in contact with skin. Another disadvantage is their high cost. In addition to these reasons, fluorinated compounds generally require a high-temperature process for their production which is not suitable for substrates with low-heat resistance (Daoud, Xin, & Tao, 2004). Therefore preparation of sol-gels using nonfluorinated compounds is essential for environmental friendly and cost effective coatings.

Table 2.5. Hydrophobic sol-gel treatments on cellulose based substrates.

Agent	Chemical composition	Precursors	Treatment Surface	Water Contact Angle	Reference
POTS	1H, 1H, 2H, 2H-perfluoroalkyl-triethoxysilanes	TEOS, NH_4OH, Ethanol	Wood	164°	(Wang, Shi, Liu, Xie, & Wang, 2011)
SA, PFTDS	stearic acid (SA), 1H, 1H, 2H, 2H-perfluorodecyl-trichlorosilane (PFTDS)	Tetrabutyl titanate, acetic acid, toluene, acetone	Cotton	142-163°	(Xue et al., 2008)
FAS-17	(heptadecafluoro-1,1,2,2-tetradecyl) trimethoxysilane	flurotitanate, Boric acid, HCl, Silver	Wood	153°	(Gao, Gan, Xiao, Zhan, & Li, 2016)
VTES	vinyltriethoxysilane	Tetrabutyl titanate, nitric acid	Wood	153°	(Liu, Qing, Wu, Liang, & Luo, 2015)
PFSC	perflurooctylated quatenary ammonium silane	TEOS, NH_4OH	Cotton	133° -145°	(Yu, Gu, Meng, & Qing, 2007)
HDTMS	Hexadecyltrimethoxy-silane	TEOS, HCl	Textiles	142°	(B. Mahltig & Böttcher, 2003)
HDTMS	Hexadecyltrimethoxy-silane	TEOS, HCl (3-Glycidyloxypropyl) trimethoxysilane	Cotton	141°	(Daoud et al., 2004)
KF-255	perfluroacrylate, benzyl methyl acrylate	TEOS, NH_4OH	Cotton	130°	(Bae et al., 2009)
APDTMS	3-aminopropyl-dimethoxymethyl-silane	TEOS, Phytic acid	Textile	129°	(Cheng, Liang, Guan, Yang, & Tang, 2018)
FAS	fluoroalkylfunctional water-born siloxane	Nano silver, reactive binder	Cotton	105°	(Tomšič et al., 2008)
MTES	methyltriethoxysilane	TEOS, HCl, propyl triethoxysilane	Wood	Lower rate of mositure sorption	(Donath et al., 2004)
HDTMS	Hexadecyltrimethoxy-silane	Methyltrimethoxy-silane, trifluroacetic acid	Wood	Lower rate of moisture and water sorption	(Tshabalala, Kingshott, Vanlandingham, & Plackett, 2002)

Chapter 3

Microstructure, Porosity and Density of Hemp Shiv

This chapter has been published as a Journal paper entitled “Cell wall microstructure, pore size distribution and absolute density of hemp shiv” in Royal Society Open Science (Jiang, Lawrence, Ansell, & Hussain, 2018).

Introductory text

The focus of this paper is the characterisation of hemp shiv by examining cell wall microstructure, porosity and density using various approaches. The microstructure of hemp shiv was studied by scanning electron microscopy and confocal microscopy. The porosity of hemp shiv was studied and characterised using mercury intrusion porosimetry. The cell wall density was evaluated by helium pycnometry, mercury intrusion porosimetry and the Archimedes' method.

The physical characterisation of hemp shiv reported in this paper is necessary to understand the internal structure of the pores that are responsible for the hygroscopic and moisture buffering capacity of hemp shiv. These pores are responsible for extremely high water absorption rate as mentioned earlier in Chapter 2. Modification of these pores would expect reduction in water absorption behaviour of hemp shiv but it is essential to retain the moisture buffering ability of hemp shiv through these pores.

To the best of our knowledge, there is no detailed study on the cell wall ultrastructure, pore size distribution and absolute density of hemp shiv. The objective of this paper is to establish the most appropriate techniques that should be used to identify the characteristic qualities of hemp shiv and to present representative data for hemp shiv typically used in construction. The study on pore size distribution and morphology is particularly of interest to compare the effect of deposition of various silica based coatings on the structure of hemp shiv. The modification of porosity, morphology, water absorption and hygroscopicity after coating the hemp shiv is reported in the next chapters.

Statement of Authorship

This declaration concerns the article entitled:									
Cell wall microstructure, pore size distribution and absolute density of hemp shiv.									
Publication status (tick one)									
draft manuscript		**Submitted**		**In review**		**Accepted**		**Published**	✓
Publication details (reference)	Jiang, Y., Lawrence, M., Ansell, M. P., & Hussain, A. (2018). Cell wall microstructure, pore size distribution and absolute density of hemp shiv. Royal Society Open Science, 5(4), 171945. http://doi.org/10.1098/rsos.171945								
Candidate's contribution to the paper (detailed, and also given as a percentage).	The candidate contributed to/ considerably contributed to/predominantly executed the… Formulation of ideas: 25% This paper was published from the work conducted during the ISOBIO project, the conceptualization mainly by M. Lawrence based on discussions with M.P Ansell, Y.Jiang and A. Hussain. Design of methodology: 25% M.Lawrence and Y.Jiang designed the methodology with inputs from M.P. Ansell and A. Hussain. Experimental work: 40% The porosity experiments were conducted by A. Hussain and he participated in data analysis. Presentation of data in journal format: 20% The paper was written by Y.Jiang with input from all co-authors. M.Lawrence, M.P Ansell and A.Hussain proofread the paper.								
Statement from Candidate	This paper reports on original research I conducted during the period of my Higher Degree by Research candidature.								
Signed	Atif				**Date**	15.09.2018			

Copyrights and Permission

ROYAL SOCIETY OPEN SCIENCE

Home Content Information for About us Sign up Submit

Article reuse

All articles in *Royal Society Open Science* are published under the latest available CC-BY open access licence. This means that readers can:

Share — copy and redistribute the material in any medium or format
Adapt — remix, transform, and build upon the material

for any purpose, even commercially, as long as attribution is given.

Attribution

- You must give appropriate credit. If supplied, you must provide the name of the creator and attribution parties, a copyright notice, a license notice, a disclaimer notice, and a link to the material. CC licenses prior to version 4.0 (current as of September 2014) also require you to provide the title of the material if supplied, and may have other slight differences.
- You must provide a link to the license.
- You must indicate if changes were made. In version CC-BY 4.0 (current as of September 2014), you must indicate if you modified the material and retain an indication of previous modifications. In 3.0 and earlier license versions, the indication of changes is only required if you create a derivative.

You may do so in any reasonable manner, but not in any way that suggests the licensor endorses you or your use.

Publication title:

Cell wall microstructure, pore size distribution and absolute density of hemp shiv.

Thesis page numbers that it spans:

68 to 82

ROYAL SOCIETY OPEN SCIENCE

rsos.royalsocietypublishing.org

Research

Cite this article: Jiang Y, Lawrence M, Ansell MP, Hussain A. 2018 Cell wall microstructure, pore size distribution and absolute density of hemp shiv. *R. Soc. open sci.* **5**: 171945.
http://dx.doi.org/10.1098/rsos.171945

Received: 22 November 2017
Accepted: 5 March 2018

Subject Category:
Engineering

Subject Areas:
materials science

Keywords:
hemp shiv, microstructure, porosity, absolute density, mercury intrusion porosimetry, helium pycnometry

Author for correspondence:
Y. Jiang
e-mail: y.jiang@bath.ac.uk

Cell wall microstructure, pore size distribution and absolute density of hemp shiv

Y. Jiang, M. Lawrence, M. P. Ansell and A. Hussain

BRE Centre for Innovative Construction Materials, Department of Architecture and Civil Engineering, University of Bath, Bath BA2 7AY, UK

YJ, 0000-0003-3292-8164

This paper, for the first time, fully characterizes the intrinsic physical parameters of hemp shiv including cell wall microstructure, pore size distribution and absolute density. Scanning electron microscopy revealed microstructural features similar to hardwoods. Confocal microscopy revealed three major layers in the cell wall: middle lamella, primary cell wall and secondary cell wall. Computed tomography improved the visualization of pore shape and pore connectivity in three dimensions. Mercury intrusion porosimetry (MIP) showed that the average accessible porosity was $76.67 \pm 2.03\%$ and pore size classes could be distinguished into micropores (3–10 nm) and macropores (0.1–1 µm and 20–80 µm). The absolute density was evaluated by helium pycnometry, MIP and Archimedes' methods. The results show that these methods can lead to misinterpretation of absolute density. The MIP method showed a realistic absolute density ($1.45\,g\,cm^{-3}$) consistent with the density of the known constituents, including lignin, cellulose and hemi-cellulose. However, helium pycnometry and Archimedes' methods gave falsely low values owing to 10% of the volume being inaccessible pores, which require sample pretreatment in order to be filled by liquid or gas. This indicates that the determination of the cell wall density is strongly dependent on sample geometry and preparation.

1. Introduction

Bio-based insulation materials, such as hemp, flax and wheat straw, offer a number of benefits in comparison with more established mineral and oil-based alternatives, such as mineral wool and PUR (polyurethane rigid foam)-based products [1,2]. Apart from timber, hemp-lime is perhaps the most researched bio-based building material because it is a cheap and low density material (bulk density: $0.08–0.16\,g\,cm^{-3}$) with associated

THE ROYAL SOCIETY PUBLISHING

low thermal conductivity (0.06–0.14 $W\,k^{-1}\,m^{-1}$) depending on the density and moisture level. Hemp-lime (often referred to a 'hempcrete') is a composite material made up of the woody core of the hemp stalk (shiv) used as an aggregate in a lime-based binder. The binders are typically based on hydraulic lime but specially formulated to avoid the inhibition of hydration caused by the sugars present in the hemp stalk.

Previous research on the physical properties of hemp-lime has demonstrated that the material presents a good balance between low mass and heat storage capacity compared with classical insulation materials. Much of the existing characterization data for natural building materials relates to structural performance such as cell wall microstructure and porosity [3–9]. Thus, concise knowledge of the cell wall microstructure, porosity and the absolute density is of high importance for the characterization of bio-aggregated materials. However, the characterization of the properties of bio-based building materials is at an early stage.

To the best of our knowledge, there is no detailed study on the cell wall ultrastructure, pore size distribution and absolute density of hemp shiv (woody core). The objective of this paper is to establish the most appropriate techniques that should be used to identify the characteristic qualities of hemp shiv and to present representative data for hemp shiv typically used in construction. This is because hemp shiv is, by far, the most commonly used bioaggregate in the construction industry and the information provided in this paper will be of great use to researchers and practitioners alike. Recently, several studies investigated the microstructure of hemp shiv. Magniont *et al*. [1] reported that hemp shiv was embedded in resin and polished and a cross section of hemp shiv was studied by scanning electron microscopy (SEM). They showed that hemp shiv is mainly composed of conducting vessels. The diameter of the vessels usually ranged from 10 to 20 µm. In addition, larger vessels were also observed in a longitudinal section [1]. Lawrence *et al*. [10] found the microstructure of hemp shiv exhibited 50 µm pores connected to 10 µm pores via 1 µm connecting pores. Dubois *et al*. [11] showed a section through one hemp shiv obtained by X-ray microtomography. The high total porosity of the vegetal particle can be clearly seen with the typical tubular structure of the mesoscopic pores. The porosity of hemp shiv is quite a simple parameter to define but is not so easy to quantify. The reason is that the void/space in hemp shiv can span from a few nanometres to millimetres or larger. There is currently no one measurement method that can adequately cover this enormous range in scale. In addition, the porosity can be modified or changed by a variety of processes during the porosity measurement such as deformation, hydrothermal alteration and the production of secondary or fracture porosity. Finally, the pore shape and connection structure (open and closed) have a significant effect on the porosity results depending on the testing approach [12–18]. Anovitz *et al*. [19] summarized 10 methods for measuring the porosity and pore size distribution (PSD) used on core or crushed rock materials (figure 1), revealing the range of pore sizes that each method is capable of measuring. It should be kept in mind that different techniques are based on different principles and have different capabilities for measurement. Depending on the natural properties of bio-aggregates, there is no best approach to determine their porosity. The combination of several techniques and comparison of results of pore structure investigations from different methods may give an insight into the complex porosity of bio-aggregates.

Similarly, the determination of cell wall density of (porous material) hemp shiv is not a simple matter. The essential requirement is that all pore spaces are freely accessible for the displacement gas or liquid. This means that all cell lumens within the hemp shiv, such as vessels and voids in the cell wall, must be reached by the displacement gas or liquid. Gas pycnometry is a very accurate method for measuring the absolute density of cell walls, which is based on the Archimedes' principle of displacement of an inert gas, such as helium, nitrogen or argon. Although the method of gas pycnometry is relatively simple compared with other methods, there are only very few publications dealing with investigations of the cell wall density or porosity of hemp shiv using this procedure, owing to the complicated sample preparation. Hill *et al*. [20] prepared samples of pine using a Soxhlet extraction for 8 h with a solvent system composed of toluene, methanol and acetone (4 : 1 : 1 by volume). Samples were then oven-dried for 12 h at 105°C and cooled in a desiccator before placing into a helium pycnometer. The cell wall density of the untreated pine sample was 1.42 $g\,cm^{-3}$. Zauer *et al*. [21] studied the cell wall density of wood determined by gas pycnometry. The results clearly showed that misinterpretation of the results is possible due to unfavourable sample preparation in relation to the different wood anatomies. The presence of a large number of uncut cells can lead to wrong results due to the inaccessible pores. Another method involves nitrogen adsorption with BET analysis to characterize pores in the 1–100 nm range. These adsorption methods do not, however, provide any information about pores larger than mesopore size, which have been shown from electron microscopy images to be present in hemp shiv samples. Some studies have been carried out using polar or non-polar liquids as the displacement medium. Nguyen

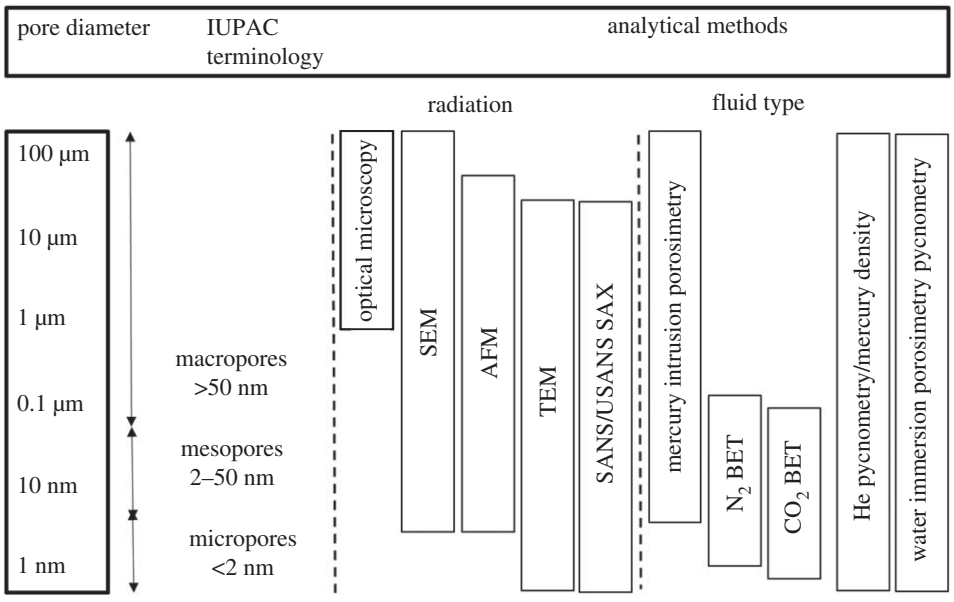

Figure 1. Methods used to determine porosity and pore size distribution (PSD) (reproduced from [19]).

et al. [22] studied the inter-porosity of hemp shiv using the pycnometer method, with toluene as the fluid filling. Pure hemp shiv aggregates possessed an inter-porosity of 60% while fibrous hemp shiv had an inter-porosity of 76.6%. Manger [23] concluded that most of the total porosity measurements are variations on bulk volume/grain volume or bulk density/grain density approaches, and the absolute porosity measurements are made by absorption methods employing different fluids or gases. However, the extent to which the cell wall density changes as a function of the sample preparation has not yet been well clarified. Mercury intrusion porosimetry (MIP) is another measurement technique for the determination of pore size distribution. It can be used to characterize pores from a few nanometres to a hundred micrometres in diameter. However, the drawbacks of MIP include the risk of crushing the sample with the high pressures required for analysis. In addition, it cannot distinguish between inter-particle and intra-particle porosity, especially for powdered samples. Finally, the MIP method only determines the diameter of the pore throat, not the actual pore size for ink bottle pores with narrow points of connection, which has the tendency to overstate smaller pore sizes at the expense of larger pore sizes. Thus, the pore size distribution given by MIP can, where ink bottle pores are present, tend to be skewed towards the smaller pores. The total porosity, however, given by this technique, can be considered to be valid as, by the time the highest intrusion pressure has been achieved, either all pores will have been intruded or the pore walls will have been crushed, and their equivalent volume effectively intruded (down to the effective limit of MIP of approximately 3.5 nm).

In this study, hemp shiv was fully characterized by examining cell wall microstructure, porosity and density using different approaches. The microstructure of hemp shiv was studied by SEM and confocal microscopy (CM). The porosity of hemp shiv was fully studied and characterized by employing MIP. The cell wall density was evaluated by helium pycnometry, MIP and the Archimedes' method.

2. Material and methods

The hemp shiv (*Cannabis sativa* L.) used in this study belonged to the herbaceous species originating from Central Asia and was sourced from industrial hemp grown and harvested in north west France by the CAVAC cooperative in 2015. The hemp shiv was produced by a mechanical de-fibring processing of removing the fibre, chopping, grading and de-dusting. During characterization of the shiv, samples from the same batch of hemp shiv from the same field plant were compared. The particles of hemp shiv used in this study were prepared with a mean length of 7.6 mm and a mean width of 2.4 mm.

For measurements performed in a dry state, the hemp shiv was dried in an oven at 60°C until a constant mass was reached (i.e. mass variation lower than 0.1% between two consecutive weighings for three consecutive weighings within a 24-hour period), then it was cooled to ambient temperature in a sealed container. The bulk density of hemp shiv is about 85–90 kg m^{-3}. The protocol followed was

based on that developed by the RILEM Technical Committee 236-BBM [24], which is a state-of-the-art report that reflects the current knowledge on the assessment of the chemical, physical and mechanical properties of bioaggregate and vegetal concrete, with the following variations: the aggregates were placed in a transparent plastic cylinder 94 mm in diameter and 204 mm in height. The quantity of aggregate was adjusted to be more or less half the volume of the container. The cylinder was upended ten times. The level was marked using a cardboard disc and the volume was measured with water. The transparent cylinder allows the technician to check that no bridges develop within the aggregate which would produce a void with a corresponding reduction in measured density. If this does occur, the cylinder is upended again or the measurement is restarted. The test was repeated three times for each aggregate. The particles of hemp shiv were cut into a mean length of 3.6 mm and a mean width of 1.4 mm to study the effect of size on the density test. The density of hemp fibre obtained from the CAVAC cooperative (France) was compared with the absolute density of hemp shiv using a liquid displacement method.

A scanning electron microscope (JEOL SEM-6480LV, Tokyo, Japan) and a field emission scanning electron microscope (JEOL FESEM6301F) were used for the microstructural analysis of the hemp shiv. All images were taken at an accelerating voltage of 10 kV. The sample surfaces were coated with a thin layer of gold using an HHV500 sputter coater (Crawley, UK) to provide electrical conductivity sending electrons to earth.

The samples of hemp shiv used for binocular microscopy (Zenith XSZ-107BN, UK) were oven-dried at 60°C for three days prior to preparation. The oven-dried material was placed in a tinfoil container and immersed in a two-part resin mixed with a blue dye. The resin was a low viscosity resin with a setting time in excess of 24 h at room temperature. The container was placed in a glass vacuum desiccator and held in a vacuum for 48 h in order to ensure maximum penetration of the resin into the pores. After the resin had set, thin sections of approximately 30 µm were prepared and mounted onto glass slides.

For CM sample preparation, the resin-embedded specimens were trimmed using an ultra-microtome with a glass knife. The slices were observed at room temperature with a confocal microscope (LSM880, Carl Zeiss) using single-track, triple-channel imaging with 405-, 488- and 543-nm laser lines.

For transmission electron microscope (TEM) sample preparation, small piece of hemp shiv were dehydrated in acetone and embedded in low viscosity SPURR resin (TAAB, UK) with vacuum treatment. Ultra-thin sections were cut with an ultra-microtome using a diamond knife. Subsequently, sections were examined with a JEO_JEM_2100 plus TEM at 120 kV.

A CT scanner (Nikon XT H 225) was used to capture the three-dimensional image of hemp shiv specimens. The scanning parameters were fixed at a voltage of 90 kV and current of 108 µA. The area of each pixel is 2.54 µm^2. The CT scan data were merged using Avizo software (FEI, Thermo Fisher Scientific). The value of white pixels is 0 which represents the pore (air) phase, while the value of blue pixels is 255 which represents the hemp shiv cell wall phase.

Gas pycnometry was carried out using the automatic pycnometers Ultrapyc 1200e (Co. Quantachrome, USA) and AccuPyc 1330 (Micromeritics, UK). Helium was employed as the displacement gas. The cell wall density was calculated from the measured cell wall volume and the known mass of the samples. The apparatus had a 10 cm^3 cell for AccuPyc and 15 cm^3 cell for Ultrapyc 1200e. Measurement of the sample volume was achieved by filling the sample cell with helium to the required filling pressure. Then the gas expanded in the expansion cell and the final pressure at equilibrium was recorded (P_f). The volume of the sample was calculated according to the following equation:

$$V_{\text{sample}} = \frac{V_{(\text{samplecell})} - V_{\text{expcell}}}{(P_r/P_f) - 1}, \tag{2.1}$$

where V_{sample} is the volume of the sample (cm^3); $V_{\text{samplecell}}$, the volume of the sample cell (cm^3); V_{expcell}, the volume of the expansion cell (cm^3); P_r, the run fill pressure; and P_f, the final pressure (psi). The volume of the sample ($V_{\text{samplecell}}$) and volume of the expansion (V_{expcell}) cells were determined by calibration and automatically stored in the set-up parameters.

Different operating conditions have to be defined by the operator before the analysis. In this test, the number of purges and procedures were fixed at ten. Standards for the volume calibration (calibration ball purchased from Micromeritics, $V_{\text{cal}} = 6.371684$ cm^3) were used at 25°C. The experiment was performed by using the cell with a 75% filling ratio. The results showed the density values and standard deviations (corresponding to the ten repetitions for each analysis).

Archimedes' method was used to measure the absolute density of hemp shiv. Canola oil with a density of 0.92 g cm^{-3} and acetone with a density of 0.79 g cm^{-3} were used for displacement liquids instead of water in order to avoid absorption of water during the experiment and to ensure that the hemp shiv

sinks. An electronic balance was used to weigh hemp shiv. Weights were measured to the nearest 0.0001 g. The hemp shiv was cut into small pieces and bundled together with hemp fibre. The dried sample was immersed into liquid and placed into the vacuum chamber. The valve was slowly opened and the air bubbles were pulled from the sample. After a period of time, the bubbles decreased in number and size. The time for the total evacuation of the air from the sample was dependent on several factors including the pore structure of the sample, its size and the power level of the vacuum. Once the bubbling had stopped, the vacuum was released by opening the relief valve. In this experiment, the vacuum was maintained for a period of 8 h. The sample was first weighed in air and its weight recorded as W_{fa}. The weight of the sample was then recorded in the displacement liquid after vacuum treatment as W_{fs}. The absolute density (ρ_A) of the sample was calculated using the following equation:

$$\rho_A = \frac{\rho_s W_{fa}}{W_{fa} - W_{fs}}, \tag{2.2}$$

where ρ_s is the density of the solvent (g cm^{-3}). All measurements were determined at 22 ± 2°C [25].

An Autopore mercury porosimeter (PASCAL, Thermo Scientific) was used to determine the porosity and pore size distribution of hemp shiv. The measurements were undertaken on four samples (between 0.15 and 0.2 g). Particle size distribution (PSD) $f(r)$ was determined using the Washburn equation. This relates the radius r of pores (assumed to be cylindrical) to the imposed pressure P as follows:

$$P = \frac{-2\gamma \cos\theta}{r},$$

where γ is interfacial energy (surface tension) of mercury and θ is contact angle of mercury with the material.

Common values of γ and θ (which assume interfaces involving a gas or vapour phase) are 485 mJ m^{-2} and 140°. While pores are rarely cylindrical, the Washburn equation is generally accepted as a practical method of analysing what are normally very complex pore systems [26]. The results were plotted in two graphical forms. In the first form, the cumulative pore volume was plotted against a logarithmically spaced abscissa, and in the second form, the differential PSD based on the logarithmic differentiation dv/dlog$R$ was calculated. The mercury in the porosimeter is intruded into the specimen at a rate of 7–28 MPa min^{-1}. The test pressure ranged from 0.0001 to 400 MPa. As a result, the ranges of the pore diameter on the cumulative curve and differential curve were 100 and 0.003 µm, respectively. This wide range allows the detection of diverse pore classes along the PSD curve.

3. Results and discussions

3.1. Microstructure of hemp shiv

The cross section of the hemp stem has been identified as the epidermis layer, the phloem layer, the xylem layer and the pith layer from the outside to the centre of its cross section, as shown in figure 2*a*. From the interior to the exterior of the hemp stem, the three zones of pith, xylem and cortex are clearly visible. It can be seen that the stem cross section has an indented shape, similar to a four-leaf clover, which enhances the rigidity of the stem. At higher magnification (figure 2*b*), the radial arrangement of cells in the vascular cambium is visible. In the vascular cambium, there is a subtle boundary between the cells in the outer secondary phloem and the inner secondary xylem. A closer view of the pith reveals the foam-like closed cell structure with some voids at the interfaces between cells. The external surface of the unretted hemp is covered in mechanical fibres (right of figure 2*b*), which are removed during the retting process and subsequently converted into yarns and woven fabrics. Field retting is a major type of retting where harvested hemp stalks are left on the ground for several weeks and the weather is relied on to facilitate the process. The length of the retting process depends on the availability of moisture and air temperature. The vessels exhibit little variation in size and there is no clear pore arrangement in a diffuse-porous distribution. The vessels are mostly solitary although some small groups of adjacent vessels exhibit shared cell walls between them. The vessels are approximately 50–80 µm in diameter and are surrounded by relatively thick cell walls. Thick-walled fibres with a diameter from 1 to 3 µm are located between the vessels. The pore frequency of hemp shiv is around 20.8 vessels mm^{-2}. There are no tyloses or other contents in the vessels.

Figure 3*a* shows a clear interface (white dotted line) between zones with smaller (lower) and larger (upper) longitudinal cells. The large parenchyma cells seen in the upper section of figure 3*a* have an average diameter of approximately 5–10 µm, whereas the size of the parenchyma cells in the lower

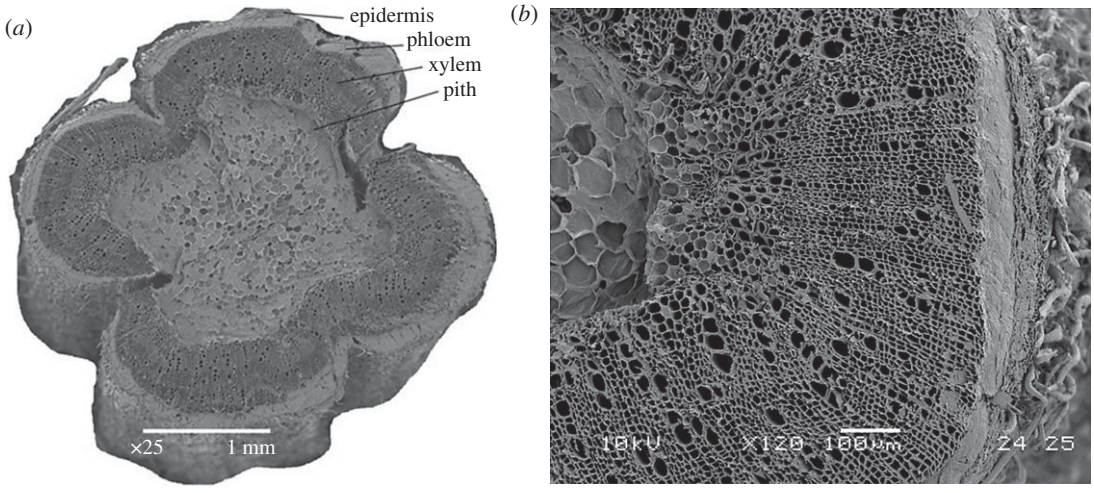

Figure 2. Cross section through hemp stem: (*a*) magnification ×25 and (*b*) magnification ×75.

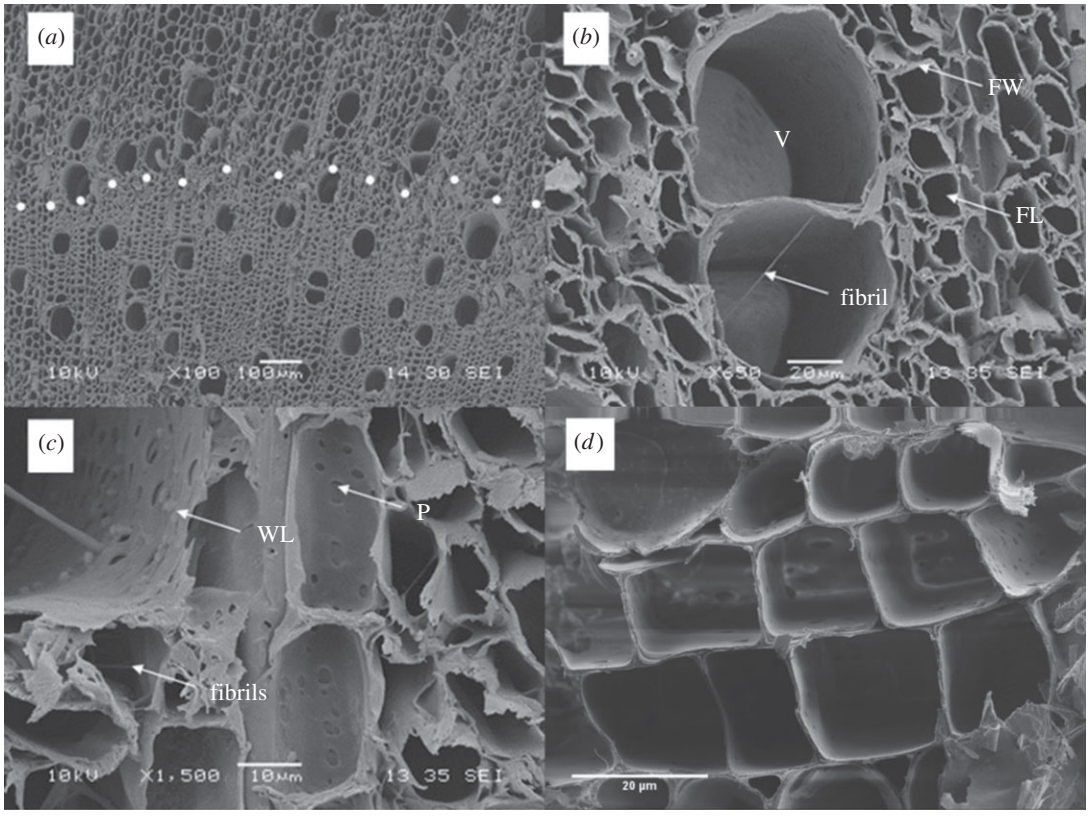

Figure 3. Scanning electron micrograph of the porous hemp shiv, showing (*a*) interface between zones with smaller (lower) and larger (upper) longitudinal cells. (*b*) A close-up view of the vessels shows a bridging fibril in the central vessel. (*c*) The secondary walls of vessels in hemp shiv are overlaid by a warty layer (WL) and several fibrils in the vessels. (*d*) A close-up view of the parenchyma cells seen in the upper section of (*a*). V, Vessel; FW, fibre wall; FL, fibre lumen; P, simple pits; WL, warty layer; dotted line indicates interface.

section of figure 3*a* is much smaller (approx. 1–5 µm). Wall thickness varies from that of fibres to that of axial parenchyma. Several bridging fibrils in vessels can be seen in figure 3*b–d*. A warty layer can just be distinguished on the surface of the secondary wall. The vessel member walls are not always covered in pits. Some walls show prolific vessel to vessel pitting, while others are completely devoid of pits. Bordered pits can be seen within the tracheid cavities. Secondary walls are present and exhibit numerous simple pits. The groups of pits on the walls of the vessel members connect with the ray cells

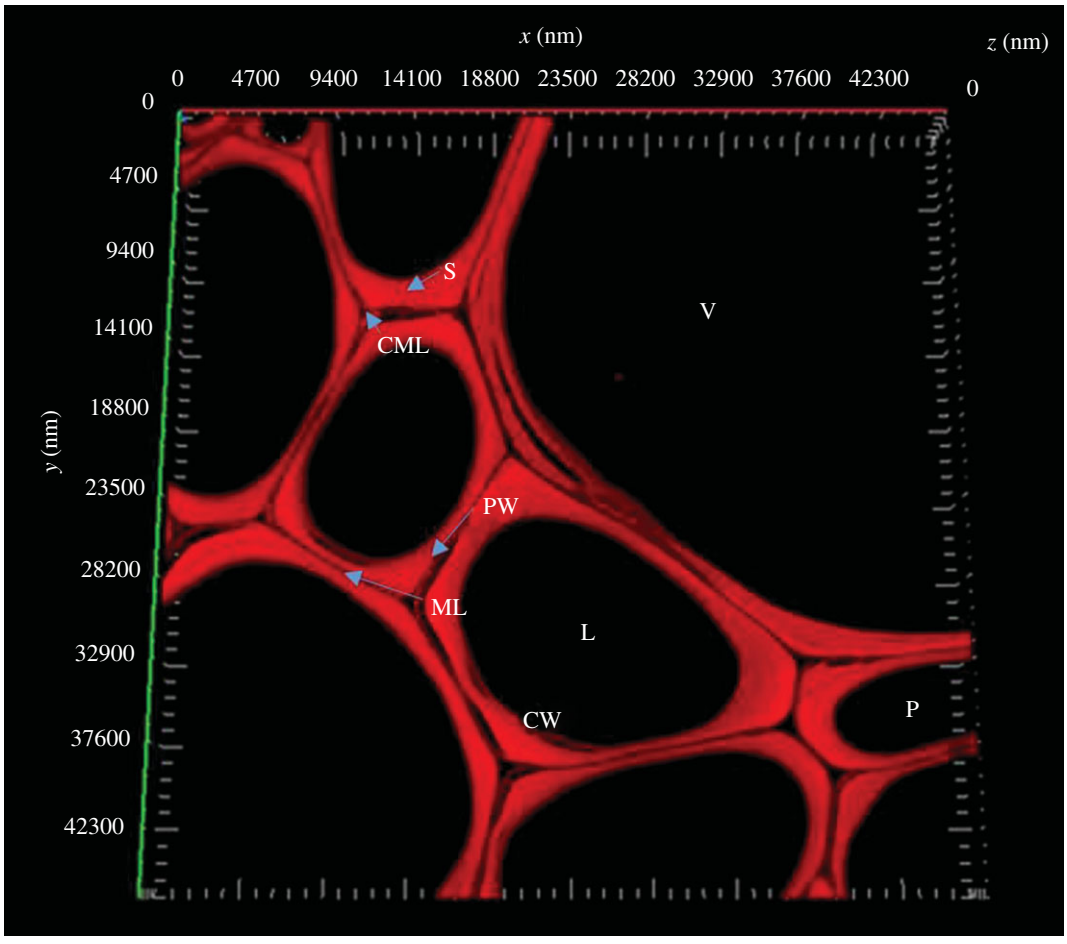

Figure 4. Confocal microscopy showing the cross-section cell wall structure with autofluorescence. V, vessel; S, second wall; P, parenchyma; L, lumen; PW, primary wall; ML, middle lamella; CML, compound middle lamella; CW, cell wall.

passing behind. The pores are arranged in radial files. The vessel members exhibit profuse vessel to vessel pitting. Small pores below 1 µm in size can be found between cell wall layers.

Figure 4 shows a cross section of the hemp shiv cell wall, imaged by CM, which is composed of intercellular material, the primary wall and the secondary wall. The secondary wall of the cell and middle lamella are clearly visible in ultra-thin transverse sections of hemp shiv. The dark staining of the middle lamella indicates that it is strongly lignified. Previous reports suggest that the secondary wall of hardwood consists of an outer layer (S1), a middle layer (S2) and an inner layer (S3) [12,27]. These could not be distinguished by CM because of the similarity in their chemical composition and the low resolution of CM. The thickness of the primary plus the secondary cell walls of hemp shiv was found to be in the range of 0.5–2 µm.

TEM was used to study the microstructure of cell wall in order to distinguish the layers of the secondary wall, as shown in figure 5. The boundary between primary wall and middle lamella was not clearly distinguishable due to its high density and extreme thinness. Therefore, both the middle lamella and the primary wall were referred to as compound middle lamella. The second wall was divided into an outer layer (S1), a middle layer (S2) and an inner layer (S3). The width of the S1 layer was about 0.2 µm. The S2 layer accounted for the largest proportion of the cell wall. The average thickness of the S2 layer was 0.6 µm. The cell wall also contained an S3 layer that was very thin and not clearly visible.

Figure 6 shows reconstructed sections of hemp shiv from CT scanning. The microtomographic constructions clearly show a high level of anatomical details, revealing the structure of larger vessels, ring boundaries, ray cells and tracheids. Figure 6*a* is a cross section of hemp shiv, which clearly shows there are some macropores with sizes between 20 and 50 µm in the hemp shiv. Figure 6*d* shows a cross-section image of hemp shiv segmented with the global LA-Kriging method [28,29] (threshold 125), which clearly shows the connection between the pores. The pore size and pore size distribution

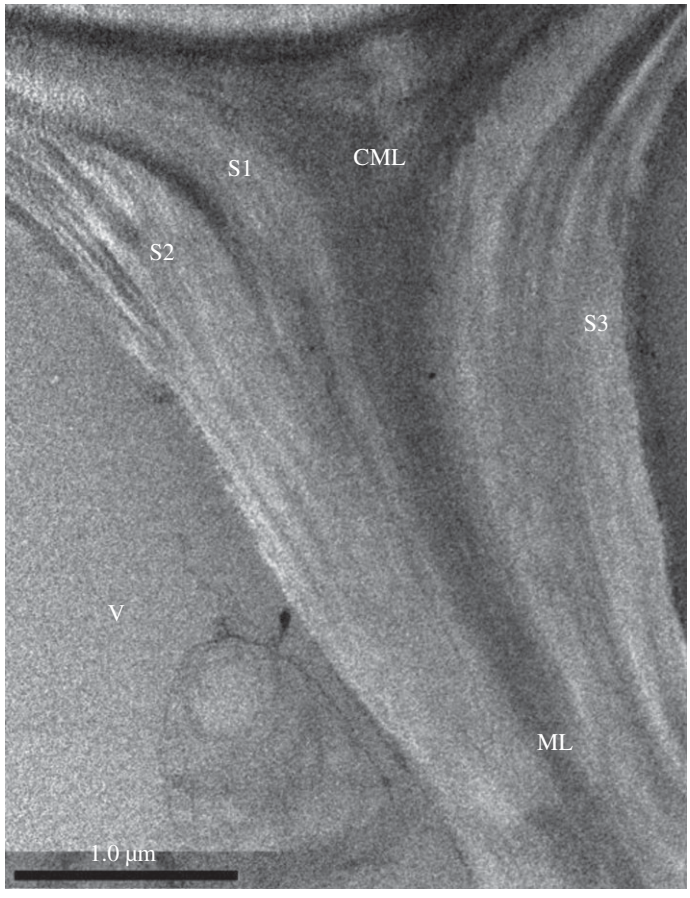

Figure 5. TEM micrographs of cross-section cell wall structure. V, vessel; S1, outer secondary wall of vessel; S2, middle secondary wall of vessel; S3, inner secondary wall of vessel; ML, middle lamella; CML, compound middle lamella.

of CT data are in good agreement with SEM images (figure 3). Figure 6*b* shows the microstructure of the inside of hemp shiv. It indicates that a large number of vessels are distributed throughout the hemp structure. The vessels are approximately 100 µm in diameter. Vessels tend to be distributed throughout the hemp shiv rather than preferentially occurring close to growth ring boundaries. Smaller hemp features, such as tracheids and fibres, are an order of magnitude smaller than vessels and require high resolution X-ray microtomography to see them. The CT images give a skeletonized view of the hemp shiv structure showing the orientation and connectivity of the vessels and tracheids. In addition, the full three-dimensional dataset shows the distribution of warts in the hemp shiv after extracting the lower density cell wall. Warts are generally developed in the inner most layer of the wood cell wall, called the warty layer. They are composed of high concentrations of lignin [30]. Figure 6*c* reveals the presence of a warty layer distinct from the S3 or S2 layer. The larger warts and aggregates with a spherical shape become clearly visible. They are not evenly distributed within the hemp shiv. The warts almost cover all the vessel and tracheid cell walls. They have a higher density compared to the cell wall. Evidence has indicated that lignin has a more condensed form in the warty layer than in other parts of the cell wall [30]. They have a wide range of particle size distribution from a few hundred nanometres to a few micrometres. They were also observed in the SEM image (figure 3*c*) and field emission SEM image (figure 7). This is the first report of a warty layer existing in a hemp shiv specimen.

Figure 7 shows the presence of a distinct warty layer with wart diameters in the range 50–200 nm. Large warts consist of an agglomeration of small ones. The warty layer is a remnant of the autolysed protoplast of the tracheal element and also the result of caving in of the S3 layer of the secondary wall inside the tracheid [30].

3.2. Porosity and pore size distribution

Table 1 shows the total mercury intrusion volume, total porosity and median pore diameter of hemp shiv studied by MIP measurement. The total intrusion volume of hemp shiv is on average

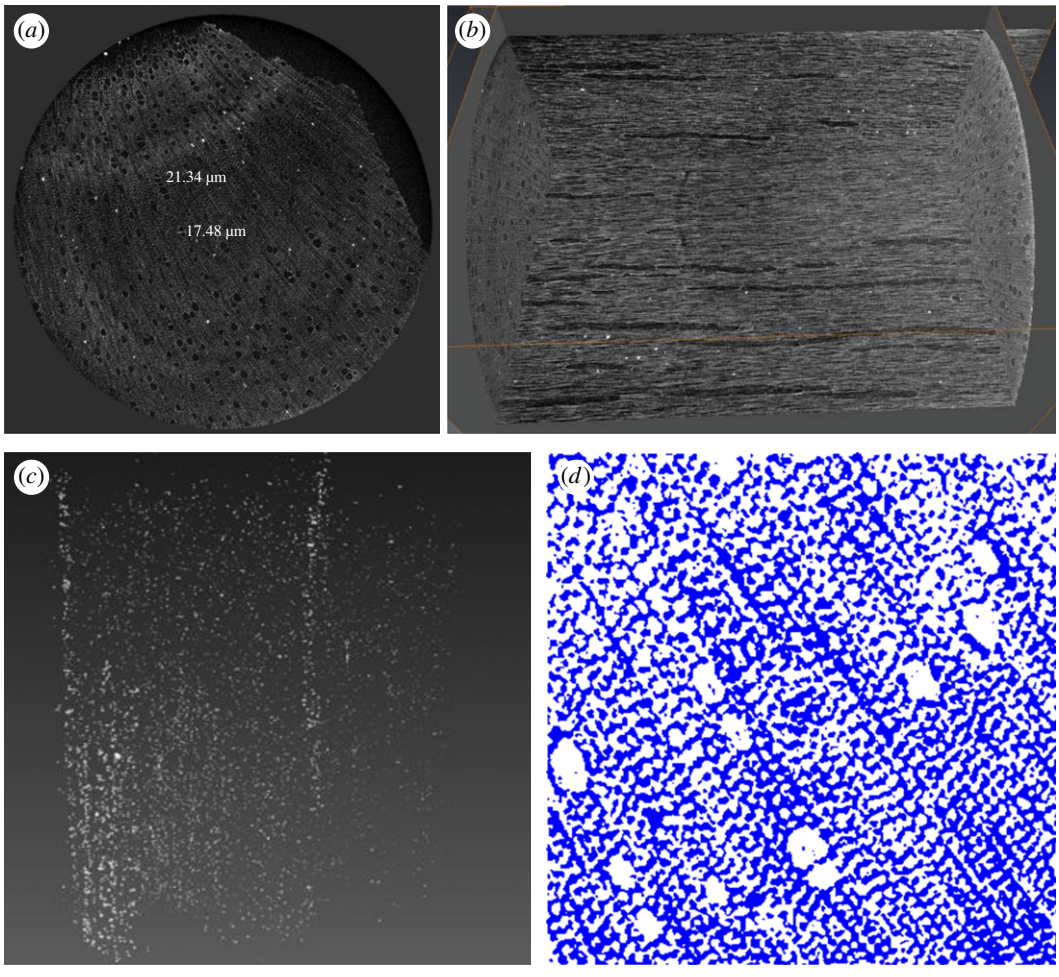

Figure 6. CT scanning measurement data: (*a*) volume rendering of a hemp shiv specimen cross section, (*b*) internal structure, (*c*) distribution of warts and (*d*) cross-section image segmented with the global LA-Kriging method (threshold 125). White is air pore and blue is solid.

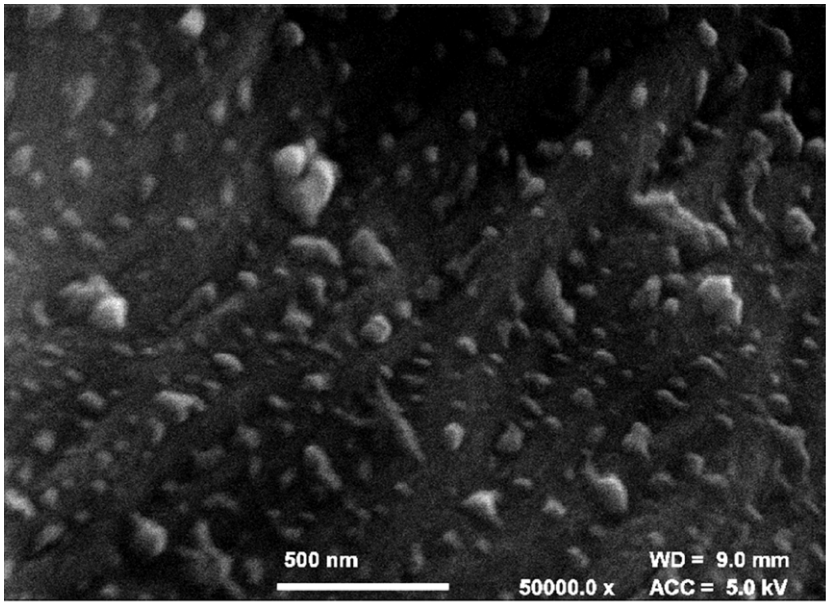

Figure 7. Field emission SEM observations of warts on the surface of cell wall of hemp shiv (radial, longitudinal section) $\times 50\,000$.

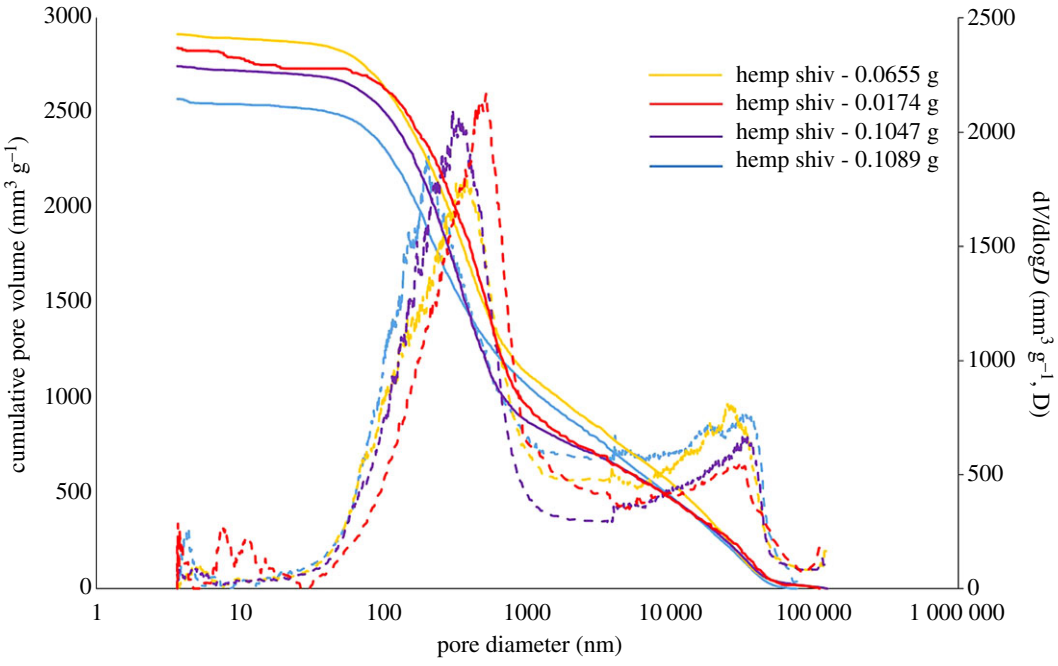

Figure 8. Cumulative pore volume and pore size distribution of hemp shiv with different sample masses determined by mercury intrusion porosimetry.

Table 1. Some porosity characteristics with ±standard errors for hemp shiv data as determined by mercury porosimetry within the pressure range of 0.0001–400 MPa.

hemp shiv (g)	total intrusion volume ($cm^3\ g^{-1}$)	total pore area ($m^2\ g^{-1}$)	median pore diameter (µm)	porosity (accessible) (%)	porosity (inaccessible) (%)
0.1047	2.429	49.81	0.52	77.93	0.24
0.0174	2.369	66.45	0.57	73.45	0.46
0.0655	2.574	63.49	0.54	78.78	0.40
0.1089	2.289	50.69	0.42	76.51	0.75
	2.415 ± 0.104	57.61 ± 7.44	0.51 ± 0.056	76.67 ± 2.03	0.46 ± 0.18

$2.415 \pm 0.104\ mm^3\ g^{-1}$ and the total pore surface area is $57.61 \pm 7.44\ m^2\ g^{-1}$. The total accessible porosity of hemp shiv is $76.67 \pm 2.03\%$. A possible compression of the samples, due to the applied high pressure during the MIP measurements, would influence the distribution of measured pore volumes. The hemp shiv used is the woody core of the hemp plant stalk (also known as hurd), as shown in figure 2*b*. Plotze *et al*. [31] showed that some wood samples (white lauan, Afzelia, Macassar ebony, Gaboon, beech, False acacia, Ramin and yew) have a very small sample compression of less than 5% of the measured cumulative pore volume. A further check was carried out by using varying amounts of hemp shiv, ranging from 0.0174 to 0.1089 g, for porosity and pore size distribution tests. No significant difference in porosity and pore size distribution was found among different amounts of sample (table 1 and figure 8). In addition, the pore size distribution measured by MIP shows a good agreement with the results of SEM (mentioned below). It indicated that the applied high pressure during the MIP measurements has little influence on the pore distribution of measured pore volumes. In this study, the common skeletal density of $1.47\ g\ cm^{-3}$ for the hemp shiv cell wall has been used to calculate the inaccessible porosity [19]. The results showed that the inaccessible porosity is about $0.46 \pm 0.18\%$. It indicates that there is only a small proportion of tiny pores or closed pores, which cannot be accessed by mercury. It is important to keep in mind that mercury porosimetry has the limitation of pore size (diameter between 3 nm and 100 µm). As shown in figure 2*b*, there are no voids in hemp shiv bigger than 100 µm. Thus, this technical restriction is not an issue for the test.

Table 2. Absolute densities of hemp shiv and fibre obtained by displacement with different liquids at 23°C.

sample type	displacement liquid	density of liquid (g cm^{-3})	size of shiv/fibre (L × W × H: mm)	number of tests	absolute density (g cm^{-3})
shiv	canola oil	0.92	7.6 × 2.4 × 1	3	0.965
shiv	canola oil	0.92	3.6 × 1.4 × 1	3	0.977
shiv	acetone	0.79	7.6 × 2.4 × 1	3	1.023
shiv	acetone	0.79	3.6 × 1.4 × 1	3	1.034
fibre	canola oil	0.92	7.6 × 0.1	3	1.545

Figure 8 shows cumulative pore volume and the pore size distribution curves for hemp shiv with various sample masses. Because of technical restrictions, the measurement of tracheids larger than 100 µm is excluded. Those pores are, on the one hand, important openings for intrusion but, on the other hand, easily accessible with very low or no applied pressure. As shown in figure 2*b*, there are no voids in hemp shiv bigger than 100 µm. Thus, this technical restriction is not an issue for the test. The pore sizes of hemp shiv show a bimodal pore size distribution with two clearly separated peaks. The main pore radius ranges from 0.03 µm to 1 µm with an average intrusion cumulative pore volume of 2.3 cm^3 g^{-1} and the second pore radius peak is between 20 µm and 80 µm with an average intrusion cumulative pore volume of 0.8 cm^3 g^{-1}. The intrusion cumulative pore volume in the range of 1 µm–20 µm pores is about 0.5 cm^3 g^{-1}. Nanoporosity is observed for smaller pores of around 3 nm with a lower peak intensity, which is at the limit of the sensitivity of the MIP technique. This could correspond to the micro-voids or cell wall capillaries. Examination of the SEM images (figure 3) shows that the 20–80 µm macro-voids are produced by the vessels. The 0.03–1 µm micro-voids correspond with the pit membrane voids, pit apertures and other small voids between cell walls. The voids in the range 1–20 µm correspond with the parenchyma cells. The MIP results show good agreement with the SEM images. All the samples show a very similar pore size distribution, although there are variations in peak heights between 3 nm and 10 nm.

3.3. Absolute density of hemp shiv substance obtained by displacement with helium gas, organic liquid and mercury

Table 2 shows the effect of different displacement liquids on the absolute density of hemp shiv with different particle sizes. The size of hemp shiv showed no effect on the densities obtained. It indicated that the equilibrium values are independent of particle size. With canola oil, a longer vacuum treatment was required to remove all of the air from the cell wall capillaries, but the results showed that the equilibrium value seems to be independent of the viscosity. There were only slight differences in the absolute density of hemp shiv obtained by using different displacement liquids. The absolute density of hemp fibre obtained by displacement with canola oil (around 1.545 g cm^{-3}) is much higher than that of hemp shiv (0.977 g cm^{-3}) measured by the same technique. It indicates that the microstructure of the cell wall has a significant effect on the density obtained. It also indicates that the displacement liquid achieves a lower penetration in hemp shiv due to the complexity of the pore structure. Repeat experiments in all cases resulted in a maximum observed deviation of 0.5% from the mean density value.

The average absolute densities of hemp fibre obtained from the displacement of liquid appear realistic. The MIP results showed that the hemp fibre contains predominantly large pores (greater than 10 µm), as evidenced by the MIP data in figure 9. The pore sizes of hemp shiv showed a totally different bimodal pore size distribution with two clearly separated peaks, as seen in figure 8. The main pore radius ranges from 0.01 to 1 µm and the second pore radius peak is between 2 and 60 µm. It can, therefore, be assumed that tracheids and cell walls of hemp fibre are freely accessible to canola oils. However, the small pores in hemp shiv (less than 2 µm) are inaccessible to the replacement liquid. The assumption can be confirmed by the colour resin filtration test. Figure 10 clearly shows that the resin cannot reach all the pores in the hemp shiv after the colour resin filtration treatment. Some cells of the lumen and nearly all large vessel pores have been filled with resin. However, there is still a high ratio of tracheid cells inaccessible to the resin. Some of them are partially filled with resin. As a result, the volume of hemp shiv determined is overstated, and consequently the calculated density is understated.

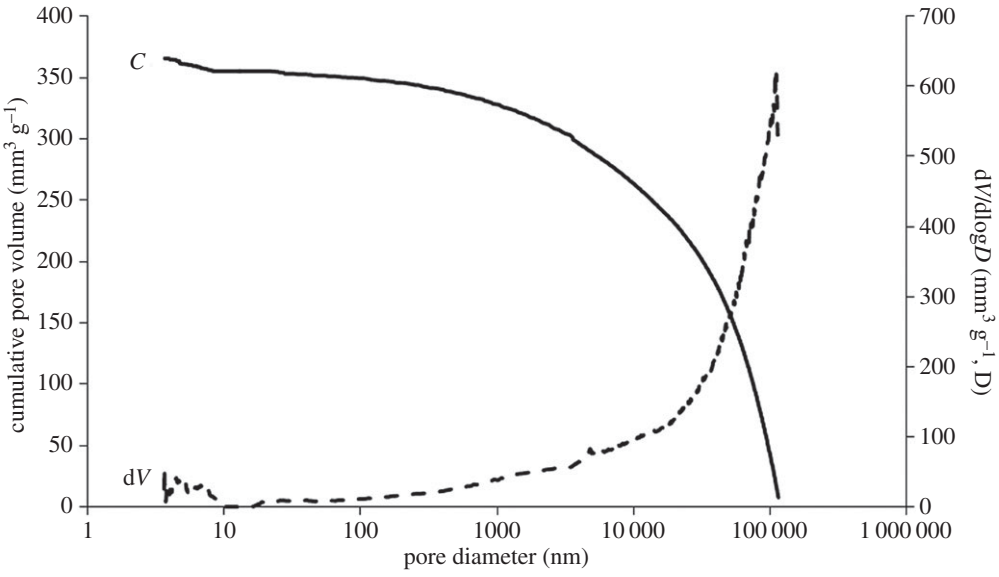

Figure 9. Cumulative pore volume versus pore size distribution for hemp fibre determined by mercury intrusion porosimetry.

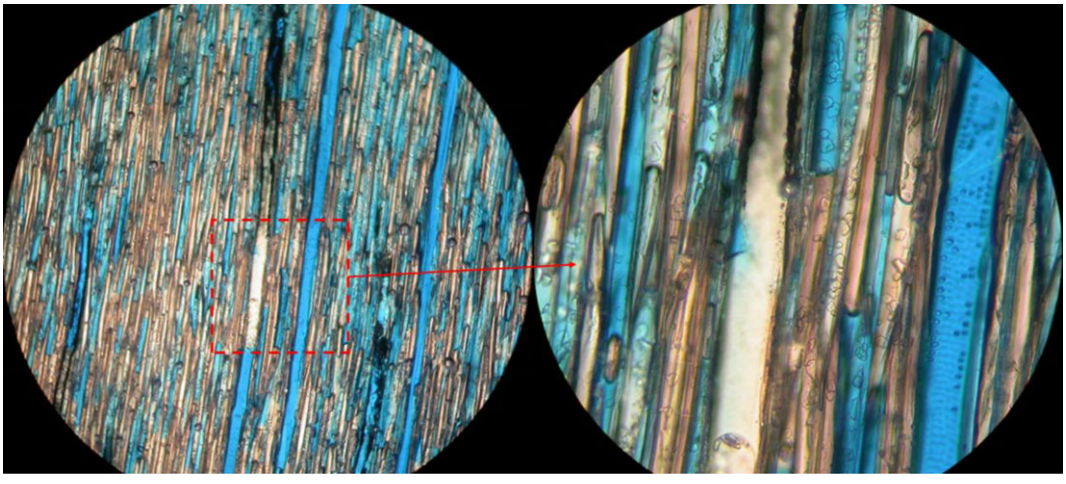

Figure 10. Optical microscopy for colour resin penetration effect in the vessels.

Table 3. Absolute density of hemp shiv, obtained by displacement with helium gas at 23°C.

displacement gas	size of shiv (L × W: mm)	number of determinations	absolute density of hemp shiv (g cm^{-3})	density s.d. (g cm^{-3})
helium	7.6 × 2.4	10	0.947	0.0023
helium	1.6 × 0.4	10	0.958	0.0031

Table 3 presents the absolute densities of oven dry hemp shiv as a function of the sample dimensions. Measurements using helium gas for displacement were undertaken on the assumption that immersion in helium gas gave the true volume of the hemp shiv. The results clearly show that the true densities of hemp shiv obtained from gas replacement are similar to the absolute density results obtained from liquid replacement. This is primarily due to the inaccessibility of some uncut cell lumens or cell walls due to the complexity of the cell wall microstructure. The results also showed that the sample size has no significant effect on the calculated density value.

Table 4. Absolute density of hemp shiv substance obtained by displacement with mercury at 23°C.

sample type	displacement liquid	size of shiv/fibre (L × W: mm)	bulk density of hemp shiv/fibre × (g cm^{-3})	absolute density (g cm^{-3})
shiv	mercury	7.6 × 2.4	0.306	1.443
shiv	mercury	1.6 × 0.4	0.321	1.454
fibre	mercury	7.6 × 0.1	0.984	1.519

It can, therefore, be considered that the displacement of gas or liquid methods is not suitable to measure the density of hemp shiv without special sample preparation, such as high temperature drying or chemical surface treatment. They will give a falsely low density due to the presence of inaccessible pores.

We already know that pressure can push liquid into small pores without special sample preparation. Thus, the real density of the hemp shiv can be measured only by MIP, if there is no sample compression or collapse under pressurization. Table 4 presents the bulk densities and absolute density of hemp shiv and fibre measured by MIP. The absolute densities of hemp shiv obtained by MIP are significantly higher than the densities obtained by the displacement of canola oil or acetone compared with the displacement of liquid measurement. However, the density of hemp fibre obtained by MIP (1.519 g cm^{-3}) is slightly lower than the density obtained by the displacement of canola oil (1.545 g cm^{-3}). The results indicate that the mercury has intruded into the small pores in the hemp shiv at high pressure. There are no extra pores that can been filled with mercury at high pressure. The pores in hemp fibre can be fully filled by replacement liquid without extra pressure due to their large pore size. The absolute density of hemp fibre being higher than that of hemp shiv can be explained by the different ratio of three main components in hemp shiv and hemp fibre. Although the hemp shiv and hemp fibre mainly consist of lignin, hemi-cellulose and cellulose, the ratio of the chemical compositions between hemp fibre and hemp shiv is slightly different. The hemp fibre contains less lignin (2–5%) than hemp shiv (19–28%) [32]. The specific density of these three chemical components is slightly different. Lignin has the lowest specific density (1.26–1.41 g cm^{-3}) compared to cellulose (1.53–1.57 g cm^{-3}) and hemicelluloses (1.50–1.54 g cm^{-3}) [32–34]. Thus, the absolute density of hemp fibre is slightly higher than that of hemp shiv. Stamm [35] measured the cell wall density of 10 wood species using three types of displacement media. The measured density ranged from 1.46 to 1.55 g cm^{-3}. Kellogg & Wangaard [36] reported that the cell wall density for wood species ranged from 1.46 to 1.53 g cm^{-3}. According to the chemical composition of hemp shiv, the cell wall density of hemp shiv should be similar to the literature values for wood species. It means that the MIP method can give a realistic absolute density of hemp shiv without a special sample pretreatment. Furthermore, according to the bulk density (0.32 g cm^{-3}) of hemp shiv from MIP data, the porosity of hemp shiv can be determined to be approximately 67% by using the absolute density of displacement of canola oil (0.97 g cm^{-3}). Compared to the porosity of hemp shiv obtained from MIP (78%), it can be deduced that around 10% of the pores in hemp shiv are inaccessible to the displacement of canola oils.

4. Conclusion

The scanning electron microscope observations of hemp shiv showed distinctive microstructures. The vessels exhibit little variation in size with no clear pore arrangement, resulting in a diffuse-porous distribution. The vessels are mostly solitary although some small groups of adjacent vessels exhibit shared cell walls between them. The vessels are approximately 50–80 µm in diameter and are surrounded by a relatively thick cell wall. Thick-walled fibres are located between the vessels with a diameter from 1 to 3 µm. The confocal images clearly showed the secondary wall and middle lamella in the ultra-thin transverse sections of hemp shiv. The dark staining of middle lamella indicated that it was strongly lignified. The TEM showed the second wall was divided into an outer layer (S1), a middle layer (S2) and an inner layer (S3). CT tomography revealed more detail of the pore shape and pore connection structures of hemp shiv and showed a three-dimensional structure of warts in the hemp shiv. The presence of a warty layer in hemp shiv is reported for the first time. The average accessible porosity of hemp shiv is 76.67 ± 2.03% by MIP measurement. The combination of several techniques and comparison of the results of cell wall structure provides an insight into the complex pore system of hemp shiv, and potentially

other similar bio-aggregates across a wide range of pore size distributions, including flax shiv, rape shiv and corn cob. Methods using the displacement of gas or liquid are not suitable for measuring the density of hemp shiv without special sample preparation, such as high temperature drying or chemical surface treatment. They will give a falsely low density due to the presence of around 10% by volume of inaccessible pores. The MIP method can give a realistic real density and porosity of hemp shiv without special sample preparation and is recommended as the appropriate technique for characterization of the pore structure of hemp shiv and other similar bio-aggregates.

Data accessibility. The datasets supporting this article can be found in the following link: http://dx.doi.org/10.5061/dryad.8t8v6 [37].

Authors' contributions. Y.H.J. and M.L. participated in the design of the study and drafted the manuscript. M.A. carried out the SEM experiments and the analyses. Y.H.J. and A.H. conducted the experiments and participated in data analysis. All authors gave final approval for publication.

Competing interests. We declare we have no competing interests.

Funding. The work presented here was carried out under the ISOBIO project, with funding from the European Union's Horizon 2020 research and innovation programme, under grant agreement no. 636835.

Acknowledgments. We thank Ursula Potter and Diana Lednitzky for helpful discussions.

References

1. Magniont C, Escadeillas G, Coutand M, Oms-Multon C. 2012 Use of plant aggregates in building ecomaterials. *Eur. J. Environ. Civil Eng.* **16**, s17–s33. (doi:10.1080/19648189.2012.682452)
2. Chabannes M, Nozahic V, Amziane S. 2015 Design and multi-physical properties of a new insulating concrete using sunflower stem aggregates and eco-friendly binders. *Mater. Struct.* **48**, 1815–1829. (doi:10.1617/s11527-014-0276-9)
3. Shea A, Lawrence M, Walker P. 2012 Hygrothermal performance of an experimental hemp–lime building. *Const. Build. Mat.* **36**, 270–275.
4. Collet F, Pretot S. 2014 Experimental highlight of hygrothermal phenomena in hemp concrete wall. *Build. Environ.* **82**, 459–466. (doi:10.1016/j.buildenv.2014.09.018)
5. Barclay M, Holcroft N, Shea AD. 2014 Methods to determine whole building hygrothermal performance of hemp–lime buildings. *Build. Environ.* **80**, 204–212. (doi:10.1016/j.buildenv.2014.06.003)
6. Mazhoud B, Collet F, Pretot S, Chamoin J. 2016 Hygric and thermal properties of hemp-lime plasters. *Build. Environ.* **96**, 206–216. (doi:10.1016/j.buildenv.2015.11.013)
7. Collet F, Pretot S. 2014 Thermal conductivity of hemp concretes: variation with formulation, density and water content. *Const. Build. Mat.* **65**, 612–619. (doi:10.1016/j.conbuildmat.2014.05.039)
8. Walker R, Pavía S. 2014 Moisture transfer and thermal properties of hemp–lime concretes. *Const. Build. Mat.* **64**, 270–276. (doi:10.1016/j.conbuildmat.2014.04.081)
9. Latif E, Tucker S, Ciupala MA, Wijeyesekera DC, Newport D. 2014 Hygric properties of hemp bio-insulations with differing compositions. *Const. Build. Mat.* **66**, 702–711. (doi:10.1016/j.conbuildmat.2014.06.021)
10. Lawrence, M, Fodde E, Paine K, Walker P. 2012 Hygrothermal performance of an experimental hemp-lime building. *Key Eng. Mater.* **517**, 413–421. (doi:10.1016/j.conbuildmat.2012.04.123)
11. Dubois S, Evrard A, Lebeau F. 2014 Modeling the hygrothermal behavior of biobased construction materials. *J. Build. Phys.* **38**, 191–213. (doi:10.1177/1744259113489810)
12. Bismarck A, Aranberri-Askargorta I, Springer J, Lampke T. 2002 Surface characterization of flax, hemp and cellulose fibers; surface properties and the water uptake behavior. *Polym. Compos.* **23**, 872–894. (doi:10.1002/pc.10485)
13. Brewer CE, Chuang VJ, Masiello CA, Gonnermann HX. 2014 New approaches to measuring biochar density and porosity. *Biomass Bioenergy* **66**, 176–185. (doi:10.1016/j.biombioe.2014.03.059)
14. Chundawat SP, Donohoe BS, Costa Sousa L, Elder T. 2011 Multi-scale visualization and characterization of lignocellulosic plant cell wall deconstruction during thermochemical pretreatment. *Energy Environ. Sci.* **4**, 973–984. (doi:10.1039/C0EE00574F)
15. Collet F, Bart M, Serres L, Miriel J. 2008 Porous structure and water vapour sorption of hemp-based materials. *Const. Build. Mat.* **22**, 1271–1280. (doi:10.1016/j.conbuildmat.2007.01.018)
16. Donato I, Lazzara G. 2012 Porosity determination with helium pycnometry as a method to characterize waterlogged woods and the efficacy of the conservation treatments. *Archaeometry* **54**, 906–915. (doi:10.1111/j.1475-4754.2011.00657.x)
17. Hamdi SE, Delisée C, Malvestio J, Da Silva N. 2015 X-ray computed microtomography and 2D image analysis for morphological characterization of short lignocellulosic fibers raw materials: a benchmark survey. *Comp. Part A Appl. Sci. Manuf.* **76**, 1–9. (doi:10.1016/j.compositesa.2015.04.019)
18. Jerram DA, Higgins MD. 2007 3D analysis of rock textures: quantifying igneous microstructures. *Elements* **3**, 239–245. (doi:10.2113/gselements.3.4.239)
19. Anovitz LM, Cole DR. 2015 Characterization and analysis of porosity and pore structures. *Rev. Mineral. Geochem.* **80**, 8061–8164. (doi:10.2138/rmg.2015.80.04)
20. Hill CAS, Forster SC, Farahani MRM, Hale MDC, Ormondroyd GA, Williams GR. 2004 An investigation of cell wall micropore blocking as a possible mechanism for the decay resistance of anhydride modified wood. *Int. Biodeterior. Biodegrad.* **55**, 69–76. (doi:10.1016/j.ibiod.2004.07.003)
21. Zauer M, Pfriem A, Wagenfuhr A. 2013 Toward improved understanding of the cell wall density and porosity of wood determined by gas pycnometry. *Wood Sci. Technol.* **47**, 1197–1211. (doi:10.1007/s00226-013-0568-1)
22. Nguyen T, Picandet V, Amziane S, Baley C. 2009 Influence of compactness and hemp hurd characteristics on the mechanical properties of lime and hemp concrete. *Eur. J. Environ. Civil Eng.* **13**, 1039–1050. (doi:10.1080/19648189.2009.9693171)
23. Manger GE. 1963 *Porosity and bulk density of sedimentary rocks*. Washington, DC: USGPO.
24. Amziane S, Collet F. 2017 Bio-aggregates based building materials: state of the art report of the RILEM technical committee 236-BBM (RILEM State-of-the-Art Reports). Dordrecht, The Netherlands: Springer. (doi:10.1007/978-94-024-1031-0)
25. Mwaikambo LY, Ansell MP. 2002 Chemical modification of hemp, sisal, jute and kapok fibers by alkalization. *J. Appl. Polym. Sci.* **84**, 2222–2234. (doi.org/10.1002/app.10460).
26. Washburn EW. 1921 The dynamics of capillary flow. *Phys. Rev.* **17**, 273–283. (doi:10.1103/PhysRev.17.273)
27. Zhou X, Ding D, Ma J, Ji Z, Zhang X, Xu F. 2015 Ultrastructure and topochemistry of plant cell wall by transmission electron microscopy. In *The transmission electron microscope: theory and applications* (ed. K Maaz), ch. 12. InTechOpen.
28. Kittler J, Illingworth J. 1986 Minimum error thresholding. *Pattern Recognit.* **19**, 41–47. (doi:10.1016/0031-3203(86)90030-0)
29. Oh W, Lindquist WB. 1999 Image thresholding by indicator Kriging. *IEEE Trans. Pattern Anal. Mach. Intell.* **21**, 590–602. (doi:10.1109/34.777370)
30. Kuo M, Manwiller F. 1986 Morphological and chemical characteristics of the warty layer in red pine (*Pinus resinosa* Ait). *Wood Fiber Sci.* **18**, 239–247.
31. Plotze M, Niezmz P. 2011 Porosity and pore size distribution of different wood types as determined by mercury intrusion porosimetry. *Eur. J. Wood Products* **69**, 649–657. (doi:10.1007/s00107-010-0504-0)

32. Thomsen AB, Rasmussen SK, Bohn V, Nielsen KV, Thygesen A. 2005 Hemp raw materials: the effect of cultivar, growth conditions and pretreatment on the chemical composition of the fibres. Risø National Laboratory, Report No.: R-1507.
33. Gibson LJ. 2012 The hierarchical structure and mechanics of plant materials. *J. R. Soc. Interf.* **9**, 2749–2766. (doi:10.1098/rsif.2012.0341)
34. Meisam KH, Lik-ho T, Denvid L, Yang L. 2016 Viscoelastic damping behavior of structural bamboo material and its microstructural origins. *Mech. Mater.* **97**, 184–198. (doi:10.1016/j.mechmat.2016.03.002)
35. Stamm AJ. 1929 Density of wood substance, adsorption by wood, and permeability of wood. *J. Phys. Chem.* **33**, 398–414. (doi:10.1021/j150297a008)
36. Kellogg R, Wangaard F. 1969 Variation in the cell wall density of wood. *Wood Fiber Sci.* **1**, 180–204.
37. Jiang Y, Lawrence M, Ansell MP, Hussain A. 2018 Data from: Cell wall microstructure, pore size distribution and absolute density of hemp shiv. Dryad Digital Repository. (http://dx.doi.org/10.5061/dryad.8t8v6)

Commentary Text

The work reported in this paper has been published in collaboration with other co-authors who are also working under the ISOBIO project. The experimental work conducted by me in this paper was focused on determining hemp shiv porosity using MIP technique. This data is useful for understanding the high water absorption and hydrophilic behaviour of hemp shiv that is discussed in the next Chapters.

In this paper, the porosity and pore structure of hemp shiv have been evaluated using various techniques. It was reported that hemp shiv has very high porosity of 76.67 ± 2.03% and a complex internal pore system. The pore size distribution curves show a bimodal distribution with two clearly separated peaks. The main pore radius ranged from 0.03 – 1 µm and the second peak pore radius was between 20 – 80 µm. Pore size distribution of hemp shiv has been reported using MIP. The microstructure of hemp shiv studied using SEM shows the presence of vessels within the cell wall having a diameter of approximately 50 – 80 µm corresponding the second peak of the MIP pore size distribution curve. The 0.3 – 1 µm pores correspond to the pit membrane voids, pit apertures and small voids between the cell walls as seen through the SEM. The pores in the range of 1 – 20 µm correspond to the parenchyma cells. The MIP data showed good agreement with the SEM analysis. It was also analysed through the SEM images, that none of the voids were larger than 100 µm which is the upper limit of the MIP technique. Therefore, MIP technique can be considered useful for studying the porosity of hemp shiv without having technical restrictions. However, a small volume of inaccessible porosity 0.46 ± 0.18% indicated that there are few tiny or closed pores which cannot be accessed by mercury. Further studies on the effect of silica deposition on both the surface and within the pores of hemp shiv is reported in the next Chapter.

Chapter 4

MTES based Water Repellent Coatings

This chapter has been published as a Journal paper entitled “Modification of hemp shiv properties using water-repellent sol-gel coatings” in Journal of Sol-Gel Science and Technology (Hussain, Calabria-Holley, Jiang, & Lawrence, 2018).

Introductory Text

This paper reports the novel use of sol-gel technology within the building industry for deposition of coatings on hemp shiv. To the best of our knowledge, this is the first time hemp shiv is modified using sol-gel based coatings. In this work, coatings were formulated using tetraethyl orthosilicate (TEOS), ethanol, water and nitric acid. Methyltriethoxysilane (MTES) was added for the hydrophobic functionalisation and dimethyl formamide (DMF) was added as the drying control additive. This formulation had been developed and used earlier on adobe bricks by one of the co-authors of this paper to provide water resistance to the material (Calabria A. et al., 2010).

The application of this coating formulation on hemp shiv for water resistance as well as its impact on moisture buffering capacity of hemp shiv has been discussed in this chapter. In addition, the effect of coating deposition and its thickness on the porosity of hemp shiv was investigated. It was seen that the number of coating layers directly influence the water absorption capacity of hemp shiv. However, increased deposition layers have a negative impact on the moisture buffering capacity as the pores within hemp shiv are blocked by the coating.

Statement of Authorship

This declaration concerns the article entitled:									
Modification of hemp shiv properties using water-repellent sol–gel coatings.									
Publication status (tick one)									
draft manuscript		**Submitted**		**In review**		**Accepted**		**Published**	✓
Publication details (reference)	Hussain, A., Calabria-Holley, J., Jiang, Y., & Lawrence, M. (2018). Modification of hemp shiv properties using water-repellent sol–gel coatings. Journal of Sol-Gel Science and Technology, 86(1), 187–197. http://doi.org/10.1007/s10971-018-4621-2								
Candidate's contribution to the paper (detailed, and also given as a percentage).	The candidate contributed to/ considerably contributed to/predominantly executed the… Formulation of ideas: 90% A. Hussain presented the main idea of this work and discussed with his supervisors M.Lawrence and J. Calabria-Holley. Design of methodology: 80% A. Hussain designed the methodology to achieve the aims of this study. The co-authors shared their expertise. Experimental work: 100% A. Hussain did all the experiments and the data analysis. Presentation of data in journal format: 90% A. Hussain prepared the manuscript. All co-authors gave feedback and comments to improve the manuscript.								
Statement from Candidate	This paper reports on original research I conducted during the period of my Higher Degree by Research candidature.								
Signed	Atif				**Date**	15.09.2018			

Copyrights and Permission

Copyright information

About this article

Check for updates

Cite this article as:
Hussain, A., Calabria-Holley, J., Jiang, Y. et al. J Sol-Gel Sci Technol (2018) 86: 187. https://doi.org/10.1007/s10971-018-4621-2

DOI
https://doi.org/10.1007/s10971-018-4621-2

Publisher Name
Springer US

Print ISSN
0928-0707

Online ISSN
1573-4846

About this journal

Reprints and Permissions

Published in cooperation with
The International Sol Gel Society

Publication title:

Modification of hemp shiv properties using water-repellent sol–gel coatings.

Thesis page numbers that it spans:

89 to 99

Journal of Sol-Gel Science and Technology (2018) 86:187–197
https://doi.org/10.1007/s10971-018-4621-2

ORIGINAL PAPER: SOL-GEL AND HYBRID MATERIALS FOR ENERGY, ENVIRONMENT AND BUILDING APPLICATIONS

Modification of hemp shiv properties using water-repellent sol–gel coatings

Atif Hussain[1] · Juliana Calabria-Holley[1] · Yunhong Jiang[1] · Mike Lawrence[1]

Received: 4 October 2017 / Accepted: 24 February 2018 / Published online: 10 March 2018

Abstract

For the first time, the hydrophilicity of hemp shiv was modified without the compromise of its hygroscopic properties. This research focused on the use of sol–gel method in preparation of coatings on the natural plant material, hemp shiv, that has growing potential in the construction industry as a thermal insulator. The sol–gel coatings were produced by cohydrolysis and polycondensation of tetraethyl orthosilicate (TEOS) using an acidic catalyst. Methyltriethoxysilane (MTES) was added as the hydrophobic precursor to provide water resistance to the bio-based material. Scanning electron microscopy (SEM) and focused ion beam (FIB) have been used to determine the morphological changes on the surface as well as within the hemp shiv. It was found that the sol–gel coatings caused a reduction in water uptake but did not strongly influence the moisture sorption behaviour of hemp shiv. Fourier transformed infrared (FTIR) spectroscopy shows that the coating layer on hemp shiv acts a shield, thereby lowering peak intensity in the wavelength range 1200–1800 cm^{-1}. The sol–gel coating affected pore size distribution and cumulative pore volume of the shiv resulting in tailored porosity. The overall porosity of shiv decreased with a refinement in diameter of the larger pores. Thermal analysis was performed using TGA and stability of coated and uncoated hemp shiv have been evaluated. Hemp shiv modified with sol–gel coating can potentially develop sustainable heat insulating composites with better hygrothermal properties.

Graphical Abstract

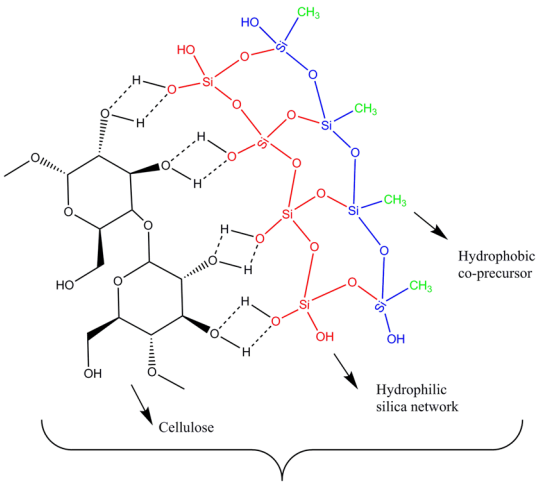

✉ Atif Hussain
A.Hussain@bath.ac.uk

[1] BRE Centre for Innovative Construction Materials, Department of Architecture and Civil Engineering, University of Bath, Bath BA2 7AY, UK

Keywords Sol–gel · Dip-coating · Water repellence · Hygroscopic · Bio-based materials

Highlights

- A novel method for modification of hemp shiv using sol-gel technology.
- Coating layer acts as a breathable membrane allowing the hemp shiv to retain its hygric characteristics.
- Hemp shiv coated with sol-gel monolayer reduces its water absorption capacity by 200%.
- The effects of sol-gel coating on surface morphology, thermal stability and porosity of the shiv increase with increase in coating thickness.

1 Introduction

The use of bio-based materials (derived from plant sources) have become increasingly popular to produce economical engineering materials in the construction industry [1]. Bio-based materials have numerous advantages over conventional non-renewable building materials such as lower embodied energy, lower CO_2 emissions of buildings and demand for in-use energy can be significantly reduced through passive environmental control [2]. Other advantages of bio-based materials include good specific strength, lower density, economic viability, biodegradability, non-irritant nature and good heat capacity [3].

Several studies have discussed the ability of bio-based materials used in construction to absorb and release moisture in response to changes in relative humidity (RH) in the surroundings which creates a breathable wall. These materials act as a hygric buffer and eventually reduce the energy demands for air conditioning [4]. The response to varying humidity conditions is linked to their pore structure and pore connectivity where the moisture condenses and evaporates on the surface of the material and within its pores. This leads to an increased effective thermal mass, allowing the bio-based material to behave as a thermal buffer in addition to their hygric buffering characteristics [5].

Towards the end of the 20th century, a bio-based building material was rediscovered which used the woody core or shiv of hemp (Cannabis Sativa L.) and lime based binders to produce hemp concrete. Hemp shiv has very low conductivity compared to lime due to its porous structure. Many studies have been conducted over the recent years to optimise the hemp characteristics, curing conditions and binder content during the production of hemp based concrete. Hemp insulation materials show good hygrothermal properties by regulating humidity inside buildings and has low environmental impact [6, 7]. The major constituents of industrial hemp shiv are: cellulose (44%), hemicellulose (18–27%), lignin (22–28%) and other components such as extractives (1–6%) and ash (1–2%) [8].

Considering bio-based insulation material to be a part of a vapour permeable wall, significant benefits can be achieved such as better indoor air quality [9] and robustness of fabric. For example when moisture is allowed to penetrate through the fabric of the wall the risk of moisture build-up is considerably reduced [10]. Under suitable environmental conditions, bio-based materials are durable and long-lasting. However, in presence of excess moisture, these materials are susceptible to decay and therefore it is not advisable to use them below damp proof courses or in areas which could get wet.

Hemp shiv has tendency to absorb large amounts of water due to its highly porous structure and presence of hydrophilic hydroxyl groups in its structure. This leads to certain disadvantages of using bio-based materials making them incompatible with hydrophobic thermoset/thermoplastic polymers causing poor adhesion in the matrix interface of the composites [11]. There is a high competition between the binders used with bio-based material due to the wide use of different binders in construction. Since the shiv competes with the binder for the available water, purely hydraulic binders like lime or cement cannot hydrate completely, leading to a powdery inner core in the hemp-lime walls which is poorly bound.

As a result, during the manufacture of hemp concrete, water is added in significant excess amounts compared to what is actually needed for the hydration of lime. This leads to long drying times ranging from several months to over a year which are not acceptable to be employed at an industrial scale [12]. Large water absorption capacity of bio-based materials can even cause problems in the end product stage when undesirable water comes in contact or if the surroundings are humid. Previous studies have reported that hemp shiv not only has higher water absorption rate but also absorb high amounts of water in the very first minutes compared with other plant materials [13].

Several studies have reported the improvement in mechanical properties of natural-fibre composites through alkali [14, 15], acetyl [16] and silane [17, 18] treatment of plant fibres. The chemical treatments react with the hydroxyl groups and improve the hydrophobic characteristics of fibres [19, 20]. The sol–gel technique is a highly versatile method to deposit silica based coatings possessing single or multi functionality [21–23]. These thin mesoporous coatings have high structural homogeneity and their adhesion can be tailored to different substrates [24, 25]. Sol–gel based hydrophobic and water-repellent coatings have been

investigated on different plant based materials such as wood [26, 27] and cellulosic based materials [28–30]. Wood and cellulosic fibres modified with sol–gel material showed significant reduction in flammability and enhanced fire-resistance properties. [31, 32].

The objective of this work was to treat the hemp shiv with a silica sol–gel coating functionalised with a hydrophobic agent in order to foster hydrophobicity of the hemp shiv. Our work focuses on creating a breathable coating around the shiv and investigate how the change in surface chemistry can alter the physical properties of the hemp shiv.

2 Materials and methods

Hemp shiv used in this study was received from CAVAC, an agricultural cooperative based in northwest France. The sol–gel was synthesised by hydrolysis and condensation of tetraethyl orthosilicate (TEOS) in ethanol and water. The reaction was catalysed by nitric acid. 1 M of TEOS was added to a mixture of 8 M distilled water, 4 M of absolute ethanol and 0.005 M of nitric acid. 0.33 M of methyltriethoxysilane (MTES) was added to the above mixture as the hydrophobic agent. Finally, 0.33 M of drying control chemical additive N, N-dimethylformamide was added. The sol was vigorously stirred at 40 °C and atmospheric pressure for nearly 2 h. All the chemicals were obtained from Sigma-Aldrich.

Gelation took place in situ in which pieces of hemp shiv were dipped in the sol for 10 min and then carefully removed and transferred onto a Petri dish. The samples were placed in an oven at 40 °C for 1 h and then dried at 80 °C for 2 h. The residual water content was calculated by sealing the oven dried samples in a glass tube under vacuum, heating them at 150°C overnight and then weighing the sample. The amount of residual water was 5 wt% for the sol–gel coated samples.

For preparation of the silica the sol was allowed to age in a container to a gel state at room temperature for 48 h The gel underwent dehydration at 80 °C for 120 h to obtain the silica.

2.1 Surface morphology

Photomicrographs of coated and uncoated hemp shiv samples were captured using a dual beam focused ion beam (FIB) system model FEI Helios NanoLab 600. This system is equipped with an extremely high resolution Elstar scanning electron microscopy (SEM) column and a fine-probe ion source. A high beam current of gallium ions was used for site specific sputtering and milling to prepare a specific area within the sample. All the samples were gold coated using an Edwards Scancoat Gold Sputter Coater. A further layer of platinum was deposited on the areas where higher beam current of gallium ions was used.

2.2 Water absorption test

To eliminate initial moisture content, the hemp shiv samples were dried overnight in an oven at 80 °C and then weighed to the nearest 0.1 mg. The samples were then completely immersed in water without using any external force. Since the density of shiv is lower than water, the samples were expected to float. Hence most of the water uptake observed was due to capillary action. The samples were removed at frequent intervals, shaking off any visible surface water and weighed to the nearest 0.1 mg within 30 s of removal from water. Mass readings were taken regularly for the next 24 h and the water absorption was calculated by the mass change (%). The readings reported were average of three measurements.

2.3 Dynamic vapour sorption

Isotherm analysis of uncoated and coated hemp shiv was carried out using a dynamic vapour sorption apparatus (DVS Advantage, Surface Measurement Systems). Hemp shiv samples were prepared weighing ~15 mg and placed on the sample holder, combined with a microbalance by a hanging wire. The instrument was maintained at constant temperature of 23 °C and the RH was increased in steps in the following sequence (0, 10, 20, 30, 40, 50, 60, 70, 80 and 90% RH), before decreasing to 0% RH in the reverse order. Each RH step change was programmed to move to the next when the moisture content was stable for duration of at least 10 minutes ($dm/dt < 0.002\%$). However, it should be noted that the maximum time allowed for each RH step to reach stability was 360 min. Previous studies have established that this value allows for obtaining equilibrium moisture content (EMC) values within 0.1% of the true equilibrium value [33]. The target RH, actual RH, running time and sample mass were recorded throughout the isotherm run.

2.4 Calculation of moisture content

Moisture content was calculated using the DVS data based on the mass of treated and untreated shiv as per the following equations:

$$\mathrm{MC} = \frac{m_2 - m_1}{m_1} \times 100 \quad (1)$$

$$\mathrm{MC_R} = \frac{m_2 - m_1}{m_0} \times 100 \quad (2)$$

where MC is the measured EMC of uncoated and coated shiv; $\mathrm{MC_R}$ is the reduced EMC of coated shiv based on the mass of shiv before coating; m_0 is the dry mass of shiv before coating; m_1 is the dry mass of shiv after coating; m_2 is the equilibrium mass of shiv at a given RH.

From the above equations, it is clear that for the uncoated hemp shiv, $EMC = MC = MC_R$. MC takes no account of the fact that the mass of the sample is increased due to the sol–gel coating layers. MC_R, however, reflects the effect of deposition of sol–gel coating layers on the adsorption–desorption isotherms of hemp shiv. However, Eq. (2) is not realistic as we are assuming that the sol–gel coating does not adsorb any moisture. To differentiate between surface effect and pore volume effect, Eq. (1) was modified to employ volume instead of mass. The new equation would be:

$$MC_{vol} = \frac{v_2}{v_1} \times 100 \quad (3)$$

where MC_{vol} is the moisture content by volume of water adsorbed, v_1 is the total accessible volume of the sample; v_2 is the volume of adsorbed moisture at a given RH.

2.5 Porosity

The pore size distribution test was performed by using Thermo Scientific Pascal Mercury Porosimeter Model 140 for low pressure and Model 440 for high pressure. The pressure range for the test was between 0.1 KPa to 400 MPa and the pore size measuring range was 116 µm to 3.6 nm. Pressure, pore diameter and intrusion volume were automatically registered.

2.6 Fourier transform infrared spectroscopy

Fourier transform infrared (FTIR) analysis on treated and untreated hemp shiv was carried out by using a PerkinElmer FTIR spectrometer model Frontier. Transmittance spectra were collected with 2 cm^{-1} resolution and 10 scans were accumulated for each spectrum in the range 4000–600 cm^{-1}. For analysis of the silica, specimens were crushed into powder and then grounded with KBr to produce pellets.

2.7 Thermal analysis

Thermal analysis of the uncoated and sol–gel coated samples was conducted by thermogravimetric analysis (TGA) using equipment STA 449 F1 Jupiter (Netzsch, Germany). The samples were heated at a rate of 10 K min^{-1} from 25 to 800 °C under nitrogen atmosphere purged at 30 ml min^{-1} using an alumina crucible.

3 Results and discussion

The water-repellent sol–gel coatings were prepared using MTES as the additive during the sol synthesis. In the present work, the co-precursor method of sol–gel synthesis was followed based on the simplicity of the process. In the sol–gel process, TEOS is hydrolysed and condensed to form a SiO_2 network which is linked to the raw material through the hydroxyl sites of cellulose present in the hemp shiv. On addition of MTES as a co-precursor during the sol–gel processing, the hydroxyl groups on the silica clusters are replaced by the –Si–CH_3 groups through –O–Si–CH_3 bonds as seen in Fig. 1. The hydrophobicity of the sol–gel coatings is due to the attachment of –Si–CH_3 groups on the SiO_2 network through oxygen bonds. Hence, by increasing the numbers of layers of the sol–gel coating a reduction of the hydroxyl sites on cellulose was obtained. Conversely the number of –$SiCH_3$ groups increased, which provided increased performance of the substrate (shiv) against water repellence.

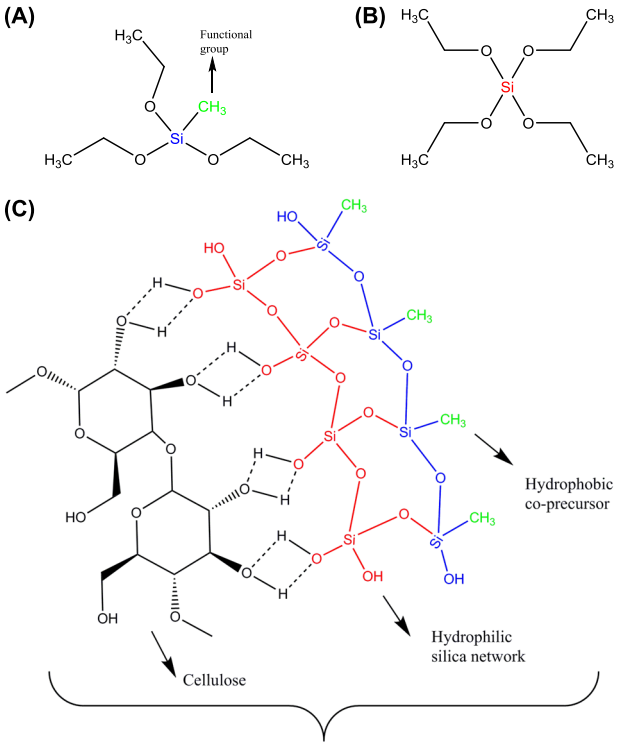

Fig. 1 Structure of an **a** MTES molecule, **b** TEOS molecule and **c** scheme for deposition of sol–gel coating on shiv surface

3.1 Characterisation of the surface morphology

The sol–gel coating affected the surface morphology of the hemp shiv. Figure 2 shows the SEM micrographs of the surface of hemp shiv before and after treatment. Hemp shiv treated with a single layer of sol–gel coating demonstrates a more uniform surface compared to the untreated shiv. However, when the hemp shiv was treated with ten layers of the sol–gel coating, the formed film showed extensive cracks as seen in Fig. 2c.

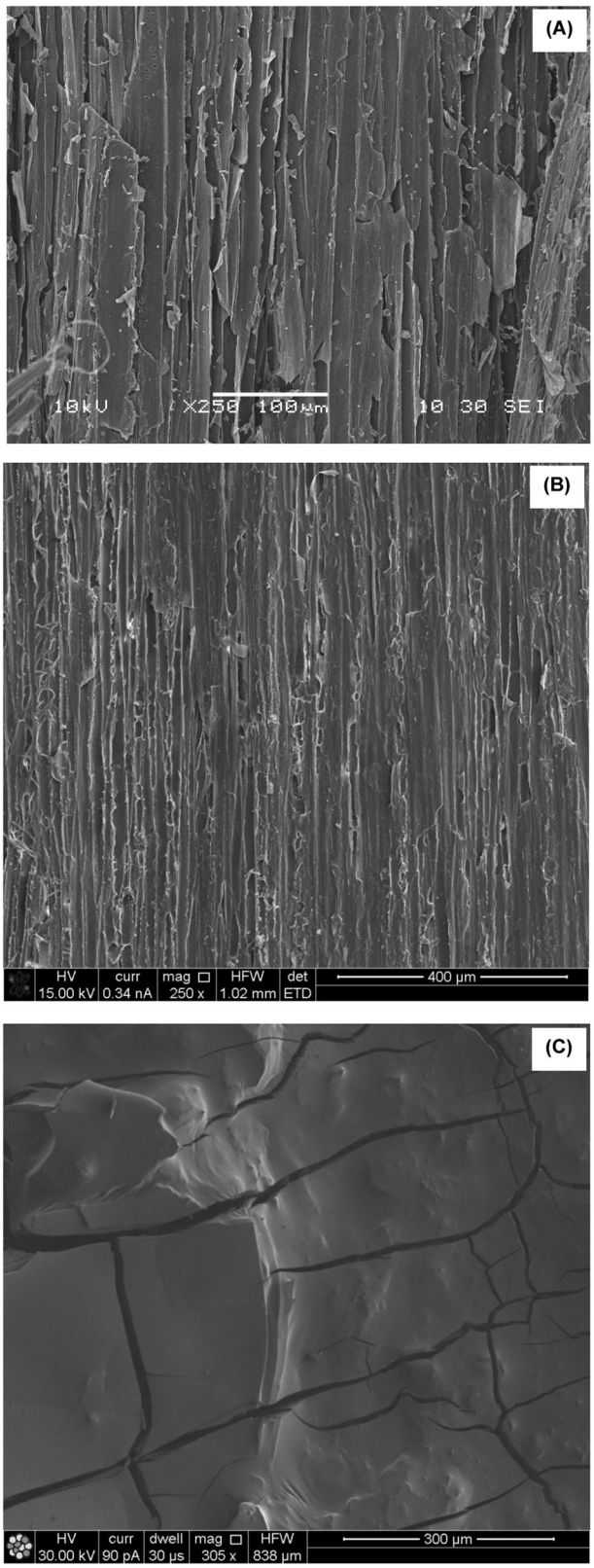

Fig. 2 SEM micrographs of hemp shiv **a** uncoated, **b** one layer of sol–gel coating and **c** ten layers of sol–gel coating

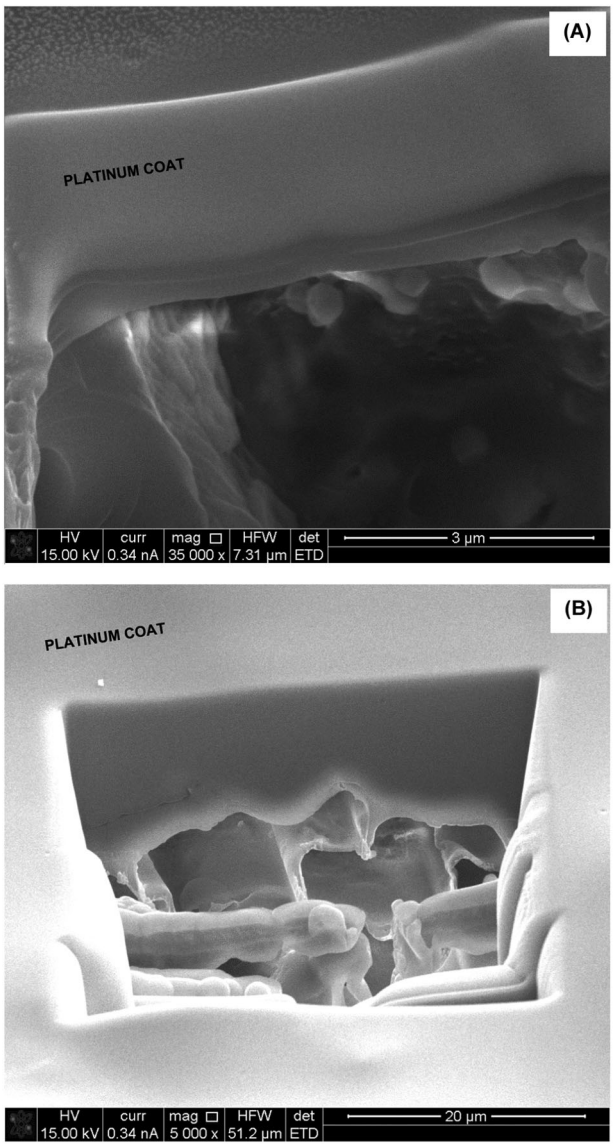

Fig. 3 SEM/FIB micrographs of hemp shiv **a** one layer of sol–gel coating and **b** ten layers of sol–gel coating

The morphology of the sol–gel modified hemp shiv was determined from an FIB cross section. Figure 3 shows the SEM micrographs of the coating layer. FIB was used to cut a section (40×30 µm and around 20 µm deep) on the surface of hemp shiv. Thin cracks were observed in the sol–gel coating formed on the surface of shiv. Ten layers of the sol–gel coating provided complete shielding of the shiv surface. FIB cross section of this piece of shiv showed that the sol–gel coating had penetrated deep into the shiv.

The sol–gel coating increased the mass of the hemp shiv as seen in Fig. 4. During the first dip, most of the sol is absorbed into the cell wall of the shiv resulting in a very thin film on the entire shiv surface including pits. A single layer of sol–gel coating on the shiv resulted in 30% overall mass gain. This is in agreement with sol–gel coatings on

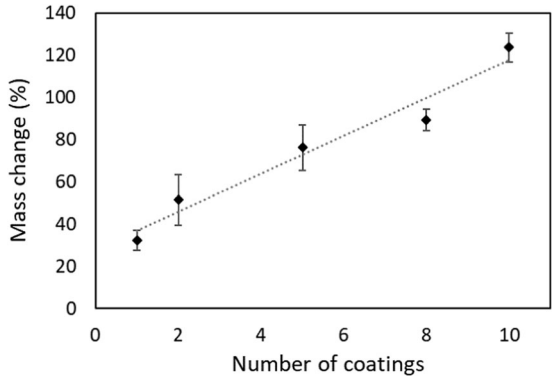

Fig. 4 Mass gain of hemp shiv with sol–gel coatings

wood resulting in 25–35% mass gain due to the absorption of coatings within the cell wall [27, 34]. Further coatings on the same piece of shiv showed that the mass gain followed a linear trend. Further layers resulted mainly in an increased thickness of the coating on the shiv surface as well as within the pits thereby the effect was a shielded pore structure as seen with the SEM (Fig. 3b).

3.2 Characterisation of surface chemistry

Figure 5 shows the FTIR spectra of uncoated and sol–gel coated hemp shiv and the peaks are listed in Table 1. The reduction of free water bands corresponding to the wave number interval 3300–3400 cm^{-1} in the coated shiv indicates that the coating has enhanced the water repellence of hemp shiv. Other wavenumbers that confirm the presence of sol–gel coating on the surface of shiv are 940 cm^{-1} corresponding to vibration of Si–OH bonds and 780 cm^{-1} associated with molecules due to incomplete hydrolysis of TEOS. It is also observed in Fig. 5b that coating the shiv results in loss of peak intensity in the region 1200–1800 cm^{-1} thereby masking the functional groups present on the surface of hemp shiv.

The region below 1000 cm^{-1} highlight the presence of Si–OH and Si–O–Si bonds although this cannot prove the covalent grafting of sol–gel coating onto C–OH of cellulose or hemicellulose. From the FTIR signals, one can prove, at best, that silica has been added on to the hemp shiv surface. For confirmation of covalent bonding between hemp shiv and the sol–gel network, further analysis is recommended.

3.3 Water absorption

The percentage of distilled water absorption (WA %) for hemp shiv was calculated using the following equation:

$$\mathrm{WA}\% = \frac{\text{Sample wet weight} - \text{Sample dry weight}}{\text{Sample dry weight}} \times 100 \quad (3)$$

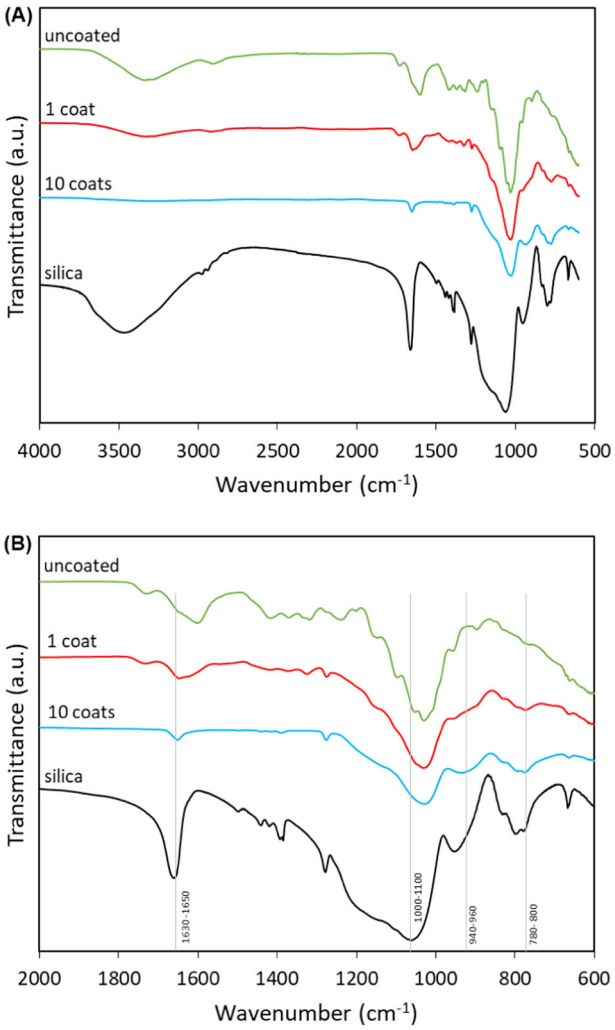

Fig. 5 FTIR spectra of silica, uncoated and coated hemp shiv in **a** 600–4000 cm^{-1} region and **b** 600–2000 cm^{-1} region

It is a measure for percent relative increase in weight due to water retention within the sample. Figure 6 depicts the distilled water absorption uptake at room temperature over a period of 24 h for different hemp shiv samples with multiple coating layers.

It can be seen that hemp shiv absorbs a large amount of water within the first few minutes of dipping. Hemp shiv without any coatings shows the maximum water absorption with 400% increase in its original mass. This was mainly due to highly porous structure of hemp shiv as well as its tendency to absorb water due to its hydrophilic nature. A single coating layer on the hemp shiv reduces the water absorption by 200%. This proves the coating layer with hydrophobic functional groups provides water resistance to the hemp shiv. Further coating layers on the shiv show an increased water resistance which can be attributed to the decrease in porosity reported in the next section of this paper.

Based on our experimental data, a water absorption model was used to determine the parameters reported in

Table 1 FTIR peaks corresponding to the source [15, 35–37]

Wavenumber (cm^{-1})	Vibration	Source
3341	O–H stretch	Polysaccharides
2918	C–H vibration	Polysaccharides
2851	CH_2 stretch	Wax
1742–1733	C=O stretch in unconjugated ketone, carbonyl and ester groups	Hemicellulose, wax
1605–1639	C=C stretch	Lignin
1630–1660	−OH	Adsorbed water
1424	CH_2 bending, C=C stretching in aromatic group, CH in plane deformation	Cellulose, lignin
1373	CH bending	Cellulose
1319	C–C stretch, CH_2 vibration	Lignin, cellulose
1027	C–C, C–OH, C–H ring and side group vibration	Hemicellulose, pectin
1000–1100	Si–O–Si	Silica
940–960	Si–OH	Silica
896	C–O–C glycosidic stretch, O–H bending	Polysaccharides
780–800	Si–O–Si, $SiOCH_2CH_3$—incomplete hydrolysis of TEOS	Silica

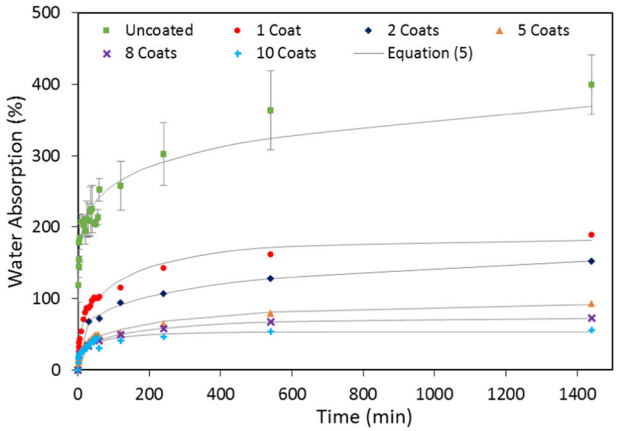

Fig. 6 Dependence of water absorption on time for varying coating layers on hemp shiv

Table 2 Water absorption parameters for hemp shiv samples

Coating layers	Eq. (5) parameters			
	a	b	c	R^2
Uncoated	1198.0	0.97×10^{-7}	0.1327	0.9504
1	182.2	0.0033	0.334	0.9814
2	173.9	0.0006	0.2446	0.9975
5	93.89	0.0019	0.307	0.9821
8	72.81	0.0027	0.2978	0.9948
10	53.41	0.0066	0.2611	0.9365

Table 2. An empirical equation proposed by Tajvidi and Azad [38] described the dependence of water absorption on time as follows:

$$\mathrm{WA}(t) = a(1 - \exp(-bt)) \tag{4}$$

where $\mathrm{WA}(t)$ is the water absorption (in percent), a and b are constants that are determined by the curve fitting procedure and t is the time in hours. This two parameter equation did not fit well with our experimental data.

Modifying Eq. (4) by an additional parameter [39, 40] describes our experimental data more accurately:

$$\mathrm{WA}(t) = a(1 - \exp(-bt))^c \tag{5}$$

where c is the third constant determined by the curve fitting procedure

The values of WA and the constants (a, b and c) for uncoated and coated hemp shiv samples were obtained from curve fitting using MATLAB. Figure 6 shows that Eq. (5) fitted well with the water absorption data of the samples with R^2 values varying between 0.9365 and 0.9975.

In our case, the coated hemp shiv samples reached equilibrium during the measurement which corresponds well with the saturation value given by parameter 'a' of Eq. (5). However, from the experimental data in Fig. 6, it can be seen that uncoated hemp shiv does not reach equilibrium and would continue to absorb water after the test. The curve fitting data for uncoated hemp shiv estimated that at saturation, the maximum water uptake would be 1200% increase in its initial mass. From Table 2, it can be seen that a single layer of sol–gel coating significantly reduces the parameter 'a' corresponding to the water absorption at saturation. This can be attributed to the water-repellent behaviour of the sol–gel coating on hemp shiv. Further coating layers enhance the water repellence of the hemp shiv thereby reducing their water uptake at saturation.

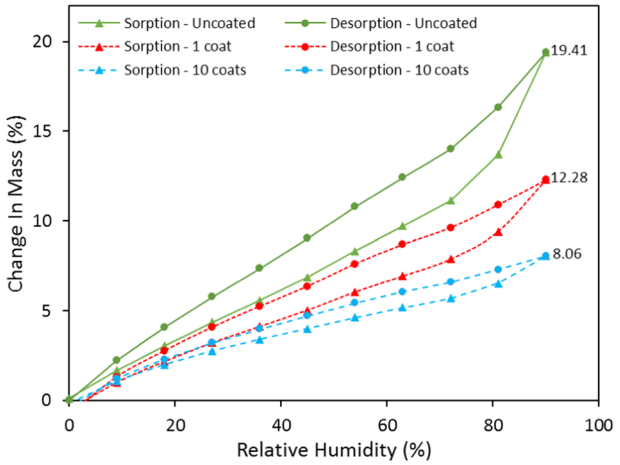

Fig. 7 Adsorption–desorption isotherm by mass of uncoated and coated hemp shiv

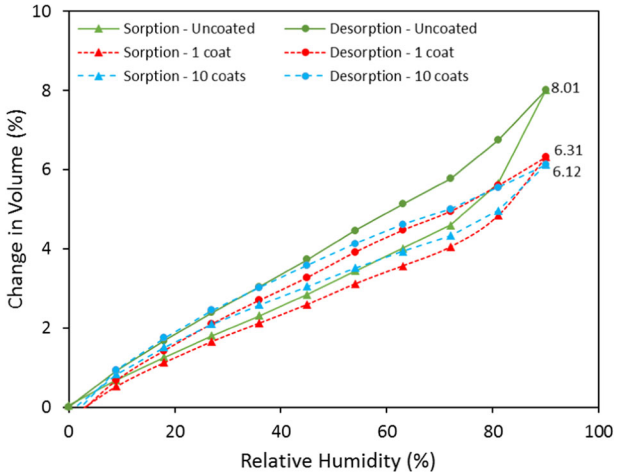

Fig. 8 Adsorption–desorption isotherm by volume of uncoated and coated hemp shiv

3.4 Dynamic vapour sorption

The adsorption–desorption isotherm of uncoated and coated hemp shiv was determined at 23 °C using the DVS equipment over a RH range 0–90% (Fig. 7). The sol–gel coating caused a reduction in measured moisture content (MC) during the adsorption–desorption process. However, the reduced moisture content (MC_R) of coated shiv calculated using Eq. (2) show only a marginal difference compared to the MC of uncoated shiv. This can be explained due to the fact that the mass of coated shiv (m_1) is always higher than the mass of untreated hemp shiv (m_0) due to coating layer. Therefore from Eqs. (1) and (2), $MC = MC_R$ for uncoated hemp shiv but for coated shiv MC is lower than MC_R [33].

At the highest RH (90%), uncoated hemp shiv reached a MC of 19.41% whereas the values obtained for the MC of the coated shiv with 1 and 10 layers were 12.28% and 8.06%, respectively. Considering the mass increased due the sol–gel coating on the hemp shiv, the MC_R of the coated shiv with 1 and 10 layers were 16.21% and 17.34%, respectively.

Figure 8 represents the moisture adsorption data relating to volume of water condensed in the pores. From the DVS data, the mass of water adsorbed at each RH can be converted into volume and compared with the total accessible volume of hemp shiv. This analysis is valid based on the assumption that water is in the liquid state upon adsorption in the pores.

It can be seen from Figs. 7 and 8 that the curves for MC and MC_{vol} are different. The lower adsorption values in for the coated shiv in Fig. 7 are due to hydrophobic groups present on the surface of hemp shiv. However, the reduced hysteresis between the adsorption and desorption curves for the coated hemp shiv indicates that the condensed water does not penetrate deep into the shiv structure. The selected sol–gel formulation is able to provide only a certain level of

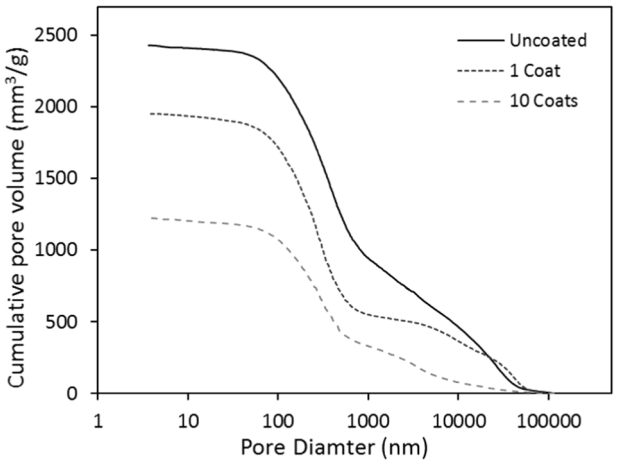

Fig. 9 Pore volume distribution of uncoated and coated hemp shiv

hydrophobicity to the hemp shiv as the concentration of the MTES is kept constant for all the coating layers. The sol–gel coating interacts with the hydroxyl groups on hemp shiv thereby reducing mass of water adsorbed. Moreover, it can be seen in Fig. 8 that hemp shiv with 10 layers of sol–gel coating still adsorbs similar vol% of water as the single coated shiv due the presence of smaller pores that are not blocked by the sol–gel coating.

The high values of EMC can be explained by the fact that raw hemp shiv has a high content of cellulose with large number of accessible OH groups. However, modifying the hemp shiv surface with sol–gel coating blocks the free OH groups on the surface, thereby reducing the moisture adsorption capability to a certain extent but does not seal the pores.

3.5 Porosity

The porosity distribution of uncoated and coated shiv is given in Figs. 9 and 10. Raw hemp shiv shows higher

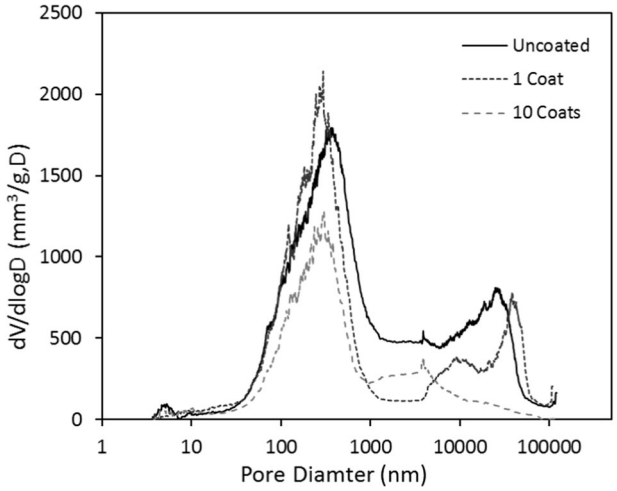

Fig. 10 Pore size distribution of uncoated and coated hemp shiv

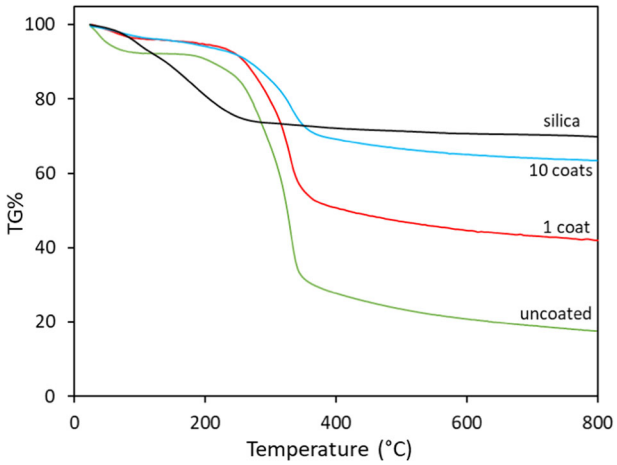

Fig. 11 TGA thermograms of silica, uncoated and coated shiv samples

porosity (78%) compared to the coated shiv with a single sol–gel layer (76%) and shiv with 10 layers of sol–gel coating (66%). From Fig. 9 it can be seen the uncoated hemp shiv has a larger cumulative pore volume compared to the coated shiv. This decrease in pore volume can be explained due the effect of the sol–gel coating reducing the size of the pores.

Figure 10 shows that the single sol–gel layer reduced the diameter of the larger pores, mainly in the range of 0.5 to 50 µm. Increasing the numbers of sol–gel layers on the shiv significantly reduce the pore size, possibly blocking some of the capillary pores completely. However, it may be noted that despite the single sol–gel layer on the shiv, the volume of smaller pores has increased and a refinement of the pore size in the range of 10 µm can be observed. It can be inferred that the deposition of the sol–gel coating has successfully taken place onto the hemp shiv surface. Therefore, the coated hemp shiv is capable of adsorbing moisture through the smaller pores whereas the water uptake is considerably reduced due to decrease in the larger pores as seen in the previous sections.

3.6 Thermal analysis

The TGA weight loss curves in a nitrogen atmosphere for silica, uncoated and sol–gel coated hemp shiv samples are shown in Fig. 11. The thermogravimetric profiles are summarised in Table 3. The uncoated and coated shiv samples degraded in three stages. The first stage which occurs below 100 °C mainly due to moisture evaporation, was higher in uncoated shiv compared to sol–gel coated shiv samples. This can be related to the binding of the silica network to the free hydroxyl groups in the coated shiv samples.

The second degradation stage occurs around 300 °C which is due to the thermal depolymerisation of hemicellulose. The third peak observed at 330 °C is mainly due to cellulose and lignin decomposition. It can be seen from Fig. 10 that increasing the number of layers of the sol–gel coating on the shiv caused a shift in the TGA curves improving the thermal stability compared to the uncoated hemp shiv.

Table 3 Decomposition temperatures of silica, uncoated and coated hemp shiv

Samples	T_5 (°C)	T_{50} (°C)	T_{max} (°C)	Residue
Uncoated shiv	50	325	329	17.5%
Shiv—1 coat	185	415	325	41.9%
Shiv—10 coats	180	–	334	63.5%
Silica	96	–	170	69.7%

4 Conclusion

Sol–gel technology has proved successful in modifying a highly hydrophilic bio-based material into a water-resistant building material. Deposited silica based sol–gel coating alters the morphology of hemp shiv, by penetrating the shiv structure thereby reducing the pore size and total pore volume of the hemp shiv. On one hand a cross linked network is formed between the silica (sol–gel coating) and the free hydroxyl groups on the surface of the shiv. On the other hand, the moisture sorption ability is not compromised which means the shiv retains its hygroscopic properties. Sol–gel coated hemp shiv showed improved thermal stability and good water resistance. It has also potential to be mixed with binders to produce composites with better interfacial adhesion, lower drying times, provide ease of handling during the manufacturing stage and ultimately a more robust bio-based thermal insulation building material.

Acknowledgements The work was supported by the ISOBIO project funded by the Horizon 2020 programme [Grant number 636835 – ISOBIO – H2020-EeB-2014-2015]. We would also like to acknowledge the EPSRC Centre for Decarbonisation of the Built Environment (dCarb) [grant number EP/L016869/1]. The ISOBIO project aims to develop and bring new bio-based insulation panels and renders into the mainstream for the purpose of creating more energy efficient buildings. The contents of this publication are the sole responsibility of the authors and can in no way be taken to reflect the views of the European Union. All data are provided in full in the Results section of this paper.

Compliance with ethical standards

Conflict of interest The authors declare that they have no conflict of interest.

References

1. Faruk O, Bledzki AK, Fink HP, Sain M (2012) Biocomposites reinforced with natural fibers: 2000-2010. Prog Polym Sci 37:1552–1596. https://doi.org/10.1016/j.progpolymsci.2012.04.003
2. Lawrence M (2015) Reducing the environmental impact of construction by using renewable. Mater J Renew Mater 3:163–174. https://doi.org/10.7569/JRM.2015.634105
3. Dhakal HN, Zhang ZY, Richardson MOW (2007) Effect of water absorption on the mechanical properties of hemp fibre reinforced unsaturated polyester composites. Compos Sci Technol 67:1674–1683. https://doi.org/10.1016/j.compscitech.2006.06.019
4. Tran LeAD, Maalouf C, Mai TH et al. (2010) Transient hygrothermal behaviour of a hemp concrete building envelope. Energy Build 42:1797–1806. https://doi.org/10.1016/j.enbuild.2010.05.016
5. Hills CAS, Norton AJ, Newman G (2009) NFI–the importance of hygroscopicity in providing indoor climate control. In: Proceedings of the 11th international conference on non-conventional. materials and technologies (NOCMAT), University of Bath, Bath, UK, 6–9 September 2009
6. Latif E, Tucker S, Ciupala MA et al. (2014) Hygric properties of hemp bio-insulations with differing compositions. Constr Build Mater 66:702–711. https://doi.org/10.1016/j.conbuildmat.2014.06.021
7. Collet F, Chamoin J, Pretot S, Lanos C (2013) Comparison of the hygric behaviour of three hemp concretes. Energy Build 62:294–303. https://doi.org/10.1016/j.enbuild.2013.03.010
8. Kidalova L, Stevulova N, Terpakova E (2015) Influence of water absorption on the selected properties of hemp hurds composites. Pollack Period. https://doi.org/10.1556/Pollack.10.2015.1.12
9. Osanyintola OF, Simonson CJ (2006) Moisture buffering capacity of hygroscopic building materials: experimental facilities and energy impact. Energy Build 38:1270–1282. https://doi.org/10.1016/j.enbuild.2006.03.026
10. Zhang H, Yoshino H, Hasegawa K (2012) Assessing the moisture buffering performance of hygroscopic material by using experimental method. Build Environ 48:27–34. https://doi.org/10.1016/j.buildenv.2011.08.012
11. Gassan J, Gutowski VS, Bledzki AK (2000) About the surface characteristics of natural fibres. Surf Eng 283:132–139. https://doi.org/10.1002/1439-2054(20001101)283:1<132::AID-MAME132>3.0.CO;2-B
12. Arnaud L, Gourlay E (2012) Experimental study of parameters influencing mechanical properties of hemp concretes. Constr Build Mater 28:50–56. https://doi.org/10.1016/j.conbuildmat.2011.07.052
13. Kymäläinen HR, Hautala M, Kuisma R, Pasila A (2001) Capillarity of flax/linseed (Linum usitatissimum L.) and fibre hemp (Cannabis sativa L.) straw fractions. Industrial Crops and products 14:41-50
14. Kabir MM, Wang H, Lau KT et al. (2012) Mechanical properties of chemically-treated hemp fibre reinforced sandwich composites. Compos Part B Eng 43:159–169. https://doi.org/10.1016/j.compositesb.2011.06.003
15. Mwaikambo LY, Ansell MP (2002) Chemical modification of hemp, sisal, jute, and kapok fibers by alkalization. J Appl Polym Sci 84:2222–2234. https://doi.org/10.1002/app.10460
16. Bledzki AK, Mamun AA, Lucka-Gabor M, Gutowski VS (2008) The effects of acetylation on properties of flax fibre and its polypropylene composites. Express Polym Lett 2:413–422. https://doi.org/10.3144/expresspolymlett.2008.50
17. Abdelmouleh M, Boufi S, Belgacem MN, Dufresne A (2007) Short natural-fibre reinforced polyethylene and natural rubber composites: effect of silane coupling agents and fibres loading. Compos Sci Technol 67:1627–1639. https://doi.org/10.1016/j.compscitech.2006.07.003
18. Abdelmouleh M, Boufi S, Ben Salah A et al. (2002) Interaction of silane coupling agents with cellulose. Langmuir 18:3203–3208. https://doi.org/10.1021/la011657g
19. Valadez-Gonzalez A, Cervantes-Uc JM, Olayo R, Herrera-Franco PJ (1999) Effect of fiber surface treatment on the fiber-matrix bond strength of natural fiber reinforced composites. Compos Part B Eng 30:309–320. https://doi.org/10.1016/S1359-8368(98)00054-7
20. Belgacem MN, Gandini A (2005) The surface modification of cellulose fibres for use as reinforcing elements in composite materials. Compos Interfaces 12:41–75. https://doi.org/10.1163/1568554053542188
21. Brinker C, Scherer G (1990) Sol-gel science: the physics and chemistry of sol-gel processing. Adv Mater 3:912. https://doi.org/10.1186/1471-2105-8-444
22. Mahadik SA, Pedraza FD, Relekar BP et al. (2016) Synthesis and characterization of superhydrophobic–superoleophilic surface. J Sol Gel Sci Technol 78:475–481. https://doi.org/10.1007/s10971-016-3974-7
23. Ismail WNW (2016) Sol–gel technology for innovative fabric finishing—a review. J Sol Gel Sci Technol 78:698–707. https://doi.org/10.1007/s10971-016-4027-y
24. Calabria AJ, Vasconcelos WL, Daniel DJ et al. (2010) Synthesis of sol–gel titania bactericide coatings on adobe brick. Constr Build Mater 24:384–389. https://doi.org/10.1016/j.conbuildmat.2009.08.020
25. Tang X, Yan X (2017) Dip-coating for fibrous materials: mechanism, methods and applications. J Sol Gel Sci Technol 81:378–404. https://doi.org/10.1007/s10971-016-4197-7
26. Wang S, Liu C, Liu G et al. (2011) Fabrication of superhydrophobic wood surface by a sol-gel process. Appl Surf Sci 258:806–810. https://doi.org/10.1016/j.apsusc.2011.08.100
27. Donath S, Militz H, Mai C (2004) Wood modification with alkoxysilanes. Wood Sci Technol 38:555–566. https://doi.org/10.1007/s00226-004-0257-1

28. Mahltig B, Böttcher H (2003) Modified silica sol coatings for water-repellent textiles. J Sol Gel Sci Technol 27:43–52. https://doi.org/10.1023/A:1022627926243
29. Bae GY, Min BG, Jeong YG et al. (2009) Superhydrophobicity of cotton fabrics treated with silica nanoparticles and water-repellent agent. J Colloid Interface Sci 337:170–175. https://doi.org/10.1016/j.jcis.2009.04.066
30. Hussain A, Calabria-Holley J, Schorr D et al. (2018) Hydrophobicity of hemp shiv treated with sol-gel coatings. Appl Surf Sci 434:850–860. https://doi.org/10.1016/j.apsusc.2017.10.210
31. Mastalska-Popławska J, Pernechele M, Troczynski T, Izak P (2017) Thermal properties of silica-coated cellulose fibers for increased fire-resistance. J Sol Gel Sci Technol 83:683–691. https://doi.org/10.1007/s10971-017-4445-5
32. Garcia AR, Júlio MF, Ilharco LM (2017) A cork–silica xerogel nanocomposite with unique properties. J Sol Gel Sci Technol 83:567–573. https://doi.org/10.1007/s10971-017-4436-6
33. Xie Y, Hill CAS, Xiao Z et al. (2010) Silane coupling agents used for natural fiber/polymer composites: a review. Compos A Appl Sci Manuf 41:806–819. https://doi.org/10.1016/j.compositesa.2010.03.005
34. Tshabalala MA, Kingshott P, Vanlandingham MR, Plackett D (2002) Surface chemistry and moisture sorption properties of wood coated with multifunctional alkoxysilanes by sol-gel process. J Appl Polym 88:2828–2841.
35. Han Y-H, Taylor A, Mantle MD, Knowles KM (2007) Sol–gel-derived organic–inorganic hybrid materials. J Non Cryst Solids 353:313–320. https://doi.org/10.1016/j.jnoncrysol.2006.05.042
36. Wang B, Sain M, Oksman K (2007) Study of structural morphology of hemp fiber from the micro to the nanoscale. Appl Compos Mater 14:89–103. https://doi.org/10.1007/s10443-006-9032-9
37. Schwarzova I, Stevulova N, Singovszka E, Terpakova E (2015) Surface treated natural fibres as filler in biocomposites. IOP Conf Ser Mater Sci Eng 96:12028. https://doi.org/10.1088/1757-899X/96/1/012028
38. Azad F, Tajvidi M (2009) Effect of particle size, fiber content and compatibilizer on the long-term water absorption and thickness swelling behavior of reed flour/polypropylene composites MEHDI. J Reinf Plast Compos 28:2341–2351. https://doi.org/10.1177/0731684408091954
39. Abu-Jdayil B, Mourad AH, Hussain A (2016) Thermal and physical characteristics of polyester-scrap tire composites. Constr Build Mater 105:472–479. https://doi.org/10.1016/j.conbuildmat.2015.12.180
40. AlMaadeed MA, Nógellová Z, Mičušík M et al. (2014) Mechanical, sorption and adhesive properties of composites based on low density polyethylene filled with date palm wood powder. Mater Des 53:29–37. https://doi.org/10.1016/j.matdes.2013.05.093

Commentary Text

For producing inexpensive hydrophobic coatings on hemp shiv, sodium silicate was used as an alternative precursor to TEOS. For preparation of the sol, sodium silicate Na_2SiO_3 solution, reagent grade (also known as water glass) was used as the silica precursor. Hydrochloric acid, HCl (37%) was diluted to a 2M solution. Hexadecyltrimethoxysilane, HDTMS (85%) was used as the hydrophobic agent. Absolute ethanol (99.8%) and distilled water were the solvents in this process. All chemicals were obtained from Sigma Aldrich.

The experimental procedure followed here is taken from Li, Xing, & Dai (2008) who prepared superhydrophobic surfaces on cotton using sodium silicate and HDTMS. The formulation was synthesised by the hydrolysis of sodium silicate solution. 10.0 ml of sodium silicate solution was added into 80 ml of distilled water and stirred at room temperature for 10 min. Then 10 ml of 2.0 M HCl solution was added dropwise to the sodium silicate solution with stirring to form a silica hydrosol. The solution temperature was continuously monitored by a probe as there is high risk involved in the reaction of acid (pH 0.7) with diluted sodium silicate solution (pH 12.3). A clear silica sol was obtained with a final pH of 11.5. In a separate beaker, HDTMS solution was prepared by adding 6.4ml water (4M) and 41.5ml ethanol (8M), stirring for 10 min and then adding 2ml HDTMS (0.05M). The solution was stirred for 30 min at room temperature.

The hemp shiv samples (20 pieces) were immersed in the silica hydrosol for 3 min, and then padded with a wet pickup of 140–150%. The samples were dried at 80 °C for 5 min. One half of the hemp shiv aggregates (10 pieces) were rinsed with distilled water for 5 min. The water was drained and the hemp shiv were rinsed again for 3 min, then dried at 80 °C for 10 min. The other half of the hemp shiv samples were not rinsed with water to study the effect of rinsing on hydrophobicity of hemp shiv. The treated hemp shiv were then immersed in the ethanol solution of hydrolysed HDTMS (4 wt%) for 4 h, dried overnight at room temperature and cured at 80 °C for 1 h in an oven.

The percentage of distilled water absorption (WA %) for hemp shiv was calculated using the following equation:

$$\text{WA } \% = \frac{\text{Sample wet weight} - \text{Sample dry weight}}{\text{Sample dry weight}} \text{ x } 100 \qquad \text{Eq (4.1)}$$

The water absorption test protocol was followed in the same manner as reported in article of this Chapter. Compared with silicon alkoxides, an ordinary aqueous solution of sodium silicate was probably the cheapest silica source. It hydrolyses under the presence of hydrochloric acid to produce silicic acid as shown in the following reaction:

$$Na_2SiO_3 + H_2O + 2HCl \rightarrow Si(OH)_4 + 2NaCl \qquad \text{Eq (4.2)}$$

The silicic acid condenses to form a silica sol, and at last a silica gel is produced as shown below:

$$Si(OH)_4 + (OH)_4Si \rightarrow (OH)_3Si - O - Si(OH)_3 + H_2O \qquad \text{Eq (4.3)}$$

Rinsing was performed to remove the excess Na^+ ions that have been obtained after the hydrolysis of sodium silicate. Some of the Na^+ ions combine with Cl^- ions from hydrochloric acid and form NaCl salt. Excess Na^+ ions can increase the hydrophilicity and therefore interfere with the hydrophobic coatings. Rinsing the hemp shiv involves additional cost on an industrial scale. Moreover it is not an easy process as hemp shiv tends to float on water. Removing the excess Na^+ ions needs a more sophisticated process such as ion exchange column which can be expensive and time consuming industrially.

The water absorption results are presented in Figure 4.1. Treatment of hemp shiv using silica sol lowers the water absorption making the hemp shiv water repellent. Hemp shiv rinsed and treated with hydrophobic coating (SS-1) absorbs the least amount of water over 24 hours. Hemp shiv samples that were not rinsed and directly treated with the HDTMS solution (SS-2) absorb more water when compared to SS-1. Although SS-1 shows the least water absorption in Figure 4.1,

the results do not provide sufficient level of hydrophobicity when compared to the MTES based sol-gel coatings reported earlier in the article of this chapter.

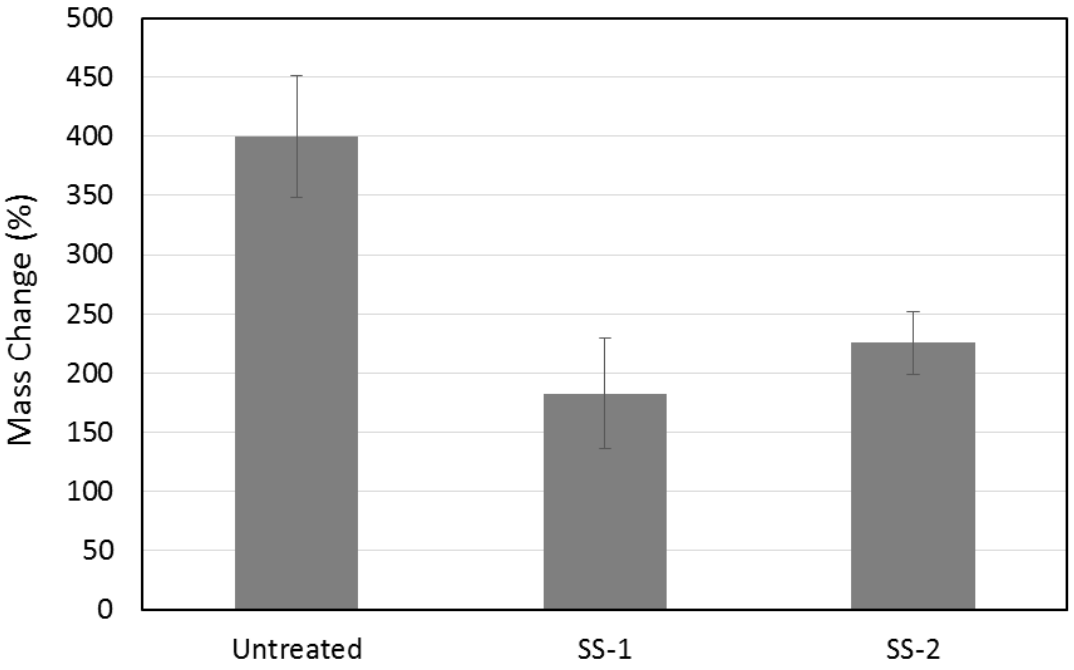

Figure 4.1 Water absorption of hemp shiv treated with sodium silicate based coatings.

The main drawbacks of using sodium silicate as an alternative precursor to TEOS for producing water repellent coatings of hemp shiv are as follows:

- High risk of mixing acid and sodium silicate solution.
- Rinsing of Na^+ ions is complicated and involves time and cost.
- Immersion in ethanol based HDTMS solution was too long (4 hours) and not practical on an industrial scale. On the other hand, only 10 min were required for the dip coating process using TEOS based formulation.
- The level of water repellence on hemp shiv achieved with sodium silicate formulation was not sufficient when compared to a single coating layer of TEOS based formulation.

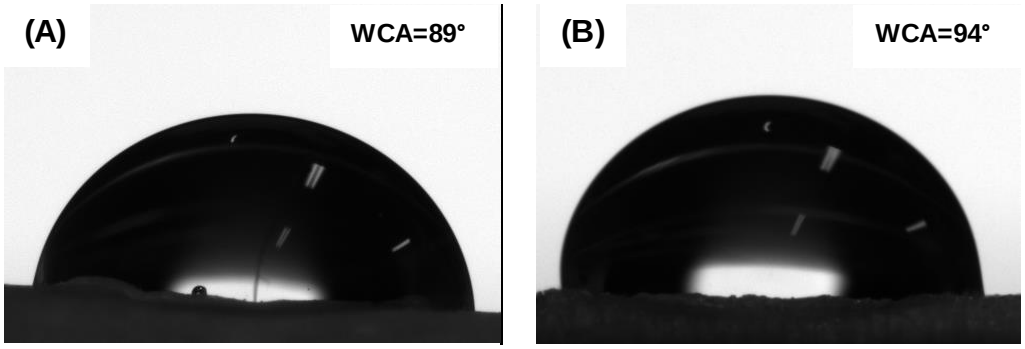

Figure 4.2 Water contact angle measurements of hemp shiv treated with MTES based coatings, (A) one coating layer and (B) ten coating layers.

From Figure 4.2, it can be seen that a single layer of MTES based coating does not provide a hydrophobic surface to hemp shiv. Hemp shiv surface coated with ten layers of MTES based coating does have a hydrophobic surface but this is not desirable as it is not deposited as a homogenous coating and greatly modifies the morphology of hemp shiv. Moreover, application of 10 coating layers would have limitations on an industrial scale such as increased cost and processing time. Therefore, new coating formulations need to be explored that can perform better in terms of hydrophobicity, use minimal reagents and are inexpensive.

Chapter 5

Effect of various HDTMS based Coatings on Hemp Shiv Hydrophobicity

This Chapter has been published as a Journal paper entitled “Hydrophobicity of Hemp Shiv treated with Sol-gel Coatings” in Applied Surface Science (Hussain et al., 2018).

Introductory Text

Although the methytriethoxysilane (MTES) based coatings reduced the water absorption significantly and did not affect the moisture buffering ability of hemp as seen in Chapter 4, the effect of the coatings on the surface hydrophobicity is not efficient as the hemp surface remains still hydrophilic.

This paper investigates the use of hexadecyltrimethoxysilane (HDTMS) as a hydrophobic precursor in the coating formulation and studies the effect of various formulations on hydrophobicity and surface morphology of hemp shiv. Moreover, the impact of acidic and basic catalysts in the formulation has been studied and it was found that acidic catalysts perform better in terms of hydrophobicity on the hemp shiv surface. The change in solvent concentration had an effect on the surface morphology and it was found that the ethanol: HDTMS ratio was optimised to achieve hydrophobic crack free coatings. The HDTMS concentration was varied to study the minimal amount needed that could provide the maximum hydrophobicity. It was found that coating formulation with HDTMS concentration as low as 1 wt% corresponding to 0.014M provided water contact angles up to 118 ° on hemp shiv. Reducing the concentration of HDTMS in the coating formulation would potentially reduce the cost of the coating as well as lower its environmental impact.

Statement of Authorship

This declaration concerns the article entitled:									
Hydrophobicity of hemp shiv treated with sol-gel coatings.									
Publication status (tick one)									
draft manuscript		**Submitted**		**In review**		**Accepted**		**Published**	✓
Publication details (reference)	Hussain, A., Calabria-Holley, J., Schorr, D., Jiang, Y., Lawrence, M., & Blanchet, P. (2018). Hydrophobicity of hemp shiv treated with sol-gel coatings. Applied Surface Science, 434, 850–860. http://doi.org/10.1016/j.apsusc.2017.10.210								
Candidate's contribution to the paper (detailed, and also given as a percentage).	The candidate contributed to/ considerably contributed to/predominantly executed the… Formulation of ideas: 90% A. Hussain presented the main idea of this work and discussed with M. Lawrence and J. Calabria-Holley. This study was conducted at Laval University, Quebec under supervision of P. Blanchet and D. Schorr. Design of methodology: 90% A. Hussain designed the methodology for this work. The co-authors shared their expertise. Experimental work: 100% A. Hussain conducted all the experiments and the data analysis. Presentation of data in journal format: 90% A. Hussain prepared the manuscript. All co-authors have feedback and comments for improving the manuscript.								
Statement from Candidate	This paper reports on original research I conducted during the period of my Higher Degree by Research candidature.								
Signed	Atif				**Date**	15.09.2018			

Copyrights and Permission

Creative Commons Attribution License (CC BY)

This article is available under the terms of the Creative Commons Attribution License (CC BY). You may copy and distribute the article, create extracts, abstracts and new works from the article, alter and revise the article, text or data mine the article and otherwise reuse the article commercially (including reuse and/or resale of the article) without permission from Elsevier. You must give appropriate credit to the original work, together with a link to the formal publication through the relevant DOI and a link to the Creative Commons user license above. You must indicate if any changes are made but not in any way that suggests the licensor endorses you or your use of the work.

Permission is not required for this type of reuse.

CLOSE WINDOW

Publication title:

Hydrophobicity of hemp shiv treated with sol-gel coatings.

Thesis page numbers that it spans:

109 to 119

Applied Surface Science 434 (2018) 850–860

Contents lists available at ScienceDirect

Applied Surface Science

journal homepage: www.elsevier.com/locate/apsusc

Full Length Article

Hydrophobicity of hemp shiv treated with sol-gel coatings

Atif Hussain[a,b,*], Juliana Calabria-Holley[a], Diane Schorr[b], Yunhong Jiang[a], Mike Lawrence[a], Pierre Blanchet[b]

[a] BRE Centre for Innovative Construction Materials, Department of Architecture and Civil Engineering, University of Bath, Bath BA2 7AY, UK
[b] NSERC Industrial Research Chair on Ecoresponsible Wood Construction, Department of Wood and Forest Sciences, Université Laval, Quebec, QC, G1 V 0A6, Canada

ARTICLE INFO

Article history:
Received 25 July 2017
Received in revised form
22 September 2017
Accepted 29 October 2017
Available online 31 October 2017

Keywords:
Sol-gel
Hydrophobicity
Coatings
Surface roughness
Hemp shiv

ABSTRACT

This is the first time sol-gel technology is used in the treatment of hemp shiv to develop sustainable thermal insulation building materials. The impact on the hydrophobicity of hemp shiv by depositing functionalised sol-gel coatings using hexadecyltrimethoxysilane (HDTMS) has been investigated. Bio-based materials have tendency to absorb large amounts of water due to their hydrophilic nature and highly porous structure. In this work, the influence of catalysts, solvent dilution and HDTMS loading in the silica sols on the hydrophobicity of hemp shiv surface has been reported. The hydrophobicity of sol-gel coated hemp shiv increased significantly when using acid catalysed sols which provided water contact angles of up to 118° at 1% HDTMS loading. Ethanol diluted sol-gel coatings enhanced the surface roughness of the hemp shiv by 36% as observed under 3D optical profilometer. The XPS results revealed that the surface chemical composition of the hemp shiv was altered by the sol-gel coating, blocking the hydroxyl sites responsible for hydrophilicity.

1. Introduction

Wettability of a solid surface is governed by a combination of chemical composition and geometric structure of the surface [1,2]. The interplay between surface chemistry and surface roughness has been an active research topic for enhancing the hydrophobicity of cellulose based materials.

The woody core of the hemp plant (*Cannabis Sativa* L.) known as shiv has gained interest in the building industry during the recent years for production of lightweight composites. Hemp shiv based composites have interesting properties such as thermal [3], hygroscopic [4], mechanical, acoustic [5] and biodegradability [6].

Hemp shiv are generally very porous with low density tending to absorb large amounts of water. Previous studies have reported that hemp shiv not only has higher water absorption rate but also absorb high amounts of water in the very first minutes compared to different plant materials [7]. Moreover, the presence of cellulose, hemicellulose and lignin in bio-based materials contributes to the presence of hydroxyl groups in their structure. This leads to certain disadvantages of using bio-based materials making them incompatible with hydrophobic thermoset/thermoplastic polymers [8]. High moisture uptake also encourages colonial fungal growth resulting in cell wall degradation and lower durability of the material [9].

The major constituents of industrial hemp shiv are: cellulose (44%), hemicellulose (18–27%), lignin (22–28%) and other components such as extractives (1–6%) and ash (1–2%) [10,11]. Cellulose is a semi crystalline polysaccharide consisting of linear chain of several D-glucose units linked together by β (1–4) glucosidal bond. Cellulose contains free hydroxyl groups, and since they form the major structural component of hemp shiv, they are responsible for the extreme hydrophilic behaviour.

One of the mechanism to convert cellulose–based material from hydrophilic to hydrophobic involves chemical modification to block the hydroxyl groups of the cell wall thereby reducing water sorption sites. Treatments include acetylation [12], silanization [13] and in situ polymerization [14] that involve incorporation of materials into the cell wall blocking the voids accessible to water molecules. Other treatments methods that are known to enhance the water repellence are plasma etching, lithography, electrospinning and sol-gel treatment that endow the material with nano-scale surface roughness [15].

Chemical pre-treatment of natural plant materials have reported better bonding with polymer matrix interface due to

* Corresponding author at: BRE Centre for Innovative Construction Materials, Department of Architecture and Civil Engineering, University of Bath, Bath BA2 7AY, UK.
E-mail addresses: A.Hussain@bath.ac.uk, atifh1187@gmail.com (A. Hussain).

https://doi.org/10.1016/j.apsusc.2017.10.210
0169-4332/

improvement of their hydrophobic characteristics [16]. There is a need to develop a novel treatment method for hemp shiv to enhance its water resistance thereby improving the shiv-binder interfacial adhesion and reduce its susceptibility to decay. The sol-gel technique is a highly versatile method to deposit silica based coatings possessing single or multi functionality [17]. These thin mesoporous coatings have high structural homogeneity and their adhesion can be tailored to different substrates.

Sol-gel based hydrophobic and water repellent coatings have been investigated on different bio-based materials such as wood [18] and cellulosic fibres [19], however for hemp shiv this is the first time. The reactive hydroxyl groups present in the polysiloxane network of the sol-gel combine with the hydroxyl groups of cellulose through a covalent bond. This study successfully delivers a sol-gel modified hemp shiv material of hydrophobic character through a simple and inexpensive, one step dip-coating method.

2. Experimental

2.1. Materials

Hemp shiv used in this study was received from MEM Inc., manufacturer of ecological materials based in Rimouski, Canada. Tetraethyl orthosilicate (TEOS, 98%) and hexadecyltrimethoxysilane (HDTMS, 85%) were obtained from Sigma-Aldrich. Anhydrous ethanol was purchased form Commercial Alcohols, Canada. Hydrochloric acid (HCl, 38%) and nitric acid (HNO_3, 70%) were obtained from Anachemia, VWR, Canada. All chemicals were used as received without further purification.

It is known that HDTMS may not be able to penetrate the outer surface layers of the cell wall due to its high molecular weight [18]. Due to this, the hydrophobicity would be compromised and it can be predicted that the coating might not be robust. Moreover, using only HDTMS would be highly expensive and would not be of interest to the construction industry. For these reasons, it was considered inappropriate to make a comparative study using purely HDTMS.

2.2. Preparation of the hydrophobic coatings

The silica based sol-gel was synthesised by hydrolysis and condensation of TEOS in ethanol and water. The reaction was catalysed using 0.005 M acid (HCl/HNO_3). Two sets of silica sols were prepared based on the difference in concentration of ethanol. The first set of formulations (sols A) were prepared stirring 1 M TEOS in a mixture of 4 M water and 4 M ethanol. For the preparation of the second set of formulations (sols B), 1 M TEOS was added to 4 M water and 16 M ethanol. After the preparation of both sets of silica formulations, the hydrophobic agent HDTMS was added in concentrations of 0.5–4 wt% of the sol. These mixtures of silica sol and HDTMS were stirred at 300 rpm for at least 20 min before performing the dip-coating process. All the sols were prepared at 40 °C and atmospheric pressure. The sols were allowed to cool down to room temperature and the pH was recorded.

The sols aged for 48 h in closed container at room temperature before the dip-coating process. Gelation took place in-situ in which pieces of hemp shiv were dipped in the sol for 10 min and then carefully removed and transferred onto a Petri dish. The samples were placed at room temperature for one hour and then dried at 80 °C for one hour. A schematic illustration of the HDTMS modified silica sol-gel coating is shown in Fig. 1.

As for the preparation of the pure sol-gel specimen, the sol aged in a container at room temperature until gel point. The gel-point was taken as the time when the sol did not show any movement on turning the container upside down. The gel-time and pH for all the prepared sols are reported in Table 1.

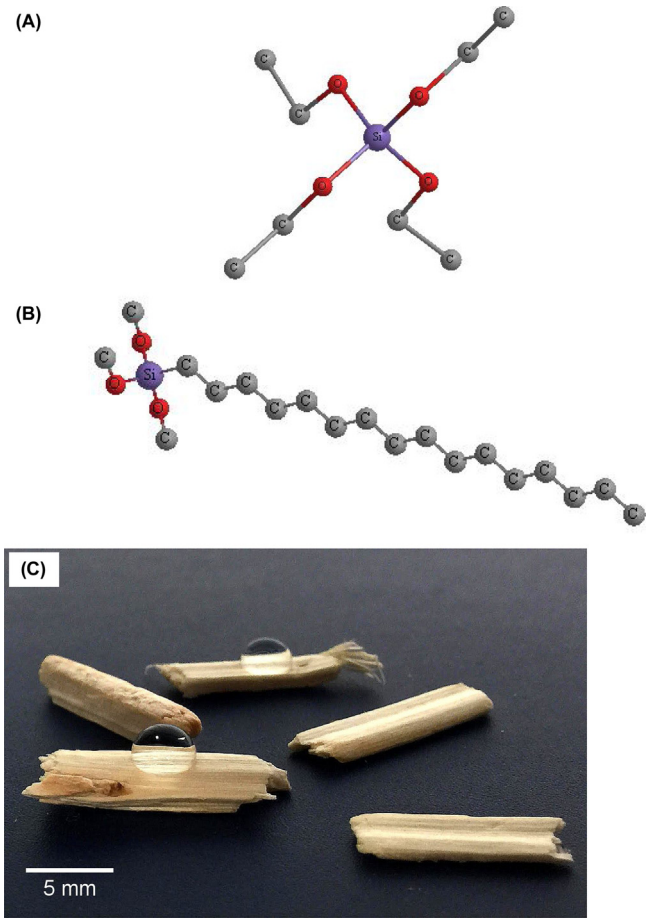

Fig. 1. 3D structure of a (A) TEOS molecule, (B) HDTMS molecule; and (C) water on coated hemp shiv samples.

2.3. Contact angle measurements

The water contact angle (WCA) of uncoated and coated hemp shiv samples were measured using a contact angle meter (First Ten Ångstroms USA, FTA200 series). The sessile drop method was employed and the contact angle was determined on at least three different positions for each sample (coated substrate). The volume of the water droplets was 5 μl for the contact angle measurements. The average value was adopted as a final value. Images were captured and analysed using the FTA32 Video 2.0 software. All the measurements were performed at room temperature (24 ± 1 °C).

2.4. Surface roughness

The topography and surface roughness of the samples was obtained using a 3D optical profilometer (Bruker Nano GmbH Germany, ContourGT-K series). The surface roughness was measured over an area at 0.25*0.30 mm^2 in non-contact mode at 20× magnification. Vision 64 on board software was then employed to analyse these data and calculate the roughness parameters. The readings were taken on at least three different positions for each sample and the average value was reported as the final value.

Table 1
Composition of the prepared sol-gel formulations and their properties.

FORMULATION	CATALYST	ETHANOL CONC. (M)	HDTMS CONC. (wt%)	GEL TIME (DAYS)	pH
sol A-1	HCl	4.0	4.0	178	1.87
sol A-2	HCl	4.0	2.0	116	1.82
sol A-3	HCl	4.0	1.0	101	1.78
sol A-4	HCl	4.0	0.5	101	1.85
sol A-5	HNO_3	4.0	4.0	150	1.73
sol A-6	HNO_3	4.0	2.0	112	1.87
sol A-7	HNO_3	4.0	1.0	101	1.92
sol A-8	HNO_3	4.0	0.5	101	1.92
sol B-1	HCl	16.0	4.0	>180	1.64
sol B-2	HCl	16.0	2.0	>180	1.68
sol B-3	HCl	16.0	1.0	>180	1.67
sol B-4	HCl	16.0	0.5	>180	1.72
sol B-5	HNO_3	16.0	4.0	>180	1.70
sol B-6	HNO_3	16.0	2.0	>180	1.76
sol B-7	HNO_3	16.0	1.0	>180	1.81
sol B-8	HNO_3	16.0	0.5	>180	1.83

2.5. X-ray photoelectron spectroscopy (XPS)

The surface elemental and chemical composition of the samples were analysed using XPS. Prior to XPS analysis, samples were oven-dried at 80 °C for 96 h. XPS spectra of uncoated and sol-gel coated hemp shiv were recorded with an X-ray photoelectron spectrometer (Kratos Axis Ultra, UK). All spectra were collected using a monochromatic Al Kα X-ray source operated at 300 W. The lateral dimensions of the samples were 800 μm × 400 μm, corresponding to those of the Al Kα X-ray used, and probing depth was approximately 5 nanometres. For each sample, two spectra were recorded: (i) survey spectra (0–1150 eV, pass energy 160 eV, and step size 1 eV) recorded for apparent composition calculation; and (ii) high-resolution C1s, O1s and Si 2p spectra (within 20 eV, pass energy 20 eV and step size within 0.05 eV) recorded to obtain information on chemical bonds. Calculation of the apparent relative atomic concentrations is performed with the CasaXPS software. Peak fitting is performed with CasaXPS, which automatically and iteratively minimizes the difference between the experimental spectrum and the calculated envelope by varying the parameters supplied in a first guess.

2.6. Scanning electron microscopy

The surface morphology of the specimens was characterised using a scanning electron microscopy (SEM), JEOL corporation – Japan Model JSM-6360 operating at 25 kV. The specimens were coated with gold to achieve maximum magnification of textural and morphological characteristics.

3. Results

3.1. Hydrophobicity of sol-gel coatings

The water contact angle was determined as soon as the water droplet encountered the sol-gel coated hemp shiv surface. The sol-gel coatings with high HDTMS loadings (4 wt%) and varying concentration of ethanol are compared in Fig. 2. It can be seen that uncoated shiv has an extremely hydrophilic surface and water droplet sinks into the substrate reducing the WCA in a short time. The sol-gel coatings yield hydrophobicity to the hemp shiv by maintaining a stable contact angle over 60 s.

Considering the coating compositions with 4% HDTMS loading listed in Table 1, it was observed that ethanol diluted sols (sol B series) performed better in terms of providing hydrophobicity to hemp shiv surface compared to undiluted sols (sol A series). Sol B-1 and sol B-5 coatings had higher contact angles (up to 105°) compared to sol A-1 and sol A-5 coatings (up to 100°).

Ethanol helps the HDTMS to be fully dissolved in water thereby promoting the hydrolysis reaction [20,21]. Fig. 2 shows the WCA measurements of sol coatings containing 4 wt% HDTMS. Sol A-1 and sol A-5 contain only 4 M ethanol whereas sol B-1 and sol B-5 contain 16 M of ethanol. At 4 wt% HDTMS concentration, using 16 M of ethanol favours the hydrolysis of HDTMS. In this way HDTMS molecules are able to self-assemble on the silica network, hence providing enhanced hydrophobicity to the material. In general, it was observed that sol-gel coatings with HNO_3 as catalyst perform slightly better in terms of hydrophobicity than coatings with HCl as catalyst.

The changes in water contact angle as a function of HDTMS loading (0.5–4.0 wt%) is presented in Fig. 3. The contact angle measurements had a standard deviation between 1.1° and 6.0°. The hydrophobic performance of the coatings is not reduced on lowering the HDTMS loading down to 1%. Surfaces coated with sol B series showed good water repellence with contact angles ranging between 96° to 108°.

3.2. Surface roughness of the coatings

The samples were analysed for their surface microstructure and roughness by the Vision64 software using a Robust Gaussian Filter (ISO 16610-31 2016) and a short wavelength cut-off 0.025 mm. The use of such filters helps to reduce the anatomical influence and optimizes the roughness profile data for evaluation of the sample surface [22,23]. The robust Gaussian filter avoids the distortions produced by some filters when applied in profiles with deep valleys [24]. Mean surface roughness (*Sa*) was calculated according to ISO 4287 (1997). *Sa* gives the description of the height variations in the surface and it is the most widely used parameter to measure the surface roughness profile of the sample. The surface roughness parameters for sol-gel coated hemp shiv with 1% and 4% HDTMS loadings are shown in Fig. 4.

The influence of different sol-gel coatings on the surface roughness of hemp shiv can be seen in Fig. 5. The 3D surface roughness profile showed that the sol A-5 coating on the hemp shiv lowered the surface roughness providing a smoother surface as seen in Fig. 5b. The non-uniform coating was also cracked, which in turn can facilitate water penetration into the hemp shiv. On the other hand, sol A-7 (contemning lower HDTMS loading) enhanced the surface roughness of hemp shiv. Overall ethanol diluted sol-gel coatings had enhanced the surface roughness of hemp shiv. Sol B-5 had the highest mean surface roughness as seen in Fig. 5c.

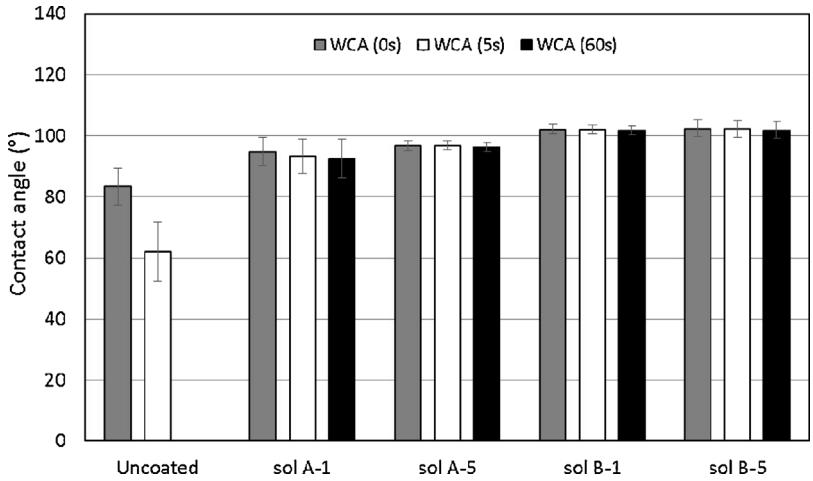

Fig. 2. Hydrophobicity of hemp shiv surface treated with different sol-gel coatings over 60 s of water contact.

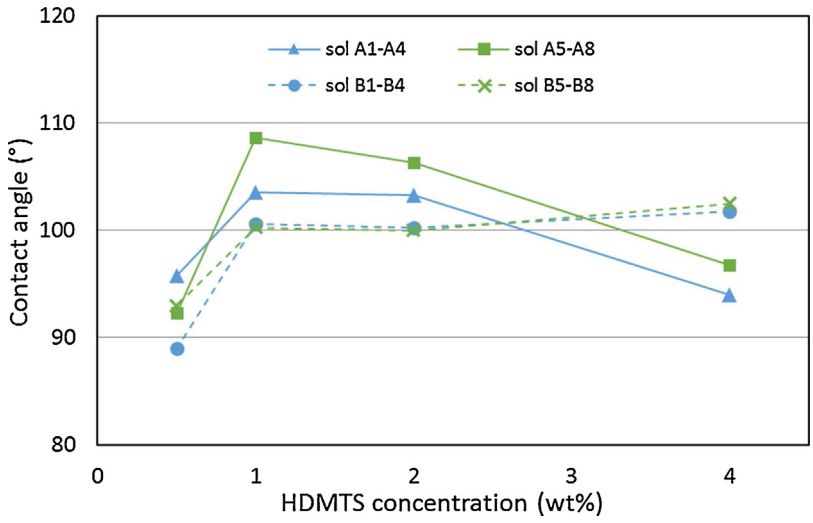

Fig. 3. Effect of ethanol dilution and varying HDTMS concentration in the sol-gel coating on hydrophobicity of hemp shiv surface.

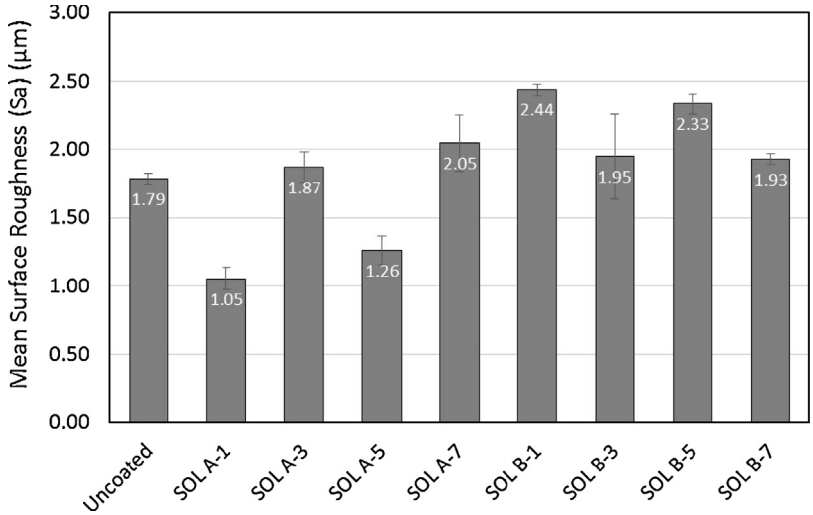

Fig. 4. Mean surface roughness (Sa) measurement of uncoated and sol-gel coated hemp shiv surfaces.

3.3. Surface morphology

Roughness parameters alone cannot describe the surface morphology and therefore microscopy analysis is beneficial to improve surface evaluations. The morphology of the uncoated and sol-gel coated surfaces was studied by scanning electron microscopy (SEM). Fig. 6 shows the micrographs of hemp shiv surface before

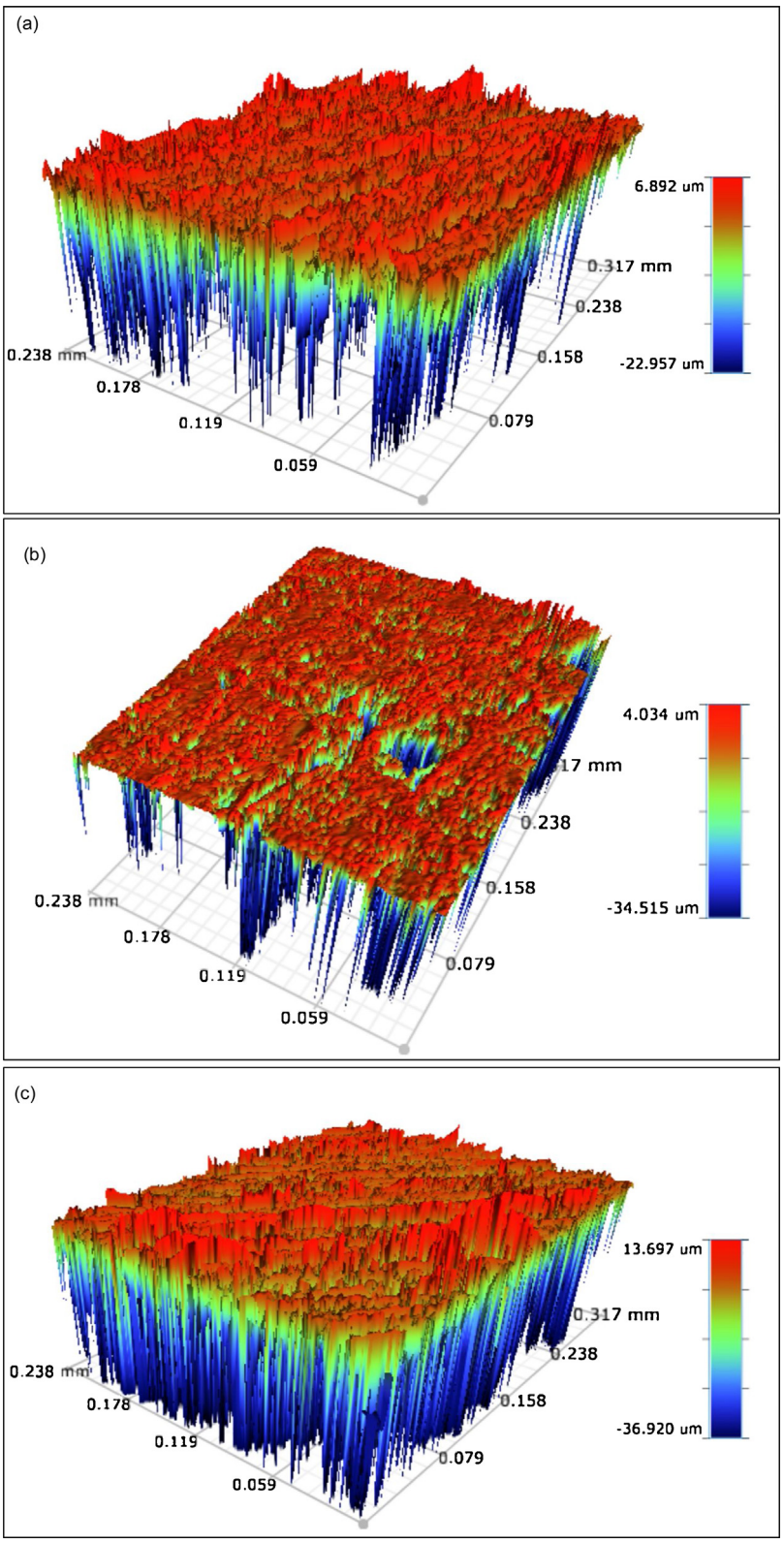

Fig. 5. Surface roughness of (a) uncoated, (b) sol A-5 and (c) sol B-5 coated hemp shiv surface.

and after modification with different sol-gel coatings. Sol A-5 and sol B-7 (Fig. 6b and e) formed a thick coating layer and changed the morphology of the shiv surface. This resulted in coating with major cracks which could be a result of shrinkage after drying the treated sample (sol-gel coated hemp shiv). On the other hand, sol A-7 and sol B-5 (Fig. 6c and d) showed uniformly coated surfaces without significantly altering the morphology of the hemp shiv.

Conventional SEM techniques proved unsuccessful in determining the coating thickness, but SEM-FIB (Focused Ion Beam) imaging of an early iteration of the formulation (Fig. 6f) measured a thick-

ness in the range 160–180 nm. It is expected that the current formulations (sol A-7 and sol B-5) would have a similar thickness.

3.4. Chemical composition

The surface chemical composition was determined by X-ray photoelectron spectroscopy. A low-resolution survey scan determined the atomic percentage of various elements present at the sample surface (Fig. 7). The relative elemental composition of the uncoated and sol-gel coated hemp shiv surface is listed in Table 2.

The main elements detected for uncoated hemp shiv were carbon and oxygen. Small amounts of other elements were present either possibly arising from the epidermal cell wall or from contamination during sample preparation. The sol-gel coated hemp shiv additionally showed high content of silicon arising from the silica based membrane on the surface (Fig. 7b).

A high-resolution scan was performed on the C1s region for the uncoated and sol-gel coated hemp shiv samples to determine the type of oxygen-carbon bonds present. The chemical bond analysis of carbon was performed by curve-fitting the C1s peak and deconvoluting it into four sub peaks corresponding to unoxidized carbon C1, and various oxidized carbons C2, C3 and C4. A ratio between oxidized carbon (C_{ox}) and unoxidized carbon (C_{unox}) was calculated by the equation [25]:

$$C_{ox/unox} = \frac{C_{ox}}{C_{unox}} = \frac{C2 + C3 + C4}{C1} \quad (1)$$

Table 2
Relative amount of atoms at sample surface determined by low-resolution XPS scan.

Element	Relative Conc. (atomic%)	
	Uncoated Hemp shiv	Sol A-7 Coated Hemp Shiv
C	69.61	28.33
O	27.06	53.57
N	2.06	–
Ca	0.64	–
P	0.14	–
K	0.30	–
S	0.09	–
Na	0.04	–
Cl	0.04	–
Co	0.03	–
Si	–	18.10

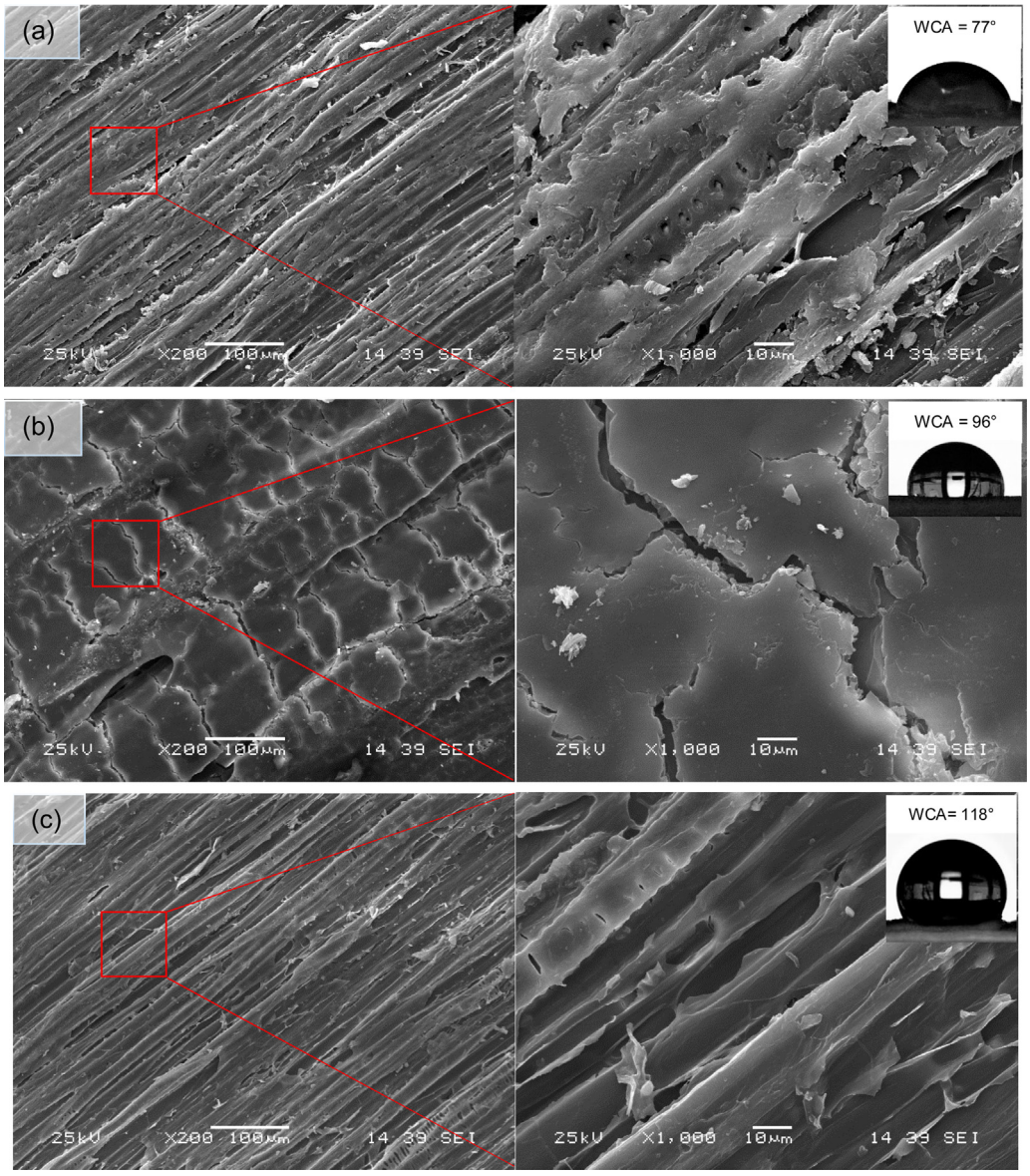

Fig. 6. Surface morphology and WCA of (a) uncoated, (b) sol A-5, (c) sol A-7, (d) sol B-5 (e) sol B-7 coated hemp shiv surface and (f) thickness of sol-gel coating.

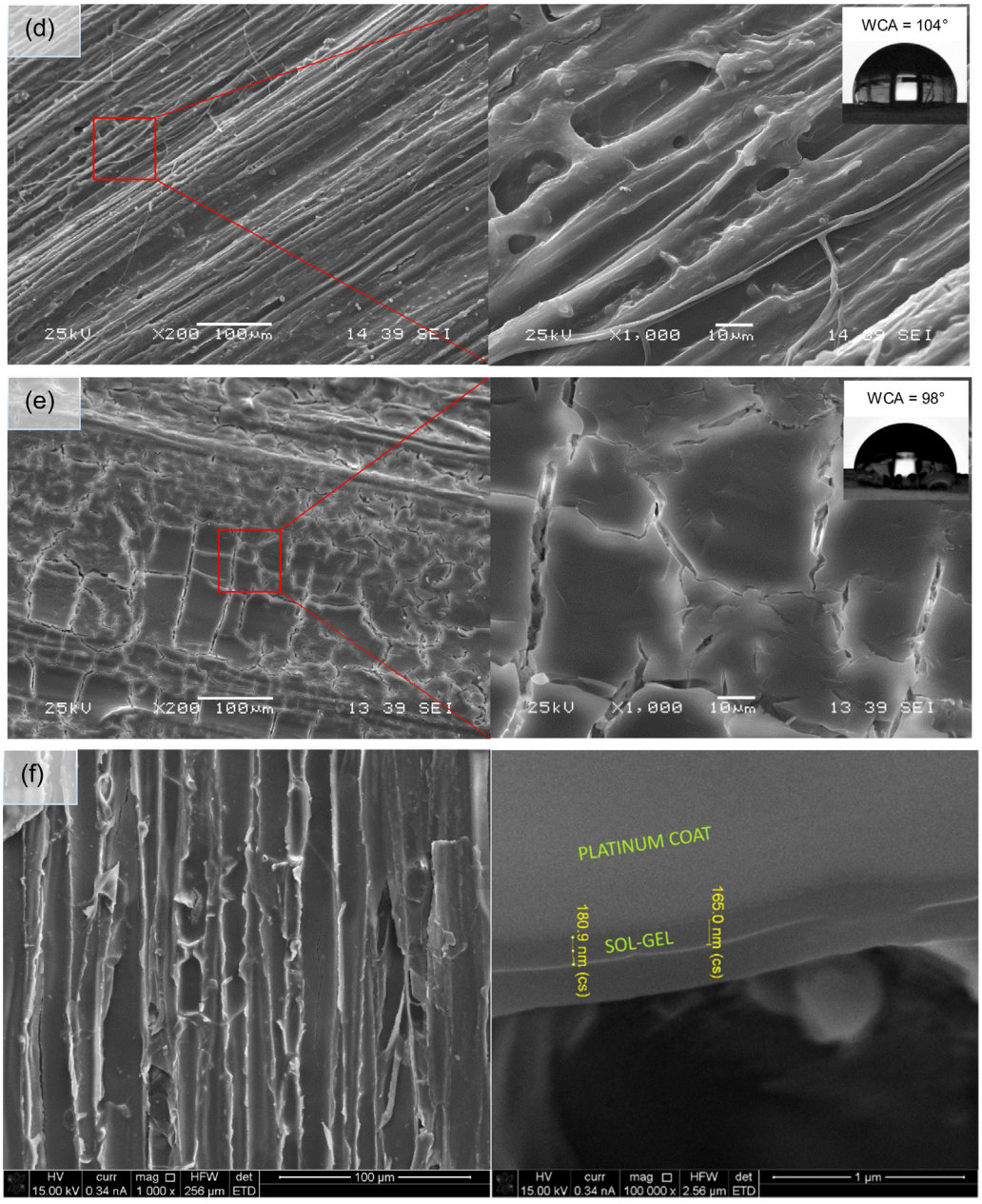

Fig. 6. (*Continued*)

Table 3
Deconvoluted peak parameters and relative amount of different carbon-to-oxygen bonds at sample surface determined by high-resolution XPS.

Carbon Group	Peak parameters		Relative amount (% area)	
	Binding Energy (eV)	Bond	Uncoated	Sol A-7 Coated
C1	285.0	C—C or C—H	48.01	91.09
C2	286.6/286.8	C—OH	36.18	8.91
C3	288.0	O—C—O or C=O	12.56	0.00
C4	289.2	O—C=O	3.24	0.00
$C_{ox/unox}$	–	–	1.08	0.09

The binding energy, corresponding bond type and their relative percentage are listed in Table 3. The ratio of $C_{ox/unox}$ has dropped significantly for sol-gel coated hemp shiv indicating that the carbon oxygen bonds have decreased on the surface of the samples.

The C1s high resolution spectra with the deconvoluted peaks for uncoated and sol-gel coated surfaces are represented in Fig. 8. The C1 peak represents carbon-carbon or carbon-hydrogen bonds whereas C2, C3, and C4 peaks possess carbon-oxygen bonds.

4. Discussion

The sol-gel coatings were functionalised using HDTMS as the hydrophobic additive during the sol-gel synthesis. The co-

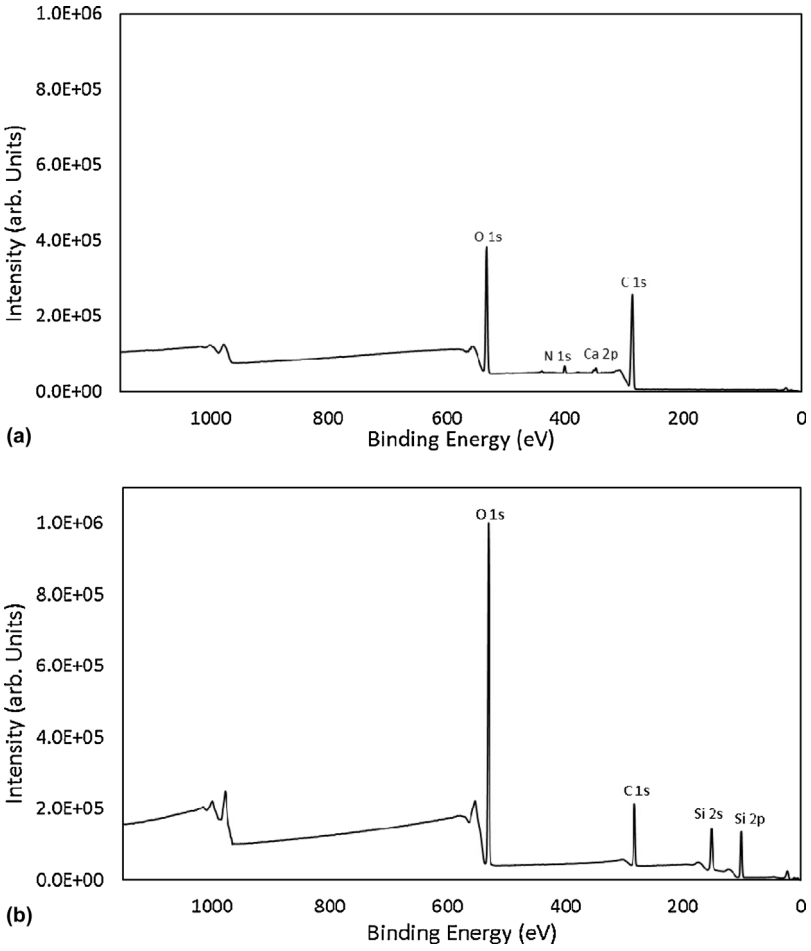

Fig. 7. XPS survey can for (a) uncoated hemp shiv, (b) sol A-7 coated hemp shiv.

precursor method of sol-gel synthesis was followed based on the simplicity of the process. In the sol-gel process, TEOS is hydrolysed and condensed to form a SiO_2 network which is covalently bonded to cell wall through the hydroxyl sites of cellulose present in the hemp shiv. On addition of hydrophobic agent as a co-precursor during the sol-gel processing, the hydroxyl groups on the silica clusters are replaced by the —Si—C_{16} groups through oxygen bonds as illustrated in Fig. 9. The hydrophobicity of the sol-gel coatings is due to the attachment of these long alkyl chains on the silica network thereby providing water resistance to the hemp shiv surface.

Overall, the acid catalysed sol-gel coatings enhance the water repellence of hemp shiv making the surface hydrophobic (WCA > 90°). The wettability of the surface is controlled by the surface chemical composition as well as by the morphology of the microstructure. Surfaces with a similar chemical composition may have different wettability behaviour due to the surface topology [26]. In this study, the surface of hemp shiv underwent microstructural changes via deposition of an organo-functionalised silica coating.

Ethanol diluted sol series enhanced the surface roughness of the hemp shiv. At higher HDTMS loading, undiluted coatings (sol A-1 and sol A-5) lowered the surface roughness of the shiv which could explain the reason for lower contact angles compared to diluted coatings. Sol A-1 and sol A-5 have HDTMS molecules that are not fully hydrolysed and being deposited onto the membrane as a flat thick film as seen in Fig. 6b. The reduced surface roughness can be attributed to the extra HDTMS molecules on the coated surface [27].

Since an organic-inorganic hybrid coating was used, the ratio of TEOS: HDTMS was critical to control the roughness of the coatings resulting in variable water repellent properties of the coated hemp shiv. Most of the coatings enhanced the surface roughness except sol A-1 and sol A-5. These coatings had smooth surfaces with cracks which could explain the lower contact angles even though it had the highest loading of hydrophobic agent. It was observed that the TEOS: HDTMS molar ratio in the coating formulations affected the hydrophobicity of the coated hemp shiv. From Fig. 3 it can be seen that varying the concentration of HDTMS in the formulations affects the water contact angle. When TEOS: HDTMS was 1: 0.01 corresponding to 0.5 wt% HDTMS, the contact angle was below 100° which suggests the concentration of the hydrophobic agent was too low to provide sufficient level of hydrophobicity. The best results were obtained with TEOS: HDTMS ratio 1: 0.02 (1 wt% HDTMS) with contact angles up to 118°. However, when the TEOS: HDTMS ratio was increased to 1: 0.06 (4 wt% HDTMS), the hydrophobicity was decreased for the undiluted sol coatings. These results can be explained by the combined effect of surface roughness and energy. TEOS is hydrophilic whereas HDTMS is hydrophobic and changing their molar ratio can affect the surface roughness and energy of the coated material. Increasing the HDTMS concentration would reduce the surface energy. However, the surface roughness can be reduced if the HDTMS concentration is high enough as the extra silane fills the inter-particle gap. Similar results have been reported in different coating systems [27,28]. Although sol B-7 coating enhanced the surface roughness, it had developed cracks which lowered the water contact angle to 98°. The presence of surface cracks arising as a result of shrinkage after drying the

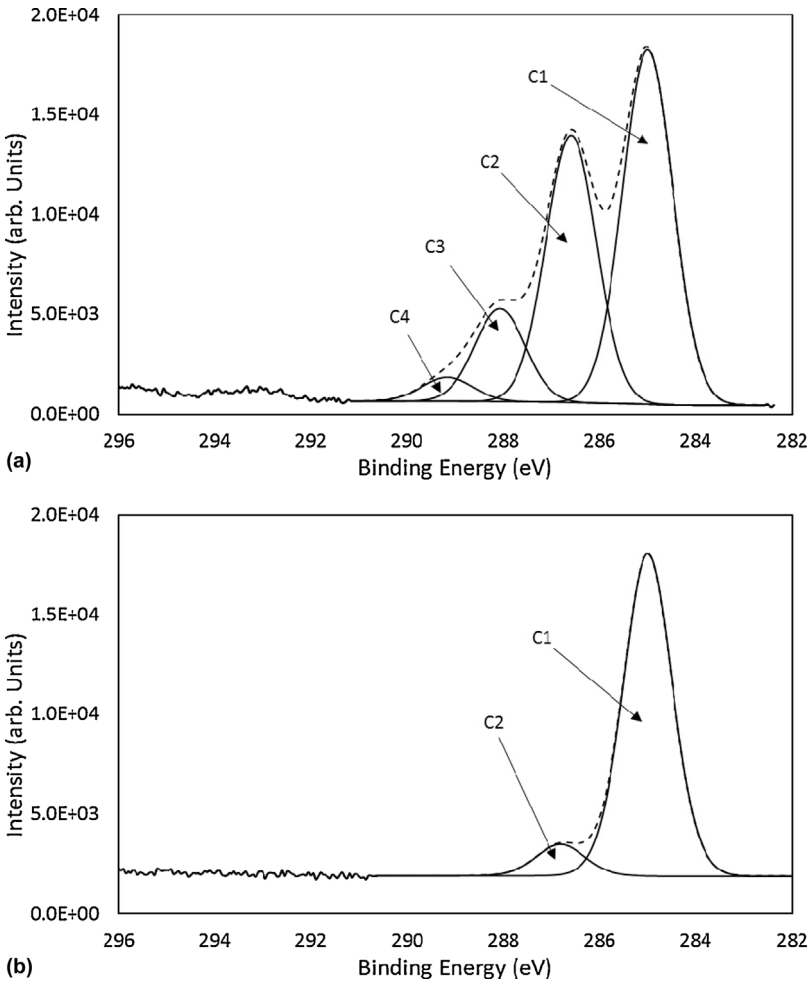

Fig. 8. XPS scan of C_{1s} region for (a) uncoated hemp shiv, (b) sol A-7 coated hemp shiv.

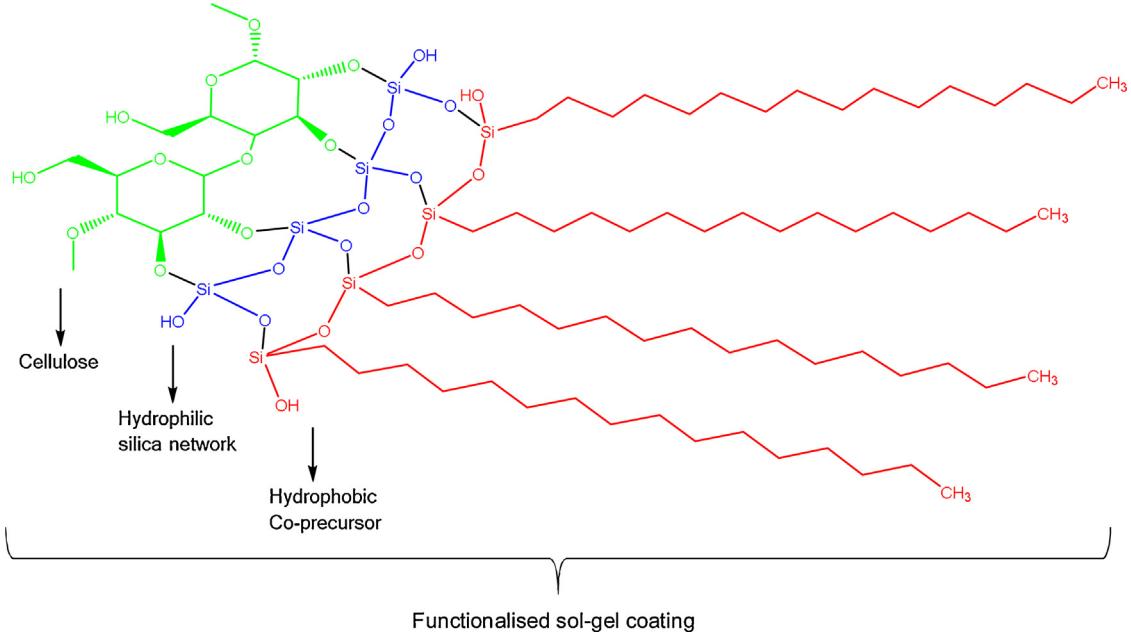

Fig. 9. Schematic illustration of sol-gel deposition on glucose units of cellulose.

coated shiv is a significant factor to be considered when hydrophobic properties are concerned. The hydrophobicity of modified hemp shiv can be compromised as the water molecules can penetrate through the cracked coating wetting the bulk of the material over time. Therefore, sol-gel coatings chemically modified the surface of hemp shiv which overall improved the hydrophobicity of the material. The high water repellence can be attributed to the long alkyl chains of HDTMS that provide high hydrophobicity.

The chemical composition of hemp shiv is mainly composed of cellulose, hemicellulose and lignin, which altogether contain a large percentage of oxidized carbon in their structure. Hydroxyl groups are known to contribute towards majority of the carbon-oxygen bonds in bio-based materials [29]. The XPS data confirmed that the sol-gel deposition on hemp shiv significantly altered the surface chemistry. The surface carbon content of the coated hemp shiv decreased by 41.28% (from 69.61 to 28.33%). On the other hand, the oxygen content increased by 26.51% (from 27.06 to 53.57%). This change in C/O ratio and increase in surface oxygen concentration can be attributed to O—CH_3 bonds present in the polysiloxane coating on the surface of the sol-gel coated hemp shiv. Moreover, the decrease in the surface carbon concentration of the sol-gel coated shiv can be attributed to the masking effect of the polysiloxane coating which reduces the detectability of surface cellulose and hemicellulose.

The C1s high resolution XPS spectra indicate that the surface has been modified by the silica based coating that led to disappearance of C3 and C4 components of the C1s peaks. A shift in the binding energy of C2 component (from 286.6 to 286.8 eV) was observed along with the decrease in the intensity of the C2 component for the sol-gel coated sample. This shift indicates the presence of a carbon atom linked to an oxygen and silicon atom (O—C—Si or C—O—Si) [18]. It has also been shown [16,30–32] that curing above room temperature drives the dehydration reaction at the adsorption sites between hydroxyl groups of the cellulose and the silanols forming —Si—O—C— bonds. These bonds are formed by the linkage between polysilanol network with the cellulose hydroxyl groups via polycondensation as illustrated in Fig. 9. The increase in the intensity of C1 component for sol-gel coated sample from 48.01% to 91.09% indicates the presence of C—H and C—C bonds from the HDTMS hydrocarbon chain.

5. Conclusion

A simple one step dip-coating process was successfully applied to form a hydrophobic surface onto an extremely hydrophilic bio-based aggregate construction material. The hydrophobic properties were achieved through a combination of topological alteration and chemical modification of the hemp shiv by the modified silica based sol-gel coatings.

The treated material (hemp shiv coated with silica based membrane) delivered the following properties when compared to the untreated hemp shiv:

- Delivered water repellence by maintaining stable water contact angles over 60 s.
- Controlled surface wettability through microstructure modification.
- Uniform and crack-free coated surface.
- Enhanced surface roughness providing water contact angles up to 118°.

It can be concluded that water based sol-gel coatings with low HDTMS precursor loading (sol A-7) would be of interest to the bio-based building industry due to its hygroscopic properties, long shelf life, reduced cost and lower environmental impact.

Acknowledgments

This study was supported by the Canadian Queen Elizabeth II Diamond Jubilee Scholarship and the ISOBIO project funded by the Horizon 2020 programme [grant number 636835-ISOBIO – H2020-EeB-2014-2015]. The authors would also like to acknowledge the EPSRC Centre for Decarbonisation of the Built Environment (dCarb) [grant number EP/L016869/1] and the NSERC project (grant number IRCPJ 461745-12). The ISOBIO project aims to develop and bring new bio-based insulation panels and renders into the mainstream for the purpose of creating more energy efficient buildings. The contents of this publication are the sole responsibility of the authors and can in no way be taken to reflect the views of the European Union. All data are provided in full in the results section of this paper.

References

[1] J. Genzer, K. Efimenko, Recent developments in superhydrophobic surfaces and their relevance to marine fouling: a review, Biofouling 22 (2006) 339–360, http://dx.doi.org/10.1080/08927010600980223.
[2] A. Nakajima, K. Hashimoto, T. Watanabe, Recent studies on super-hydrophobic films, Monatsh. Chem. (2001) 31–41, http://dx.doi.org/10.1007/s007060170142.
[3] S. Benfratello, C. Capitano, G. Peri, G. Rizzo, G. Scaccianoce, G. Sorrentino, Thermal and structural properties of a hemp-lime biocomposite, Constr. Build. Mater. 48 (2013) 745–754, http://dx.doi.org/10.1016/j.conbuildmat.2013.07.096.
[4] A.D. Tran Le, C. Maalouf, T.H. Mai, E. Wurtz, F. Collet, Transient hygrothermal behaviour of a hemp concrete building envelope, Energy Build. 42 (2010) 1797–1806, http://dx.doi.org/10.1016/j.enbuild.2010.05.016.
[5] L. Arnaud, E. Gourlay, Experimental study of parameters influencing mechanical properties of hemp concretes, Constr. Build. Mater. 28 (2012) 50–56, http://dx.doi.org/10.1016/j.conbuildmat.2011.07.052.
[6] M. Theis, B. Grohe, Biodegradable lightweight construction boards based on tannin/hexamine bonded hemp shaves, Holz. Als. Roh. Und. Werkst. 60 (2002) 291–296, http://dx.doi.org/10.1007/s00107-002-0306-0.
[7] H. Kyma, M. Hautala, R. Kuisma, A. Pasila, Capillarity of flax/linseed (Linum usitatissimum L.) and fibre hemp (Cannabis sati 6 a L.) straw fractions, Ind. Crops Prod. 14 (2001) 41–50.
[8] J. Gassan, V.S. Gutowski, A.K. Bledzki, About the surface characteristics of natural fibres, Surf. Eng. 283 (2000) 132–139, http://dx.doi.org/10.1002/1439-2054(20001101)283:1<132:AID-MAME132>3.0.CO;2-B.
[9] S. Marceau, P. Glé, M. Guéguen-Minerbe, E. Gourlay, S. Moscardelli, I. Nour, S. Amziane, Influence of accelerated aging on the properties of hemp concretes, Constr. Build. Mater. 139 (2017) 524–530, http://dx.doi.org/10.1016/j.conbuildmat.2016.11.129.
[10] L. Kidalova, N. Stevulova, E. Terpakova, Influence of water absorption on the selected properties of hemp hurds composites, Pollack Period 10 (2015) 123–132, http://dx.doi.org/10.1556/Pollack.10.2015.1.12.
[11] M.R. Vignon, D. Dupeyre, Steam explosion of woody hemp ch nevotte, Int. J. Biol. Macromol. 17 (1995) 395–404.
[12] M.M. Kabir, H. Wang, K.T. Lau, F. Cardona, Chemical treatments on plant-based natural fibre reinforced polymer composites: an overview, Compos. Part B Eng. 43 (2012) 2883–2892, http://dx.doi.org/10.1016/j.compositesb.2012.04.053.
[13] S. Donath, H. Militz, C. Mai, Wood modification with alkoxysilanes, Wood Sci. Technol. 38 (2004) 555–566, http://dx.doi.org/10.1007/s00226-004-0257-1.
[14] E. Cabane, T. Keplinger, V. Merk, P. Hass, I. Burgert, Renewable and functional wood materials by grafting polymerization within cell walls, ChemSusChem 7 (2014) 1020–1025, http://dx.doi.org/10.1002/cssc.201301107.
[15] J. Song, O.J. Rojas, Approaching super-hydrophobicity from cellulosic materials: a review, Pap. Chem. 28 (2013) 216–238, http://dx.doi.org/10.3183/NPPRJ2013-28-02-p216-238.
[16] A. Valadez-Gonzalez, J.M. Cervantes-Uc, R. Olayo, P.J. Herrera-Franco, Effect of fiber surface treatment on the fiber-matrix bond strength of natural fiber reinforced composites, Compos. Part B Eng. 30 (1999) 309–320, http://dx.doi.org/10.1016/S1359-8368(98)00054-7.
[17] C. Brinker, G. Scherer, Sol-gel science: the physics and chemistry of sol-gel processing, Adv. Mater. 3 (1990) 912, http://dx.doi.org/10.1186/1471-2105-8-444.
[18] M.A. Tshabalala, P. Kingshott, M.R. Vanlandingham, D. Plackett, Surface Chemistry and Moisture Sorption Properties of Wood Coated with Multifunctional Alkoxysilanes by Sol- Gel Process, 2002.
[19] B. Tomšič, B. Simončič, B. Orel, L. Černe, P.F. Tavčer, M. Zorko, I. Jerman, A. Vilčnik, J. Kovač, Sol–gel coating of cellulose fibres with antimicrobial and repellent properties, J. Sol-Gel Sci. Technol. 47 (2008) 44–57, http://dx.doi.org/10.1007/s10971-008-1732-1.

[20] L. Xu, W. Zhuang, B. Xu, Z. Cai, Superhydrophobic cotton fabrics prepared by one-step water-based sol-gel coating, J. Text. Inst. 103 (2012) 311–319, http://dx.doi.org/10.1080/00405000.2011.569238.
[21] S. Sankaraiah, J.M. Lee, J.H. Kim, S.W. Choi, Preparation and characterization of surface-functionalized polysilsesquioxane hard spheres in aqueous medium, Macromolecules 41 (2008) 6195–6204, http://dx.doi.org/10.1021/ma8003345.
[22] Y. Fujiwara, Y. Fujii, Y. Sawada, S. Okumura, Assessment of wood surface roughness: comparison of tactile roughness and three-dimensional parameters derived using a robust Gaussian regression filter, J. Wood Sci. 50 (2004) 35–40, http://dx.doi.org/10.1007/s10086-003-0529-7.
[23] L. Gurau, H. Mansfield-Williams, M. Irle, Filtering the roughness of a sanded wood surface, Holz. Als. Roh. Und. Werkst. 64 (2006) 363–371, http://dx.doi.org/10.1007/s00107-005-0089-1.
[24] B. Ugulino, R.E. Hernández, Assessment of surface properties and solvent-borne coating performance of red oak wood produced by peripheral planing, Eur. J. Wood Wood Prod. (2016) 1–13, http://dx.doi.org/10.1007/s00107-016-1090-6.
[25] N.M. Stark, L.M. Matuana, Surface chemistry changes of weathered HDPE/wood-flour composites studied by XPS and FTIR spectroscopy, Polym. Degrad. Stab. 86 (2004) 1–9, http://dx.doi.org/10.1016/j.polymdegradstab.2003.11.002.
[26] Q.F. Xu, J.N. Wang, K.D. Sanderson, Organic-inorganic composite nanocoatings with superhydrophobicity, good transparency, and thermal stability, ACS Nano 4 (2010) 2201–2209, http://dx.doi.org/10.1021/nn901581j.
[27] H. Wang, H. Zhou, S. Liu, H. Shao, S. Fu, G.C. Rutledge, T. Lin, Durable, self-healing, superhydrophobic fabrics from fluorine-free, waterborne, polydopamine/alkyl silane coatings, RSC Adv. 7 (2017) 33986–33993, http://dx.doi.org/10.1039/C7RA04863G.
[28] C. Zeng, H. Wang, H. Zhou, T. Lin, Self-cleaning, superhydrophobic cotton fabrics with excellent washing durability, solvent resistance and chemical stability prepared from an SU-8 derived surface coating, RSC Adv. 5 (2015) 61044–61050, http://dx.doi.org/10.1039/C5RA08040A.
[29] N.M. Stark, L.M. Matuana, Ultraviolet weathering of photostabilized wood-flour-filled high-density polyethylene composites, J. Appl. Polym. Sci. 90 (2003) 2609–2617, http://dx.doi.org/10.1002/app.12886.
[30] Y. Xie, C.A.S. Hill, Z. Xiao, H. Militz, C. Mai, Silane coupling agents used for natural fiber/polymer composites: a review, Compos. Part A Appl. Sci. Manuf. 41 (2010) 806–819, http://dx.doi.org/10.1016/j.compositesa.2010.03.005.
[31] M. Castellano, A. Gandini, P. Fabbri, M.N. Belgacem, Modification of cellulose fibres with organosilanes: under what conditions does coupling occur? J. Colloid Interface Sci. 273 (2004) 505–511, http://dx.doi.org/10.1016/j.jcis.2003.09.044.
[32] M. Abdelmouleh, S. Boufi, M.N. Belgacem, A. Dufresne, Short natural-fibre reinforced polyethylene and natural rubber composites: effect of silane coupling agents and fibres loading, Compos. Sci. Technol. 67 (2007) 1627–1639, http://dx.doi.org/10.1016/j.compscitech.2006.07.003.

Commentary Text

A set of sols was also prepared using basic catalysts instead of acidic catalysts. The formulations were prepared by stirring 1M TEOS in a mixture of 4M water and 4M ethanol. The basic catalysts used for the study were NaOH and NH_4OH in the concentration 0.05M. The hydrophobic agent HDTMS was added in concentrations of 4 wt% of the sol. These mixtures of silica sol and HDTMS were stirred for at least 20 minutes before performing the dip-coating process. The coating process was followed in the same manner as reported earlier in the article of this Chapter (experimental section). The prepared sols and their gel-time are listed in Table 5.1.

Table 5.1 Basic sol compositions and gel-time.

FORMULATION	CATALYST	CONC. (M)	GEL TIME (DAYS)
sol C-1	NaOH	0.05	6
sol C-2	NH_4OH	0.05	5

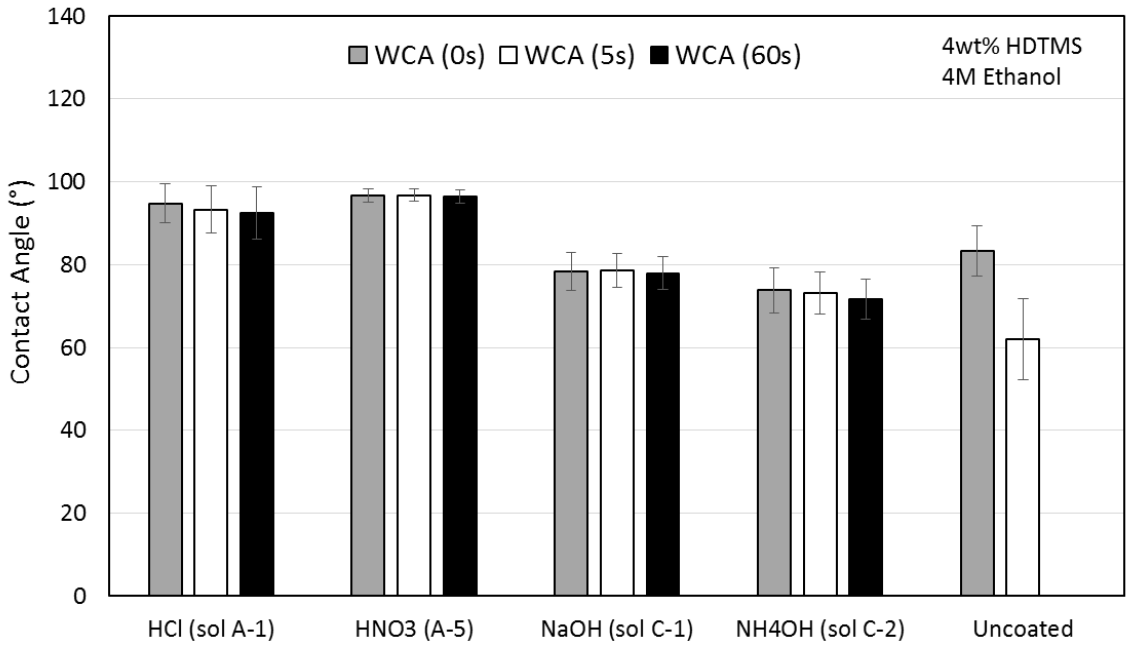

Figure 5.1 WCA measurements for acidic and basic sols over 60 seconds of contact.

Keeping the HDTMS and ethanol concentration constant between the acidic and basic sols, it was seen that the coatings prepared using acidic catalysts showed better contact angles as seen in Figure 5.1. Both acidic and basic sol-gel coatings tend to reduce the hydrophilicity of the hemp shiv by maintaining a stable contact angle over 60 seconds. However, it is clear that using this process of sol-gel dip coating, the basic sols are unable to provide a hydrophobic surface (WCA<90°) on the hemp shiv.

It is well known that the in the sol-gel process, basic sols result in the production of silica nanoparticles. Cellulose based fibres can be covered by silica nanoparticles by simple dip coating (Zhou, Wang, Niu, Gestos, & Lin, 2013), by spraying SiO2 nanoparticles suspended in alcohol (Ogihara, Xie, Okagaki, & Saji, 2012) or by heat treatment (Xu, Zhuang, Xu, & Cai, 2011) resulting in a chemical bond formation between silica and the hydroxyl groups of cellulose. Silica nanoparticles prepared by the sol-gel process are usually negatively charged and the surface of cellulose fiber carries negative charges in aqueous solution as well. Therefore, the coverage of silica nanoparticles on cellulose based fibers without pre-treatment is quite poor (Bae et al., 2009; Yu, Gu, Meng, & Qing, 2007), which may affect the strength of the functionality it is expected to provide on the material. This may be the reason for the lower WCA on hemp shiv coated with basic sols. In order to enhance the hydrophobic functionality, the nanoparticle coverage and roughness needs to be increased. This can be obtained by depositing multilayers of silica nanoparticles and combining the basic sol-gel suspension with cationic polyelectrolytes (Song & Rojas, 2013). Sols prepared using acid catalysts are deposited as continuous thin membranes rather than nanoparticles.

Since the acidic sols enhanced the water repellence of hemp shiv making the surface hydrophobic (WCA>90°), they were further studied in this Chapter. The selected formulation is sol A-7 and its effect on the porosity and hygroscopic properties of hemp shiv is studied in the next chapter.

Chapter 6

Effect of Selected HDTMS based Coating on Hemp Shiv Properties

This Chapter has been submitted as a Journal paper entitled “Preparation of hydrophobic surface on hemp shiv while retaining its moisture buffering ability” to Construction and Building Materials.

Introductory Text

This paper further investigates the effect of the selected HDTMS based formulation (sol A-7) from Chapter 5 on the hygroscopic properties of hemp shiv. In particular, the objective of this paper was to demonstrate that hemp shiv treated with HDTMS based coating retains its ability to exchange moisture as seen with the vapour sorption experiment. The HDTMS based coating reported in this chapter performs better than the MTES based coating reported in Chapter 4 in terms of reduction in water absorption capacity of hemp shiv. The reduced hysteresis in the vapour sorption isotherm reveal that the moisture does not penetrate deep into the shiv due to the deposition of the hydrophobic coating. Chemical analysis of HDTMS based silica glass, uncoated and coated hemp shiv has also been reported in this paper.

Statement of Authorship

<table>
<tr><th colspan="9">This declaration concerns the article entitled:</th></tr>
<tr><td colspan="9">Preparation of hydrophobic surface on hemp shiv while retaining its moisture buffering ability</td></tr>
<tr><td colspan="9">Publication status (tick one)</td></tr>
<tr><td>draft manuscript</td><td></td><td>Submitted</td><td></td><td>In review</td><td>✓</td><td>Accepted</td><td></td><td>Published</td><td></td></tr>
<tr><td>Publication details (reference)</td><td colspan="8">Hussain, A., Calabria-Holley, J., Lawrence. M., & Jiang, Y., Preparation of hydrophobic surface on hemp shiv while retaining its moisture buffering ability. Construction and Building Materials.</td></tr>
<tr><td>Candidate's contribution to the paper (detailed, and also given as a percentage).</td><td colspan="8">The candidate contributed to/ considerably contributed to/predominantly executed the…

Formulation of ideas: 90%
The concept was presented by A. Hussain and discussed with this supervisors M. Lawrence and J. Calabria-Holley.

Design of methodology: 90%
A. Hussain designed the methodology for this paper. All co-authors shared their expertise.

Experimental work: 100%
A. Hussain did all the experimental work and the data analysis.

Presentation of data in journal format: 90%
A. Hussain prepared the manuscript. The co-authors provided feedback and comments.</td></tr>
<tr><td>Statement from Candidate</td><td colspan="8">This paper reports on original research I conducted during the period of my Higher Degree by Research candidature.</td></tr>
<tr><td>Signed</td><td colspan="4">  </td><td>Date</td><td colspan="3">15.09.2018</td></tr>
</table>

Submitted Article: Preparation of hydrophobic surface on hemp shiv while retaining its moisture buffering ability

Atif Hussain*, Juliana Calabria- Holley, Mike Lawrence, Yunhong Jiang

BRE Centre for Innovative Construction Materials, Department of Architecture and Civil Engineering, University of Bath, Bath BA2 7AY, UK
*Corresponding Author: Atif Hussain (A.Hussain@bath.ac.uk)

Abstract

This study focuses on the surface treatment of an extremely hydrophilic natural plant material, hemp shiv, using a silica based coating functionalised with hexadecyltrimethoxysilane (HDTMS). The chemical composition and physical structure of bio-based materials results in their extremely hydrophilic behaviour. In this work, a simple and inexpensive one step coating process was used to enhance the hydrophobicity of hemp shiv without compromising its moisture buffering property. The coating modified the morphology and surface roughness of hemp shiv providing a hydrophobic surface having a water contact angle of 118° and reduced the bulk water absorption by 250% over 24 hours. The coating reduced the size the larger pores in hemp shiv but did not block the smaller pores thereby allowing hemp shiv to adsorb and release moisture. Fourier-transform infrared spectroscopy (FTIR) revealed the chemical composition was modified by the coating, reducing the hydroxyl groups. Hemp shiv surface treated with hydrophobic silica coating shows potential for the development of new resilient building materials with engineered hygroscopic properties.

Keywords: hemp shiv, bio-based, moisture buffering, hydrophobicity, coating, surface engineering.

Introduction

Bio-based aggregates in the building industry has become popular due to their lower embodied energy, lower CO2 emissions and good hygrothermal properties reducing the energy demands of buildings [1]. Hemp shiv is the woody core obtained from the stem of the hemp (*Cannabis Sativa* L.). Hemp shiv based composites have been actively researched due to their high moisture buffering and good thermal insulation properties [2,3]. The moisture buffering property, absorb and release moisture at dynamic relative humidity levels, of hemp shiv is associated with its pore structure [4]. Hemp shiv has a dry bulk density of 107 ± 3 kg/m^3 [5] and porosity of 76-78% [6] tending to absorb huge volume of water when compared with other plant materials [7]. The chemical composition of industrial hemp shiv are: 44-46% cellulose, 18-27% hemicellulose, 22-28% lignin, 1-6% extractives and 1-2% ash [8,9]. Cellulose forms the main structural part of hemp shiv containing free hydroxyl groups which are responsible for the extreme hydrophilicity. As a result, hemp shiv based building composites have extremely long drying times when mixed with lime [10], or they have poor interfacial adhesion with the polymeric matrix [11]. Moisture sensitivity also results in microbial growth causing degradation of the aggregate cell wall and deterioration of the composite durability [12].

The wetting behaviour of any solid surface is governed by the surface chemical composition and its geometric structure [13,14]. The interaction between surface roughness and chemistry is actively researched for improving the hydrophobic properties of plant based materials. One of the mechanisms to enhance the hydrophobicity of plant based materials involves altering the chemical composition by blocking the cell wall hydroxyl group. Some of the approaches include addition of silanes [15], acetylation [16] or in situ polymerization [17] that involve chemical modification of the aggregate cell wall. Other approaches that can enhance surface roughness and hydrophobicity of the material include sol-gel coatings, plasma treatment or lithography. The sol-gel technique can be carried at room temperature and it is widely used for enhancing surface hydrophobicity by depositing coatings with low surface energy and increased roughness [18]. Sol-gel coatings have been used on various bio-based materials

for improving their hydrophobicity [15,19–22] however there is limited knowledge on the impact of sol-gel coatings on hemp shiv. Sol-gel treatment has also proven to improve the fire resistance and reduce the flammability of cellulose based materials [23].

This work focuses on modification of hemp shiv surface using a functionalised silica based coating to enhance to hydrophobicity of hemp shiv without compromising its moisture buffering capacity. Our work reports the application of a breathable coating on hemp shiv using a simple inexpensive one step process. The objective of this work was to investigate the effect of a hydrophobic silica coating on the porosity, moisture buffering ability and surface morphology of hemp shiv.

Experimental

Materials

The hemp shiv aggregates (Figure 1) were received from an agricultural cooperative CAVAC, France. Tetraethyl orthosilicate (TEOS, 98%), nitric acid (HNO_3, 70%), hexadecyltrimethoxysilane (HDTMS, 85%) and absolute ethanol were received from Sigma-Aldrich.

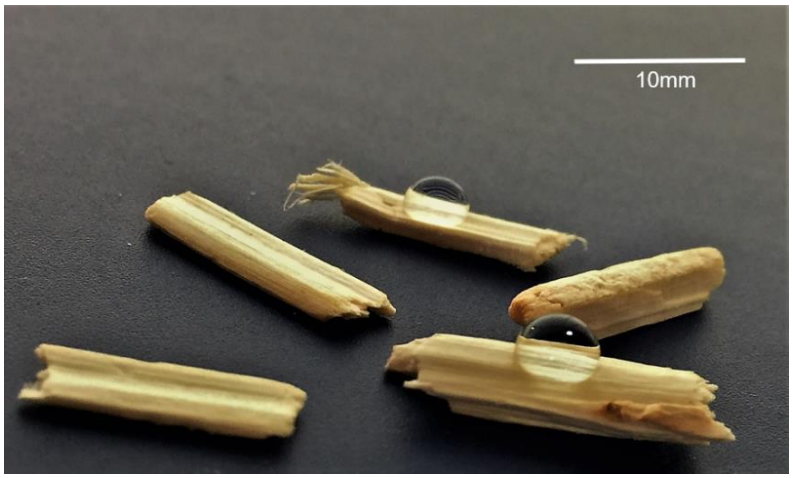

Figure 1. Water droplets on hemp shiv treated with silica coating.

Coating preparation

The coating was prepared by hydrolysis and condensation of TEOS in water and ethanol and nitric acid was added as the catalyst. The coating formulation was 1M of TEOS, 4M water, 4M ethanol and 0.005M nitric acid. The solution was stirred using a magnetic stirrer for 30 minutes at 300 rpm and 40 °C. After the preparation of silica formulation, 1 wt. % of HDTMS was added as the hydrophobic agent and the sol was stirred for another 20 minutes at 300rpm. The pH of the prepared sol was measured to be 1.92.

The prepared sol aged in a sealed vial for 48 hours at 20 °C. Hemp shiv aggregates were immersed in the sol for 10 min and then carefully placed on a Petri dish for drying at room temperature 20 °C for an hour. The aggregates were then dried at 80 °C for an hour in a laboratory oven. The treated samples were stored in a sealed vial for further sample characterisation. The treated samples had an average mass gain of 18% due to the deposition of the silica coating on the hemp shiv. For calculating the amount of residual water, the treated samples

were vacuum sealed in a glass tube, heated at 150°C overnight and then weighed. The residual water content was found to be 5 wt. % for coated hemp shiv samples. The silica glass was prepared by aging the sol in a sealed vial for 48 hours at 20 °C and then placed in oven at 80 °C for at least 120 hours to undergo dehydration. The gel time of the prepared sol was 101 days when stored in a sealed vial at 20 °C.

Contact Angle Measurements

The determination of water contact angle (WCA) was performed by a contact angle meter (First Ten Ångstroms USA, FTA200 series) using the sessile drop method. The WCA readings were taken for a minimum of 3 different samples. The water droplets used during the test had a volume of 5µl. The recorded images were analysed by FTA32 Video 2.0 software. The experiment was performed at room temperature (20 ± 1 °C).

Water absorption test

Prior to the test, the samples were dried overnight in an oven at 80 °C and then weighed for recording the initial mass. The samples were placed in beaker containing water and since they have a density lower than water, the samples floated and only one side of the shiv was in contact with water. Therefore, the water uptake was mainly due to capillary behaviour. The readings were taken at frequent intervals for 24 hours, in which the sample was taken out of water using a tweezer, shaken off to remove any visible surface water and then weighed within 30s. Mass readings were recorded to the nearest 0.1 mg and an average of three readings from different samples was reported as the final measurement.

Dynamic vapour sorption

For the analysis of the adsorption-desorption isotherm in response to varying humidity levels, a dynamic vapour sorption equipment DVS Advantage, SMS, UK was used. The detailed test protocol is reported in a previous paper [6]. The samples weighed around 15 mg and experiment temperature was maintained at 23 °C. The relative humidity (RH) was increased in steps from 0-90% and then decreased back to 0%. The actual and target RH, sample mass and running time were continuously recorded during the experiment.

The data obtained from the isotherms was used to calculate the moisture content of the samples at any given RH using the following equations:

$$MC = \frac{m_2 - m_1}{m_1} \times 100 \quad (1)$$

$$MC_R = \frac{m_2 - m_1}{m_0} \times 100 \quad (2)$$

Where MC is the measured equilibrium moisture content of the sample; MC_R is the reduced equilibrium moisture content of the sample before coating; m_0 is mass of oven dried uncoated shiv sample; m_1 is the mass of oven dried coated shiv sample; m_2 is the mass of shiv sample at any given RH.

Scanning Electron Microscopy

Photomicrographs of the samples were captured using a scanning electron microscope (SEM), JEOL Corporation - Japan Model JSM-6360 operating at 25 kV. The samples were gold coated to obtain high magnification of morphology and texture.

Surface Roughness

For measurement of sample surface roughness, a 3D optical profilometer, Bruker Nano GmbH ContourGT-K series, Germany was used in non-contact mode. The area analysed for each test was 0.25*0.30 mm^2 and magnification was set to 20X. The data was analysed by Vision 64 software and the surface roughness was calculated. The test was performed for at least 3 different samples and the average value was reported.

Fourier transform infrared (FTIR) spectroscopy

For identification of the chemical bonds, FTIR analysis was performed with a PerkinElmer FTIR spectrometer, Model Frontier. Transmittance spectra were recorded in the range of 4000-600 cm^{-1} with a resolution of 2 cm^{-1} and 10 scans were run for each test. Hemp shiv samples were tested as individual pieces whereas the silica glass sample was crushed to powder form and then mixed with potassium bromide to form pellets.

Results

The water contact angles were recorded from 0-60 seconds of contact between the droplet and the hemp shiv surface. From Figure 2, it was observed that hemp shiv surface that have not been coated have highly hydrophilicity. The initial contact angle was 79° and the droplet sinks into the bulk of the sample completely in less than 20 seconds. On the other hand, the sol-gel coated samples have an initial contact angle of 118° making the surface hydrophobic. The contact angle remains stable over 60 seconds of contact.

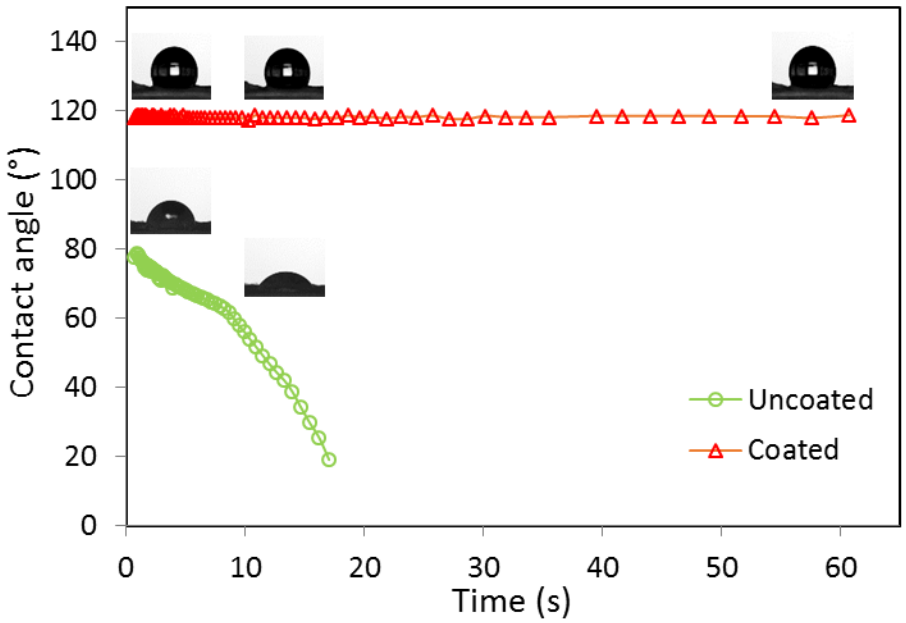

Figure 2. Water contact angles of coated and uncoated hemp shiv over time.

Water absorption (WA %) measures the relative percentage increase in mass due to the retention of water within the bulk of the sample. It is calculated using the following equation:

$$\text{WA } \% = \frac{\text{Sample wet weight} - \text{Sample dry weight}}{\text{Sample dry weight}} \text{ x } 100 \quad (3)$$

Figure 3 shows the absorption of water for coated and uncoated hemp shiv samples over 24 hour period. It was observed that within the initial few minutes of contact with water, hemp shiv can absorb a huge volume of water corresponding the significantly high mass increase. Uncoated hemp shiv shows extremely high water absorption reaching up to 4 times its initial mass after 24 hours. This tendency of absorbing water is mainly caused by the hydrophilic

behaviour of hemp shiv and its highly porous structure. Hemp shiv treated with the silica coating shows a significant reduction in water absorption by almost 250%. The treated shiv sample absorbs water only 1.5 times its initial mass over 24 hours.

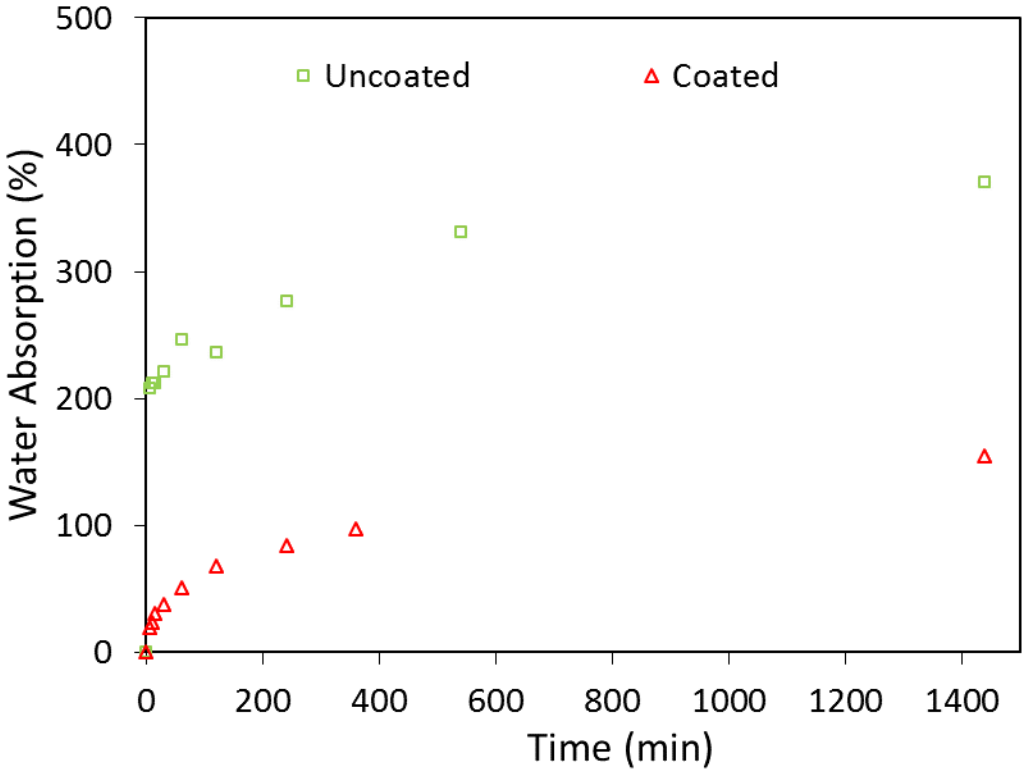

Figure 3. Water absorption of coated and uncoated hemp shiv samples.

The sorption isotherm of coated and uncoated hemp shiv was determined over a RH range 0-90%. It was observed the coating lowered the measured moisture content (MC) in the isotherm. The coating decreased the measured MC of the hemp shiv sample by 30%. Coated shiv showed a maximum measured MC of 12.81% at the highest humidity level of 90% whereas uncoated hemp shiv had a measured MC value of 19.41% at 90 % relative humidity level as seen in Figure 4a.

It should be noted that the coating increases the mass of hemp shiv and therefore the reduced moisture content (MC_R) of the coated shiv was calculated to be 15.12%. The MC_R of uncoated shiv remains the same as its MC which is 19.41% which means that the moisture adsorption capacity of the coated shiv is not

significantly different than the uncoated shiv. The fact that the coating increases the mass of the shiv, equations (1) and (2) show that for uncoated hemp shiv MC = MC_R but for coated shiv MC < MC_R [6,24].

The hysteresis values between adsorption and desorption curves of uncoated and coated shiv are presented in Figure 4b. It can be seen from the hysteresis curves that coated shiv shows lower hysteresis when compared to uncoated shiv. It was observed that the difference in hysteresis between coated and uncoated shiv increased at each higher RH step.

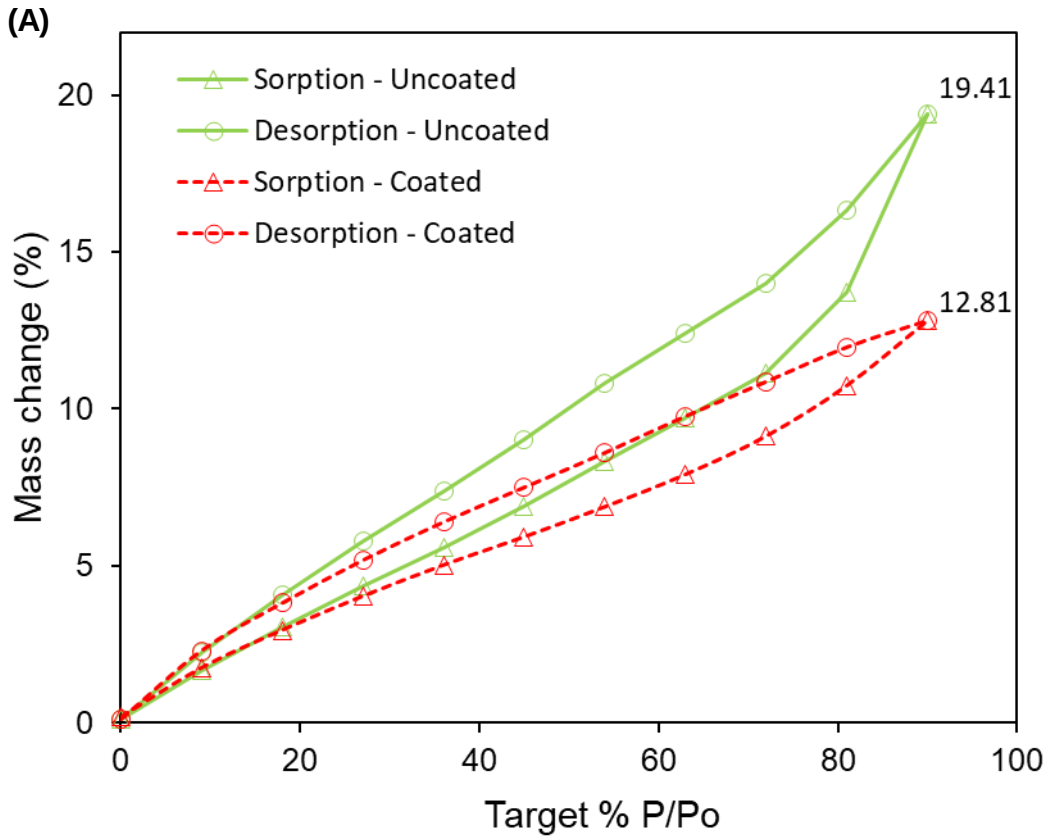

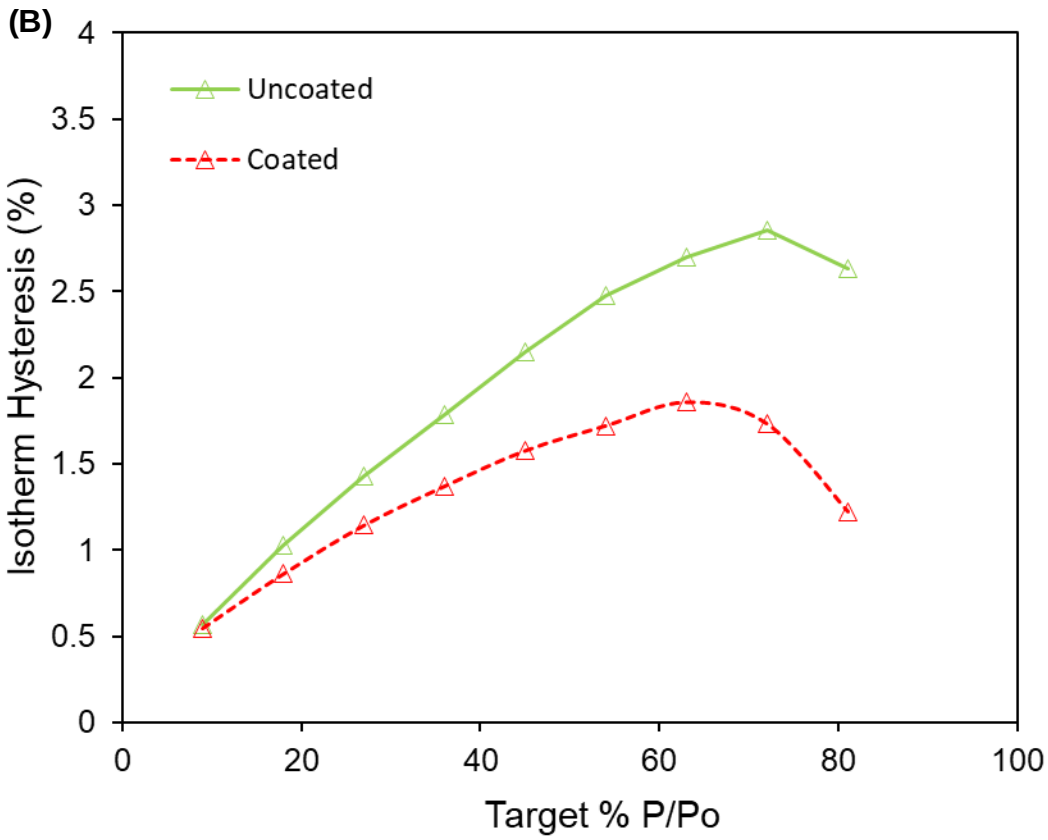

Figure 4. (A) Sorption isotherms; (B) isotherm hysteresis curves of uncoated and coated samples.

The pore size distribution of uncoated and coated shiv is given in Figure 5. The overall porosity of hemp shiv is unaffected by the coating and both samples have a porosity of 78 ± 0.7%. The cumulative pore volume is found to be very similar as well, 2428 mm^3/g and 2377 mm^3/g for uncoated and coated samples respectively. Figure 5 shows that the coating reduced the diameter of the larger pores, mainly in the range of 1 µm to 10 µm. The pores over 50 µm remain unaffected by the coating suggesting that the layer of coating deposited is very thin and in the nanometer scale.

Another observation from Figure 5 is that the coated shiv has increased number of smaller pores in the range of 100-800 nm compared to the uncoated shiv. The overall porosity remaining the similar for both samples suggest that the overall pore volume is not reduced but only the pores have been refined from micron size to nano size.

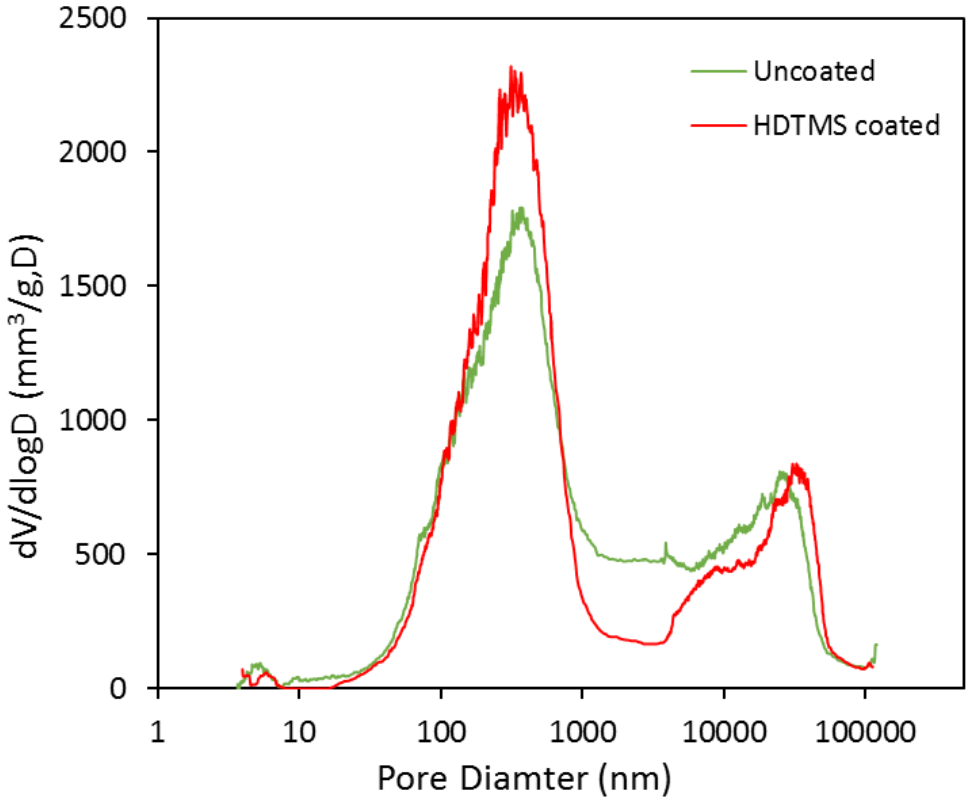

Figure 5. Pore size distribution of uncoated and coated hemp shiv.

The surface roughness of uncoated and coated hemp shiv samples was analysed by the software Vision64 and a Robust Gaussian Filter (ISO 16610-31 2016) was applied. The anatomical influence can be reduced with the help of such filters and the roughness profile can be optimised for surface evaluation of the sample [25,26]. Moreover, when analysing deep valleys on the sample surface, the robust Gaussian filter does not produce distortions that maybe formed by other filters [27]. The mean surface roughness (*Sa*) is the most widely used parameter for describing the variations in surface height and was calculated according to ISO 4287 (1997).

The 3D roughness profile for uncoated and coated hemp shiv surfaces is shown in Figure 6. It was observed that the coating enhanced the surface roughness of the samples with a mean *Sa* value of 2.07 µm compared to uncoated shiv having a mean *Sa* value of 1.79 µm.

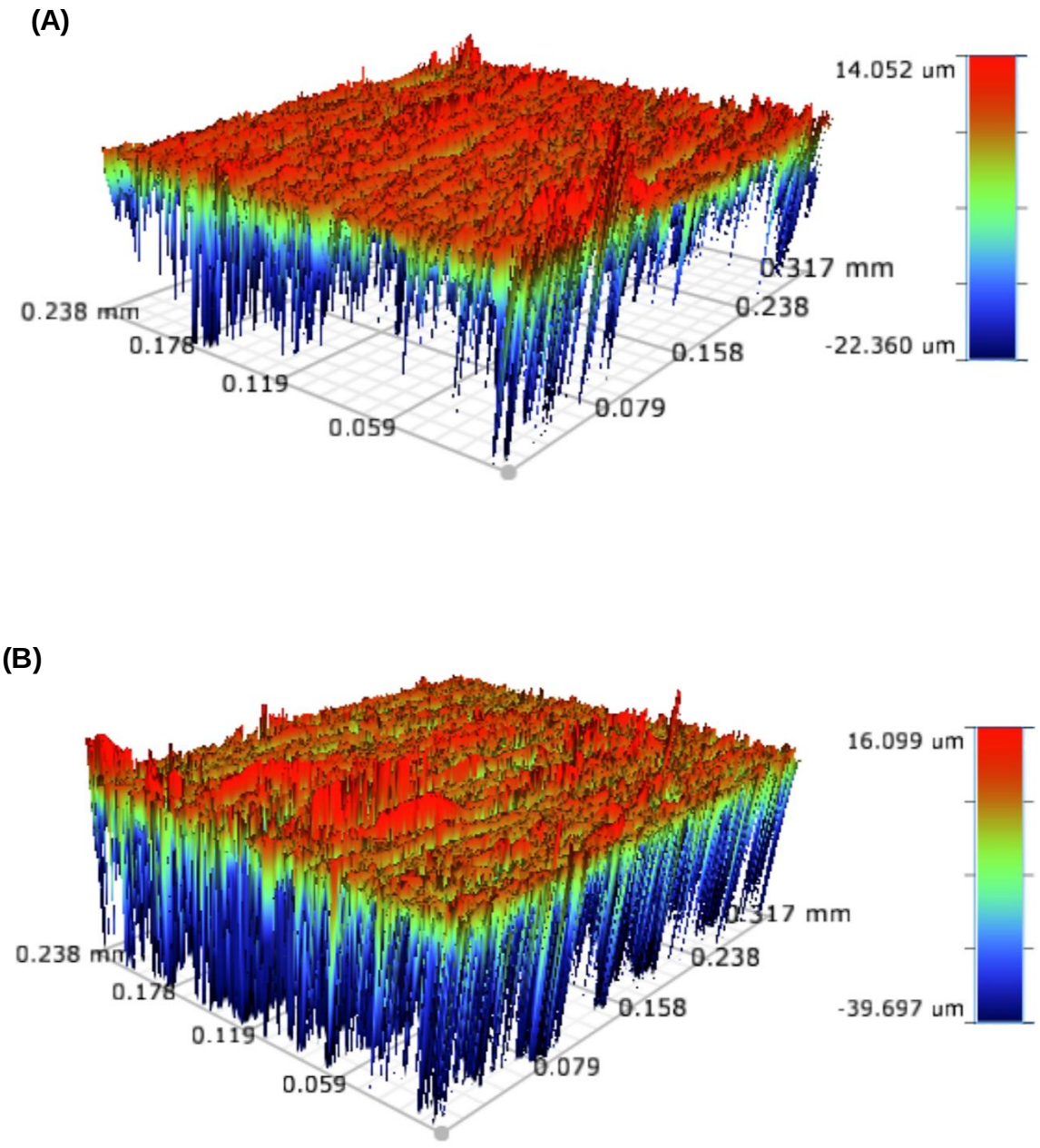

Figure 6.3D surface roughness profiles of (a) uncoated; (b) coated shiv.

Morphological characterisation cannot be performed by roughness parameters alone and therefore microscopic examination is advantageous for better surface evaluations. The surface morphology of the uncoated and coated surfaces was further evaluated using SEM. From SEM micrographs in Figure 7, it can be seen that the coating has been uniformly deposited over the hemp shiv surface without significantly modifying its microstructure.

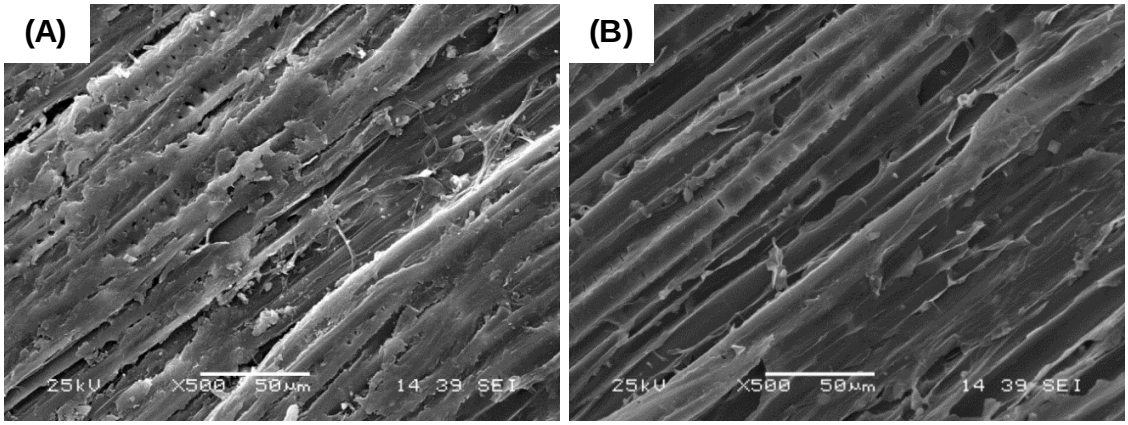

Figure 7. SEM micrographs showing (A) uncoated; (B) coated hemp shiv surface.

The FTIR spectra of silica glass, coated and uncoated hemp shiv is shown in Figure 8. Free water bands corresponding to the wave number interval 3300-3400 cm^{-1} have been reduced in the coated shiv samples as seen in Figure 8A. This decrease in signal indicates that the hydrophobicity of the shiv has been enhanced by the deposition of the silica coating. The peaks at 2918 cm^{-1} and 2851 cm^{-1} correspond to C-H vibration and CH_2 stretching from polysaccharides, wax and the alkyl chains. The peaks at wavenumber 1605-1630 cm^{-1} correspond to adsorbed water. From figure 8B, it was observed that coated shiv showed lower peak intensity corresponding to wavenumbers 1742-1733 cm^{-1} (C=O from hemicellulose), 1424 cm^{-1} (CH_2, C=C from cellulose and lignin), 1373 cm^{-1} (C-H from cellulose), 1319 cm^{-1} (C-C, CH_2 from cellulose and lignin), 1027 cm^{-1} (C-C, C-OH, C-H from hemicellulose) and 896 cm^{-1} (C-O-C glycosidic bonds from polysaccharides). The deposition of the silica coating can be confirmed by wavenumbers 940 cm^{-1} associated with Si-OH bonds vibration and 780 cm^{-1} incomplete hydrolysis of TEOS molecules. The peak at 1000-1100 cm^{-1} for the silica glass corresponds to Si-O-Si bonds.

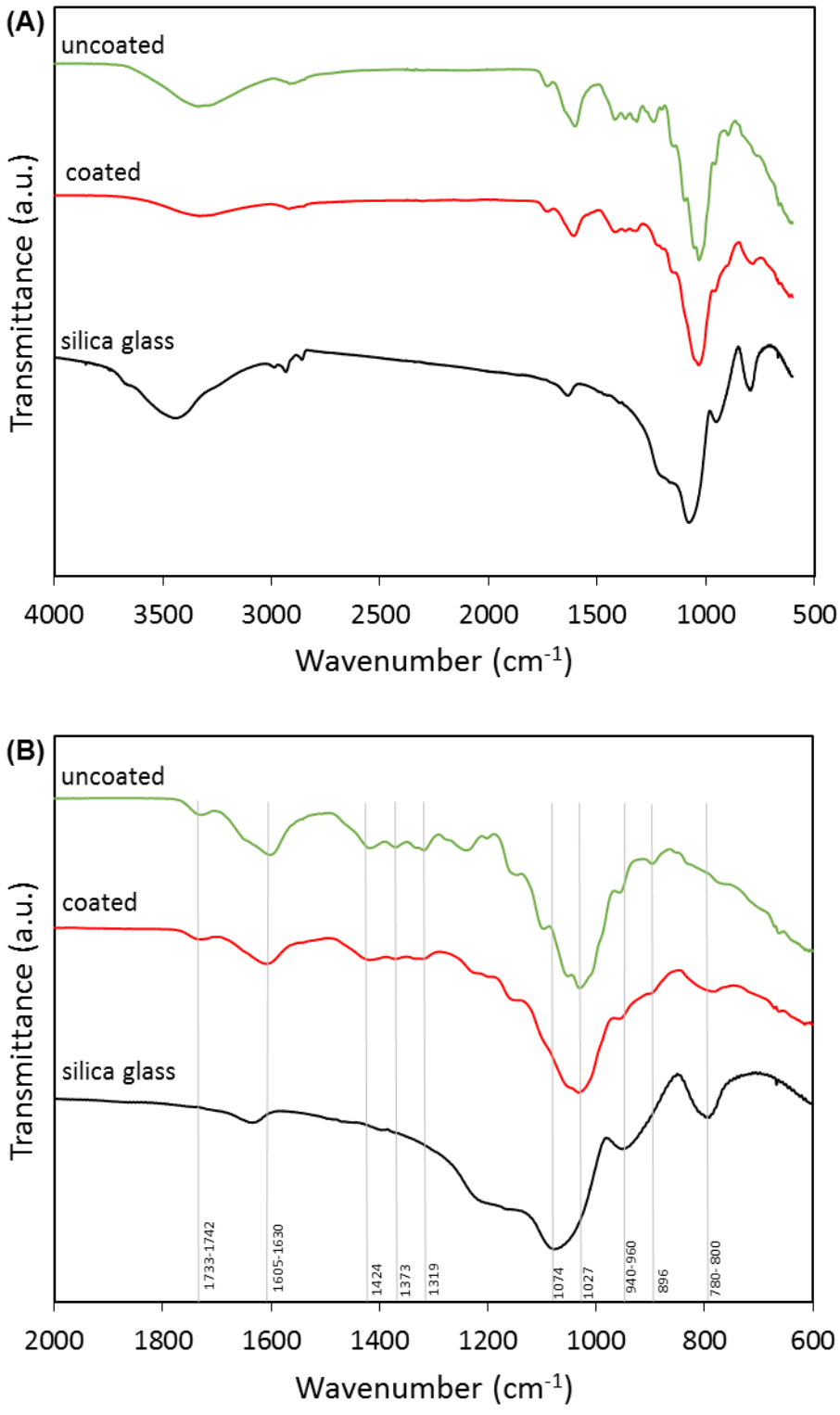

Figure 8. FTIR spectra of silica, coated and uncoated shiv samples for (A) 600-4000 cm-1 region; (B) 600-2000 cm-1 region.

Discussion

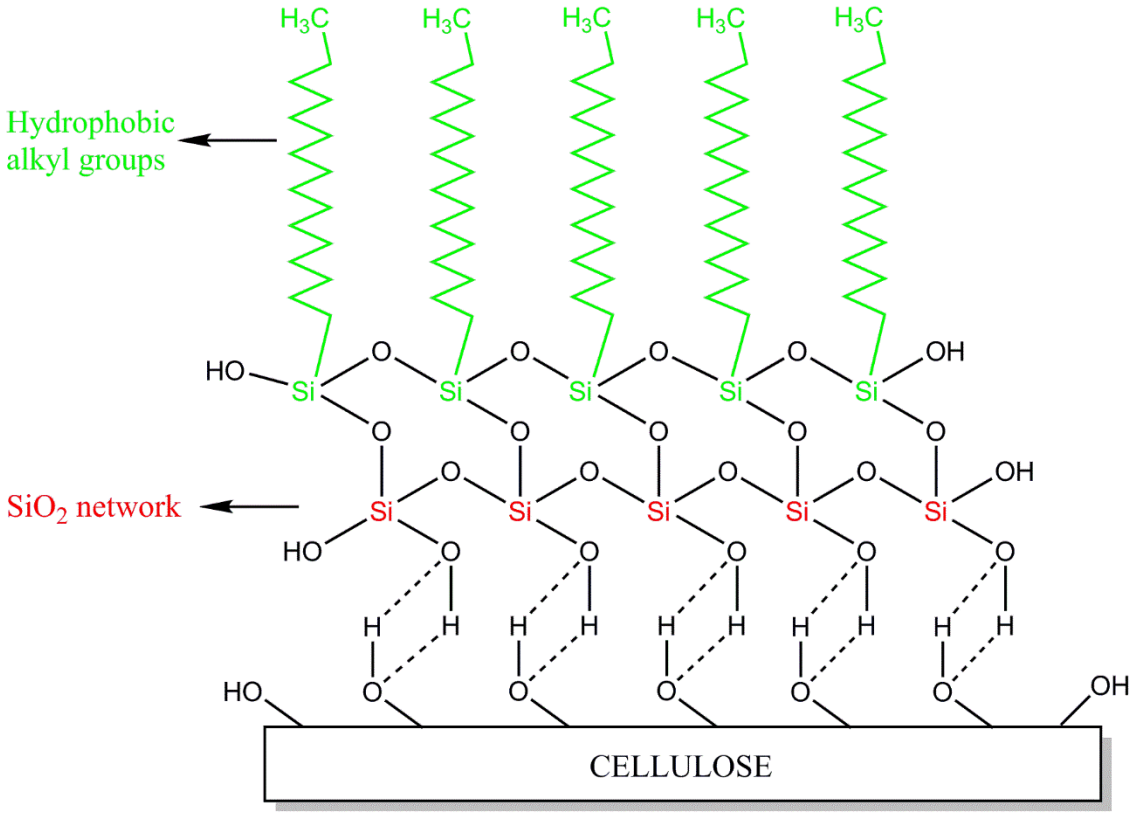

Figure 9. Schematic illustration of sol-gel deposition on hemp shiv surface.

The silica based coatings were prepared through the sol-gel process and HDTMS was added as the hydrophobic agent in the sol formulation. A schematic illustration of deposition of the coating on hemp shiv surface through the hydroxyl sites of cellulose is presented in Figure 9. During the sol-gel process, hydrolysis and condensation of TEOS forms a silica (SiO_2) network. The HDTMS molecules self-assemble replacing the hydroxyls on silica network and long alkyl chains (–Si–C_{16}) are attached on the silica network. Coating the hemp shiv results in attachment of the silica network to the shiv surface through the cellulose hydroxyl groups which are also chemically linked to the alkyl groups responsible for providing hydrophobicity to the shiv surface.

The surface wettability of hemp shiv is controlled by the chemical composition and the morphology. Hemp shiv tends to absorb huge volume of water within a few minutes of contact as hydroxyl sites are present in large numbers on its surface and in this structure. Moreover, the extreme hydrophilicity of hemp shiv

can also be assigned to its high roughness profile. Surface roughness can cause an increase or decrease in the water contact angle depending on the nature of the material. For a hydrophilic surface, high surface roughness provides a large surface area increasing the interaction with a water droplet, thereby providing a low water contact angle. On the other hand, for a hydrophobic surface, higher surface roughness leads to enhanced hydrophobicity due to entrapped air resulting in higher contact angles [28]. The hydrophobicity of the coated hemp shiv surface is due to the self-assembled layer of HDTMS on the silica network reducing the cellulose hydroxyl sites. Moreover, the surface roughness of the hemp shiv was enhanced due the deposition of the coating. The coated hemp shiv exhibited excellent hydrophobicity with WCA up to 118° due to the combination of enhanced surface roughness and low surface energy of the HDTMS chains.

The microstructure of hemp shiv remained unaltered after sol-gel treatment. From SEM results, it was observed that the coating was deposited as a uniform layer and no cracks were observed after drying the shiv. The hydrophobicity of the substrate can be affected by cracks in the coating layer as water molecules can penetrate, wetting the substrate over time. The water absorption results showed that the sol-gel coating layer provided excellent resistance to water due to the hydrophobic functional groups in the coating. The water uptake for the coated hemp shiv was massively reduced within the first few minutes of contact and the water absorption was reduced by 250% over 24 hours when compared to the uncoated shiv.

The high values of moisture adsorption for hemp shiv can be assigned to its chemical composition with a large number of hydroxyl groups being accessible. The lower water vapour sorption values for the coated shiv can be attributed to the hydrophobic alkyl chains present on the coated surface. Modifying the surface of hemp shiv with the silica coating blocked the surface hydroxyl sites and reduced the mass of water adsorbed at high humidity levels. The silica coating interacts with the hemp shiv subsequently lowering its moisture buffering capacity to a limited extent but the coating does not completely block the pores. This is also in agreement with the SEM micrographs showing this coating formulation

had least altered the surface morphology of hemp shiv. From the porosity and DVS results, it can be determined that the coated hemp shiv is capable of adsorbing moisture through the smaller pores whereas the water uptake is considerably reduced due to decrease in the larger pores. Coated shiv showed significant reduction in hysteresis by 54% when compared to uncoated shiv at 90% RH. The reduction in hysteresis curves of the coated shiv shows that water is condensed only on the surface and does not go further deep into the bulk of the hemp shiv structure due to the presence of hydrophobic chains.

Conclusions

Sol-gel technology has been successfully applied for surface modification of hemp shiv enhancing its hydrophobicity without compromising its moisture buffering capacity. A simple and inexpensive one step coating process has been used to provide a hydrophobicity to a highly hydrophilic bio-based material. The coated surface exhibited excellent hydrophobic properties through the synergistic effect of enhanced surface roughness and modified chemical composition. Uniform crack-free monolayer surface coatings delivered contact angles up to 118° and significantly lowered the water absorption rate. The sol-gel coating does not significantly alter the microstructure of the shiv thereby retaining the ability to adsorb and desorb humidity. Silica coated hemp shiv has the potential to be used as a superior aggregate and mixed with binders to produce water-resistant bio-based building composites.

Funding

The work was supported by the ISOBIO project funded by the Horizon 2020 programme [Grant number 636835 – ISOBIO – H2020-EeB-2014-2015] and the EPSRC Centre for Decarbonisation of the Built Environment (dCarb) [grant number EP/L016869/1]. The contents of this publication are the sole responsibility of the authors and can in no way be taken to reflect the views of the European Union.

Acknowledgments

The authors thank Prof Pierre Blanchet and Dr Diane Schorr for access to 3D profilometer at Université Laval.

Data access statement

All data are provided in full in the results section of this paper.

Disclosure statement

The authors declare that they have no conflict of interest.

References

[1] M. Lawrence, Reducing the Environmental Impact of Construction by Using Renewable Materials, J. Renew. Mater. 3 (2015) 163–174. doi:10.7569/JRM.2015.634105.

[2] E. Latif, M. Lawrence, A. Shea, P. Walker, Moisture buffer potential of experimental wall assemblies incorporating formulated hemp-lime, Build. Environ. 93 (2015) 199–209. doi:10.1016/j.buildenv.2015.07.011.

[3] F. Collet, J. Chamoin, S. Pretot, C. Lanos, Comparison of the hygric behaviour of three hemp concretes, Energy Build. 62 (2013) 294–303. doi:10.1016/j.enbuild.2013.03.010.

[4] Y. Jiang, M. Lawrence, M.P. Ansell, A. Hussain, Cell wall microstructure, pore size distribution and absolute density of hemp shiv, R. Soc. Open Sci. 5 (2018) 171945. doi:10.1098/rsos.171945.

[5] B. Mazhoud, F. Collet, S. Pretot, C. Lanos, Mechanical properties of hemp-clay and hemp stabilized clay composites, Constr. Build. Mater. 155 (2017) 1126–1137. doi:10.1016/j.conbuildmat.2017.08.121.

[6] A. Hussain, J. Calabria-Holley, Y. Jiang, M. Lawrence, Modification of hemp shiv properties using water-repellent sol–gel coatings, J. Sol-Gel Sci. Technol. (2018). doi:10.1007/s10971-018-4621-2.

[7] H.R. Kymainen, M. Hautala, R. Kuisma, A. Pasila, Capillarity of flax/linseed (Linum usitatissimum L.) and fibre hemp (Cannabis sativa L.) straw fractions, Ind. Crops Prod. 14 (2001) 41–50. doi:10.1016/S0926-6690(00)00087-X.

[8] L. Kidalova, N. Stevulova, E. Terpakova, Influence of water absorption on

the selected properties of hemp hurds composites, Pollack Period. (2015). doi:10.1556/Pollack.10.2015.1.12.

[9] M.R. Vignon, D. Dupeyre, Steam explosion of woody hemp ch nevotte, 17 (1995) 395–404.

[10] L. Arnaud, E. Gourlay, Experimental study of parameters influencing mechanical properties of hemp concretes, Constr. Build. Mater. 28 (2012) 50–56. doi:10.1016/j.conbuildmat.2011.07.052.

[11] J. Gassan, V.S. Gutowski, A.K. Bledzki, About the surface characteristics of natural fibres, Surf. Eng. 283 (2000) 132–139. doi:10.1002/1439-2054(20001101)283:1<132::AID-MAME132>3.0.CO;2-B.

[12] S. Marceau, P. Glé, M. Guéguen-Minerbe, E. Gourlay, S. Moscardelli, I. Nour, S. Amziane, Influence of accelerated aging on the properties of hemp concretes, Constr. Build. Mater. 139 (2017) 524–530. doi:10.1016/j.conbuildmat.2016.11.129.

[13] J. Genzer, K. Efimenko, Recent developments in superhydrophobic surfaces and their relevance to marine fouling: a review., Biofouling. 22 (2006) 339–360. doi:10.1080/08927010600980223.

[14] A. Nakajima, K. Hashimoto, T. Watanabe, Recent studies on super-hydrophobic films, in: Monatshefte Fur Chemie, 2001: pp. 31–41. doi:10.1007/s007060170142.

[15] S. Donath, H. Militz, C. Mai, Wood modification with alkoxysilanes, Wood Sci. Technol. 38 (2004) 555–566. doi:10.1007/s00226-004-0257-1.

[16] M.M. Kabir, H. Wang, K.T. Lau, F. Cardona, Chemical treatments on plant-based natural fibre reinforced polymer composites: An overview, Compos. Part B Eng. 43 (2012) 2883–2892. doi:10.1016/j.compositesb.2012.04.053.

[17] E. Cabane, T. Keplinger, V. Merk, P. Hass, I. Burgert, Renewable and functional wood materials by grafting polymerization within cell walls, ChemSusChem. 7 (2014) 1020–1025. doi:10.1002/cssc.201301107.

[18] J. Song, O.J. Rojas, Approaching super-hydrophobicity from cellulosic materials : A Review, Pap. Chem. 28 (2013) 216–238. doi:10.3183/NPPRJ-2013-28-02-p216-238.

[19] S. Wang, C. Liu, G. Liu, M. Zhang, J. Li, C. Wang, Fabrication of superhydrophobic wood surface by a sol-gel process, Appl. Surf. Sci. 258 (2011) 806–810. doi:10.1016/j.apsusc.2011.08.100.

[20] B. Mahltig, H. Böttcher, Modified silica sol coatings for water-repellent textiles, J. Sol-Gel Sci. Technol. 27 (2003) 43–52. doi:10.1023/A:1022627926243.

[21] G.Y. Bae, B.G. Min, Y.G. Jeong, S.C. Lee, J.H. Jang, G.H. Koo,

Superhydrophobicity of cotton fabrics treated with silica nanoparticles and water-repellent agent, J. Colloid Interface Sci. 337 (2009) 170–175. doi:10.1016/j.jcis.2009.04.066.

[22] A. Hussain, J. Calabria-Holley, D. Schorr, Y. Jiang, M. Lawrence, P. Blanchet, Hydrophobicity of hemp shiv treated with sol-gel coatings, Appl. Surf. Sci. 434 (2018) 850–860. doi:10.1016/j.apsusc.2017.10.210.

[23] J. Mastalska-Popławska, M. Pernechele, T. Troczynski, P. Izak, Thermal properties of silica-coated cellulose fibers for increased fire-resistance, J. Sol-Gel Sci. Technol. 83 (2017) 683–691. doi:10.1007/s10971-017-4445-5.

[24] Y. Xie, C.A.S. Hill, Z. Xiao, H. Militz, C. Mai, Silane coupling agents used for natural fiber/polymer composites: A review, Compos. Part A Appl. Sci. Manuf. 41 (2010) 806–819. doi:10.1016/j.compositesa.2010.03.005.

[25] Y. Fujiwara, Y. Fujii, Y. Sawada, S. Okumura, Assessment of wood surface roughness: Comparison of tactile roughness and three-dimensional parameters derived using a robust Gaussian regression filter, J. Wood Sci. 50 (2004) 35–40. doi:10.1007/s10086-003-0529-7.

[26] L. Gurau, H. Mansfield-Williams, M. Irle, Filtering the roughness of a sanded wood surface, Holz Als Roh - Und Werkst. 64 (2006) 363–371. doi:10.1007/s00107-005-0089-1.

[27] B. Ugulino, R.E. Hernández, Assessment of surface properties and solvent-borne coating performance of red oak wood produced by peripheral planing, Eur. J. Wood Wood Prod. (2016) 1–13. doi:10.1007/s00107-016-1090-6.

[28] H. Teisala, M. Tuominen, J. Kuusipalo, Superhydrophobic Coatings on Cellulose-Based Materials: Fabrication, Properties, and Applications, Adv. Mater. Interfaces. 1 (2014) 1–20. doi:10.1002/admi.201300026.

Commentary Text

Figure 6.1 shows the water vapour adsorption and desorption isotherms for the silica glass samples prepared using the MTES based formulation (used in Chapter 4) and the selected HDTMS based formulation reported in this Chapter. The HDTMS based silica does not show capillary condensation of water as seen with the MTES based silica. Moreover the HDTMS based silica shows very low mass increase and almost negligible hysteresis between the adsorption and desorption curves. This is possibly due to the increased hydrophobic behaviour, thereby decreasing the surface energy of the pore walls, lowering the tendency for capillary condensation (Jiang et al., 2018).

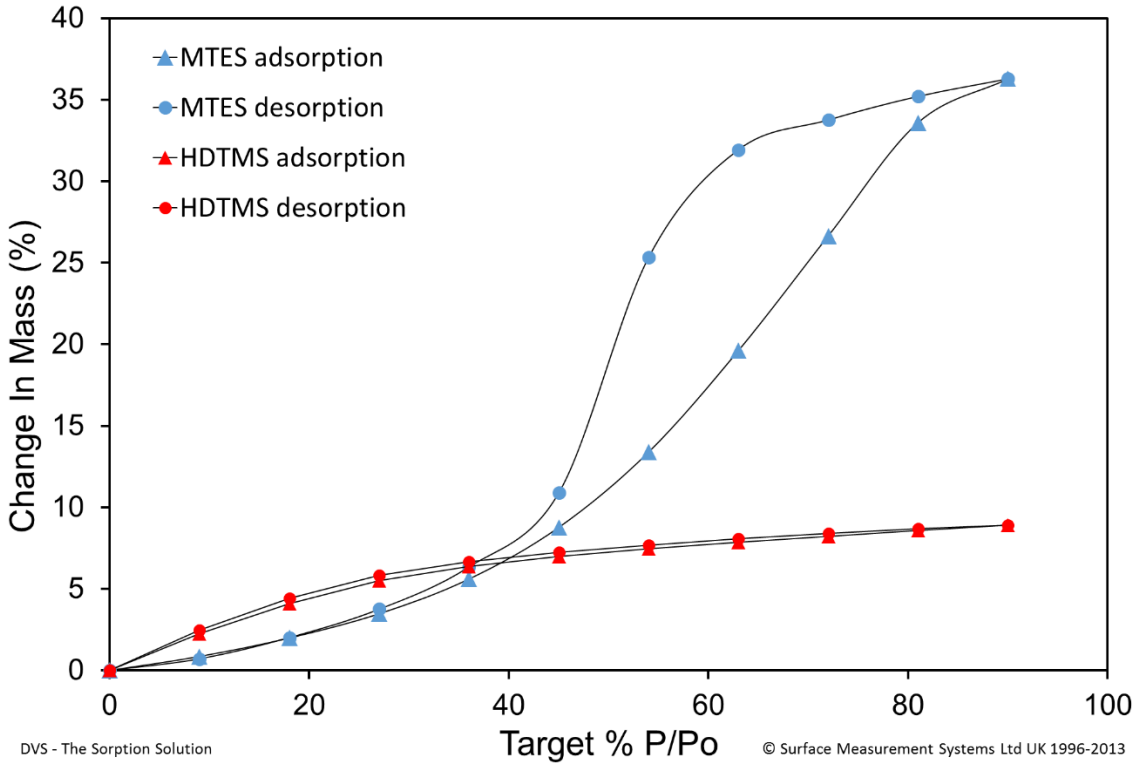

Figure 6.1. DVS isotherms of MTES based silica and HDTMS based silica.

From this paper, it can be summarised that the selected HDTMS based coating formulation has been successful in providing hydrophobicity to hemp shiv yet allowing the hemp shiv to retain its moisture buffering ability. The water absorption of hemp shiv has been reduced significantly with just a single layer of the HDTMS based coating. The coated hemp shiv retains high porosity that is essential for the development of a high performance thermal insulation composite material reported in the next chapters.

Chapter 7

Novel Composites using Hemp Shiv and Multi-Functional Silica Matrix

This Chapter has been published as a Journal paper entitled “Development of novel building composites based on hemp and multi-functional silica matrix” in Composites Part B: Engineering (Hussain, Calabria-Holley, Lawrence, et al., 2018).

Introductory Text

From the previous chapter it can be seen that the treated hemp shiv has successfully retained the moisture buffering characteristics. The coated shiv has also shown a massive reduction in water uptake which makes it a superior aggregate for the development of high performance composites. This paper discusses the applicability of treated hemp shiv for the development of robust composites for the building and construction industry.

In this paper, novel bio-based composites have been prepared using hemp shiv and the selected HDTMS silica formulation. The dual-functional use of silica sol: as a hydrophobic treatment as well as a binder for hemp shiv has been reported for the first time in this paper. The change in silica chemistry due to interaction with hemp shiv has been identified through X-ray photoelectron spectroscopy (XPS), gas chromatography-mass spectrometry (GC-MS) and energy dispersive X-ray (EDX) analysis. The durability of the composites was tested by water immersion tests followed by comparative compressive strength analysis.

Statement of Authorship

This declaration concerns the article entitled:									
Development of novel building composites based on hemp and multi-functional silica matrix.									
Publication status (tick one)									
draft manuscript		**Submitted**		**In review**		**Accepted**		**Published**	✓
Publication details (reference)	Hussain, A., Calabria-Holley, J., Lawrence, M., Ansell, M. P., Jiang, Y., Schorr, D., & Blanchet, P. (2018). Development of novel building composites based on hemp and multi-functional silica matrix. Composites Part B: Engineering, 156, 266–273. http://doi.org/10.1016/J.COMPOSITESB.2018.08.093								
Candidate's contribution to the paper (detailed, and also given as a percentage).	The candidate contributed to/ considerably contributed to/predominantly executed the… Formulation of ideas: 90% A.Hussain conceptualized this study and discussed with M. Lawrence and J. Calabria-Holley. All co-authors shared their expertise for building up on this idea. Design of methodology: 90% A. Hussain designed the methodology of this study with guidance from M.Lawrence, M.P. Ansell and J.Calabria-Holley. Experimental work: 80% A.Hussain perfomed majority of the experimental work and data analysis. Morphological studies were done by M.P. Ansell. Some experiments were also conducted at Laval University under supervision of P. Blanchet and D. Schorr. Presentation of data in journal format: 90% A. Hussain prepared the manuscript. M.P. Ansell proofread the manuscript. All co-authors gave feedback and comments to improve the quality.								
Statement from Candidate	This paper reports on original research I conducted during the period of my Higher Degree by Research candidature.								
Signed	Atif				**Date**	15.09.2018			

Copyrights and Permission

Creative Commons Attribution License (CC BY)

This article is available under the terms of the Creative Commons Attribution License (CC BY). You may copy and distribute the article, create extracts, abstracts and new works from the article, alter and revise the article, text or data mine the article and otherwise reuse the article commercially (including reuse and/or resale of the article) without permission from Elsevier. You must give appropriate credit to the original work, together with a link to the formal publication through the relevant DOI and a link to the Creative Commons user license above. You must indicate if any changes are made but not in any way that suggests the licensor endorses you or your use of the work.

Permission is not required for this type of reuse.

CLOSE WINDOW

Publication title:

Development of novel building composites based on hemp and multi-functional silica matrix.

Thesis page numbers that it spans:

152 to 159

Composites Part B 156 (2019) 266–273

Contents lists available at ScienceDirect

Composites Part B

journal homepage: www.elsevier.com/locate/compositesb

Development of novel building composites based on hemp and multi-functional silica matrix

Atif Hussain[a,b,*], Juliana Calabria-Holley[a], Mike Lawrence[a], Martin P. Ansell[a], Yunhong Jiang[a], Diane Schorr[b], Pierre Blanchet[b]

[a] BRE Centre for Innovative Construction Materials, Department of Architecture and Civil Engineering, University of Bath, Bath, BA2 7AY, UK
[b] Department of Wood and Forest Sciences, Université Laval, Quebec, QC, G1V 0A6, Canada

ARTICLE INFO

Keywords:
Hemp
B. Adhesion
D. Chemical analysis
Mechanical testing

ABSTRACT

This study focuses on the development of novel bio-composites using a silica matrix that provides dual functionality: as a hydrophobic surface treatment and as a binder for hemp-shiv. The hydrophilic nature of hemp shiv, a plant based aggregate, results in composites having poor interfacial adhesion, weak mechanical properties and long drying times. In this work, sol-gel process has been utilised to manufacture durable low density hemp based composites. Morphological characterisation by scanning electron microscopy (SEM) showed that hemp shiv was embedded well in the matrix. Detailed chemical analysis using x-ray photoelectron spectroscopy (XPS) and gas chromatography-mass spectrometry (GC-MS) indicate the presence of water soluble and ethanol soluble extractives leached from the hemp shiv which are incorporated into the silica matrix inducing the binding effect. The composites were water resistant and showed good mechanical performance having the potential to develop novel thermal insulation building materials.

1. Introduction

Bio-based materials have become increasingly popular for producing economical engineering materials in the building and construction industry. Composites manufactured using the woody core of the hemp plant (*Cannabis Sativa* L.) known as shiv have been adopted by the building industry. Lightweight composites from hemp shiv possess excellent hygroscopic [1,2], thermal [3,4] and biodegradable [5] properties.

Hemp shiv has low density due to its high porosity and it tends to absorb large amounts of water [6]. The hydrophilic nature of bio-based materials makes them incompatible with hydrophobic thermoset/thermoplastic polymers [7]. On the other hand, since the shiv competes with the binder for the available water, purely hydraulic binders like lime or cement cannot hydrate completely, leading to a powdery inner core in the hemp-lime walls which is poorly bound [8]. The issue of adhesion with hemp-lime has stimulated considerable investment in hemp-specific lime based binders. The most recent generation of binders utilises high specific surface area lime in order to obtain a more reactive binder, however, they are still susceptible to adhesion issues. Pre-fabrication of panels or blocks ensures factory controlled conditions which reduce the extremes of adhesion issues (e.g. extensive flouring), but there still remains the inherent issue that the soluble sugars on the surface of the shiv interfere with the hydration of the binders, resulting in lower strength composites [9]. The durability of the material is compromised due to high moisture uptake as colonial fungal growth is encouraged resulting in cell wall degradation [10].

The major constituents of industrial hemp shiv are: cellulose (44%), hemicellulose (18–27%), lignin (22–28%) and other components such as extractives (1–6%) and ash (1–2%) [11,12]. Extractives include numerous low molecular mass compounds such as fatty acids, waxes, sterols, triglycerides, steryl esters, glycosides, fatty alcohols, terpenes, phenolics, simple sugars, alkaloids, pectins, gums and essential oils. It is well known that extractives can be isolated using polar and non-polar solvents. Volatile extractives are represented by highly volatile compounds which can be separated by water distillation. They are mainly composed of monoterpenes and other volatile terpenes including terpenoids as well as many different low molecular weight compounds. Water-soluble compounds consist of various phenol compounds, carbohydrates, glycosides and soluble salts, which can be extracted by cold or hot water [13–15]. Lipophilic extractives are insoluble in water but soluble in organic solvents such as hexane, dichloromethane, diethyl

* Corresponding author. BRE Centre for Innovative Construction Materials, Department of Architecture and Civil Engineering, University of Bath, Bath, BA2 7AY, UK.
E-mail address: A.Hussain@bath.ac.uk (A. Hussain).

https://doi.org/10.1016/j.compositesb.2018.08.093
Received 1 May 2018; Received in revised form 26 July 2018; Accepted 23 August 2018
Available online 25 August 2018

ether, acetone or ethanol [16]. Lipophilic extractives also known as plant-resins are divided into free acids, e.g. resin acid and fatty acid, and neutral compounds, e.g. fats and waxes. Extractives from bio-based materials can have a tacky nature forming pitch deposits which is considered to be a major problem in the paper and pulp industry [17].

Natural fibre composites have low durability and tend to absorb large amounts of moisture weakening interfacial adhesion and degradation, although this property can be improved by treatment of the fibres [18–20]. Physical approaches such as plasma, ultraviolet or corona treatment modify the fibre surface for enhancing roughness and interfacial adhesion. Chemical treatments such as alkaline, silane and acetylation offer better improvements than physical methods enhancing hydrophobicity and roughness of the fibres resulting in better interfacial bonding [20–24]. Addition of silica particles into polymeric matrix has also been used to enhance the mechanical properties of natural fibre reinforced composites [25]. Hydrolysed silanes can chemically attach to the hydroxyl group of fibres, but they are known to provide only a limited improvement in the mechanical properties of the resulting fibre composite due to their physical compatibility with the matrix. The strength of natural fibre composites can be increased if covalent bonds are present between the silane treated fibre and matrix [19,20]. Therefore there is a need to develop novel composites that possess good interfacial bonding and at the same time utilise the benefits of chemically treated bio-based aggregates being resistant to water and degradation.

The work reported in this paper is carried out under the ISOBIO project which aims to develop hygrothermally efficient bio-based building insulation panels with low embodied energy and low embodied carbon. We have previously reported that the silica based treatment can provide hydrophobicity to hemp shiv [26] without compromising its moisture buffering capacity as the pores are not totally blocked by the coating [27]. The aim of this paper is to demonstrate the use of a hydrophobic silica treatment as a binder for hemp shiv to produce novel robust light weight composites with enhanced water resistance.

2. Materials

Hemp shiv used in this study was received from CAVAC, an agricultural cooperative based in north-west France. Tetraethyl orthosilicate (TEOS, 98%), hexadecyltrimethoxysilane (HDTMS, 85%), nitric acid (70%) and absolute ethanol were obtained from Sigma-Aldrich.

2.1. Silica formulation and preparation

The silica based binder was synthesised by hydrolysis and condensation of TEOS in ethanol and water. The reaction was catalysed by nitric acid. For the preparation of the silica, 1 M of TEOS was added to a mixture of 4 M distilled water, 4 M of absolute ethanol and 0.005 M of nitric acid. 0.015 M of HDTMS was added to the above mixture as the hydrophobic agent. The sol was vigorously stirred at 40 °C and atmospheric pressure for nearly 2 h. The sols were allowed to age for 96 h in closed container at room temperature.

For the preparation of the silica glass, the sol was aged in a container at room temperature until the gel point was reached. The gel-point was taken as the time when the sol did not show any movement on turning the container upside down. For analysis of the binder, the left-over sol contaminated with leached out hemp shiv extractives was aged in a container until the gel point was reached and the specimen was termed the “binding matrix”. A schematic illustration of silica glass has been presented in Fig. 1.

2.2. Binder characterisation

The surface morphology of the specimens was characterised using a scanning electron microscope (SEM), JEOL Corporation Model SEM-6480LV (Tokyo, Japan) operating at an accelerating voltage of 10 kV. The specimens were coated with gold using an HHV500 sputter coater (Crawley, UK) to prevent charging and to achieve high quality images of morphological characteristics. Energy dispersive X-ray spectroscopy (Oxford INCA) was used to characterise the elemental composition of the specimens.

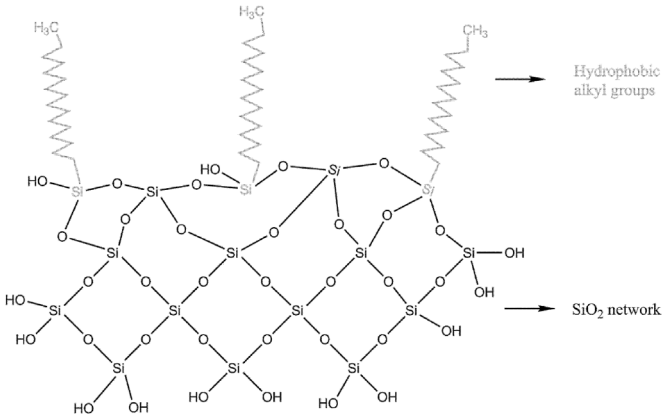

Fig. 1. Schematic illustration of the silica glass.

The surface elemental and chemical composition of the specimens were analysed using X-ray photoelectron spectroscopy (XPS). Prior to XPS analysis, samples were oven-dried at 80 °C for 96 h. XPS spectra of the samples were recorded with an X-ray photoelectron spectrometer (Kratos Axis Ultra, UK). All spectra were collected using a monochromatic Al Kα X-ray source operated at 300 W. The lateral dimensions of the samples were 800 μm × 400 μm, corresponding to spot size of the Al Kα X-ray used, and probing depth was approximately 5 nm. For each sample, two spectra were recorded: (i) survey spectra (0–1150 eV, pass energy 160 eV, and step size 1eV) recorded for apparent composition calculation; and (ii) high-resolution C1s, O1s and Si 2p spectra (within 20 eV, pass energy 20 eV and step size within 0.05eV) recorded to obtain information on chemical bonds. Calculation of the apparent relative atomic concentrations was performed with the CasaXPS software. Peak fitting was performed with CasaXPS, which automatically and iteratively minimizes the difference between the experimental spectrum and the calculated envelope by varying the parameters supplied in a first guess.

Thermal analysis of the samples was carried out by simultaneous thermogravimetric analysis (TGA) and differential scanning calorimetry (DSC) using the STA 449 F1 Jupiter thermal analyser (Netzsch, Germany). The specimens were heated at a rate of 10 °C/min from 25 to 950 °C under nitrogen atmosphere purged at 30 ml/min using an alumina crucible.

2.3. Extractive analysis

For isolation of the extractives, oven dried hemp shiv pieces were immersed in a solution containing a mixture of ethanol and water in the molar ratio 1:1 to represent the solvent ratio used in the sol formulation. Extraction of the hemp shiv samples was done using Soxhlet apparatus for 2 h at 80 °C. The extract was evaporated to dryness using a rotary evaporator and placed overnight in a vacuum oven. The dried extract was re-suspended in hexane and methylene chloride for chromatographic analysis of the lipophilic fraction. Gas chromatography–mass spectrometry (GC-MS) analysis was performed on a Varian CP 3800 gas chromatograph coupled to a mass spectrometer detector (Varian Saturn, 2000 MS/MS, 40–650 a.m.u.). The GC oven was kept at 50 °C for 5 min and then heated to 250 °C at 5 °C/min. The final temperature was held for 2 min. The injector temperature was set at 250 °C. Helium was used as the carrier gas at a flow rate 1.0 ml/min 1 μl of oil (solvent extractive) was injected using a rear injector type

1177 with a split ratio 1:10. The spectrometer was operated in the electron impact mode using 30 μA emission current and mass range *m/z* 40–600. Peaks were quantified by area and the compounds were identified by comparing the mass spectra with those from Wiley and NIST computer libraries.

2.4. Preparation of composite samples

Mixing of the constituent materials, hemp shiv (75 vol%) and sol (25 vol%), were carried out manually to achieve a uniform mixture. The mass of the materials was pre-calculated to target a final density of 175 kg/m^3 for the composites. Aggregates of hemp shiv were mixed with the sol and then placed into a phenolic ply mould, tamped down and left overnight in the oven at 80 °C. The specimens were removed from the moulds and transferred to a conditioning room at 19 °C and 50% relative humidity. Another set of samples were prepared by mixing hemp shiv (75 vol%) and ethanol-water solution (25 vol%) and rest of the conditions were kept constant as described above.

2.5. Composite characterisation

Compressive tests were conducted on 100 mm cube samples using an Instron 50 KN testing rig at a controlled displacement rate of 3 mm/min; the inbuilt instrumentation was used to both record load and platen displacement at a resolution of one data point per 0.1 s. A durability test was performed to determine the robustness of the binder. Composite samples were fully immersed in water for 24 h at 20 °C. The samples were removed from water and placed in an oven at 80° for complete drying until no further mass change was observed. Compression tests were performed on these samples and the results were compared with control samples. Prior to compression testing, the samples were placed in a conditioning room at 19 °C and 50% relative humidity for at least 24 h. The tests were performed in triplicate and the average reading was reported.

3. Results

3.1. Morphology characterisation

The morphology of the silica glass, hemp shiv composite and the binding matrix is presented in Fig. 2. The silica glass (Fig. 2A) has a smooth texture and is classically brittle when compared to the binding matrix (Fig. 2B) which exhibits some spallation. In general, the hemp shiv particles are well embedded in the matrix due good interaction between the hemp shiv and binding matrix. However, some minor cracks appear in the matrix (Fig. 2C) which could be a result of shrinkage during drying of the gel.

3.2. Chemical characterisation

The EDX analysis (Table 1) shows the surface composition of the silica specimens. The percentage of carbon is significantly higher in the binding matrix than the silica glass. The presence of carbon in the silica glass is due to the alkyl groups providing functionalisation.

The chemical composition of the silica glass and the binding matrix was determined by X-ray photoelectron spectroscopy. The atomic percentage of various elements present at the sample surface was determined by a low-resolution survey scan. The relative elemental composition for the specimens is listed in Table 2.

The main elements detected for both the silica specimens were carbon, oxygen and silicon. The binding matrix showed higher content of carbon as seen in Fig. 3.

A high-resolution scan was performed on the C1s region for the silica glass and the binding matrix (Fig. 4) to determine the type of oxygen-carbon bonds present. The chemical bond analysis of carbon was performed by curve-fitting the C1s peak and deconvoluting it into four sub peaks corresponding to unoxidized carbon C1, and various oxidised carbons C2, C3 and C4. The binding energy, corresponding bond type and their relative percentage are listed in Table 3. The silica based binder shows additional oxidised carbon sub peaks, C3 and C4.

The C1s high resolution spectra with the deconvoluted peaks for silica glass and binding matrix are represented in Fig. 4. The C1 peak is related carbon-carbon or carbon-hydrogen bonds whereas C2, C3, and C4 peaks are associated with carbon-oxygen bonds.

3.3. Physical characterisation

The thermal analysis of the silica glass and the binding matrix is reported in Fig. 5. From the TGA weight loss curves, it is seen that silica glass has a residual mass of 84.1% whereas the binding matrix has a residual mass of 80.7% at 950 °C. The maximum decomposition peak determined from the first derivative of the weight loss thermogram (DTG) curve is at 525 °C for silica glass and 495 °C for the binding matrix.

The DSC graph of the binding matrix shows a stronger endothermic peak at 102 °C when compared to the endothermic peak at 128 °C for silica glass. The endothermic peaks corresponding to the maximum decomposition rate are at 489 °C and 530 °C for the binding matrix and silica glass respectively.

3.4. Identification of extractives

The identification of the extracted compounds was performed using GCMS. The polar components of the extractives were analysed for identification of the lipophilic extractives which are responsible for their tacky nature [28] and would contribute to the adhesive properties of the binding matrix. The yield of total extractives (polar and non-polar) in hemp shiv was 6.23% (dry weight %). The hexane yield and methylene chloride yield in the total extract was 9.05% and 5.00% respectively.

The chromatographs for hexane extract and methylene chloride extract are presented in Figs. 6 and 7 respectively. All the compounds identified by GCMS are listed in Tables 4 and 5. The individual compounds were identified based on a comparison with GC retention times and mass spectra from the NIST library. Over twenty compounds were identified in the hexane extract and twelve compounds were identified in the methylene chloride extract. For the analysis of the GCMS data, peaks lower than 30000 counts were rejected. From the chromatograms, it was determined that fatty acids esters, mainly lauric acid and phthalic acid, gave the highest peaks.

3.5. Composite characterisation

The compression testing of the composite samples prepared with hemp shiv and binding matrix is imaged in Fig. 8 and stress versus strain curves for the before and after immersion samples are presented in Fig. 9. The moisture sensitivity of the composite was determined by comparing the mechanical properties of the hemp shiv composite before and after immersion in water for 24 h. Preparation of composite samples using hemp shiv and ethanol-water solution (see section 2.4) was unsuccessful as the hemp shiv particles were not able to bind.

From Fig. 9, the results from three test samples before immersion reveal that the composite reaches an average compressive stress of 0.48 ± 0.02 MPa at 30% strain. After the immersion test, a slight reduction in compressive stress by 15% was observed for the three samples and the average reading was 0.41 ± 0.01 MPa at 30% strain. It was noted that further compression led to densification of the sample. After compression, the sample showed some elastic behaviour as seen in Fig. 8.

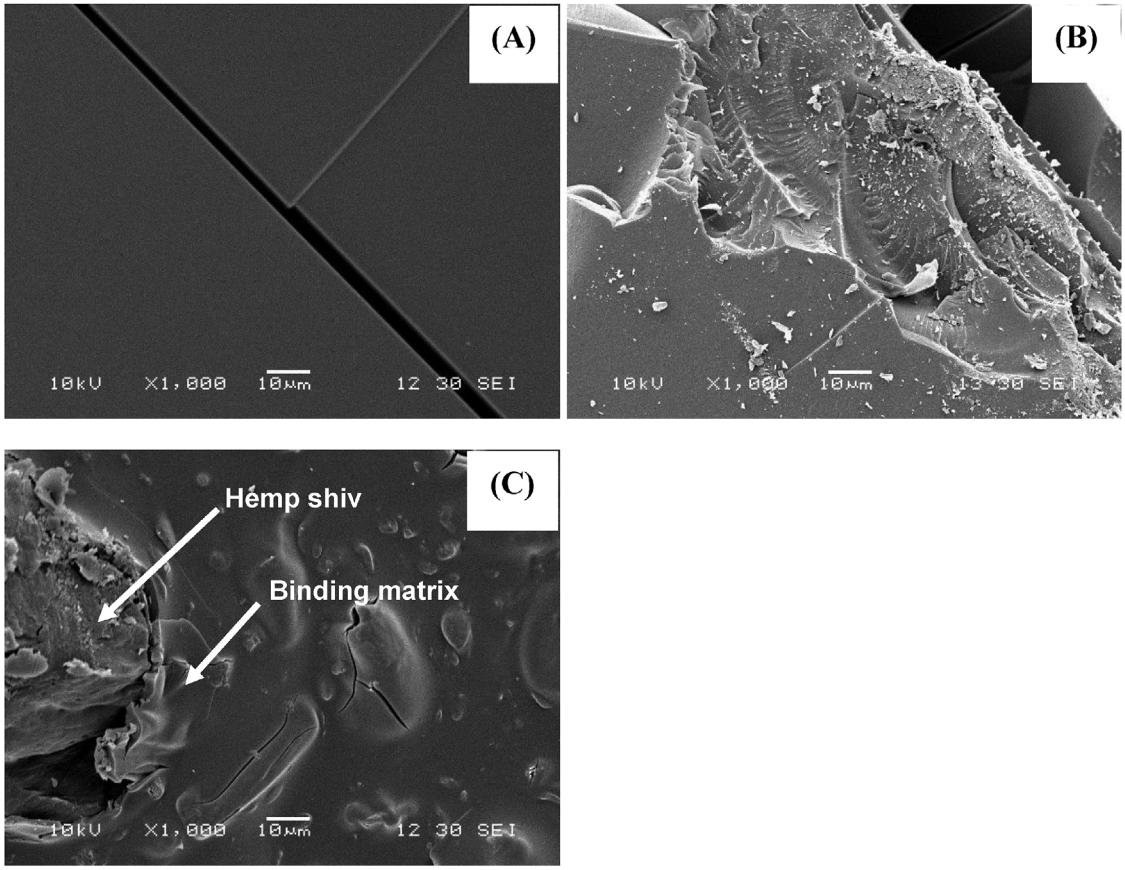

Fig. 2. SEM micrographs of (A) silica glass, (B) binding matrix and (C) hemp shiv composite.

Table 1
EDX analysis of silica glass and binding matrix.

Element	Silica glass		Binding matrix	
	Weight %	Atomic %	Weight %	Atomic %
C K	19.41 ± 3.8	28.69 ± 4.5	51.45 ± 5.3	61.94 ± 4.9
O K	43.21 ± 3.3	51.07 ± 7.1	34.86 ± 3.2	31.65 ± 3.7
Si K	43.33 ± 7.6	29.48 ± 7.3	7.15 ± 1.8	3.71 ± 1.1
Other	0.35 ± 0.1	0.26 ± 0.1	6.54 ± 0.2	2.69 ± 0.2

Table 2
Relative amount of atoms in the sample determined by low-resolution XPS scan.

Element	Relative Concentration (Atomic %)	
	Silica Glass	Binding matrix
C	19.86	46.09
O	61.50	40.34
Si	18.64	13.58

4. Discussion

In the present study, hemp shiv based composites have been manufactured by using silica sol as a binder. The binding matrix has been characterised and its morphology, chemical composition and physical properties have been studied in comparison with silica glass. The binder is prepared by the hydrolysis and condensation of TEOS in water in the presence of ethanol as the mediator solvent. HDTMS is added for functionalisation thereby providing hydrophobic alkyl groups in the silica network. The formulation has been used earlier for treatment of hemp shiv particles for imparting hydrophobicity to the material [26].

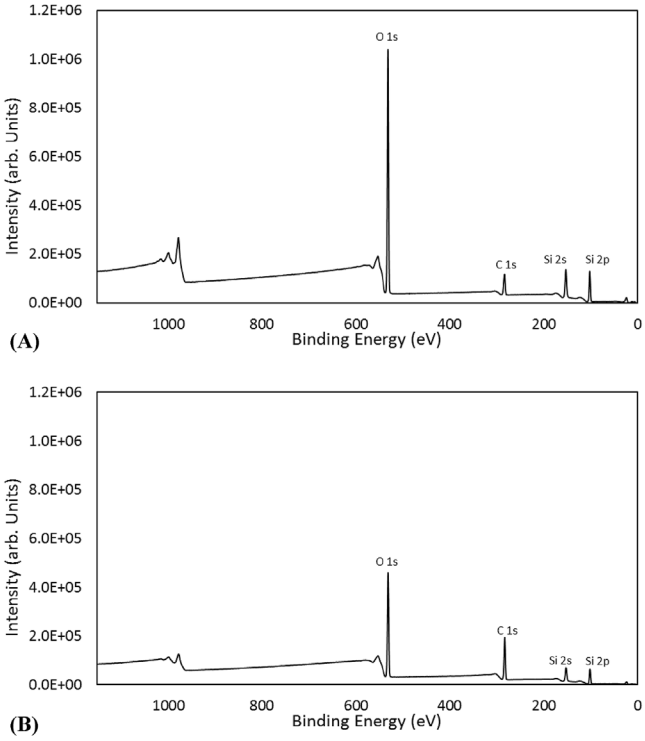

Fig. 3. XPS survey scan for (A) silica glass, (B) binding matrix.

Here we report the binding properties of silica when mixed with hemp shiv. The silica sol interacts with hemp shiv leaching out extractives and waxes which leads to visual changes turning the silica matrix from

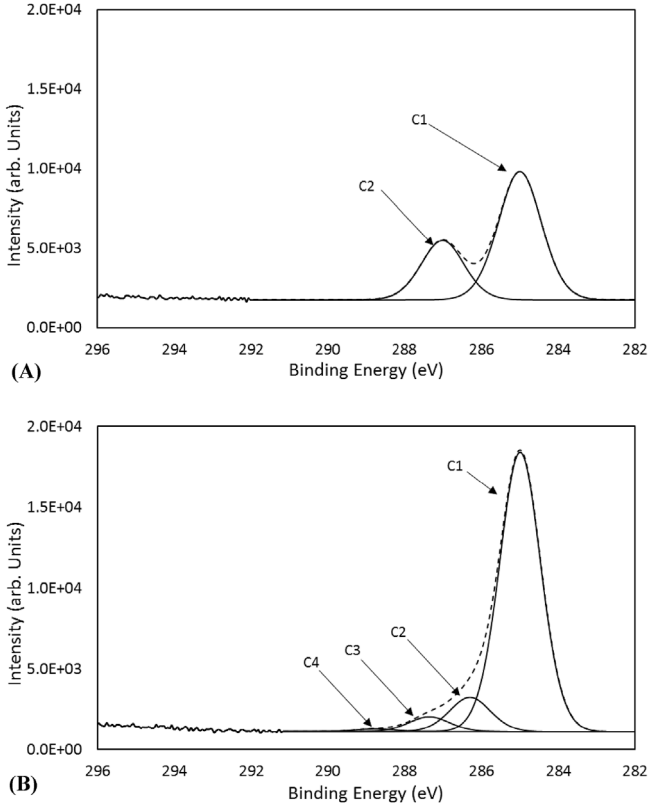

Fig. 4. XPS scan of C1s region for (A) silica glass, (B) binding matrix.

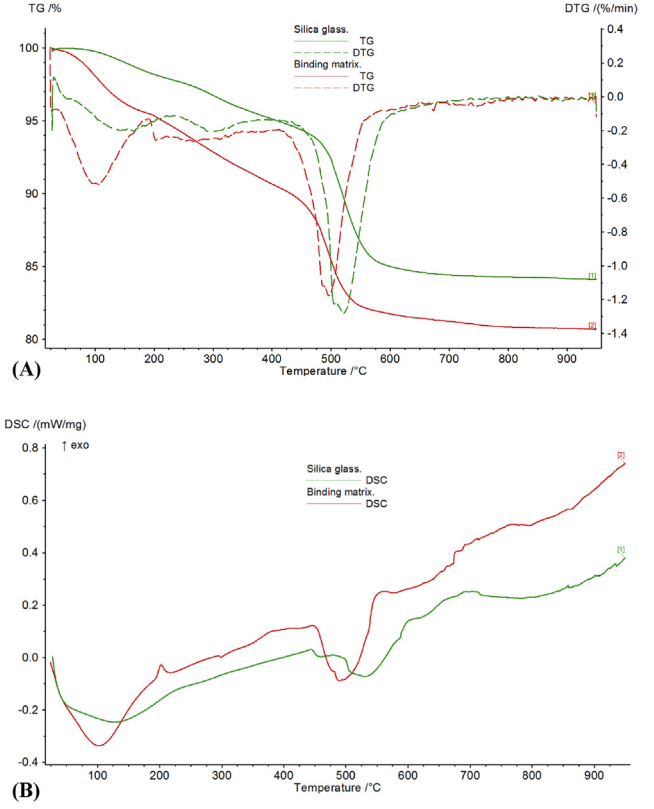

Fig. 5. Thermal analysis of silica glass and binding matrix; (A) TGA and DTG curves, (B) DSC curves.

Table 3
Deconvoluted peak parameters and relative amount of different carbon-to-oxygen bonds at sample surface determined by high-resolution XPS.

Carbon Group	Peak parameters		Relative amount (% area)	
	Binding Energy (eV)	Bond	Silica Glass	Binding matrix
C1	285.0	C–C or C–H	68.65	84.30
C2	286.6/286.8	C–OH	31.35	10.40
C3	288.0	O–C–O or C=O	0.00	4.50
C4	289.2	O–C=O	0.00	0.81

colourless transparent to yellowish opaque.

The silica is able to covalently bond to hemp shiv through the hydroxyl groups of cellulose [26]. During the drying process, the gel starts condensing, releasing ethanol and water and develops a silica network. The extracts from the shiv that are entrapped in the silica network alter the characteristics of the silica. From the SEM analysis, it was seen that the silica morphology is modified. The structure of the new modified silica with incorporated extracts is less brittle when compared to the pure silica glass.

The chemical composition of the silica specimens is mainly composed of carbon, oxygen and silicon. Chemical characterisation using EDX reveals that the modified silica (binding matrix) has a higher carbon content than the pure silica. Detailed XPS analysis indicates that due to sol interaction with hemp shiv, the silica chemistry has been significantly altered. The surface carbon content of the binding matrix increased by 27% (from 19% to 46%). On the other hand, the oxygen content decreased by 21% (from 61% to 40%). This change in C/O ratio and increase in the surface carbon content can be attributed to the additional extracts that have been identified in the modified network of the binding matrix. The decrease in surface oxygen content can be related to the masking effect of the hemp shiv extracts reducing the detectability of the oxygen bonds in the silica network.

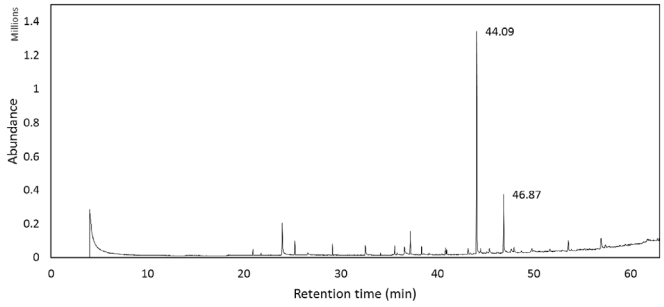

Fig. 6. The chromatogram of hexane extractives from hemp shiv.

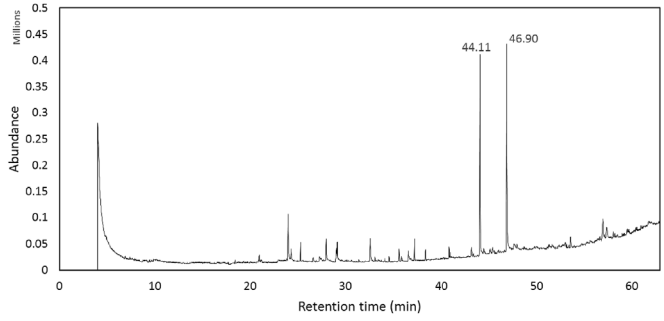

Fig. 7. The chromatogram of methylene chloride extractives from hemp shiv.

The C1s high resolution XPS spectra reveal that the hemp shiv extracts have modified the silica network leading to the appearance of C3 and C4 peaks which are not present in the pure silica glass. Furthermore, the increase in the intensity of the C1 component for the

Table 4
GCMS peak area and retention time of lipophilic extractives identified in hemp shiv hexane extract.

Compound (Hexane Extract)	Retention time (min)	Peak Area
4-Hydroxy-3-nitrobenzaldehyde	23.961	732645
14-Methyl-8-hexadecen-1-ol	34.108	42090
Pentadecanoic acid	36.601	235957
Hexadecanoic acid, ethyl ester	37.202	346033
Heptadecanoic acid, 15-methyl-, ethyl ester	40.988	79364
Tetradecanal (Myristaldehyde)	43.402	32795
Dodecanoic acid (lauric acid), tetradecyl ester	44.086	4120000
Heptadecanoic acid, ethyl ester	44.484	94511
Oleyl alcohol	45.124	37702
1,2-Benzenedicarboxylic acid (phthalic acid), isodecyl octyl ester	46.872	1124000
Tricosanoic acid, methyl ester	47.939	159469
13-Heptadecyn-1-ol	48.691	31836
Tetracosanoic acid, methyl ester	49.676	33092
Eicosanoic acid	49.815	181870
Hexadecanoic acid, octadecyl ester	51.163	31625
Pentacosanoic acid, methyl ester	51.658	113374
Ergost-5-en-3-ol	52.97	48769
Tricosane	53.592	327306
9,19-Cyclochloestene-3,7-diol,4,14-dimethyl-,3-acetate	53.91	38821
Cholestra-4,6 dien-3-ol	55.287	88534
Stigmasterol	55.784	34398
7-Dehydrodiosgenin	56.974	371899
Stigmastan-3-ol, 5-chloro-, acetate, (3.beta.,5.alpha.)	57.416	91981
Stigmastan-3-ol, 5-chloro-, acetate, (3.beta.,5.alpha.)	57.447	81052

Table 5
GCMS peak area and retention time of lipophilic extractives identified in methylene chloride extract of hemp shiv.

Compound (Methylene Chloride Extract)	Retention time (min)	Peak Area
4-Hydroxy-3-nitrobenzaldehyde	23.97	450485
2,6-Dimethoxybenzoquinone	27.945	287931
4-Hydroxy-3-nitrobenzoic acid	29.049	93543
Phenol,2,4-dinitro-6-methoxy	32.602	216393
Pentadecanoic acid	36.589	65679
Hexadecanoic acid, ethyl ester	37.221	111908
Octadecanoic acid, ethyl ester	41.011	28187
Dodecanoic acid (lauric acid), tetradecyl ester	44.108	1.70E + 06
1,2-Benzenedicarboxylic acid (phthalic acid), mono (2-ethylhexyl) ester	46.899	2.75E + 06
Octadecane, 3-ethyl-5-(2-ethylbutyl)-	53.625	106470
Stigmasta-5, 22-dien-3-ol, acetate, (3.beta.)-	57.009	348774
Cholest-1-eno [2,1-a]naphthalene,3′,4′-dihydro-	57.396	263327

binding matrix from 68% to 84% indicates the presence of C—C and C—H bonds from the incorporated extracts. To analyse the extracts that were leaching out from hemp shiv during the silica based treatment, the process was simplified by using a solution of ethanol and water for the extraction process. Ethanol is able to dissolve waxes and isolate lipophilic extractives. These ethanol-soluble extractives were analysed using GCMS and it was found that the extract was mainly composed of lauric acid and phthalic acid with many other fatty acids. The majority of the compounds identified using GCMS belong to the group of lipophilic extractives which are hydrophobic in nature [16,29]. This could possibly be one of the factors for the compatibility between the lipophilic extractives and the sol-gel chemistry due to their hydrophobic nature.

The thermal decomposition patterns of the silica specimens were studied by TGA. The binding matrix had a higher weight loss below 100 °C and a greater endothermic peak that can be attributed to the presence of fatty acids in addition to the physically adsorbed water [30]. The embedded extracts in the silica network changed the decomposition range of the organic fragments of the silane corresponding to the temperature range of 270–600 °C [31]. Due to the higher percentage of the organic compounds in the binding matrix, the weight loss was greater and a peak shift was observed in the first derivative of the weight loss thermogram (DTG). The maximum decomposition rate in the DTG curve for silica glass was at 520 °C attributed to the loss of silanol groups. The modification of silica network with hemp shiv extracts lowered the thermal stability of the binding matrix.

Composites were prepared using hemp shiv and silica sol and their mechanical performance was evaluated. The composites were light weight with a density of 175 kg/m^3 and the compressive stress of 0.48 MPa attained at 30% strain is relatively good when compared to other hemp shiv based composites such as hemp-lime (0.02–0.39 MPa at density 360 kg/m^3) [32], hemp-starch (0.4 MPa at density 177 kg/m^3) [33] and hemp-clay (0.39 at density 373 kg/m^3) [34]. Higher strains corresponded with higher compressive stresses leading to densification of the sample without reaching a failure point. This suggests that the interfacial adhesion between the shiv and binding matrix is good and the shear forces are low.

After the immersion test, the decrease in mechanical strength can be related to the swelling of the shiv when placed in water for 24 h. Since the binder also provides hydrophobicity to the hemp shiv, the compressive stress versus strain characteristics are not compromised to a great extent. However, the swelling could be related to the slow penetration of water through micro-cracks on the coated surface or due to the presence of small uncovered pores within the hemp shiv. The binder can provide hydrophobicity to the hemp shiv but it cannot fully protect the hemp shiv against long-term water interaction. The slight decrease in compressive stress reached at 30% strain can be attributed to the weakening of the interfacial bonding between the hemp shiv and the binding matrix. However, composites produced using an ethanol-water mixture instead of silica sol was unsuccessful as the hemp shiv fell apart on demoulding. The ethanol is responsible for isolation of the extractives and waxes from hemp shiv but the extractives cannot bind hemp shiv on their own. The extractives modify the silica chemistry and the binding matrix holds the hemp particles together resulting in the production of coherent composite blocks.

When compared to conventional hemp-lime composites, it is evident that the production costs of the hemp-silica composites would be higher due to the hydrophobic treatment on hemp shiv. However, this cost could be off-set by savings elsewhere, both in production ingredients (reduction in water usage, lower drying times) as well as an extension in service life, potentially reducing the whole life cost. Moreover, the commercial availability of sol-gel solution on an industrial scale would significantly lower the cost of this novel composite. The preparation of hemp-silica composite results in the reduction of 2 L of mixing water per 1 kg of hemp shiv when compared to a conventional hemp-lime composite. The thermal performance of the new composite is expected to be better due to their significantly lower density than hemp-lime. Overall early indications are that the global warming potential of this composite would be approximately 5% lower than that of a conventional composite. The life span is expected to increase by 50% due the improved resistance to water that is responsible for degradation of the composite.

5. Conclusions

In this work, the novel use of sol-gel treatment as a binding agent has been identified, providing multi-functionality from a single treatment using a simple, economical one-step process. Thorough investigation of the binder and its chemical interaction with hemp shiv has been performed. Lipophilic extractives from the shiv are integrated within the silica network, modifying chemical, morphological and physical characteristics of the glass material. The prepared composites show good mechanical performance as a non-load bearing material and

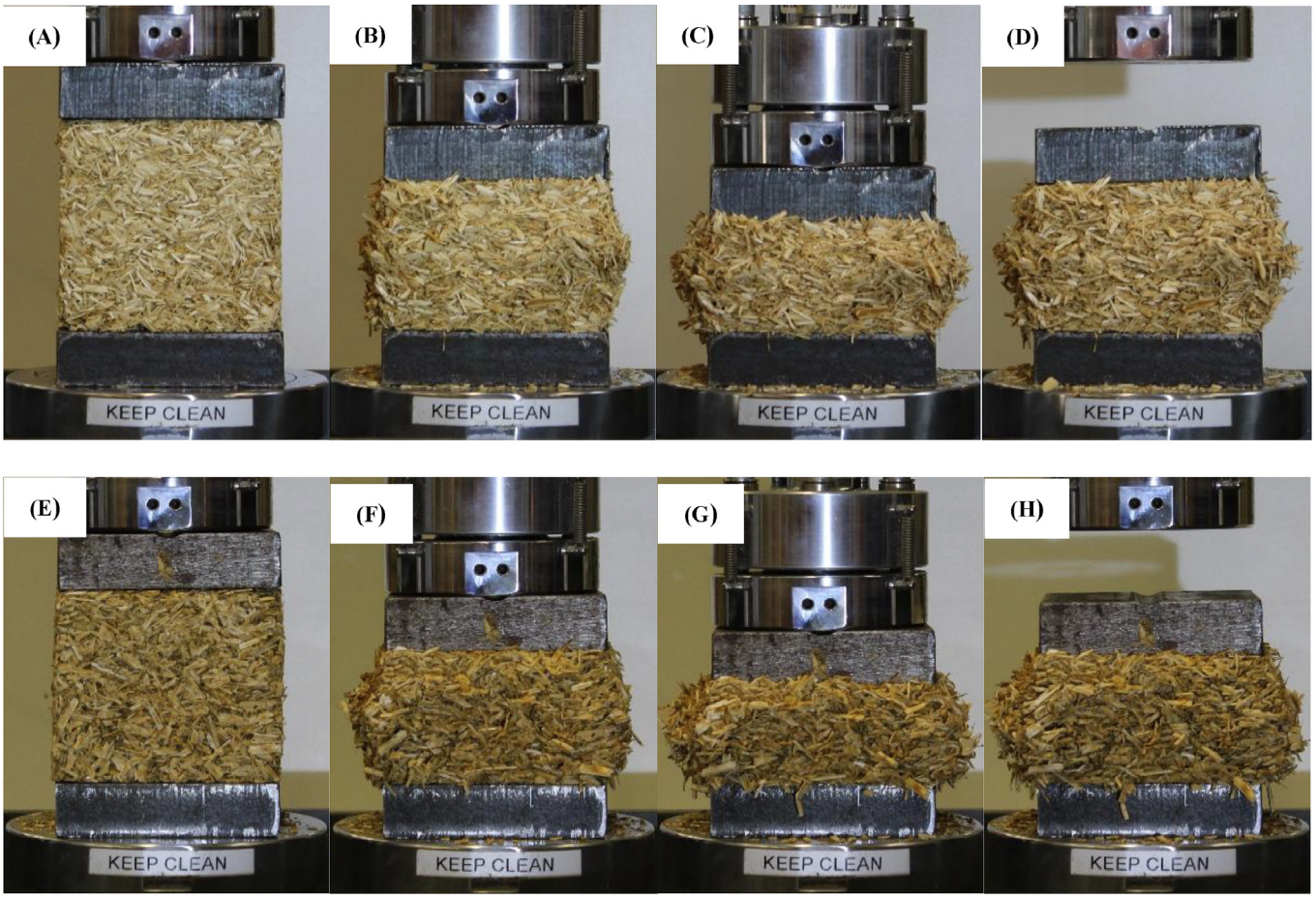

Fig. 8. Compression testing of hemp shiv composites at; (A) 0% strain, (B) 30% strain, (C) 50% strain, (D) after 50% strain, and after immersion in water at (E) 0% strain, (F) 30% strain, (G) 50% strain, (H) after 50% strain.

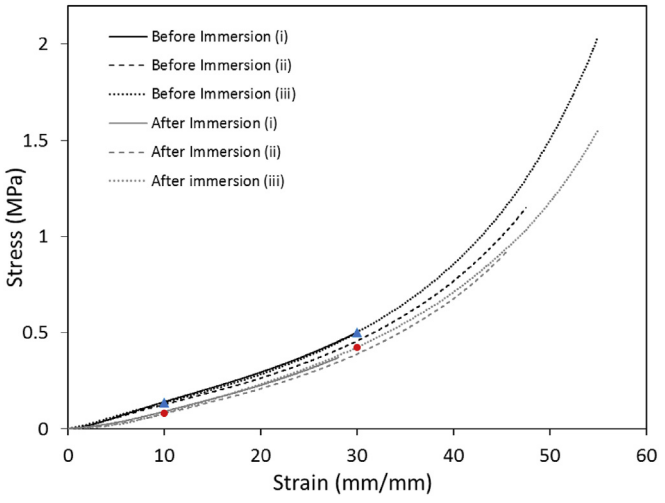

Fig. 9. Compressive stress versus strain characteristics of hemp shiv composites before and after immersion in water.

has great potential as a thermal insulation material due to their low density as well as the high porosity of hemp shiv. Durability tests evaluated the robustness of the composite and the hydrophobic silica treatment was seen to enhance the water resistance of the material. This study is applicable to not only the hemp shiv material but also to any bio-based material which has cellulose and lipophilic extractives in its composition. This therefore transforms the current use of the sol-gel treatment as a surface modifier agent alone to dual functionality as a binder agent leading to economical and sustainable bio-based building materials.

Disclosure statement

The authors declare that they have no conflict of interest.

Acknowledgments

This study was supported by the ISOBIO project funded by the Horizon 2020 programme [grant number 636835 – ISOBIO – H2020-EeB-2014-2015] and the Canadian Queen Elizabeth II Diamond Jubilee Scholarship. The authors would also like to acknowledge the EPSRC Centre for Decarbonisation of the Built Environment (dCarb) [grant number EP/L016869/1]. The contents of this publication are the sole responsibility of the authors and cannot be taken to reflect the views of the European Union. All data are provided in full in the results section of this paper.

Appendix A. Supplementary data

Supplementary data related to this article can be found at https://doi.org/10.1016/j.compositesb.2018.08.093.

References

[1] Tran Le AD, Maalouf C, Mai TH, Wurtz E, Collet F. Transient hygrothermal behaviour of a hemp concrete building envelope. Energy Build 2010;42:1797–806.

https://doi.org/10.1016/j.enbuild.2010.05.016.
[2] Latif E, Lawrence M, Shea A, Walker P. Moisture buffer potential of experimental wall assemblies incorporating formulated hemp-lime. Build Environ 2015;93:199–209. https://doi.org/10.1016/j.buildenv.2015.07.011.
[3] Benfratello S, Capitano C, Peri G, Rizzo G, Scaccianoce G, Sorrentino G. Thermal and structural properties of a hemp-lime biocomposite. Construct Build Mater 2013;48:745–54. https://doi.org/10.1016/j.conbuildmat.2013.07.096.
[4] Shea A, Lawrence M, Walker P. Hygrothermal performance of an experimental hemp-lime building. Construct Build Mater 2012;36:270–5. https://doi.org/10.1016/j.conbuildmat.2012.04.123.
[5] Theis M, Grohe B. Biodegradable lightweight construction boards based on tannin/hexamine bonded hemp shaves. Holz als Roh- Werkst 2002;60:291–6. https://doi.org/10.1007/s00107-002-0306-0.
[6] Jiang Y, Lawrence M, Ansell MP, Hussain A. Cell wall microstructure, pore size distribution and absolute density of hemp shiv. R Soc Open Sci 2018;5:171945. https://doi.org/10.1098/rsos.171945.
[7] Gassan J, Gutowski VS, Bledzki AK. About the surface characteristics of natural fibres. Surf Eng 2000;283:132–9. https://doi.org/10.1002/1439-2054(20001101)283:1<132:AID-MAME132>3.0.CO;2-B.
[8] Elfordy S, Lucas F, Tancret F, Scudeller Y, Goudet L. Mechanical and thermal properties of lime and hemp concrete ("hempcrete") manufactured by a projection process. Construct Build Mater 2008;22:2116–23. https://doi.org/10.1016/j.conbuildmat.2007.07.016.
[9] Ahmad MR, Bing C, Oderji SY, Mohsan M. Development of a new bio-composite for building insulation and structural purpose using corn stalk and magnesium phosphate cement; Physical, mechanical, thermal and hygric evaluation. Energy Build 2018. https://doi.org/10.1016/j.enbuild.2018.06.007.
[10] Marceau S, Glé P, Guéguen-Minerbe M, Gourlay E, Moscardelli S, Nour I, et al. Influence of accelerated aging on the properties of hemp concretes. Construct Build Mater 2017;139:524–30. https://doi.org/10.1016/j.conbuildmat.2016.11.129.
[11] Kidalova L, Stevulova N, Terpakova E. Influence of water absorption on the selected properties of hemp hurds composites. Pollack Period 2015. https://doi.org/10.1556/Pollack.10.2015.1.12.
[12] Gandolfi S, Ottolina G, Riva S, Fantoni GP, Patel I. Complete chemical analysis of carmagnola hemp hurds and structural features of its components. BioResources 2013;8:2641–56. https://doi.org/10.15376/biores.8.2.2641-2656.
[13] PETTERSEN RC. The Chemical Composition of Wood 1984:57–126. https://doi.org/10.1021/ba-1984-0207.ch002.
[14] Yang G, Jaakkola P. Wood chemistry and isolation of extractives from wood. Lit Study BIOTULI Proj Univ Appl Sci 2011;10–22.
[15] Nascimento MS, Santana ALBD, Maranhão CA, Oliveira LS, Bieber L. Phenolic extractives and natural resistance of wood. Biodegrad - Life Sci 2013. https://doi.org/10.5772/56358.
[16] Sun RC, Tomkinson J. Comparative study of organic solvent-soluble and water-soluble lipophilic extractives from wheat straw 2: spectroscopic and thermal analysis. J Wood Sci 2002;48:222–6. https://doi.org/10.1007/BF00771371.
[17] Gutiérrez A, Del Río JC, Martínez MJ, Martínez AT. The biotechnological control of pitch in paper pulp manufacturing. Trends Biotechnol 2001;19:340–8. https://doi.org/10.1016/S0167-7799(01)01705-X.
[18] Kabir MM, Wang H, Lau KT, Cardona F, Aravinthan T. Mechanical properties of chemically-treated hemp fibre reinforced sandwich composites. Compos B Eng 2012;43:159–69. https://doi.org/10.1016/j.compositesb.2011.06.003.
[19] Xie Y, Hill CAS, Xiao Z, Militz H, Mai C. Silane coupling agents used for natural fiber/polymer composites: a review. Composer Part A Appl Sci Manuf 2010;41:806–19. https://doi.org/10.1016/j.compositesa.2010.03.005.
[20] Pickering KL, Efendy MGA, Le TM. A review of recent developments in natural fibre composites and their mechanical performance. Composer Part A Appl Sci Manuf 2016;83:98–112. https://doi.org/10.1016/j.compositesa.2015.08.038.
[21] Valadez-Gonzalez A, Cervantes-Uc JM, Olayo R, Herrera-Franco PJ. Effect of fiber surface treatment on the fiber-matrix bond strength of natural fiber reinforced composites. Compos B Eng 1999;30:309–20. https://doi.org/10.1016/S1359-8368(98)00054-7.
[22] Sepe R, Bollino F, Boccarusso L, Caputo F. Influence of chemical treatments on mechanical properties of hemp fiber reinforced composites. Compos B Eng 2018;133:210–7. https://doi.org/10.1016/J.COMPOSITESB.2017.09.030.
[23] Sullins T, Pillay S, Komus A, Ning H. Hemp fiber reinforced polypropylene composites: the effects of material treatments. Compos B Eng 2017;114:15–22. https://doi.org/10.1016/j.compositesb.2017.02.001.
[24] Kabir MM, Wang H, Lau KT, Cardona F. Chemical treatments on plant-based natural fibre reinforced polymer composites: an overview. Compos B Eng 2012;43:2883–92. https://doi.org/10.1016/j.compositesb.2012.04.053.
[25] Da Silva LJ, Panzera TH, Velloso VR, Christoforo AL, Scarpa F. Hybrid polymeric composites reinforced with sisal fibres and silica microparticles. Compos B Eng 2012;43:3436–44. https://doi.org/10.1016/j.compositesb.2012.01.026.
[26] Hussain A, Calabria-Holley J, Schorr D, Jiang Y, Lawrence M, Blanchet P. Hydrophobicity of hemp shiv treated with sol-gel coatings. Appl Surf Sci 2018;434:850–60. https://doi.org/10.1016/j.apsusc.2017.10.210.
[27] Hussain A, Calabria-Holley J, Jiang Y, Lawrence M. Modification of hemp shiv properties using water-repellent sol–gel coatings. J Sol Gel Sci Technol 2018. https://doi.org/10.1007/s10971-018-4621-2.
[28] Marques G, del Río JC, Gutiérrez A. Lipophilic extractives from several nonwoody lignocellulosic crops (flax, hemp, sisal, abaca) and their fate during alkaline pulping and TCF/ECF bleaching. Bioresour Technol 2010;101:260–7. https://doi.org/10.1016/j.biortech.2009.08.036.
[29] Hardell HL, Nilvebrant NO. A rapid method to discriminate between free and esterified fatty acids by pyrolytic methylation using tetramethylammonium acetate or hydroxide. J Anal Appl Pyrolysis 1999;52:1–14. https://doi.org/10.1016/S0165-2370(99)00035-2.
[30] Knothe G, Dunn RO. A comprehensive evaluation of the melting points of fatty acids and esters determined by differential scanning calorimetry. J Am Oil Chem Soc 2009;86:843–56. https://doi.org/10.1007/s11746-009-1423-2.
[31] Hemsri S, Asandei AD, Grieco K, Parnas RS. Biopolymer composites of wheat gluten with silica and alumina. Composer Part A Appl Sci Manuf 2011;42:1764–73. https://doi.org/10.1016/j.compositesa.2011.07.032.
[32] Walker R, Pavia S, Mitchell R. Mechanical properties and durability of hemp-lime concretes. Construct Build Mater 2014;61:340–8. https://doi.org/10.1016/j.conbuildmat.2014.02.065.
[33] Benitha Sandrine U, Isabelle V, Ton Hoang M, Maalouf C. Influence of chemical modification on hemp-starch concrete. Construct Build Mater 2015;81:208–15. https://doi.org/10.1016/j.conbuildmat.2015.02.045.
[34] Mazhoud B, Collet F, Pretot S, Lanos C. Mechanical properties of hemp-clay and hemp stabilized clay composites. Construct Build Mater 2017;155:1126–37. https://doi.org/10.1016/j.conbuildmat.2017.08.121.

Commentary Text

In this paper, it was reported that the selected HDTMS based formulation provides dual functionality: as a hydrophobic treatment on hemp shiv and, as a binder for hemp shiv aggregates for the development of a novel hemp shiv composite material. The detailed chemical analysis of the binder revealed that hemp shiv extractives were leached out during the treatment process which were then incorporated within the silica network. The change in silica chemistry provided a binding matrix where the hemp shiv aggregates were well embedded. The composite durability was tested in this paper which showed high resistance to water due to the hydrophobic silica treatment. The mechanical performance was considerably good even after the exposing the composite to water for prolonged periods. The performance of the composite as a thermal insulation material is reported in the next Chapter.

Chapter 8

Hygroscopic, Thermal & Mechanical Properties of Novel Hemp Composites

This Chapter has been submitted as a Journal paper entitled “Hygrothermal and mechanical characterisation of novel hemp shiv based thermal insulation composites” to Construction and Building Materials.

Introductory Text

This paper reports the characterisation of the novel hemp-silica composites discussed in the Chapter 7. In addition to these composites, two new composites were prepared: (i) using coated hemp shiv and a starch based binder and; (ii) raw hemp shiv and starch based binder (control samples). The objective of this paper was to study the effect of hydrophobic treatment on hemp shiv on the overall performance of the composites. The effect of binder matrix on the composite strength was also investigated.

Statement of Authorship

This declaration concerns the article entitled:									
Hygrothermal and mechanical characterisation of novel hemp shiv based thermal insulation composites.									
Publication status (tick one)									
draft manuscript		**Submitted**		**In review**	✓	**Accepted**		**Published**	
Publication details (reference)	Hussain, A., Calabria-Holley, J., Lawrence, M., & Jiang, Y. Hygrothermal and mechanical characterisation of novel hemp shiv based thermal insulation composites. Construction and Building Materials.								
Candidate's contribution to the paper (detailed, and also given as a percentage).	The candidate contributed to/ considerably contributed to/predominantly executed the… Formulation of ideas: 90% A. Hussain presented the main idea for this work and discussed with his supervisors M. Lawrence and J. Calabria-Holley. Design of methodology: 90% A. Hussain designed the methodology with input from the co-authors. Experimental work: 100% A. Hussain performed all the experiments and the data analysis. Presentation of data in journal format: 90% A. Hussain prepared the manuscript. The co-authors provided feedback and comments.								
Statement from Candidate	This paper reports on original research I conducted during the period of my Higher Degree by Research candidature.								
Signed	Atif					**Date**	15.09.2018		

Submitted Article: Hygrothermal and mechanical characterisation of novel hemp shiv based thermal insulation composites

Atif Hussain*, Juliana Calabria- Holley, Mike Lawrence, Yunhong Jiang

BRE Centre for Innovative Construction Materials, Department of Architecture and Civil Engineering, University of Bath, Bath BA2 7AY, UK

*Corresponding Author: Atif Hussain (A.Hussain@bath.ac.uk)

Abstract

This study focuses on the development of advanced water resistant bio-based composites with enhanced hygrothermal performance for building applications. The highly porous structure of hemp shiv is responsible for low thermal conductivity and allows the material to adapt to varying humidity conditions providing comfortable indoor environment. However, the pore network and the hydrophilic nature of hemp shiv affects the compatibility and durability of the material in presence of excess moisture conditions. In this work, novel hemp shiv composites were prepared in a starch based or silica based matrix and characterised for their hygroscopic, thermal and mechanical properties. The hemp shiv based composites were resistant to water yet permeable to vapour and showed excellent moisture buffering capacity when compared to conventional hemp-lime composites. The composites prepared were light weight with low thermal conductivity values of 0.051-0.058 W/mK and showed good mechanical performance. Hemp shiv composites with superior hygrothermal characteristics have immense potential as robust thermal insulation building materials.

Keywords: Hemp shiv, hygrothermal, moisture buffering, vapour permeability, thermal conductivity, bio-based composites.

Introduction

Bio-based materials have gained interest in the building industry since the last decade due to their hygroscopic and insulation properties. The use of these materials not only enhances the energy efficiency of the building but is also beneficial for the health and comfort of the occupants [1,2]. Using bio-based materials can also have a positive impact on the environment since they have the ability to capture CO_2 from the atmosphere during their lifetime. When these materials are used to produce building materials, the sequestered CO_2 is locked up within the building resulting in the production of extremely low embodied energy materials [3].

Several studies have discussed the moisture buffering property of bio-based materials. The ability to absorb and release moisture in response to changes in surrounding relative humidity can impact indoor comfort levels and reduce the energy demands for air conditioning [4]. Creating a vapour permeable wall and maintaining indoor relative humidity levels between 40 and 60% can have a positive impact on wellbeing of residents, reducing bacterial growth, allergies and controlling respiratory problems [5].

Numerous studies have reported the use of hemp shiv in the production of hemp based composites with majority of the research being conducted on hemp lime [6–12]. However, the manufacture of hemp lime requires significantly high volume of water than what is actually required for lime hydration as a lot of water is absorbed by the hemp shiv [13]. As a result, the hemp lime blocks need long drying times of approximately several months to a year which are not preferred on an industrial scale [14]. Mixing hemp shiv with binders is quite a challenge so far as the shiv competes with the binder for the available water due to its hydrophilic nature. Therefore, hemp lime walls tend to have a powdery inner core resulting in poor interfacial adhesion as hydraulic binders like lime or cement undergo incomplete hydration. Moreover, the use of mineral binders for the production of hemp based composites result in an increased thermal conductivity of the overall composite undermining the insulation property of hemp shiv aggregates.

The large water absorption capacity of hemp shiv is due to its highly porous structure and its chemical composition. Hemp shiv has low bulk density (90-110 kg/m^3) and high porosity (76-78%) due to the structure of the plant stem from which they are derived [15]. Moreover, the presence of high amounts of cellulose (44%) and hemicellulose (27%) in hemp shiv contributes to the presence of hydrophilic hydroxyl groups in their chemical composition [16,17]. High moisture sensitivity in bio-based materials can be responsible for colonial fungal growth leading to degradation of their cell wall and the durability of the material can be compromised [18]. Furthermore, high water absorption capacity of these materials can affect the manufacturing quality of the end product if they encounter humid surroundings or come in contact with water unexpectedly.

On the positive side, the highly porous structure of hemp shiv is responsible for the excellent hygroscopic and insulation properties of the material. Therefore, there is a need to develop new hemp based composites to address the existing issues as well as to retain the maximum insulating and moisture buffering properties of the bio-based aggregate. The use of silica based coatings on hemp shiv has proven to be successful in lowering the water absorption capacity of hemp shiv yet retaining its moisture buffering ability due to presence of small pores not blocked by the coating [19] .

This research focuses on the development of water resistant hemp shiv based composites for use as a building thermal insulator. The novel composites were produced either in starch matrix or silica matrix without using any additional mineral binders. The composites have been characterised for their hygroscopic, thermal insulation, water resistance and mechanical properties.

Materials

Bio-aggregate

Hemp shiv was received from CAVAC, an agricultural cooperative based in north-west France. The hemp shiv aggregates used for this study are shown in Figure 1.

Figure 1. Hemp shiv aggregates used in this study.

Treatment formulation

For the preparation of the hydrophobic treatment, the sol-gel process was followed. 1M of TEOS was added to a mixture of 4M distilled water, 4M of absolute ethanol and 0.005M of nitric acid. 0.015M of HDTMS was added to the above mixture as the hydrophobic agent. The sol was vigorously stirred at 40 °C and atmospheric pressure for nearly 2 hours. The sols were allowed to age for 96 hours in closed container at room temperature before the treatment process. Figure 2 shows the surface of hemp shiv before and after the silica treatment.

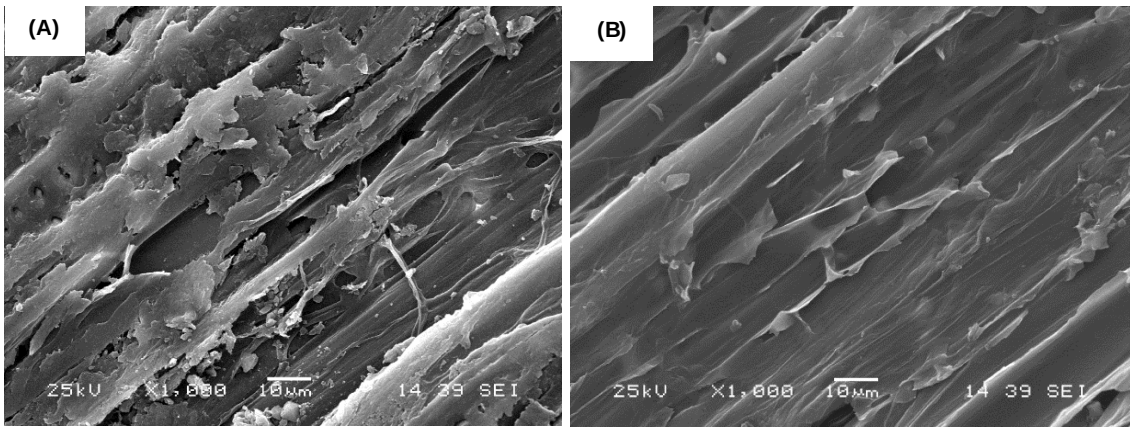

Figure 2.Micrographs of hemp shiv surface (A) untreated, (B) after hydrophobic silica treatment.

Composite formulations

Composite C1 - Hemp shiv aggregates and silica treatment as binder: Mixing of the constituent materials, raw hemp shiv and sol was carried out manually to achieve a uniform mixture. The weight ratio for raw hemp shiv: dry binder was 5:1. The mass of the materials was pre-calculated to target a final density of 175 kg/m^3 for the composites. Aggregates of hemp shiv were mixed with the sol and then placed into a phenolic ply mold of desired dimension, tamped down and left for overnight in the oven at 80 °C. The specimens were removed from the molds and transferred to a conditioning room at 19 °C and 50% relative humidity.

Composite C2 - Treated hemp shiv aggregates and polysaccharide binder: Prior to composite preparation, hemp shiv aggregates were dipped in the sol for 10 min and then removed and transferred onto an open tray. The treated aggregates were dried at 80 °C overnight. C2 composites were then prepared by mixing treated hemp shiv aggregates with a bio-based binder formulated by CAVAC using a starch derivative and a crosslinker. The weight ratio for treated hemp shiv: dry binder was 9:1. The mixture was placed into a steel mold of desired dimension with a target density of 240 kg/m^3, compacted at 0.5 MPa using a hot press (PressMasters 40T GEM series). The upper and lower plates were then heated to 180 °C and the temperature was maintained for one hour. The specimens were demolded after cooling down to room temperature and then transferred to a conditioning room at 19 °C and 50% relative humidity.

Composite C3 – raw hemp shiv aggregates and polysaccharide binder: C3 composites were prepared by mixing raw hemp shiv aggregates with the same bio-based binder as in formulation C2. The weight ratio for raw hemp shiv: dry binder was 9:1. The mixture was placed into a steel mold of desired dimension with a target density of 200 kg/m^3, and the rest of the conditions for the manufacturing process using the thermal press remained constant as for Composite C2. The specimens were demolded after cooling down to room temperature and then transferred to a conditioning room at 19 °C and 50% relative humidity. The target density of C3 is lower than C2 due to the absence of silica treatment that increases the mass of hemp shiv aggregates by 18 ± 1%.

Methods

Vapour permeability

The ability of a porous material to transfer moisture due to a vapour pressure gradient can be expressed by the vapour permeability of the material. The transfer of moisture during this process can take place due to three factors: diffusion (self-collision of water molecules), effusion (collision of water molecules with the pore walls) and liquid transfer (associated with capillary condensation) [20].

The water vapour permeability and the diffusion resistance factor of thermal insulation materials can be measured using the British Standard (BS EN 12086) [21] under isothermal conditions (23 °C) and at two sets of relative humidity: dry cup and wet cup. Three samples with dimensions 100mm x 100mm and thickness 20mm were conditioned for at least 6 h at 23 °C and 50% relative humidity to reach constant mass. The samples were then placed on plastic containers filled either with desiccant (dry cup test) or salt solution (for wet cup test). The sides of the samples were properly sealed to achieve unidirectional moisture flow. The test assembly is shown in Figure 3.

The test assembly containing the sealed specimens were placed in a climate chamber where the temperature and humidity were controlled constantly. For the dry cup test, the relative humidity inside the container was maintained between 0-2% using silica beads and the climate chamber was set at 50% relative humidity. For wet cup test, the relative humidity inside the container was maintained at 93% using saturated KNO_3 salt solution and the climate chamber was set at 50%.

Figure 3 Test assembly of hemp composites for vapour permeability testing.

The test assembly was then conditioned in the climate chamber for 24 h. The partial pressure gradient between the container and the climate chamber drives the vapour through the specimen. The test assembly was weighed every 24 h until three successive determinations of change in mass per unit time for each specimen was within ±5% of its mean value.

The rate of change in mass (G) (mg/hr) was calculated using the equation:

$$G_{1,0} = \frac{(m_1 - m_0)}{(t_1 - t_0)} \qquad \text{Eq (1)}$$

where m_1 (mg) is the mass of the test assembly at time t_1, m_0 is the mass of the test assembly at time t_0. G is the mean of at least three successive determinations of $G_{1,0}$ (mg/h) provided $G_{1,0}$ is within ±5% of G.

The water vapour transmission rate (g) (mg/m^2) was calculated using the equation:

$$g = \frac{G}{A} \qquad \text{Eq (2)}$$

where A is the upper exposed surface area (m^2) of the test specimen.

Water vapour permeance *(W)* (mg/m^2.hr.Pa) is determined from the following equation:

$$W = \frac{G}{A.\Delta P} \qquad \text{Eq (3)}$$

where ΔP is the pressure difference (Pa) as described in BS EN 12086.

Water vapour resistance (Z) (m^2.hr.Pa/mg) was calculated using the equation:

$$Z = \frac{1}{W} \quad \text{Eq (4)}$$

Water vapour permeability δ (mg/m.hr.Pa) is calculated from the following equation:

$$\delta = W.d \quad \text{Eq (5)}$$

where *d* is the test specimen thickness (m).

The water vapour diffusion resistance factor (μ) was calculated using the equation:

$$\mu = \frac{\delta_a}{\delta} \quad \text{Eq (6)}$$

where δ_a is the vapour permeability of air [kg/(m s Pa)] and δ is the vapour permeability of the insulation material [kg/(m s Pa)]

It should be noted that this method of measuring vapour diffusion resistance factor does not consider the surface vapour resistance of the material.

Moisture buffering

The moisture buffering ability of a hygroscopic material can be measured by the moisture buffer value (MBV). Hygroscopic materials have the ability to adsorb and release moisture responding to changes in surrounding relative humidity in order to create an equilibrium. Moisture buffering capacity can regulate the fluctuations in humidity in internal spaces.

The MBV was measured according to the NORDTEST method [22]. This method was used to measure the practical moisture buffer value of the specimens under dynamic conditions. This value represents the amount of moisture adsorption and desorption, per unit open surface area, under daily cyclic variation of relative humidity according to following equation:

$$MBV = \frac{\Delta m}{A.(RH_{high} - RH_{low})} \quad \text{Eq (7)}$$

where MBV: moisture buffer value (g/(m^2 %RH)), Δm is moisture uptake/release during the period (kg), A is open surface area (m^2), $RH_{high/low}$ is relative humidity level (%) respectively.

The specimens were tested in triplicates. Each sample was exposed only from a single side having a surface area of at least 100 mm x 100 mm. The other five sides of the sample were sealed with aluminium foil tape. The thickness of each sample was the actual product thickness ranging between 50-60 mm.

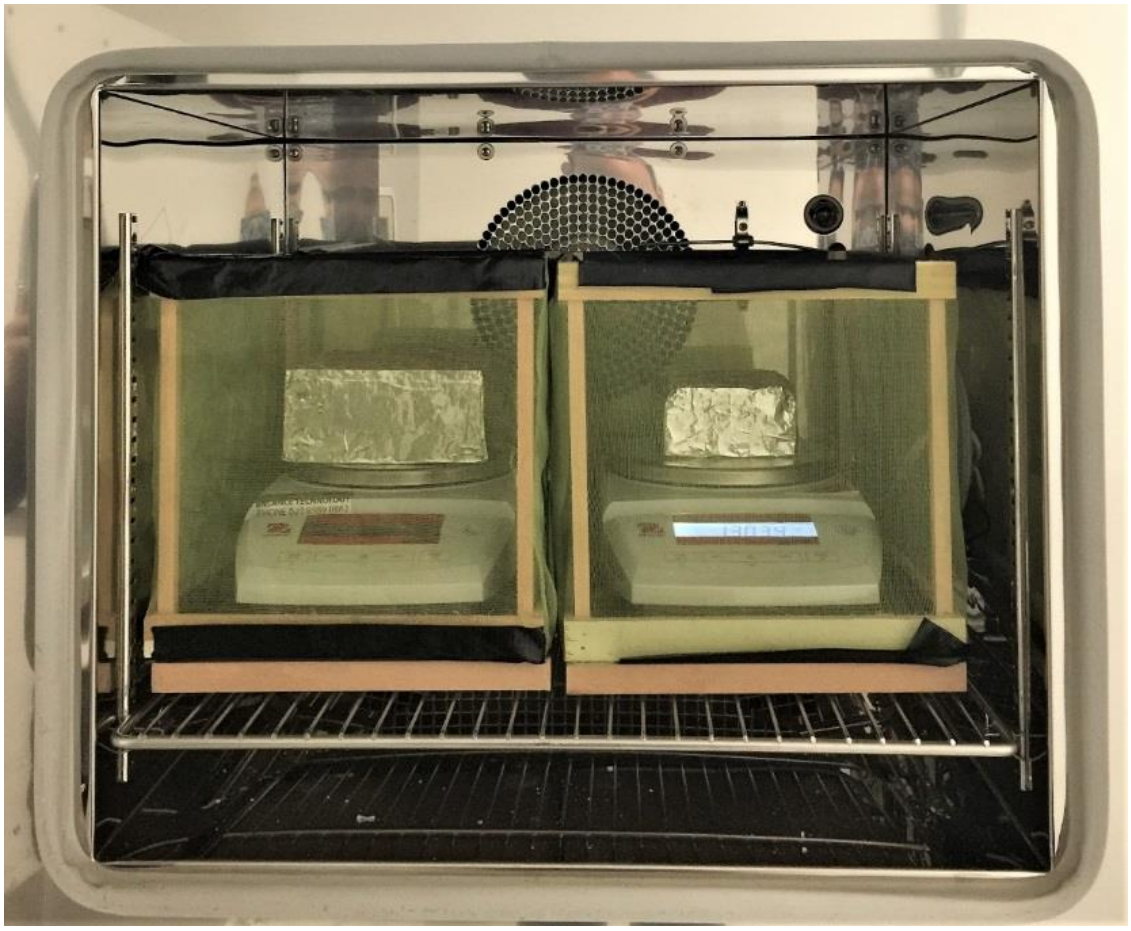

Figure 4. Moisture buffering setup in climate chamber.

A climate chamber (ACS Angelantoni Test Technologies, model DY110 SP, Italy) was used for the MBV experiment that can be controlled in the range -40 to 180 °C and 10 to 95% relative humidity. The samples were preconditioned at 23 °C and 50% relative humidity for at least 6 hours before the test. The samples were then exposed to cyclic relative humidity conditions where each 24h cycle was a combination of 8h exposure to 75% relative humidity and 16h exposure to 33% relative humidity at 23 °C temperature. Temperature and relative humidity were measured and maintained constantly with the sensor of the climate chamber. The

measurement of mass was performed by a precision scale with readability and repeatability of 0.001grams (g). The sample mass was logged every min by a computer connected to the scale. A screen was placed around the balance to minimise the influence of air movement over the sample surface during the test as seen in Figure 4. The wind speed was measured by an anemometer and found to be 0.1 m/s at the sample surface. The experiment was continued until the change in mass between three consecutive cycles was not greater than 5%. The surface vapour resistance was assumed to be constant during the test.

Thermal conductivity

The thermal conductivity of the samples was measured using a hand-held measuring instrument ISOMET 2114 which is used for direct measurement of heat transfer properties of a wide range of isotropic materials including cellular insulating materials, plastics, glasses and minerals. The ISOMET is equipped with two types of measurement probes: needle probes for soft materials, and surface probes for hard materials. It applies a dynamic measurement method, which enables a reduced measurement time in comparison with steady state measurement methods. Measurement is based on analysis of the temperature response of the analysed material to heat flow impulses. Heat flow is induced by the electrical heating of a resistor heater inserted into the probe which is in direct heat contact with the tested specimen. In order to obtain the best measurement accuracy on specific materials, surface probes are used for measurement on solid and hard materials.

Figure 5. Thermal conductivity setup using ISOMET.

For measuring the thermal conductivity of the composite samples, the surface probe was used which is a heating plate as seen in Figure 5. The evaluation of thermal conductivity and heat capacity is based on periodically sampled temperature records as a function of time. The samples had a flat surface with dimensions of at least 100 x 100 mm. Greater accuracy of surface flatness is required with increasing thermal conductivity of the tested material. The minimal thickness of the samples was 50 mm.

Water absorption

The short term water absorption of the specimens was determined by the British Standard EN 1609:2013 [23]. The specimens were preconditioned for at least 6 h at 23 °C and 50% relative humidity. The specimens were partially immersed in water for a period of 24 hours by applying a sufficient load on the top face as seen in Figure 6A. The water level was maintained such that the bottom face of the specimen was 10 ± 2 mm below the surface of water during the entire test. After 24 hr ± 30 min, the test specimen was removed and drained for 10 min by placing it vertically on a mesh, inclined at an angle of 45° as shown in Figure 6B. This step allowed draining any excess water adhering to the surface but not absorbed by the specimen. The test was carried out at 23 ± 2 °C and 50 ± 5 % relative humidity. The specimens were tested in triplicates. The test specimens had a bottom surface area of at least 100 mm x 100 mm and the thickness of each sample was the actual product thickness ranging between 50-60 mm.

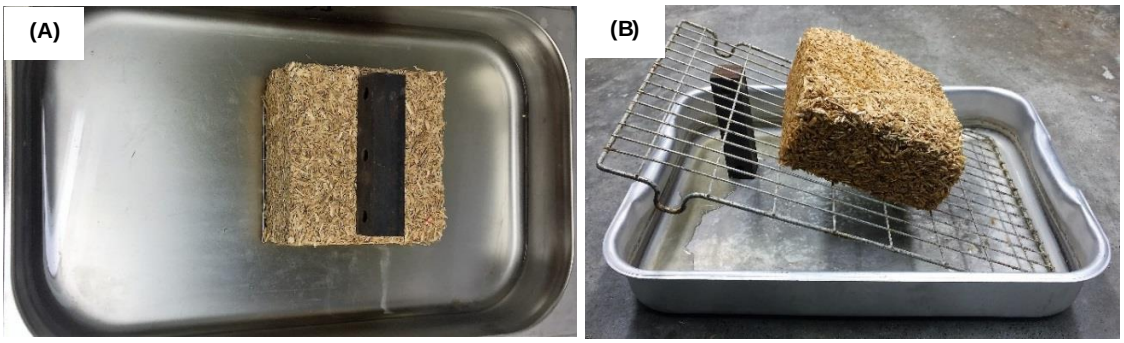

Figure 6. Water absorption test showing (A) sample placed in water for 24 hours, (B) draining at an inclined angle.

The water absorption was calculated as the change in mass according to the following equation:

$$WA = \frac{m_{24} - m_0}{A_p} \quad \text{Eq (8)}$$

where *WA* is the water absorption (kg/m^2), m_0 is the initial mass of the test specimen (kg), m_{24} is the mass of the test specimen after partial immersion for 24 h (kg), A_p is the bottom surface area of the test specimen (m^2).

The percentage of water absorption was calculated according to the following equation:

$$WA\ \% = \frac{m_{24} - m_0}{m_0} * 100 \quad \text{Eq (9)}$$

where *WA%* is the water absorption percentage.

Compression

Compressive tests were conducted on 100 mm cube samples using an Instron 50 KN testing rig at a controlled displacement of 3 mm/min; the inbuilt instrumentation was used to both record load and platen displacement at a resolution of one data point per 0.1 s. Prior to compression testing, the samples were placed in a conditioning room at 19 °C and 50% relative humidity for at least 24 hours. The tests were performed in triplicates and the average reading was reported.

Results and discussion

The transfer of moisture takes place in porous materials when a vapour pressure gradient is present between the opposite surfaces (top and bottom) of the material. The water vapour permeability results of the hemp shiv based composites are summarised in Table 1 for both dry cup and wet cup tests. The kinetics of mass change during the water vapour permeability test is presented in Figure 7 for the composites. The vapour diffusion resistance μ was calculated using Equation 6, and it was found that for the dry cup, C2 had the lowest value of μ, and for the wet cup C1 had the lowest value of μ. All the composites showed higher permeability (lower resistance factor) during higher relative humidity conditions with the maximum increase observed in C1 composite.

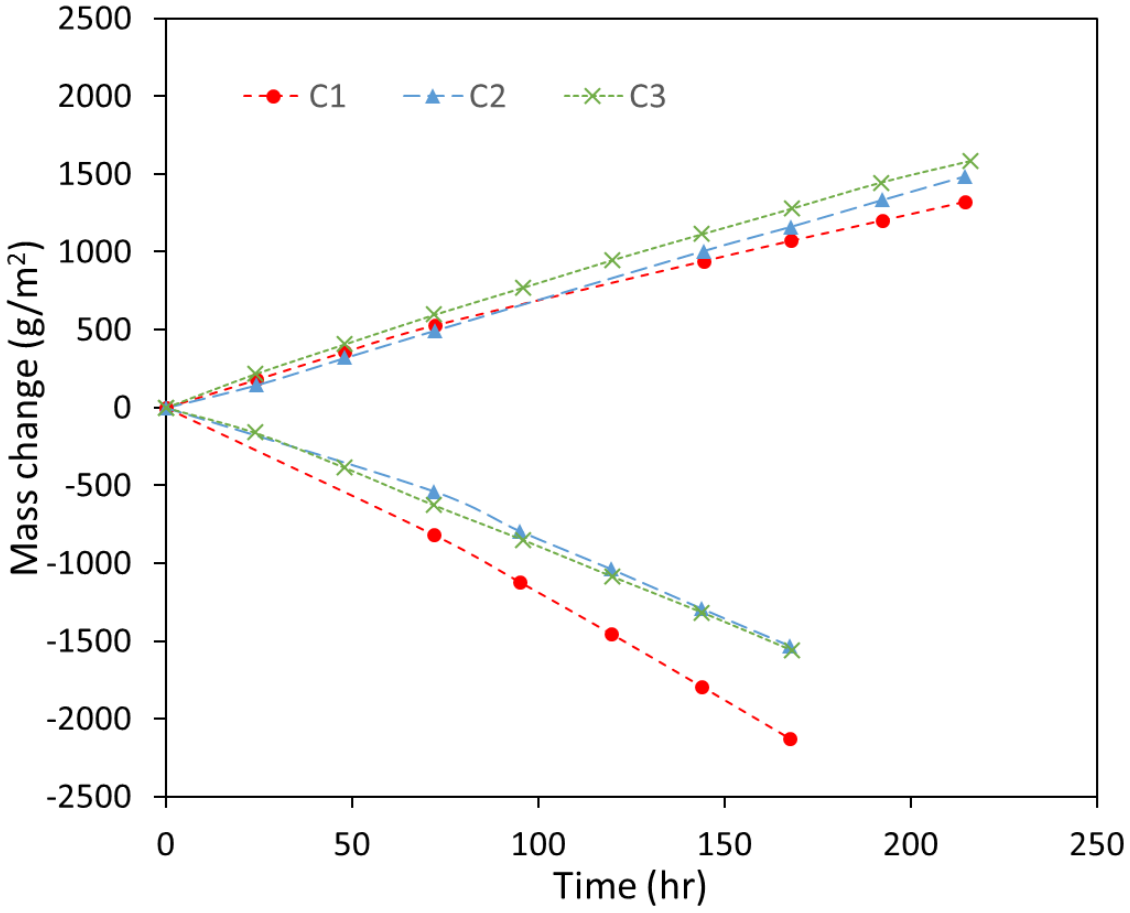

Figure 7. Mass change of the specimens during the vapour permeability test.

Table 1. Vapour permeability results of the hemp shiv based composites.

Parameters	C1 composite		C2 composite		C3 composite	
	Dry cup	**Wet Cup**	**Dry cup**	**Wet Cup**	**Dry cup**	**Wet Cup**
Water vapour transmission rate, g (mg/hr)	5675.65	15538.89	7224.33	9605.63	6343.75	9833.33
Water vapour permeance, W ($mg/m^2.hr.Pa$)	4.22	12.84	5.37	7.94	4.72	8.13
Water vapour resistance, Z ($m^2.hr.Pa/mg$)	0.24	0.08	0.18	0.13	0.21	0.12
Water vapour permeability δ (mg/m.hr.Pa)	0.08	0.26	0.11	0.16	0.09	0.16
Water vapour resistance factor μ	8.42	2.77	6.62	4.48	7.54	4.37

It can be seen the hydrophobic treatment in composites C1 and C2 does not significantly affect the water vapour permeability results when compared to the untreated C3 composites. The increase in the water vapour permeability at higher humidity level is related to the enhanced transport of moisture. This phenomenon is induced by the transfer of liquid in the microscopic pores of the material that are filled with water due to capillary condensation [20]. For materials that show hysteresis in their sorption isotherm, it has been reported earlier that their water vapour permeability is dependent on the moisture content [24].

The fluctuations in humidity within internal spaces of a building can be regulated by the moisture buffering ability of the construction materials. The kinetics of mass change for the MBV test is presented in Figure 8. The mass change was calculated per m^2 exposed surface of the samples and plotted against time. The sampling frequency was every 1 min and the data is plotted using a running average of every 60 min.

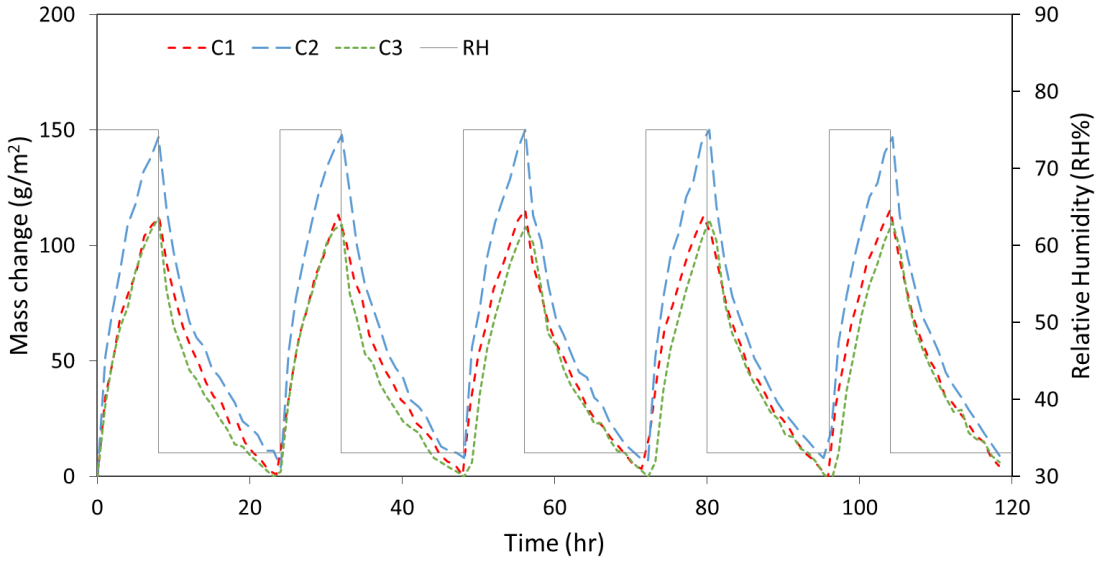

Figure 8. Mass change of the composites when exposed to varying relative humidity at 23 °C.

Table 2. MBV values of the composites using NORDTEST.

Sample	**MBV (g/m^2.RH)**
C1	3.07 ± 0.05
C2	3.63 ± 0.01
C3	2.93 ± 0.02

The moisture buffering capacity of the materials can be classified in terms of their moisture buffer value (MBV) as: Excellent (MBV ≥2.0 g/m^{2}RH), Good (MBV 1.0-2.0 g/m^{2}RH), Moderate (MBV 0.5-1.0 g/m^{2}RH), Limited (MBV 0.2-0.5 g/m^{2}RH) and Negligible (MBV ≤0.2 g/m^{2}RH) [25]. From Table 2, it can be seen that all the prepared composites showed "excellent" moisture buffering capacity with the highest MBV obtained for the C2 composites. The MBV of all hemp shiv composites (C1, C2 and C3) is higher than previously reported MBV for hemp concrete (1.75-2.15 g/m^{2}RH) [11,10,26]. This can be attributed to the higher hemp shiv: binder ratio in the prepared composites inducing lower density and enhanced permeability.

The thermal properties were analysed using a dynamic measurement system and they are reported in Table 3. It was observed that the thermal conductivity was in the range 0.051-0.058 W/mK and the thermal diffusivity ranged 0.28-0.35 m^2/s. The thermal conductivity values were lower when compared to the values for hemp lime composites (0.08 – 0.16 W/mK) previously reported in literature [27,28]. An obvious reason for the low conductivity is that the density of the prepared composites is much lower than hemp-lime composites. The higher hemp shiv: binder ratio used for the prepared composites takes greater advantage of the insulation properties of hemp shiv. The increased hemp shiv content in the matrix results in higher porosity thereby producing low density composites when compared to hemp-lime.

The specific heat capacity for the composites ranged from 760 – 1050 J/kg.K (Table 3). It can be seen that C1 and C3 composites have a high specific heat capacity for their respective densities. A hemp concrete composite is reported to have specific heat capacity of 1000 J/kg.K for a density of 413 kg/m^3 [10]. C1 composite in comparison to hemp concrete has less than half its density but a higher heat capacity. This could be attributed to the presence of chemically bound water (heat capacity 2200 J/kg.K) [29] in the silica coating that may affect the specific heat of the C1 and C2 composites when compared to the untreated C3 composite. In addition to the lowest density of C1 composite, it comprises of a silica matrix as opposed to C2 consisting of a starch matrix, thereby having superior insulating properties.

Table 3. Thermal conductivity data obtained from transient method using ISOMET.

Sample	**Thermal conductivity (W/mK)**	**Thermal diffusivity (10^{-6}) (m^2/s)**	**Specific heat capacity (J/kg.K)**	**Bulk Density (kg/m^3)**
C1	0.052	0.28	1050.28	175.0 ± 3
C2	0.057	0.30	782.71	240.0 ± 5
C3	0.053	0.35	763.00	200.0 ± 5

The relationship between density and thermal conductivity of the three prepared hemp shiv composites is shown in Figure 9. It is clearly seen that increasing the density increases the thermal conductivity of the composite which has also been previously reported in several studies [27,28,30].

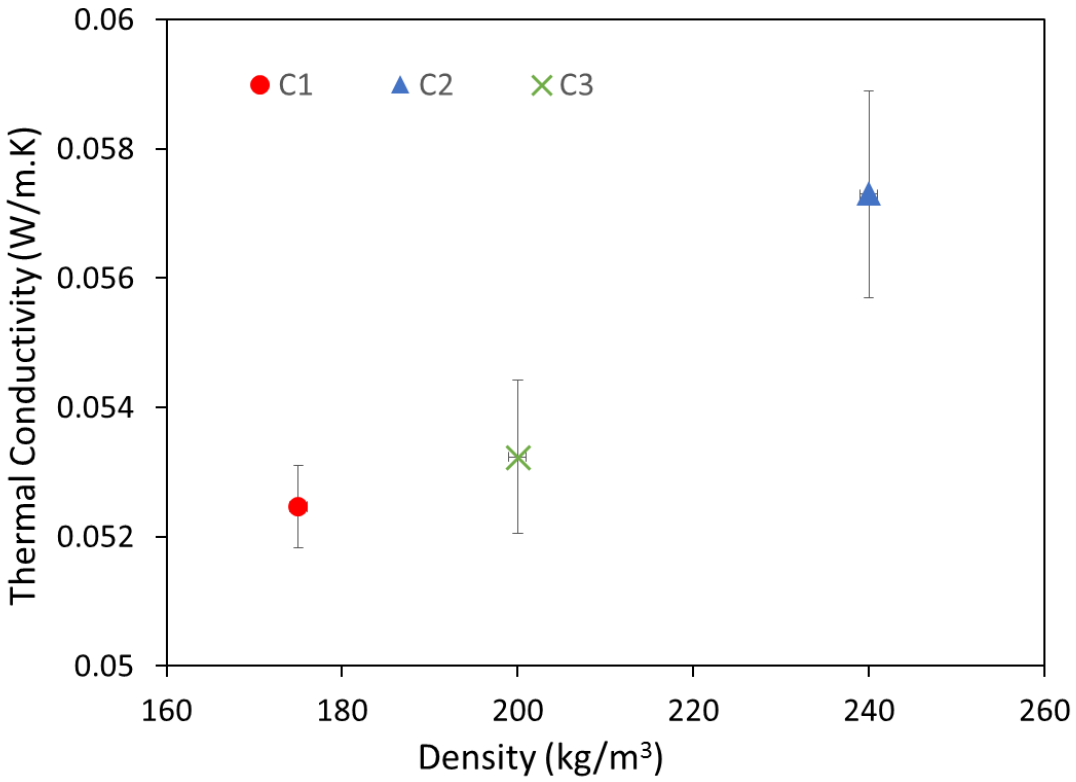

Figure 9. Thermal conductivity vs density of the composites.

The water absorption of the composites is calculated in two ways: (i) as change in mass over exposed surface area (WA) using Equation 8 and; (ii) as percentage of absorption with respect to initial mass (WA%) using Equation 9. The water absorption results are presented in Table 4. C3 shows the highest values for WA and WA% due to the absence of hydrophobic silica treatment on hemp shiv in the composites. For C2, the hydrophobic treatment reduced the WA by 50% and the WA% reduced by 123%. For C1, the reduction in water absorption is not as significant as C2. This is due to the fact that C1 has a much lower density than C2, therefore having more voids in the composite where water may get trapped during the test. Nevertheless, the C1 water absorption values show that the

treatment was still effective and absorbed less water when compared to untreated C3 composite.

Table 4. Water absorption measurements of composites.

Sample	WA (kg/m^2)	WA%
C1	18.48 ± 0.1	180.41 ± 2.2
C2	11.04 ± 0.6	98.02 ± 3.5
C3	22.11 ± 0.7	221.10 ± 1.3

The stress versus strain curves for the prepared hemp shiv composites are presented in Figure 10. The results show that C3 has a compressive stress of 0.92 ± 0.01 MPa at 30% strain. C2 composites show the highest compressive stress of 1.05 ± 0.04 MPa at 30% strain which is 14% higher than C3. On the other hand, the compressive stress of C1 is 0.49 ± 0.02 MPa at 30% strain which is 47% lower than C2. For all composites, it was observed that higher strain levels lead to further densification of the composites. The behaviour of the composites at varying strain levels (0%, 10%, 50%, after test) are imaged in Figure 11. After the compression test, C1 and C3 composites showed some elastic behaviour as seen in Figures 11D and 11H.

In general, the prepared light weight composites showed good mechanical performance. The composites attained compressive stress ranging between 0.49 – 1.05 MPa at very low densities (175-240 kg/m^3) which are relatively good when compared with other hemp shiv based composites such as hemp-lime (0.02 - 0.39 MPa at density 360 kg/m^3) [12], hemp-clay (0.39 at density 373 kg/m^3) [31] or hemp-starch (0.4 MPa at density 177 kg/m^3) [32]. The prepared composites did not reach failure even at 60% strains, which suggests good interfacial adhesion between the hemp shiv and the matrix.

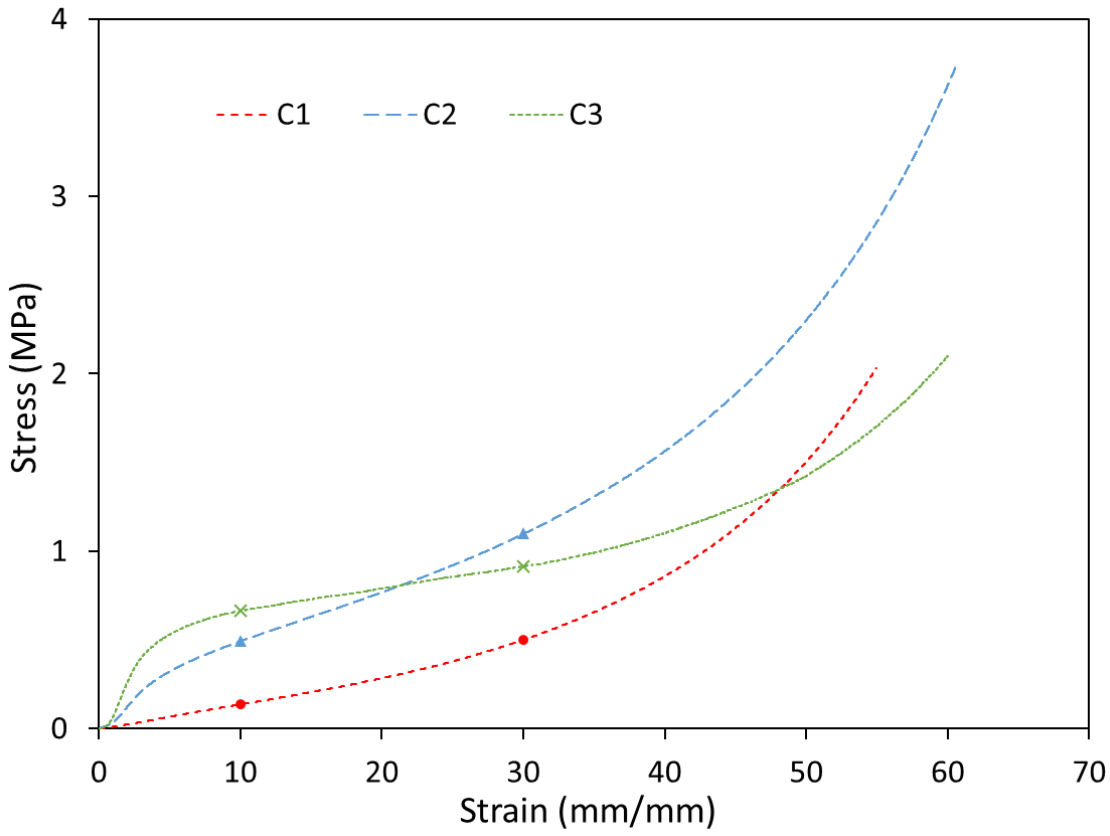

Figure 10. Compressive strength of the hemp based composites.

Figure 11. Compression testing of different hemp shiv composites; C1 at (A) 0% strain, (B) 30% strain, (C) 50% strain, (D) after 50% strain; C2 at (E) 0% strain, (F) 30% strain, (G) 50% strain, (H) after 50% strain; and C3 at (I) 0% strain, (J) 30% strain, (K) 50% strain, (L) after 50% strain.

Conclusion

In this work, manufacturing and testing of novel hemp shiv based composites have been reported. The composites showed a significant enhancement of hygrothermal performance when compared to traditional hemp based insulation composites. Vapour permeability and Nordtest results validate that hemp shiv composites retain their hygroscopic and moisture buffering ability even after hydrophobic treatment of the aggregate. The silica treatment reduced the hydrophilicity of hemp shiv as seen with the water absorption tests making them water resistant and less susceptible to degradation. The binding matrix did not degrade the thermal properties, and the prepared composites had thermal conductivity values of 0.052 W/mK. Preparation of composites with high hemp shiv: binder ratio had a significant benefit for enhancing their thermal insulation properties. The composites showed good mechanical properties as a non-load bearing material and final composites with density as low as 175 kg/m^3 were prepared successfully. Using economical methods, high performance hemp shiv based insulation composites have been developed that have great potential in the construction industry by reducing the embodied energy and the in-use energy demands of buildings.

Acknowledgments

The work was supported by the ISOBIO project funded by the Horizon 2020 programme [Grant number 636835 – ISOBIO – H2020-EeB-2014-2015] and the EPSRC Centre for Decarbonisation of the Built Environment (dCarb) [grant number EP/L016869/1]. The authors thank CAVAC for providing the starch binder for preparation of the composites. The contents of this publication are the sole responsibility of the authors and can in no way be taken to reflect the views of the European Union. All data are provided in full in the results section of this paper.

Disclosure statement

The authors declare that they have no conflict of interest.

References

[1] O.F. Osanyintola, C.J. Simonson, Moisture buffering capacity of hygroscopic building materials: Experimental facilities and energy impact, Energy Build. 38 (2006) 1270–1282. doi:10.1016/j.enbuild.2006.03.026.

[2] M. Woloszyn, T. Kalamees, M.O. Abadie, M. Steeman, A. Sasic Kalagasidis, The effect of combining a relative-humidity-sensitive ventilation system with the moisture-buffering capacity of materials on indoor climate and energy efficiency of buildings, Build. Environ. 44 (2009) 515–524. doi:10.1016/j.buildenv.2008.04.017.

[3] M. Lawrence, Reducing the Environmental Impact of Construction by Using Renewable Materials, J. Renew. Mater. 3 (2015) 163–174. doi:10.7569/JRM.2015.634105.

[4] A.D. Tran Le, C. Maalouf, T.H. Mai, E. Wurtz, F. Collet, Transient hygrothermal behaviour of a hemp concrete building envelope, Energy Build. 42 (2010) 1797–1806. doi:10.1016/j.enbuild.2010.05.016.

[5] D. Maskell, A. Thomson, P. Walker, M. Lemke, Determination of optimal plaster thickness for moisture buffering of indoor air, Build. Environ. 130 (2018) 143–150. doi:10.1016/j.buildenv.2017.11.045.

[6] A. Shea, M. Lawrence, P. Walker, Hygrothermal performance of an experimental hemp-lime building, Constr. Build. Mater. 36 (2012) 270–275. doi:10.1016/j.conbuildmat.2012.04.123.

[7] J. Williams, M. Lawrence, P. Walker, The influence of constituents on the properties of the bio-aggregate composite hemp-lime, Constr. Build. Mater. 159 (2018) 9–17. doi:10.1016/j.conbuildmat.2017.10.109.

[8] B. Mazhoud, F. Collet, S. Pretot, J. Chamoin, Hygric and thermal properties of hemp-lime plasters, Build. Environ. 96 (2016) 206–216. doi:10.1016/j.buildenv.2015.11.013.

[9] E. Latif, M. Lawrence, A. Shea, P. Walker, Moisture buffer potential of experimental wall assemblies incorporating formulated hemp-lime, Build. Environ. 93 (2015) 199–209. doi:10.1016/j.buildenv.2015.07.011.

[10] A.D. Tran Le, C. Maalouf, T.H. Mai, E. Wurtz, F. Collet, Transient hygrothermal behaviour of a hemp concrete building envelope, Energy Build. 42 (2010) 1797–1806. doi:10.1016/j.enbuild.2010.05.016.

[11] F. Collet, S. Pretot, Experimental investigation of moisture buffering capacity of sprayed hemp concrete, Constr. Build. Mater. 36 (2012) 58–65. doi:10.1016/j.conbuildmat.2012.04.139.

[12] R. Walker, S. Pavia, R. Mitchell, Mechanical properties and durability of hemp-lime concretes, Constr. Build. Mater. 61 (2014) 340–348.

doi:10.1016/j.conbuildmat.2014.02.065.

[13] S. Elfordy, F. Lucas, F. Tancret, Y. Scudeller, L. Goudet, Mechanical and thermal properties of lime and hemp concrete (“hempcrete”) manufactured by a projection process, Constr. Build. Mater. 22 (2008) 2116–2123. doi:10.1016/j.conbuildmat.2007.07.016.

[14] L. Arnaud, E. Gourlay, Experimental study of parameters influencing mechanical properties of hemp concretes, Constr. Build. Mater. 28 (2012) 50–56. doi:10.1016/j.conbuildmat.2011.07.052.

[15] Y. Jiang, M. Lawrence, M.P. Ansell, A. Hussain, Cell wall microstructure, pore size distribution and absolute density of hemp shiv, R. Soc. Open Sci. 5 (2018) 171945. doi:10.1098/rsos.171945.

[16] L. Kidalova, N. Stevulova, E. Terpakova, Influence of water absorption on the selected properties of hemp hurds composites, Pollack Period. (2015). doi:10.1556/Pollack.10.2015.1.12.

[17] A. Hussain, J. Calabria-Holley, D. Schorr, Y. Jiang, M. Lawrence, P. Blanchet, Hydrophobicity of hemp shiv treated with sol-gel coatings, Appl. Surf. Sci. 434 (2018) 850–860. doi:10.1016/j.apsusc.2017.10.210.

[18] S. Marceau, P. Glé, M. Guéguen-Minerbe, E. Gourlay, S. Moscardelli, I. Nour, S. Amziane, Influence of accelerated aging on the properties of hemp concretes, Constr. Build. Mater. 139 (2017) 524–530. doi:10.1016/j.conbuildmat.2016.11.129.

[19] A. Hussain, J. Calabria-Holley, Y. Jiang, M. Lawrence, Modification of hemp shiv properties using water-repellent sol–gel coatings, J. Sol-Gel Sci. Technol. (2018). doi:10.1007/s10971-018-4621-2.

[20] F. Collet, J. Chamoin, S. Pretot, C. Lanos, Comparison of the hygric behaviour of three hemp concretes, Energy Build. 62 (2013) 294–303. doi:10.1016/j.enbuild.2013.03.010.

[21] BS EN 12086, BSI Standards Publication Thermal insulating products for building applications — Determination of water vapour transmission properties, (2013).

[22] C. Rode, Moisture Buffering of Building Materials Department of Civil Engineering Technical University of Denmark, 2005.

[23] N.O. Copying, W. Bsi, P. Except, A.S. Permitted, B.Y. Copyright, BS EN 1609 : 2013 BSI Standards Publication Thermal insulating products for building applications — Determination of short term water absorption by partial immersion, (2013).

[24] D. Derome, H. Derluyn, W.A. Zillig, J. Carmeliet, Model for hysteretic moisture behaviour of wood, in: Proc. Nord. Symp. Build. Phys. 2008, 2008: pp. 959–966.

[25] C. Rode, R. Peuhkuri, L.H. Mortensen, K.K. Hansen, A. Gustavsen, T. Ojanen, J. Ahonen, K. Svennberg, L.-E. Harderup, J. Arfvidsson, Moisture Buffering of Building Materials, 2005. http://orbit.dtu.dk/fedora/objects/orbit:75984/datastreams/file_2415500/content.

[26] S. Dubois, A. Evrard, F. Lebeau, Modeling the hygrothermal behavior of biobased construction materials, J. Build. Phys. 38 (2014) 191–213.

[27] V. Cérézo, Propriétés mécaniques, thermiques et acoustiques d'un matériau à base de particules végétales: approche expérimentale et modélisation théorique, Inst. Natl. Des Sci. Appliquées, Lyon. (2005).

[28] R. Walker, S. Pavía, Moisture transfer and thermal properties of hemp-lime concretes, Constr. Build. Mater. 64 (2014) 270–276. doi:10.1016/j.conbuildmat.2014.04.081.

[29] D.P. Bentz, M.A. Peltz, A. Durán-Herrera, P. Valdez, C.A. Juárez, Thermal properties of high-volume fly ash mortars and concretes, J. Build. Phys. 34 (2011) 263–275. doi:10.1177/1744259110376613.

[30] B. Abu-Jdayil, A.-H. Mourad, A. Hussain, Thermal and physical characteristics of polyester-scrap tire composites, Constr. Build. Mater. 105 (2016). doi:10.1016/j.conbuildmat.2015.12.180.

[31] B. Mazhoud, F. Collet, S. Pretot, C. Lanos, Mechanical properties of hemp-clay and hemp stabilized clay composites, Constr. Build. Mater. 155 (2017) 1126–1137. doi:10.1016/j.conbuildmat.2017.08.121.

[32] U. Benitha Sandrine, V. Isabelle, M. Ton Hoang, C. Maalouf, Influence of chemical modification on hemp-starch concrete, Constr. Build. Mater. 81 (2015) 208–215. doi:10.1016/j.conbuildmat.2015.02.045.

Commentary Text

In this paper, three new composites were prepared and characterised for their hygrothermal and mechanical properties. The composites were prepared in either a silica matrix or a starch matrix without the use of any additional mineral binders. Two composites comprised of coated hemp shiv using the selected HDTMS based coating formulation. The third composite was prepared with hemp shiv that did not have any hydrophobic coating and this was used as the control sample to study the influence of the hydrophobic coated hemp shiv on the hygrothermal performance of the composites.

All three composites were characterised for their vapour permeability, moisture buffer value, water absorption capacity and compressive strength. Composites with density as low as 175 kg/m^3 were prepared successfully showing good mechanical performance when compared to conventional hemp based composites. The prepared composites were vapour permeable and showed retained excellent moisture buffering capacity despite the hydrophobic treatment of the hemp shiv aggregates. The water resistance was significantly enhanced due to the HDTMS based coating on hemp shiv reducing the water absorption capacity by 123%. The composites possessed low thermal conductivity values ranging between 0.051-0.058 W/m.K. The selected HDTMS based formulation significantly reduced the hydrophilicity of hemp shiv making water resistant composites that are expected to be less susceptible to degradation. The developed composites show a great potential in the building industry as novel bio-based thermal insulation materials with engineered hygroscopic properties.

Chapter 9

Conclusions and Recommendations

This chapter summarises the key findings reported in this thesis based on the objectives set out in Chapter 1. A critical analysis of the importance and novelty of this work in relation to international state of the art research has been highlighted. Further work has been suggested for an increased understanding of the newly developed composites.

Conclusions

Based on the objectives listed out in Chapter 1, the specific aims of this thesis have been successfully accomplished. The main focus of this thesis was formulation and development of hydrophobic coatings using sol-gel process for improvement of the water repellence of hemp shiv yet retaining its moisture buffering ability. The next focus was to utilise the coated hemp shiv to develop sustainable thermal insulating composites with better hygrothermal properties.

Hemp shiv has a tendency to absorb huge amounts of water due its extremely porous structure and the presence of surface hydroxyl groups. The geometric structure and chemical composition of a material are the two main features that control the wettability of any material (Genzer & Efimenko, 2006; Nakajima, Hashimoto, & Watanabe, 2001). Therefore for interpreting the extremely hydrophilic behaviour of hemp shiv, it is essential to investigate in detail the morphology, porosity and pore structure of hemp shiv. Previous studies reported in literature only provide limited knowledge on the microstructure of hemp shiv as reported in Chapter 2. Previous work has on hemp shiv microstructure reported the presence of conducting vessels (Magniont, Escadeillas, Coutand, & Oms-Multon, 2012), macro- and micro-pores (Lawrence, Shea, Walker, & De Wilde, 2013) and tubular structured pores (Dubois, Evrard, & Lebeau, 2014). However, the total porosity, detailed pore structure and the pore size distribution of hemp shiv has not been studied in literature.

The pore structure of hemp shiv is not only responsible for the high hydrophilicity but also for the excellent moisture buffering and thermal properties. Hemp-lime, a composite material made out of hemp shiv and lime binder, has been the most researched bio-based material apart from timber, due to its low thermal conductivity (0.06 – 0.014 W/mK) which is related to its low bulk density (0.08 – 0.016 g/cm^{-3}). Hemp-lime demonstrates a good balance between low mass and heat storage capacity and has excellent moisture buffering ability (Collet & Pretot, 2014; Latif, Tucker, Ciupala, Wijeyesekera, & Newport, 2014; Mazhoud, Collet, Pretot, & Chamoin, 2016; Shea, Lawrence, & Walker, 2012; Walker & Pavía,

2014). These characteristics are related to the microstructure and porosity of hemp shiv but their knowledge in the field is limited. Therefore concise knowledge of hemp shiv microstructure is of high importance to characterise the performance of hemp based composite materials.

An extensive characterisation of the porosity, pore structure and pore size distribution of hemp shiv has been reported in Chapter 3. The combination of several techniques and comparison of the results of cell wall structure provides an insight into the high porosity and complex pore system of hemp shiv. It was seen that hemp shiv had a very high porosity of 76.67 ± 2.03% using MIP technique and the pore size distribution curve followed a bimodal trend with two clearly separated peaks. The main pores were in the range 0.3 – 1 µm and the second peak showed pores in the range 20 – 80 µm. The high porosity values can be related to the low thermal conductivity and excellent hygroscopic properties of hemp based composites. The published article in Chapter 3 also presents the most appropriate techniques used for characterization of the cell wall microstructure, pore size distribution and absolute density of hemp shiv. Hemp shiv has gained considerable interest as a bio-aggregate in the building and construction industry for the production sustainable insulation materials as mentioned in Chapter 2 and the work reported in this article would be useful to researchers and practitioners alike.

The use of bio-aggregates within construction have their own challenges as mentioned in Chapter 1 which mainly include durability and degradation. The high sensitivity of hemp shiv to water is the main factor that limits the use of these materials within industry to their maximum potential. Therefore, this thesis provides a successful method for the pre-treatment of hemp shiv aggregates to render them more resistant to degradation, while maintaining their valuable hygrothermal qualities. In this thesis, the sol-gel process has been used to develop hydrophobic coating formulations that can be deposited on hemp shiv as a thin breathable membrane allowing exchange of vapour but blocking water molecules in liquid state.

The published article in Chapter 4 reports for the first time that the hydrophilicity of hemp shiv was modified without the compromise of its hygroscopic properties. The sol-gel process can be used for the formulation of highly versatile coatings with single or multi-functional properties. Various researchers have reported the use of hydrophobic sol-gel coatings on bio-based materials such as wood (Steffen Donath, Militz, & Mai, 2004; S. Wang, Shi, Liu, Xie, & Wang, 2011) and cellulose based materials (Bae et al., 2009; Mahltig & Böttcher, 2003) but so far the use of sol-gel technology on hemp shiv remains unexplored. The coatings formulated in this thesis aimed towards deposition of thin membranes or films on hemp shiv so as to not modify the physical properties of hemp shiv to a great extent but achieve maximum hydrophobicity on its surface. This kind of modification was necessary to retain the high porosity of hemp shiv which was responsible for its excellent hygrothermal qualities.

The researchers in the past have used sol-gel coatings for hydropobization of wood completely blocking all the pores thus not allowing water and moisture to permeate (S. Donath, Militz, & Mai, 2007). This was not the objective of this PhD work, as we aimed towards deposition of a hydrophobic coating but with breathable characteristics to allow water vapour to permeate through the surface of hemp shiv. The coating was also required to be deposited as an extremely thin film thus not lowering the overall porosity of hemp shiv.

The first coating formulation was prepared using tetraethyl orthosilicate (TEOS), ethanol, water, nitric acid and a hydrophobic additive, methyltriethoxysilane (MTES) using the sol-gel process. The co-precursor method of sol-gel synthesis was followed based on the simplicity of the process. During the process, TEOS was hydrolysed and condensed to form a SiO_2 network that links to cell wall through the hydroxyl sites of cellulose present in the hemp shiv. On addition of hydrophobic agent as a co-precursor during the sol-gel processing, the hydroxyl groups on the silica clusters are replaced by the alkyl groups through oxygen bonds. The hydrophobicity of the coated surface is due to the presence of alkyl groups on silica network.

From the article in Chapter 4, it was seen a single layer of MTES based coating significantly lowered the water absorption of hemp shiv by 200% and did not modify the porosity of hemp shiv to a great extent. Although the water-repellence of hemp shiv was increased with the MTES based coating, it was not sufficient enough to create a hydrophobic surface as seen with the water contact angle (WCA) results. It has been reported earlier that superhydrophobic surfaces (WCA>150°) can be prepared on cellulose based materials using sol-gel coatings (Chang, Tu, Wang, & Liu, 2015; Gao, Gan, Xiao, Zhan, & Li, 2016; S. Wang et al., 2011; Xue, Jia, Chen, & Wang, 2008), but the use of fluoro based precursors in the coating was not considered in this work due to their harmful nature and high cost.

An inexpensive coating formulation was prepared using sodium silicate as an alternative precursor to TEOS. The formulation has been reported earlier to provide superhydrophobic surface on cotton substrates (Li, Xing, & Dai, 2008). The formulation does not contain any fluorinated compounds and the hydrophobic precursor used was hexadecyltrimethoxysilane (HDTMS). Following the same coating methodology from the paper, the formulation was unable to provide sufficient level of water-repellence to hemp shiv. The water absorption was reduced by 150 – 200% which is similar to the results obtained by the MTES based coating. Moreover, the methodology has certain drawbacks such as multi step process, long immersion time in HDTMS for 4 hours and rinsing of sodium ions which are costly, time-consuming and not favourable on an industrial scale.

Chapter 4 studies new formulations using TEOS, ethanol, water, HDTMS and different catalysts. The concentration of HDTMS and ethanol was varied to study different formulations for producing coatings with maximum hydrophobicity and minimal cost. HDTMS is a silane molecule with 16-carbon alkyl chain and known to provide good level of hydrophobicity to other cellulose based materials (Daoud, Xin, & Tao, 2004; Mahltig & Böttcher, 2003; Tshabalala, Kingshott, Vanlandingham, & Plackett, 2002). The coating formulations chemically modified the surface of hemp shiv which overall improved the hydrophobicity of the material. The high water repellence can be attributed to the long alkyl chains of HDTMS that provide high hydrophobicity.

The coated hemp shiv showed good resistance to water although the precursors and reagent concentrations played a significant role in providing hydrophobicity to the surface. The effect of acidic and basic catalyst on the hydrophobicity of the coating was analysed. Both acidic and basic sol-gel coatings tend to reduce the hydrophilicity of the hemp shiv by maintaining a stable contact angle over 60 seconds. However, it was found that the basic sols were unable to provide a hydrophobic surface (WCA<90°) on the hemp shiv.

It is well known that when basic catalysts are used in the sol-gel process silica nanoparticles are usually produced. Cellulose based materials have been covered by silica nanoparticles by simple dip coating (Zhou, Wang, Niu, Gestos, & Lin, 2013), by spraying SiO2 nanoparticles suspended in alcohol (Ogihara, Xie, Okagaki, & Saji, 2012) or by heat treatment (L. Xu, Zhuang, Xu, & Cai, 2011). However, studies have reported that the coverage of silica nanoparticles on cellulose based materials without pre-treatment is quite poor (Bae et al., 2009; Yu, Gu, Meng, & Qing, 2007), which may affect the strength of the functionality it is expected to provide on the material. This may be the reason for the lower WCA on hemp shiv coated with basic sols. In order to enhance the hydrophobic functionality, the nanoparticle coverage and roughness needs to be increased. This can be obtained by depositing multilayers of silica nanoparticles and combining the basic sol-gel suspension with cationic polyelectrolytes (Song & Rojas, 2013). The deposition of multilayers is time consuming and expensive on an industrial scale. In this thesis, the sols prepared with acidic catalysts were deposited as films rather than nanoparticles.

The acidic coatings performed better showing higher contact angles making the surface hydrophobic (WCA>90°) and particularly nitric acid based coatings showed the highest contact angles. The wettability of the surface is controlled by the surface chemical composition as well as the morphology of the microstructure. Surfaces with a similar chemical composition may have different wettability behaviour due to the surface topology (Q. F. Xu, Wang, & Sanderson, 2010).

The effect of varying ethanol concentrations in acidic coatings revealed that controlling the ethanol: HDTMS ratio was important to achieve crack free coatings with enhanced surface roughness. Ethanol dilution enhanced the surface roughness of hemp shiv whereas the undiluted sols with high HDTMS concentration had lower surface roughness and were deposited as flat thick membranes. This was mainly due to the presence of HDTMS molecules that are not fully hydrolysed and being deposited onto the membrane as a flat thick film. The reduced surface roughness can be attributed to the extra HDTMS molecules on the coated surface (H. Wang et al., 2017).

On the other hand, ethanol diluted sols with low HDTMS concentration developed cracks which lowered the water contact angle to 98°. The presence of surface cracks arising as a result of shrinkage after drying the coated shiv is a significant factor to be considered when hydrophobic properties are concerned. The hydrophobicity of modified hemp shiv can be compromised as the water molecules can penetrate through the cracked coating wetting the bulk of the material over time. The highest hydrophobicity was obtained when ethanol: HDTMS ratio was 4M: 0.014M and the coatings were deposited as a thin crack-free uniform layer without altering the morphology of hemp shiv surface

Another factor that controlled the hydrophobicity of the coatings with TEOS: HDTMS ratio since an organic-inorganic hybrid coating was used. When using TEOS: HDTMS ratio as 1M: 0.014M, highest contact angles were obtained even at low HDTMS concentration due to the combined effect of chemical modification and surface roughness. Although higher HDTMS concentration would be expected to decrease the surface energy, experimental analysis revealed that the surface roughness can be reduced if the HDTMS concentration is too high as the extra silane fills the inter-particle gap. Similar results have been reported in different coating systems (H. Wang et al., 2017; Zeng, Wang, Zhou, & Lin, 2015).

The published article in Chapter 5 has been useful in the field of surface science and has been already cited over 5 times by various researchers reporting on silica coatings on hemp shiv (Bourebrab, Durand, & Taylor, 2017; Jiang et al., 2018)

and TEOS based organic-inorganic hybrid formulations (Dezfuli & Sabzi, 2018; Mersagh Dezfuli & Sabzi, 2018; Saputra, Astuti, & Darmawan, 2018)

The coatings modified the chemical composition of hemp shiv mainly reducing the surface hydroxyl groups that are responsible for the extreme hydrophilic behaviour of hemp shiv. From the XPS analysis, it was seen that the surface carbon content of the coated hemp shiv decreased by 41.28% (from 69.61 to 28.33%) and the oxygen content increased by 26.51% (from 27.06 to 53.57%). This change in C/O ratio and increase in surface oxygen concentration can be attributed to O-Si-CH_3 bonds present in the polysiloxane coating on the surface of the sol-gel coated hemp shiv. The decrease in the surface carbon concentration of the coated shiv can be attributed to the masking effect of the polysiloxane coating which reduces the detectability of surface cellulose and hemicellulose. The masking effect of the coating was also observed in the FTIR analysis.

Covalent bonding has been observed between the hydroxyl groups of cellulose and the silanols of the coating. From XPS analysis, the C1s high resolution indicates a shift in the binding energy of C2 component (from 286.6 to 286.8 eV) which was observed along with the decrease in the intensity of the C2 component for the sol-gel coated sample. This shift indicates the presence of a carbon atom linked to an oxygen and silicon atom (O-C-Si or C-O-Si) (Tshabalala et al., 2002). It has also been shown (Abdelmouleh, Boufi, Belgacem, & Dufresne, 2007; Castellano, Gandini, Fabbri, & Belgacem, 2004; Valadez-Gonzalez, Cervantes-Uc, Olayo, & Herrera-Franco, 1999; Xie, Hill, Xiao, Militz, & Mai, 2010a) that curing above room temperature drives the dehydration reaction at the adsorption sites between hydroxyl groups of the cellulose and the silanols forming –Si-O-C- bonds. These bonds are formed by the linkage between polysilanol network with the cellulose hydroxyl groups via polycondensation. The C1 component of the C1s peak shows an increase in intensity for the coated sample indicating presence of C-H and C-C bonds from the HDTMS hydrocarbon chain.

The chemical composition of the selected coating formulation was TEOS: Ethanol: Water: Nitric acid: HDTMS = 1M: 4M: 4M: 0.005M: 0.014M. Contact

angles up to 118 ° were achieved on coated hemp shiv surface with enhanced surface roughness. It was seen that HDTMS based coatings performed better than MTES based coatings even at lower concentration of the hydrophobic additive. The water absorption of hemp shiv was reduced by 250% over 24 hours with selected HDTMS based coating. On the other hand, hemp shiv treated with single layer of MTES based coating showed water contact angles up to 89° and reduced the water absorption of shiv by 200% over 24 hours.

The selected HDTMS based coating formulation does not significantly alter the microstructure and porosity of the shiv thereby retaining its ability to adsorb and desorb moisture. The high values of moisture adsorption for hemp shiv can be assigned to its chemical composition with a large number of hydroxyl groups being accessible. The lower water vapour sorption values for the coated shiv can be attributed to the hydrophobic alkyl chains present on the coated surface. Modifying the surface of hemp shiv with the silica coating blocked the surface hydroxyl sites and reduced the mass of water adsorbed at high humidity levels. Although, the silica coating interacts with the hemp shiv subsequently lowering its moisture buffering capacity to a limited extent but the coating does not completely block the pores. The SEM micrographs confirmed that the coating formulation had least altered the surface morphology of hemp shiv. From the porosity and DVS results, it was determined that the coated hemp shiv is capable of adsorbing moisture through the smaller pores whereas the water uptake was considerably reduced due to decrease in the larger pores. Coated shiv showed significant reduction in hysteresis by 54% when compared to uncoated shiv at 90% RH. The reduction in hysteresis curves of the coated shiv showed that water is condensed only on the surface and does not go further deep into the bulk of the hemp shiv structure due to the presence of hydrophobic chains.

From Chapters 5 and 6 it can be established that a simple and inexpensive one step coating process was used to provide a hydrophobicity to a highly hydrophilic bio-based material. The coated surface exhibited excellent hydrophobic properties through the synergistic effect of enhanced surface roughness and modified chemical composition. The hemp shiv samples were found to retain their moisture buffering ability even after deposition of the silica coatings.

The next part of the thesis focused on the development of a novel hemp based thermal insulation composite that is reported in Chapter 7. Light weight hemp shiv composites were prepared in a silica based binding matrix for the first time. The selected HDTMS based silica sol formulation was used as the binding agent. The novel use of sol-gel treatment as a binding agent was identified, providing multi-functionality from a single treatment using an economical single step process.

The silica sol interacted with hemp shiv leaching out extractives and waxes which lead to visual changes turning the silica matrix from colourless transparent to yellowish opaque. On drying the gel undergoes condensation and develops into a network of silica entrapping the extracts the hemp shiv. It was seen that lipophilic extractives from the shiv were integrated within the silica network, modifying the chemical, morphological and physical characteristics of silica.

Chemical characterisation of the binding matrix revealed the presence of higher carbon content when compared to pure silica glass. The surface carbon content of the binding matrix increased by 27% (from 19% to 46%). On the other hand, the oxygen content decreased by 21% (from 61% to 40%). This change in C/O ratio and increase in the surface carbon content can be attributed to the additional extracts in the modified network of the binding matrix that were identified by GCMS analysis.

The C1s high resolution XPS spectra revealed that the hemp shiv extracts modified the silica network leading to the appearance of C3 and C4 peaks which were not present in the pure silica glass. Moreover, the increase in the intensity of the C1 component for the binding matrix from 68% to 84% indicated the presence of C-C and C-H bonds from the incorporated extracts. To analyse the extracts that were leaching out from hemp shiv during the silica based treatment, the process was simplified by using a solution of ethanol and water for the extraction process. Lipophilic extractives are insoluble in water but soluble in organic solvents such as hexane, dichloromethane, diethyl ether, acetone or ethanol (Sun & Tomkinson, 2002). These ethanol-soluble extractives were analysed using GCMS and it was found that the extract was mainly composed of

lauric acid and phthalic acid with many other fatty acids. The majority of the compounds identified using GCMS belong to the group of lipophilic extractives which are hydrophobic in nature (Hardell & Nilvebrant, 1999; Sun & Tomkinson, 2002). This could possibly be one of the factors for the compatibility between the lipophilic extractives and the sol-gel chemistry due to their hydrophobic nature. It has also been reported earlier that extractives from bio-based materials can have a tacky nature forming pitch deposits which is considered to be a major problem in the paper and pulp industry (Gutiérrez, Del Río, Martínez, & Martínez, 2001). It must be noted that composites produced using an ethanol-water mixture instead of silica sol were unsuccessful as the hemp shiv fell apart on demoulding. The ethanol is responsible for isolation of the extractives and waxes from hemp shiv but the extractives cannot bind hemp shiv on their own. The extractives modify the silica chemistry and the binding matrix holds the hemp particles together resulting in the production of coherent composite blocks.

Composites were prepared using hemp shiv and silica sol and their mechanical performance was evaluated. The composites were light weight with a density of 175 kg/m^3 and the compressive stress of 0.48 MPa attained at 30% strain is relatively good when compared to other hemp shiv based composites such as hemp-lime (0.02 - 0.39 MPa at density 360 kg/m^3) (Walker, Pavia, & Mitchell, 2014), hemp-starch (0.4 MPa at density 177 kg/m^3) (Benitha Sandrine, Isabelle, Ton Hoang, & Maalouf, 2015) and hemp-clay (0.39 at density 373 kg/m^3) (Mazhoud, Collet, Pretot, & Lanos, 2017). It is known that hydrolysed silanes can chemically attach to the hydroxyl group of fibres, but they are known to provide only a limited improvement in the mechanical properties of the resulting fibre composite due to their physical compatibility with the matrix. The strength of natural fibre composites can be increased if covalent bonds are present between the silane treated fibre and matrix (Pickering, Efendy, & Le, 2016; Xie, Hill, Xiao, Militz, & Mai, 2010b). This presence of covalent bonding between the silica and hemp shiv is possibly the reason for good mechanical properties of the prepared composite.

The developed composites were durable and the silica treatment enhanced their resistance to water. The durability test was performed by immersion of the

composites in water for 24 hours and comparing their mechanical performance before and after the immersion. Since the binder also provides hydrophobicity to the hemp shiv, the compressive stress versus strain characteristics are not compromised to a great extent. However, minor swelling was observed in the composites that could be related to the slow penetration of water through micro-cracks on the coated surface or due to the presence of small uncovered pores within the hemp shiv.

The study reported in Chapter 7 is applicable to not only the hemp shiv material but also to any bio-based material which has cellulose and lipophilic extractives in its composition. This published article in Chapter 7 enlightens and broadens the current use of the sol-gel treatment as a dual functionalised agent: (i) as a hydrophobic surface treatment (ii) and as a binding agent leading to the development of high performance bio-based building materials.

Chapter 8 reports the physical and mechanical characterisation of the novel hemp-silica matrix composites and the results have been compared with starch matrix composites prepared with either coated or uncoated hemp shiv aggregates. The composites showed a significant enhancement of hygrothermal performance when compared to traditional hemp based insulation composites. The prepared hemp shiv composites retained their hygroscopic and moisture buffering ability even after hydrophobic treatment of the aggregate. The silica treatment reduced the hydrophilicity of hemp shiv making them water resistant and less susceptible to degradation.

The binding matrix did not degrade the thermal properties, and the prepared composites had thermal conductivity values of 0.051 – 0.058 W/mK. Preparation of composites with high hemp shiv: binder ratio had a significant benefit for enhancing their thermal insulation properties compared to conventional hemp-lime composites having thermal conductivity values in the range (0.08 – 0.16 W/mK) previously reported in literature (Cérézo, 2005; Walker & Pavía, 2014). The reason for the low conductivity is that the density of the prepared composites is much lower than hemp-lime composites. The higher hemp shiv: binder ratio used for the prepared composites takes greater advantage of the insulation

properties of hemp shiv. The increased hemp shiv content in the matrix results in higher porosity thereby producing low density composites when compared to hemp-lime.

The prepared composites showed “excellent” moisture buffering capacity with MBV values in the range of 3.1 – 3.6 g/m^{2}RH. The MBV of both hemp shiv composites, in starch matrix and silica matrix, is higher than previously reported MBV for hemp concrete (1.75-2.15 g/m^{2}RH) (Collet & Pretot, 2012; Dubois et al., 2014; Tran Le, Maalouf, Mai, Wurtz, & Collet, 2010). This can be attributed to the higher hemp shiv: binder ratio in the prepared composites inducing lower density and high vapour permeability. The hydrophobic treatment of hemp shiv in the prepared composites did not significantly affect the water vapour permeability results when compared to the control samples with untreated hemp shiv. The water absorption capacity of the prepared composites was greatly reduced due to the hydrophobic hemp shiv aggregates used in the composite. The treatment lowered the WA% of the composites down to 123% when compared to the control composites.

From Chapter 8 it can be concluded that the prepared composites showed a significant enhancement of hygrothermal performance when compared to traditional hemp based insulation composites. The composites possessed good mechanical properties as a non-load bearing material and final composites with density as low as 175 – 240 kg/m^3 were prepared successfully. The silica treatment reduced the hydrophilicity of hemp shiv as seen with the water absorption tests making them water resistant and less susceptible to degradation. Preparation of composites with high hemp shiv: binder ratio had a significant benefit for enhancing their thermal insulation properties. The binding matrix did not degrade the thermal properties, and the prepared composites had thermal conductivity values of 0.051 – 0.058 W/mK. The objectives of this PhD have been met and high performance thermal insulation composites with enhanced hygroscopic properties have been successfully prepared using hemp shiv treated with the selected HDTMS based coating formulation.

From this thesis the following points can be concluded:

- Sol–gel technology has proved successful in modifying a highly hydrophilic bio-based material into a water-resistant building material. A cross linked network was formed between the coating and the surface hydroxyl groups of the shiv. The vapour sorption ability was not compromised which means the shiv retained its moisture buffering capacity.

- A simple one step dip-coating process was successfully applied on hemp shiv. The hydrophobic properties were achieved through a combination of topological alteration and chemical modification of the hemp shiv by the silica based coating. The selected formulation has low HDTMS concentration (1 wt%) that would be of interest to the industry due to its hygroscopic properties, long shelf life, reduced cost and lower environmental impact.

- The novel use of sol-gel treatment as a binding agent has been identified. This transforms the current use of the sol-gel treatment as a surface modifier agent alone to dual functionality as a binder agent leading to economical and sustainable bio-based building materials.

- Using economical methods, high performance hemp shiv based composites with enhanced hygrothermal properties were developed that have great potential in the construction industry by reducing the embodied energy and the in-use energy demands of buildings.

Recommendation for future work

The work in this thesis mainly focuses on the development of robust engineered thermal insulation composites. The research has demonstrated that the elements responsible for decay and degradation of hemp based composites have been addressed by reducing the water absorption capacity of the composites. The author recommends further work for a deeper understanding of the composite behaviour.

- Studies on decay and fungal growth would provide insight into the potential of the hydrophobic coating towards mould resistance.

- The life cycle assessment (LCA) would give an overview on the environmental impact of the treated composites.

- Characterisation of the composites for their resistance to fire. Silica deposition has theoretical potential to confer fire resistance to the material.

Bibliography

Abdelmouleh, M., Boufi, S., Belgacem, M. N., & Dufresne, A. (2007). Short natural-fibre reinforced polyethylene and natural rubber composites: Effect of silane coupling agents and fibres loading. *Composites Science and Technology*, *67*(7–8), 1627–1639. https://doi.org/10.1016/j.compscitech.2006.07.003

Abdelmouleh, M., Boufi, S., Salah, A. Ben, Belgacem, M. N., & Gandini, A. (2002). Interaction of silane coupling agents with cellulose. *Langmuir*, *18*(8), 3203–3208. https://doi.org/10.1021/la011657g

Agency for Natural Resources and Energy. (2017). Key World Energy statistics. *IEA International Energy Agency*. https://doi.org/10.1017/CBO9781107415324.004

Agoua, E., Allognon-Houessou, E., Adjovi, E., & Togbedji, B. (2013). Thermal conductivity of composites made of wastes of wood and expanded polystyrene. *Construction and Building Materials*, *41*, 557–562. https://doi.org/10.1016/j.conbuildmat.2012.12.016

Ahmad, M. R., Bing, C., Oderji, S. Y., & Mohsan, M. (2018). Development of a new bio-composite for building insulation and structural purpose using corn stalk and magnesium phosphate cement; Physical, mechanical, thermal and hygric evaluation. *Energy and Buildings*. https://doi.org/10.1016/j.enbuild.2018.06.007

Aigbomian, E. P., & Fan, M. (2013). Development of Wood-Crete building materials from sawdust and waste paper. *Construction and Building Materials*, *40*, 361–366. https://doi.org/10.1016/j.conbuildmat.2012.11.018

Al-Homoud, M. S. (2005). Performance characteristics and practical applications of common building thermal insulation materials. *Building and Environment*, *40*(3), 353–366. https://doi.org/10.1016/j.buildenv.2004.05.013

Al Rim, K., Ledhem, A., Douzane, O., Dheilly, R. M., & Queneudec, M. (1999). Influence of the proportion of wood on the thermal and mechanical performances of clay-cement-wood composites. *Cement and Concrete Composites*, *21*(4), 269–276. https://doi.org/10.1016/S0958-9465(99)00008-6

Amziane, S., & Arnaud, L. (2013). *Bio-aggregate-based building materials: applications to hemp concretes*. John Wiley & Sons.

Amziane, S., & Collet, F. (2017). *Bio-aggregates Based Building Materials* (Vol. 23). https://doi.org/10.1007/978-94-024-1031-0

Anovitz, L. M., & Cole, D. R. (2015). Characterization and Analysis of Porosity

and Pore Structures. *Reviews in Mineralogy and Geochemistry*, *80*(1), 61–164. https://doi.org/10.2138/rmg.2015.80.04

Arnaud, L., & Gourlay, E. (2012). Experimental study of parameters influencing mechanical properties of hemp concretes. *Construction and Building Materials*, *28*(1), 50–56. https://doi.org/10.1016/j.conbuildmat.2011.07.052

Association, E. I. H. (2018). Industrial Hemp Cultivation Area 2017. Retrieved September 10, 2018, from http://eiha.org/document/eu-hemp-cultivation-area-2017/

Bae, G. Y., Min, B. G., Jeong, Y. G., Lee, S. C., Jang, J. H., & Koo, G. H. (2009). Superhydrophobicity of cotton fabrics treated with silica nanoparticles and water-repellent agent. *Journal of Colloid and Interface Science*, *337*(1), 170–175. https://doi.org/10.1016/j.jcis.2009.04.066

Balčiunas, G., Vejelis, S., Vaitkus, S., & Kairyte, A. (2013). Physical properties and structure of composite made by using hemp hurds and different binding materials. *Procedia Engineering*, *57*, 159–166. https://doi.org/10.1016/j.proeng.2013.04.023

Bedetti, R., & Ciareli, N. (1976). Variazione del contenuto della cellulosa durante il periodo vegetativo della canapa. *Cellulosa E Carta*, *26*, 27–30.

Belgacem, M. N., & Gandini, A. (2005). The surface modification of cellulose fibres for use as reinforcing elements in composite materials. *Composite Interfaces*, *12*(1–2), 41–75. https://doi.org/10.1163/1568554053542188

Benfratello, S., Capitano, C., Peri, G., Rizzo, G., Scaccianoce, G., & Sorrentino, G. (2013). Thermal and structural properties of a hemp-lime biocomposite. *Construction and Building Materials*, *48*, 745–754. https://doi.org/10.1016/j.conbuildmat.2013.07.096

Benitha Sandrine, U., Isabelle, V., Ton Hoang, M., & Maalouf, C. (2015). Influence of chemical modification on hemp-starch concrete. *Construction and Building Materials*, *81*, 208–215. https://doi.org/10.1016/j.conbuildmat.2015.02.045

Biofib'. Biofib'Hemp. Available at: http://www.biofib.com/files/en/BIOFIB-Hemp.pdf [Accessed August 20, 2018].

Black Mountain Insulation. NatuHemp technica, 76. Retrieved from http://www.blackmountaininsulation.com/NatuHemp_Technical_Sheet.pdf [Accessed August 20, 2018].

Bledzki, A. K., Mamun, A. A., Lucka-Gabor, M., & Gutowski, V. S. (2008). The effects of acetylation on properties of flax fibre and its polypropylene composites. *Express Polymer Letters*, *2*(6), 413–422. https://doi.org/10.3144/expresspolymlett.2008.50

Bourebrab, M. A., Durand, G. G., & Taylor, A. (2017). Development of highly repellent silica particles for protection of hemp shiv used as insulation

materials. *Materials*, *11*(1). https://doi.org/10.3390/ma11010004

British Columbia, M. of A. and F. F. (1999). Industrial Hemp - Factsheet.

BS EN 12086. (2013). BSI Standards Publication Thermal insulating products for building applications — Determination of water vapour transmission properties.

C. Brinker, & Scherer, G. (1990). Sol-Gel Science: The Physics and Chemistry of Sol-Gel Processing. *Advanced Materials*. https://doi.org/10.1186/1471-2105-8-444

Calabria A., J., Vasconcelos, W. L., Daniel, D. J., Chater, R., McPhail, D., & Boccaccini, A. R. (2010). Synthesis of sol-gel titania bactericide coatings on adobe brick. *Construction and Building Materials*, *24*(3), 384–389. https://doi.org/10.1016/j.conbuildmat.2009.08.020

Carus, M. (2013). Market data on Industrial Hemp – fibres , shivs and seeds, (October).

Carus, M. (2017). The European Hemp Industry: Cultivation, processing and applications for fibres, shivs, seeds and flowers, *1994*, 1–9. Retrieved from http://eiha.org/media/2017/12/17-03_European_Hemp_Industry.pdf

Castellano, M., Gandini, A., Fabbri, P., & Belgacem, M. N. (2004). Modification of cellulose fibres with organosilanes: Under what conditions does coupling occur? *Journal of Colloid and Interface Science*, *273*(2), 505–511. https://doi.org/10.1016/j.jcis.2003.09.044

Cérézo, V. (2005). Propriétés mécaniques, thermiques et acoustiques d'un matériau à base de particules végétales: approche expérimentale et modélisation théorique. *Institut National Des Sciences Appliquées, Lyon*.

Chang, H., Tu, K., Wang, X., & Liu, J. (2015). Fabrication of mechanically durable superhydrophobic wood surfaces using polydimethylsiloxane and silica nanoparticles. *RSC Advances*, *5*(39), 30647–30653. https://doi.org/10.1039/c5ra03070f

Cheng, X. W., Liang, C. X., Guan, J. P., Yang, X. H., & Tang, R. C. (2018). Flame retardant and hydrophobic properties of novel sol-gel derived phytic acid/silica hybrid organic-inorganic coatings for silk fabric. *Applied Surface Science*, *427*, 69–80. https://doi.org/10.1016/j.apsusc.2017.08.021

Collet, F., Chamoin, J., Pretot, S., & Lanos, C. (2013). Comparison of the hygric behaviour of three hemp concretes. *Energy and Buildings*, *62*, 294–303. https://doi.org/10.1016/j.enbuild.2013.03.010

Collet, F., & Pretot, S. (2012). Experimental investigation of moisture buffering capacity of sprayed hemp concrete. *Construction and Building Materials*, *36*, 58–65. https://doi.org/10.1016/j.conbuildmat.2012.04.139

Collet, F., & Pretot, S. (2014a). Experimental highlight of hygrothermal

phenomena in hemp concrete wall. *Building and Environment*, *82*, 459–466. https://doi.org/10.1016/j.buildenv.2014.09.018

Collet, F., & Pretot, S. (2014b). Thermal conductivity of hemp concretes: Variation with formulation, density and water content. *Construction and Building Materials*, *65*, 612–619. https://doi.org/10.1016/j.conbuildmat.2014.05.039

Danks, A. E., Hall, S. R., & Schnepp, Z. (2016). The evolution of "sol–gel" chemistry as a technique for materials synthesis. *Mater. Horiz.*, *3*, 91–112. https://doi.org/10.1039/C5MH00260E

Danny Harvey, L. D. (2007). Net climatic impact of solid foam insulation produced with halocarbon and non-halocarbon blowing agents. *Building and Environment*, *42*(8), 2860–2879. https://doi.org/10.1016/j.buildenv.2006.10.028

Daoud, W. A., Xin, J. H., & Tao, X. (2004). Superhydrophobic silica nanocomposite coating by a low-temperature process. *Journal of the American Ceramic Society*, *87*(9), 1782–1784. https://doi.org/10.1111/j.1551-2916.2004.01782.x

de Groot, B. (1998). *Alkaline hemp woody core pulping: impregnation characteristics, kinetic modelling and papermaking qualities*. sn].

Dezfuli, S. M., & Sabzi, M. (2018). Effect of yttria and benzotriazole doping on wear/corrosion responses of alumina-based nanostructured films. *Ceramics International*, (July), 0–1. https://doi.org/10.1016/j.ceramint.2018.07.313

Dinwoodie, J. M. (1989). *Wood: Nature's Cellular, Polymeric, Fibre-composite*. Maney Pub.

Diquélou, Y., Gourlay, E., Arnaud, L., & Kurek, B. (2015). Impact of hemp shiv on cement setting and hardening: Influence of the extracted components from the aggregates and study of the interfaces with the inorganic matrix. *Cement and Concrete Composites*, *55*, 112–121. https://doi.org/10.1016/j.cemconcomp.2014.09.004

Donath, S., Militz, H., & Mai, C. (2004). Wood modification with alkoxysilanes. *Wood Science and Technology*, *38*(7), 555–566. https://doi.org/10.1007/s00226-004-0257-1

Donath, S., Militz, H., & Mai, C. (2007). Weathering of silane treated wood. *Holz Als Roh - Und Werkstoff*, *65*(1), 35–42. https://doi.org/10.1007/s00107-006-0131-y

Dubois, S., Evrard, A., & Lebeau, F. (2014). Modeling the hygrothermal behavior of biobased construction materials. *Journal of Building Physics*, *38*(3), 191–213.

Elfordy, S., Lucas, F., Tancret, F., Scudeller, Y., & Goudet, L. (2008).

Mechanical and thermal properties of lime and hemp concrete ("hempcrete") manufactured by a projection process. *Construction and Building Materials*, *22*(10), 2116–2123. https://doi.org/10.1016/j.conbuildmat.2007.07.016

EU. (2010). Directive 2010/31/EU of the European Parliament and of the Council of 19 May 2010 on the energy performance of buildings (recast). *Official Journal of the European Union*, 13–35. https://doi.org/doi:10.3000/17252555.L_2010.153.eng

European Commission. (2018). The Energy Performance of Buildings Directive. Retrieved September 10, 2018, from https://ec.europa.eu/energy/en/topics/energy-efficiency/buildings

Faruk, O., Bledzki, A. K., Fink, H. P., & Sain, M. (2012). Biocomposites reinforced with natural fibers: 2000-2010. *Progress in Polymer Science*, *37*(11), 1552–1596. https://doi.org/10.1016/j.progpolymsci.2012.04.003

Fibranatur. Isolant chanvre. Available at: http://www.fibranatur.com/isolant-naturel-chanvre-fibranatur-p2.php [Accessed August 20, 2018].

Gandolfi, S., Ottolina, G., Riva, S., Fantoni, G. P., & Patel, I. (2013). Complete chemical analysis of carmagnola hemp hurds and structural features of its components. *BioResources*, *8*(2), 2641–2656. https://doi.org/10.15376/biores.8.2.2641-2656

Gao, L., Gan, W., Xiao, S., Zhan, X., & Li, J. (2016). A robust superhydrophobic antibacterial Ag-TiO2 composite film immobilized on wood substrate for photodegradation of phenol under visible-light illumination. *Ceramics International*, *42*(2), 2170–2179. https://doi.org/10.1016/j.ceramint.2015.10.002

Gassan, J., Gutowski, V. S., & Bledzki, A. K. (2000). About the surface characteristics of natural fibres. *Surface Engineering*, *283*(1), 132–139. https://doi.org/10.1002/1439-2054(20001101)283:1<132::AID-MAME132>3.0.CO;2-B

Genzer, J., & Efimenko, K. (2006). Recent developments in superhydrophobic surfaces and their relevance to marine fouling: a review. *Biofouling*, *22*(5–6), 339–360. https://doi.org/10.1080/08927010600980223

Gourlay, E., & Arnaud, L. (2010). Comportement hygrothermique des murs de béton de chanvre. *Proceedings of the Actes Du Congrès SFT, France, Le Touquet*, (February).

Gutiérrez, A., Del Río, J. C., Martínez, M. J., & Martínez, A. T. (2001). The biotechnological control of pitch in paper pulp manufacturing. *Trends in Biotechnology*. https://doi.org/10.1016/S0167-7799(01)01705-X

Hardell, H. L., & Nilvebrant, N. O. (1999). A rapid method to discriminate between free and esterified fatty acids by pyrolytic methylation using tetramethylammonium acetate or hydroxide. *Journal of Analytical and*

Applied Pyrolysis, *52*(1), 1–14. https://doi.org/10.1016/S0165-2370(99)00035-2

Hemptechnology. Breathe Natural Fibre Insulation. Available at: http://americanlimetechnology.com/wp-content/uploads/2011/11/Breathe-Datasheet.pdf [Accessed August 20, 2018].

Hill, C. A. S., Forster, S. C., Farahani, M. R. M., Hale, M. D. C., Ormondroyd, G. A., & Williams, G. R. (2005). An investigation of cell wall micropore blocking as a possible mechanism for the decay resistance of anhydride modified wood. *International Biodeterioration and Biodegradation*, *55*(1), 69–76. https://doi.org/10.1016/j.ibiod.2004.07.003

Hills, C. A. S., Norton, A. J., & Newman, G. (2009). NFI–The importance of hygroscopicity in providing indoor climate control. In *Proceedings of the 11th International Conference on Non-conventional Materials and Technologies–NOCMAT*.

Hirst, E. A. J. (2013). Characterisation of Hemp-Lime As a Composite Building Material. *Doctoral Dissertation, University of Bath*.

Hoang, C. P., Kinney, K. A., Corsi, R. L., & Szaniszlo, P. J. (2010). Resistance of green building materials to fungal growth. *International Biodeterioration and Biodegradation*, *64*(2), 104–113. https://doi.org/10.1016/j.ibiod.2009.11.001

Hussain, A., Calabria-Holley, J., Jiang, Y., & Lawrence, M. (2018). Modification of hemp shiv properties using water-repellent sol–gel coatings. *Journal of Sol-Gel Science and Technology*, *86*(1), 187–197. https://doi.org/10.1007/s10971-018-4621-2

Hussain, A., Calabria-Holley, J., Lawrence, M., Ansell, M. P., Jiang, Y., Schorr, D., & Blanchet, P. (2018). Development of novel building composites based on hemp and multi-functional silica matrix. *Composites Part B: Engineering*, *156*, 266–273. https://doi.org/10.1016/J.COMPOSITESB.2018.08.093

Hussain, A., Calabria-Holley, J., Schorr, D., Jiang, Y., Lawrence, M., & Blanchet, P. (2018). Hydrophobicity of hemp shiv treated with sol-gel coatings. *Applied Surface Science*, *434*, 850–860. https://doi.org/10.1016/j.apsusc.2017.10.210

Hustache, Y., & Arnaud, L. (2008). Synthèse des connaissances sur les bétons et mortiers de chanvre. *Construire En Chanvre*.

International Energy Agency. (2012). *Energy Policies of IEA Countries - The United Kingdom 2012 Review*. https://doi.org/10.1787/9789264171497-en

International Energy Agency. (2015). Key World Energy Statistics 2009. *Statistics*, 82. https://doi.org/10.1787/9789264039537-en

International Energy Agency. (2017). United Kingdom - Energy System Overview, 2016.

Jiang, Y., Bourebrab, M. A., Sid, N., Taylor, A., Collet, F., Pretot, S., … Lawrence, M. (2018a). Improvement of Water Resistance of Hemp Woody Substrates through Deposition of Functionalized Silica Hydrophobic Coating, while Retaining Excellent Moisture Buffering Properties. *ACS Sustainable Chemistry and Engineering*, *6*(8), 10151–10161. https://doi.org/10.1021/acssuschemeng.8b01475

Jiang, Y., Bourebrab, M. A., Sid, N., Taylor, A., Collet, F., Pretot, S., … Lawrence, M. (2018b). Improvement of Water Resistance of Hemp Woody Substrates through Deposition of Functionalized Silica Hydrophobic Coating, While Retaining Excellent Moisture Buffering Properties. *ACS Sustainable Chemistry & Engineering*, *6*(8), 10151–10161. https://doi.org/10.1021/acssuschemeng.8b01475

Jiang, Y., Lawrence, M., Ansell, M. P., & Hussain, A. (2018). Cell wall microstructure, pore size distribution and absolute density of hemp shiv. *Royal Society Open Science*, *5*(4), 171945. https://doi.org/10.1098/rsos.171945

Kabir, M. M., Wang, H., Lau, K. T., Cardona, F., & Aravinthan, T. (2012). Mechanical properties of chemically-treated hemp fibre reinforced sandwich composites. *Composites Part B: Engineering*, *43*(2), 159–169. https://doi.org/10.1016/j.compositesb.2011.06.003

Kymainen, H. R., Hautala, M., Kuisma, R., & Pasila, A. (2001a). Capillarity of flax/linseed (Linum usitatissimum L.) and fibre hemp (Cannabis sativa L.) straw fractions. *Industrial Crops and Products*, *14*(1), 41–50. https://doi.org/10.1016/S0926-6690(00)00087-X

Kymainen, H. R., Hautala, M., Kuisma, R., & Pasila, A. (2001b). Capillarity of flax/linseed (Linum usitatissimum L.) and fibre hemp (Cannabis sativa L.) straw fractions. *Industrial Crops and Products*, *14*(1), 41–50. https://doi.org/10.1016/S0926-6690(00)00087-X

Latif, E., Lawrence, M., Shea, A., & Walker, P. (2015). Moisture buffer potential of experimental wall assemblies incorporating formulated hemp-lime. *Building and Environment*, *93*(P2), 199–209. https://doi.org/10.1016/j.buildenv.2015.07.011

Latif, E., Tucker, S., Ciupala, M. A., Wijeyesekera, D. C., & Newport, D. (2014). Hygric properties of hemp bio-insulations with differing compositions. *Construction and Building Materials*, *66*, 702–711. https://doi.org/10.1016/j.conbuildmat.2014.06.021

Lawrence, M. (2015). Reducing the Environmental Impact of Construction by Using Renewable Materials. *Journal of Renewable Materials*, *3*(3), 163–174. https://doi.org/10.7569/JRM.2015.634105

Lawrence, M., Heath, A., & Walker, P. (2009). Determining moisture levels in straw bale construction. *Construction and Building Materials*, *23*(8), 2763–2768. https://doi.org/10.1016/j.conbuildmat.2009.03.011

Lawrence, M., & Jiang, Y. (2017). Porosity, Pore Size Distribution, Micro-structure BT - Bio-aggregates Based Building Materials : State-of-the-Art Report of the RILEM Technical Committee 236-BBM. In S. Amziane & F. Collet (Eds.) (pp. 39–71). Dordrecht: Springer Netherlands. https://doi.org/10.1007/978-94-024-1031-0_2

Lawrence, M., Shea, A., Walker, P., & De Wilde, P. (2013). Hygrothermal performance of bio-based insulation materials. *Proceedings of the Institution of Civil Engineers - Construction Materials*, *166*(4), 257–263. https://doi.org/10.1680/coma.12.00031

Lekavicius, V., Shipkovs, P., Ivanovs, S., & Rucins, A. (2015). Thermo-insulation properties of hemp-based products. *Latvian Journal of Physics and Technical Sciences*, *52*(1), 38–51. https://doi.org/10.1515/lpts-2015-0004

Lenofon. lenofon Holteg: How do you feel? Available at: http://www.lenofon.com/grafiken/lenofon-catalog-2013-en.pdf [Accessed August 20, 2018].

Li, Z., Xing, Y., & Dai, J. (2008). Superhydrophobic surfaces prepared from water glass and non-fluorinated alkylsilane on cotton substrates. *Applied Surface Science*, *254*(7), 2131–2135. https://doi.org/10.1016/j.apsusc.2007.08.083

Liu, M., Qing, Y., Wu, Y., Liang, J., & Luo, S. (2015). Facile fabrication of superhydrophobic surfaces on wood substrates via a one-step hydrothermal process. *Applied Surface Science*, *330*, 332–338. https://doi.org/10.1016/j.apsusc.2015.01.024

Magniont, C., Escadeillas, G., Coutand, M., & Oms-Multon, C. (2012). Use of plant aggregates in building ecomaterials. *European Journal of Environmental and Civil Engineering*, *16*(SUPPL. 1). https://doi.org/10.1080/19648189.2012.682452

Mahltig, B., & Böttcher, H. (2003). Modified silica sol coatings for water-repellent textiles. *Journal of Sol-Gel Science and Technology*, *27*(1), 43–52. https://doi.org/10.1023/A:1022627926243

Mahltig, B., Swaboda, C., Roessler, A., & Böttcher, H. (2008). Functionalising wood by nanosol application. *Journal of Materials Chemistry*, *18*, 3180. https://doi.org/10.1039/b718903f

Mai, C., & Militz, H. (2004). Modification of wood with silicon compounds. Inorganic silicon compounds and sol-gel systems: A review. *Wood Science and Technology*, *37*(5), 339–348. https://doi.org/10.1007/s00226-003-0205-5

Manger, G. E. (1963). Porosity and bulk density of sedimentary rocks.

Manitoba Agriculture Canada. (2018). Hemp | Manitoba Agriculture | Province of Manitoba. Retrieved July 23, 2018, from

https://www.gov.mb.ca/agriculture/crops/production/hemp.html

Marceau, S., Glé, P., Guéguen-Minerbe, M., Gourlay, E., Moscardelli, S., Nour, I., & Amziane, S. (2017). Influence of accelerated aging on the properties of hemp concretes. *Construction and Building Materials*, *139*, 524–530. https://doi.org/10.1016/j.conbuildmat.2016.11.129

Maskell, D., Thomson, A., Walker, P., & Lemke, M. (2018). Determination of optimal plaster thickness for moisture buffering of indoor air. *Building and Environment*, *130*(November 2017), 143–150. https://doi.org/10.1016/j.buildenv.2017.11.045

Mazhoud, B., Collet, F., Pretot, S., & Chamoin, J. (2016). Hygric and thermal properties of hemp-lime plasters. *Building and Environment*, *96*, 206–216. https://doi.org/10.1016/j.buildenv.2015.11.013

Mazhoud, B., Collet, F., Pretot, S., & Lanos, C. (2017). Mechanical properties of hemp-clay and hemp stabilized clay composites. *Construction and Building Materials*, *155*, 1126–1137. https://doi.org/10.1016/j.conbuildmat.2017.08.121

Mersagh Dezfuli, S., & Sabzi, M. (2018). A study on the effect of presence of CeO_2 and benzotriazole on activation of self-healing mechanism in ZrO_2 ceramic-based coating. *International Journal of Applied Ceramic Technology*, *15*(5), 1248–1260. https://doi.org/10.1111/ijac.12901

Morrell, P. (2010). Low Carbon Construction. *Innovation*, 231.

Mwaikambo, L. Y., & Ansell, M. P. (2002). Chemical modification of hemp, sisal, jute, and kapok fibers by alkalization. *Journal of Applied Polymer Science*, *84*(12), 2222–2234. https://doi.org/10.1002/app.10460

Nakajima, A., Hashimoto, K., & Watanabe, T. (2001). Recent studies on super-hydrophobic films. In *Monatshefte fur Chemie* (Vol. 132, pp. 31–41). https://doi.org/10.1007/s007060170142

Naono, H., & Hakuman, M. (1993). Analysis of porous texture by means of water vapor adsorption isotherm with particular attention to lower limit of hysteresis loop. *Journal of Colloid and Interface Science*, *158*(1), 19–26.

NaturePRO. NaturePRO Hemp technical sheet. Available at: http://www.natureproinsulation.co.uk/pdf/Hemp-Leaflet-High-Res.pdf [Accessed August 20, 2018].

Nguyen, T. T., Picandet, V., Amziane, S., & Baley, C. (2009). Influence of compactness and hemp hurd characteristics on the mechanical properties of lime and hemp concrete. *European Journal of Environmental and Civil Engineering*, *13*(9), 1039–1050. https://doi.org/10.1080/19648189.2009.9693171

Nielsen, K. F., Holm, G., Uttrup, L. P., & Nielsen, P. A. (2004). Mould growth on building materials under low water activities. Influence of humidity and

temperature on fungal growth and secondary metabolism. *International Biodeterioration and Biodegradation*, *54*(4), 325–336. https://doi.org/10.1016/j.ibiod.2004.05.002

Ogihara, H., Xie, J., Okagaki, J., & Saji, T. (2012). Simple method for preparing superhydrophobic paper: Spray-deposited hydrophobic silica nanoparticle coatings exhibit high water-repellency and transparency. *Langmuir*, *28*(10), 4605–4608. https://doi.org/10.1021/la204492q

Osanyintola, O. F., & Simonson, C. J. (2006). Moisture buffering capacity of hygroscopic building materials: Experimental facilities and energy impact. *Energy and Buildings*, *38*(10), 1270–1282. https://doi.org/10.1016/j.enbuild.2006.03.026

Papadopoulos, A. M. (2005). State of the art in thermal insulation materials and aims for future developments. *Energy and Buildings*, *37*(1), 77–86. https://doi.org/10.1016/j.enbuild.2004.05.006

Pickering, K. L., Efendy, M. G. A., & Le, T. M. (2016). A review of recent developments in natural fibre composites and their mechanical performance. *Composites Part A: Applied Science and Manufacturing*, *83*, 98–112. https://doi.org/10.1016/j.compositesa.2015.08.038

Rode, C. (2005). *Moisture Buffering of Building Materials Department of Civil Engineering Technical University of Denmark*.

Rowell, R. M. (2012). *Handbook of wood chemistry and wood composites*. CRC press.

Saputra, R. E., Astuti, Y., & Darmawan, A. (2018). Hydrophobicity of silica thin films: The deconvolution and interpretation by Fourier-transform infrared spectroscopy. *Spectrochimica Acta - Part A: Molecular and Biomolecular Spectroscopy*, *199*, 12–20. https://doi.org/10.1016/j.saa.2018.03.037

Sedan, D., Pagnoux, C., Smith, A., & Chotard, T. (2008). Mechanical properties of hemp fibre reinforced cement: Influence of the fibre/matrix interaction. *Journal of the European Ceramic Society*, *28*(1), 183–192. https://doi.org/10.1016/j.jeurceramsoc.2007.05.019

Shea, A., Lawrence, M., & Walker, P. (2012). Hygrothermal performance of an experimental hemp-lime building. *Construction and Building Materials*, *36*, 270–275. https://doi.org/10.1016/j.conbuildmat.2012.04.123

Silva, C., & Airoldi, C. (1997). Acid and Base Catalysts in the Hybrid Silica Sol-Gel Process. *Journal of Colloid and Interface Science*, *195*(2), 381–387. https://doi.org/10.1006/jcis.1997.5159

Song, J., & Rojas, O. J. (2013). Approaching super-hydrophobicity from cellulosic materials : A Review. *Paper Chemistry*, *28*(2), 216–238. https://doi.org/10.3183/NPPRJ-2013-28-02-p216-238

Stefanidou, M., Assael, M., Antoniadis, K., & Matziaroglou, G. (2010). Thermal

conductivity of building materials employed in the preservation of traditional structures. *International Journal of Thermophysics*, *31*(4–5), 844–851. https://doi.org/10.1007/s10765-010-0750-8

STEICO. STEICO natural building products. Available at: http://merodax.com/images/dokumentai/steico_canaflex_merodax_en.pdf [Accessed August 20, 2018].

Stevulova, N., Cigasova, J., Estokova, A., Terpakova, E., Geffert, A., Kacik, F., … Holub, M. (2014). Properties characterization of chemically modified hemp hurds. *Materials*, *7*(12), 8131–8150. https://doi.org/10.3390/ma7128131

Straube, J., & Schumacher, C. (2003). Monitoring the Hygrothermal Performance of Strawbale Walls. *East*.

Sun, R. C., & Tomkinson, J. (2002). Comparative study of organic solvent-soluble and water-soluble lipophilic extractives from wheat straw 2: Spectroscopic and thermal analysis. *Journal of Wood Science*, *48*(3), 222–226. https://doi.org/10.1007/BF00771371

Sutton, A., Black, D., Walker, P., & BRE. (2011). Natural fibre insulation. *Bre Ip 18/11*, 1–4. Retrieved from http://www.bre.co.uk/filelibrary/pdf/projects/low_impact_materials/IP14_11.pdf

Taoukil, D., El Bouardi, A., Sick, F., Mimet, A., Ezbakhe, H., & Ajzoul, T. (2013). Moisture content influence on the thermal conductivity and diffusivity of wood-concrete composite. *Construction and Building Materials*, *48*, 104–115. https://doi.org/10.1016/j.conbuildmat.2013.06.067

Technichanvre. Technilaine. Available at: http://www.technichanvre.com/1411-2/1499-2/hemp-insulationrolls-and-panels/?lang=en#dws_first_tab33 [Accessed August 20, 2018].

Teisala, H., Tuominen, M., & Kuusipalo, J. (2014). Superhydrophobic Coatings on Cellulose-Based Materials: Fabrication, Properties, and Applications. *Advanced Materials Interfaces*, *1*(1), 1–20. https://doi.org/10.1002/admi.201300026

Thermafleece. Thermafleece NATRA natural insulation. Available at: http://www.thermafleece.com/uploads/Thermafleece-NatraHemp-Factsheet.pdf [Accessed August 20, 2018].

Thermo-Hemp. Thermo-Hemp natural insulation. Available at: http://www.ecologicalbuildingsystems.com/docs/Thermo-Hemp-Insulation-Data-Sheet.pdf [Accessed August 20, 2018].

Thomsen, A. B., Rasmussen, S., Bohn, V., Nielsen, K. V., & Thygesen, A. (2005). Hemp raw materials : The effect of cultivar , growth conditions and pretreatment on the chemical composition of the fibres. *Risø-R Report*, *1507*(March), 6–30.

Thygesen, A., Daniel, G., Lilholt, H., & Thomsen, A. B. (2005). Hemp Fibre Microstructure and Use of Fungal Defibration to Obtain Fibres for Composite Materials. *Journal of Natural Fibers*, *2*(4), 19–37. https://doi.org/10.1300/J395v02n04

Tomšič, B., Simončič, B., Orel, B., Černe, L., Tavčer, P. F., Zorko, M., … Kovač, J. (2008). Sol--gel coating of cellulose fibres with antimicrobial and repellent properties. *Journal of Sol-Gel Science and Technology*, *47*(1), 44–57. https://doi.org/10.1007/s10971-008-1732-1

Tran Le, A. D., Maalouf, C., Mai, T. H., Wurtz, E., & Collet, F. (2010). Transient hygrothermal behaviour of a hemp concrete building envelope. *Energy and Buildings*, *42*(10), 1797–1806. https://doi.org/10.1016/j.enbuild.2010.05.016

Tshabalala, M. A., Kingshott, P., Vanlandingham, M. R., & Plackett, D. (2002). Surface Chemistry and Moisture Sorption Properties of Wood Coated with Multifunctional Alkoxysilanes by Sol- Gel Process.

United Nations. (2009). *Buildings and Climate Change: Summary for Decision Makers*. *Buildings and Climate Change: Summary for Decision-Makers*. https://doi.org/10.1127/0941-2948/2006/0130

Valadez-Gonzalez, A., Cervantes-Uc, J. M., Olayo, R., & Herrera-Franco, P. J. (1999). Effect of fiber surface treatment on the fiber-matrix bond strength of natural fiber reinforced composites. *Composites Part B: Engineering*, *30*(3), 309–320. https://doi.org/10.1016/S1359-8368(98)00054-7

Van der Werf, H. (1994). *Crop physiology of fibre hemp (Cannabis sativa L.)*. Van der Werf.

Végétal, I. Une isolation thermique et acoustique performante et une grande souplesse de mise en oeuvre. Retrieved from http://www.isonat.com/uploads/files/produits/IsonatVegetal/Fiche_Vegetal_1113_BDEF.pdf [Accessed August 20, 2018].

Vignon, M. R., & Dupeyre, D. (1995). Steam explosion of woody hemp ch nevotte, *17*(6), 395–404.

Walker, R., & Pavía, S. (2014). Moisture transfer and thermal properties of hemp-lime concretes. *Construction and Building Materials*, *64*, 270–276. https://doi.org/10.1016/j.conbuildmat.2014.04.081

Walker, R., Pavia, S., & Mitchell, R. (2014). Mechanical properties and durability of hemp-lime concretes. *Construction and Building Materials*, *61*, 340–348. https://doi.org/10.1016/j.conbuildmat.2014.02.065

Wang, H., Zhou, H., Liu, S., Shao, H., Fu, S., Rutledge, G. C., & Lin, T. (2017). Durable, self-healing, superhydrophobic fabrics from fluorine-free, waterborne, polydopamine/alkyl silane coatings. *RSC Adv.*, *7*(54), 33986–33993. https://doi.org/10.1039/C7RA04863G

Wang, S., Liu, C., Liu, G., Zhang, M., Li, J., & Wang, C. (2011). Fabrication of

superhydrophobic wood surface by a sol-gel process. *Applied Surface Science*, *258*(2), 806–810. https://doi.org/10.1016/j.apsusc.2011.08.100

Wang, S., Shi, J., Liu, C., Xie, C., & Wang, C. (2011). Fabrication of a superhydrophobic surface on a wood substrate. *Applied Surface Science*, *257*(22), 9362–9365. https://doi.org/10.1016/j.apsusc.2011.05.089

Xie, Y., Hill, C. A. S., Xiao, Z., Militz, H., & Mai, C. (2010a). Silane coupling agents used for natural fiber/polymer composites: A review. *Composites Part A: Applied Science and Manufacturing*, *41*(7), 806–819. https://doi.org/10.1016/j.compositesa.2010.03.005

Xie, Y., Hill, C. A. S., Xiao, Z., Militz, H., & Mai, C. (2010b). Silane coupling agents used for natural fiber/polymer composites: A review. *Composites Part A: Applied Science and Manufacturing*, *41*(7), 806–819. https://doi.org/10.1016/j.compositesa.2010.03.005

Xu, L., Zhuang, W., Xu, B., & Cai, Z. (2011). Fabrication of superhydrophobic cotton fabrics by silica hydrosol and hydrophobization. *Applied Surface Science*, *257*(13), 5491–5498. https://doi.org/10.1016/j.apsusc.2010.12.116

Xu, Q. F., Wang, J. N., & Sanderson, K. D. (2010). Organic-inorganic composite nanocoatings with superhydrophobicity, good transparency, and thermal stability. *ACS Nano*, *4*(4), 2201–2209. https://doi.org/10.1021/nn901581j

Xue, C.-H., Jia, S.-T., Chen, H.-Z., & Wang, M. (2008). Superhydrophobic cotton fabrics prepared by sol–gel coating of TiO 2 and surface hydrophobization. *Science and Technology of Advanced Materials*, *9*(3), 35001. https://doi.org/10.1088/1468-6996/9/3/035001

Yang, J., Yeh, S. K., Chiou, N. R., Guo, Z., Daniel, T., & Lee, L. J. (2009). Synthesis and foaming of water expandable polystyrene-activated carbon (WEPSAC). *Polymer*, *50*(14), 3169–3173. https://doi.org/10.1016/j.polymer.2009.05.007

Yohanis, Y. G., & Norton, B. (2002). Life-cycle operational and embodied energy for a generic single-storey office building in the UK. *Energy*, *27*(1), 77–92. https://doi.org/10.1016/S0360-5442(01)00061-5

Yu, M., Gu, G., Meng, W. D., & Qing, F. L. (2007). Superhydrophobic cotton fabric coating based on a complex layer of silica nanoparticles and perfluorooctylated quaternary ammonium silane coupling agent. *Applied Surface Science*, *253*(7), 3669–3673. https://doi.org/10.1016/j.apsusc.2006.07.086

Zauer, M., Pfriem, A., & Wagenführ, A. (2013). Toward improved understanding of the cell-wall density and porosity of wood determined by gas pycnometry. *Wood Science and Technology*, *47*(6), 1197–1211. https://doi.org/10.1007/s00226-013-0568-1

Zeng, C., Wang, H., Zhou, H., & Lin, T. (2015). Self-cleaning, superhydrophobic cotton fabrics with excellent washing durability, solvent resistance and

chemical stability prepared from an SU-8 derived surface coating. *RSC Adv.*, *5*(75), 61044–61050. https://doi.org/10.1039/C5RA08040A

Zhang, H., Yoshino, H., & Hasegawa, K. (2012). Assessing the moisture buffering performance of hygroscopic material by using experimental method. *Building and Environment*, *48*(1), 27–34. https://doi.org/10.1016/j.buildenv.2011.08.012

Zhou, H., Wang, H., Niu, H., Gestos, A., & Lin, T. (2013). Robust, self-healing superamphiphobic fabrics prepared by two-step coating of fluoro-containing polymer, fluoroalkyl silane, and modified silica nanoparticles. *Advanced Functional Materials*, *23*(13), 1664–1670. https://doi.org/10.1002/adfm.201202030